Contribution of artificial intelligence in model predictive control of smart sewer networks

Khalid El Ghazouli

Université de Lille

Université Mohammed V de Rabat

Laboratoire Génie Civil et GéoEnvironnement- (LGCGE)

Laboratoire Analyse des Systèmes, Traitement de l'information et Management Intégré (LASTIMI)

Thèse en cotutelle présentée par :

EL GHAZOULI Khalid

Soutenue le: 15 Décembre 2021

Pour l'obtention du grade de Docteur en Génie Civil

Contribution de l'intelligence artificielle dans la gestion prédictive des réseaux d'assainissement intelligents

Contribution of Artificial Intelligence in Model Predictive Control of Smart Sewer Networks

Membres du jury :

Isam SHAHROUR	Professeur, Université de Lille	Président du Jury
Jamal EL KHATTABI	Maitre de Conférences, Université de Lille	Directeur de thèse
Aziz SOULHI	Professeur, Ecole Nationale Supérieure des Mines de Rabat	Co-Directeur de thèse
Lahcen ZOUHRI	Professeur, Unilasalle	Rapporteur
Ahmed MOUHSEN	Professeur, Faculté des Sciences et Techniques Settat	Rapporteur
Oras ABBAS	Directrice de laboratoire de contrôle, Trescal Groupe	Examinateur
Mounia EL HAJI	Professeur, Ecole Nationale Supérieur d'Electricité et Mécanique	Examinateur
Toufik CHERRADI	Professeur, Ecole Mohammadia d'Ingénieurs	Examinateur

ABSTRACT

Urbanization and an increase in precipitation intensities due to climate change, in addition to limited urban drainage systems (UDS) capacity, are the main causes of combined sewer overflows (CSOs) that cause serious water pollution problems in many cities around the world. Model predictive control (MPC) systems offer a new approach to mitigate the impact of CSOs. This thesis aimed to develop an MPC system to minimize the environmental impact of CSOs during the rainy season.

Data forecasts are a key component for every MPC system. The first part of this work comprises the development and validation of two flow forecasting models, namely, a wastewater flow forecasting model (WWFFM) to forecast dry weather flows (DWFs) and a stormwater forecasting model (SWFM) to predict stormwater flows in sewer networks. These models have shown their ability to provide valuable input data with sufficient lead time for predictive model control systems to enhance efficiency in UDSs and reduce CSOs. Moreover, the second part of this work discusses the development of an MPC system based on the SWFM and the WWFFM for predicting flows, the SWMM for flow conveying, and a genetic algorithm for optimizing the operation of the sewer system to reduce the impact of CSOs on the receiving environment. MPC demonstrates high efficiency in reducing CSOs in the receiving environment by generating the optimal temporally and spatially varied dynamic control strategies of the gate valves of the sewer system.

Keywords: artificial intelligence, combined sewer overflows, genetic algorithm, hydraulic modeling, model predictive control, neural network, optimization, real-time control, sewer network

RESUME

Du fait de l'urbanisation et du changement climatique, les agglomérations mondiales sont confrontées à des enjeux environnementaux majeurs liés à la pollution causée par les déversements des réseaux d'assainissement (RA) par temps de pluie. Les systèmes de contrôle prédictif offrent une nouvelle approche permettant de piloter les réseaux d'assainissement en temps réel et limiter l'impact des déversements vers le milieu récepteur. Cette thèse a visé à développer un système de modélisation prédictif basé sur l'intelligence artificielle pour minimiser l'impact environnemental des rejets urbains par temps de pluie (RUTP).

Les données issues des modèles de prévisions sont des paramètres essentiels pour tout système de modélisation prédictif. La première partie de cette thèse a consisté à développer et valider deux modèles basés sur de l'intelligence artificielle (IA) pour la prévision des débits dans les RA. Le premier modèle basé sur le NARX Neural Network a été développé et validé pour la prévision des débits des eaux usées par temps sec. Le deuxième modèle développé dans le cadre de ce travail permet la prévision des débits des eaux pluviales aux exutoires des bassins versants et aux points de contrôles stratégiques et a fait l'objet d'une comparaison des performances de quatre modèles IA .

La dernière partie de ce travail a porté sur le développement d'un système de contrôle prédictif (SCP) qui prend comme données d'entrée les prévisions des débits, un modèle hydraulique EPA-SWMM, et un algorithme génétique pour l'optimisation du fonctionnement du RA. Le SCP a démontré une grande efficacité dans la réduction des RUTP en générant des stratégies de contrôle dynamiques et optimales qui permettent de maximiser le volume traité en station d'épuration avant rejet vers le milieu naturel.

Mots clés : Intelligence artificielle, déversements des réseaux d'assainissement unitaires, algorithme génétique, modélisation hydraulique, modèle de contrôle prédictif, réseau de neurones, optimisation, contrôle en temps réel, réseau d'assainissement

SYNTHESE

Les agglomérations mondiales sont confrontées à des enjeux environnementaux majeurs liés aux problèmes d'inondations et à la pollution qui impacte les milieux récepteurs, du fait de l'urbanisation et du changement climatique. Dans de nombreuses villes, les réseaux d'assainissement existants ne peuvent pas acheminer toutes les eaux polluées vers les stations d'épuration lors d'épisodes pluvieux, ce qui entraîne de fréquents déversements d'eau polluée qui impactent significativement l'écosystème en déséquilibrant sa cinétique.

Plusieurs stratégies de contrôle ont été mises en œuvre pour minimiser les rejets urbains par temps de pluie (RUTP) et améliorer la résilience des villes face aux inondations. Les techniques alternatives jouent un rôle important dans la limitation des volumes de ruissellement, des débits de pointe et de la pollution. Elles désengorgent le réseau d'assainissement aval en régulant le débit ou en infiltrant l'eau. Les bassins de stockage permettent de stocker un volume important d'eau polluée lors d'épisodes pluvieux et de les rejeter dans les RA une fois les événements pluvieux terminés. Cependant, ces solutions restent difficiles à réaliser en raison des coûts de réalisation et d'entretien ainsi que la problématique du foncier dans les zones fortement urbanisées. L'une des techniques émergentes pour réduire les RUPT repose du le contrôle prédictif des différents composants du RA afin d'atteindre des objectifs de réduction de la pollution vers le milieu récepteur et des inondations urbaines.

Cette thèse a visé à développer un système de modélisation prédictive pour le contrôle du réseau d'assainissement de la ville de Casablanca au Maroc. Ce système permet de définir des stratégies de contrôle optimales des différentes vannes motorisées afin de minimiser l'impact environnemental des RUTP pendant la saison des pluies.

Le premier chapitre de cette thèse présente l'évolution des systèmes d'assainissement, les processus de génération de pollution dans les bassins versants urbains, et les techniques

utilisées pour minimiser l'impact des RUTP sur les milieux récepteurs.

Le deuxième chapitre est une présentation des systèmes de distribution d'eau potable et d'assainissement du Grand Casablanca, au Maroc, et qui a servi de site expérimental pour ce travail de recherche.

La prévision des débits d'eaux usées est un élément clé dans la gestion à court et à long terme des réseaux d'assainissements (RA). Cette prévision constitue souvent une incertitude considérable pour les exploitants en raison de la relation non linéaire entre les variables causales et les débits d'eaux usées. Le troisième chapitre a visé à compléter les travaux de recherche existants sur la prévision des débits d'eaux usées par temps sec dans les RA en proposant un nouveau modèle de prévision des débits d'eaux usées (WWFFM) basé sur les réseaux de neurones NARX-NN. Ce travail de recherche a permis de comparer deux approches du modèle de prévision. La première approche consiste à prédire les débits d'eaux usées sur la base de la consommation d'eau potable en temps réel et les débits d'eaux claires parasites (ECP), et la seconde approche considère les mêmes données d'entrée en plus des prévisions de besoin en eau potable sur les différents secteurs du bassin versant.

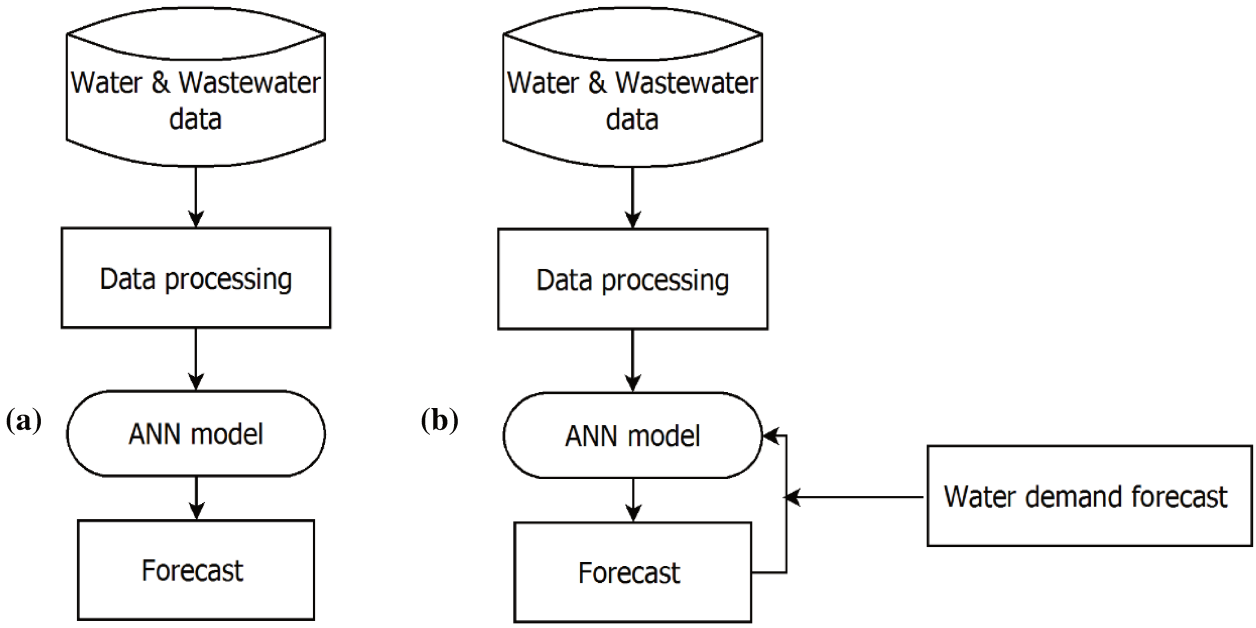

Processus de fonctionnement du WWFFM : (a) Sans prévision de la demande en eau et (b) avec prévision de la demande en eau

Les résultats de ce travail ont montré que les deux approches présentent des performances similaires dans la prévision des débits d'eaux usées, tant que l'horizon de prévision ne dépasse pas le temps de réponse (Lag) du bassin versant. Pour les horizons de prévision qui dépassent le lag du bassin versant, le WWFFM basé les prévisions des besoins en eau potable fourni des résultats plus fiables pour des horizons de prévisions plus longs. Le WWFFM proposé pourrait profiter aux opérateurs en fournissant des données d'entrée fiables pour les besoins du contrôle en temps réel des composants du système d'assainissement.

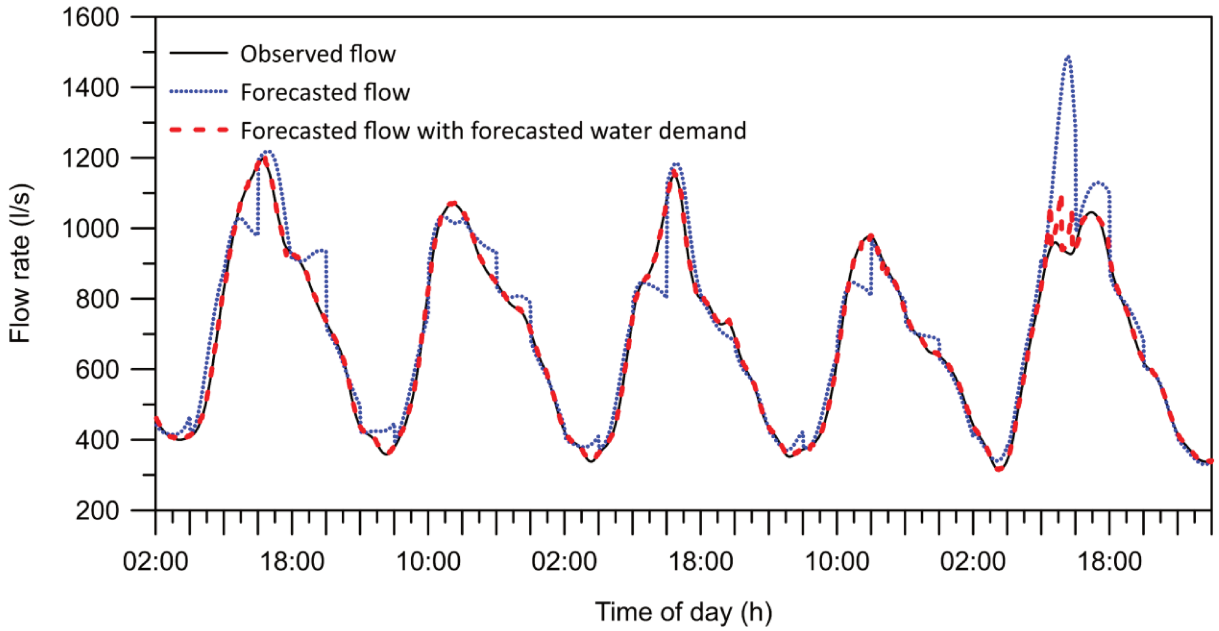

Résultats du WWFFM pour un horizon de prévision de 4 h

Le quatrième chapitre présente le développement d'un modèle de prévision des débits des eaux pluviales (SWFM) à travers une étude comparative de quatre techniques d'intelligence artificielle. Le NARX-NN, M5T, Random Forest (RF) et le système adaptatif d'inférence neuro-floue (ANFIS) ont été utilisés pour la prévision des eaux pluviales prenant comme données d'entrée les prévisions des précipitations. Ces algorithmes ont été testés et comparés sur la base de données collectées sur un bassin versant de 3 315 ha situé à Casablanca au Maroc. Les résultats de cette étude confirment que les modèles NARX, M5T et RF fournissent de bons résultats là où l'algorithme

ANFIS échoue dans la transformation de la pluie en débit. Le modèle NARX montre de bonnes performances dans la modélisation de toutes les gammes de débits avec une légère surestimation des débits de pointe pour les intensités de pluies faibles à moyennes. Les modèles M5T et RF donnent de bons résultats dans la prévision des débits de pointe. Les modèles NARX, M5T, ANFIS et RF sous-estiment les débits de pointe pour les pluies avec une période de retour de 10 ans. Cette sous-estimation est principalement due à la non-représentativité des pluies décennales qui représentent à peine 2% du jeu de données utilisé pour l'apprentissage de ces algorithmes. Cette sous-estimation peut être adressé dans le temps avec l'utilisation d'un jeu de données plus large et un apprentissage en continu des modèles d'IA. Le SWFM basé sur les modèles NARX, M5T et RF pourrait être facilement mis en œuvre pour une utilisation pratique dans les systèmes d'assainissement.

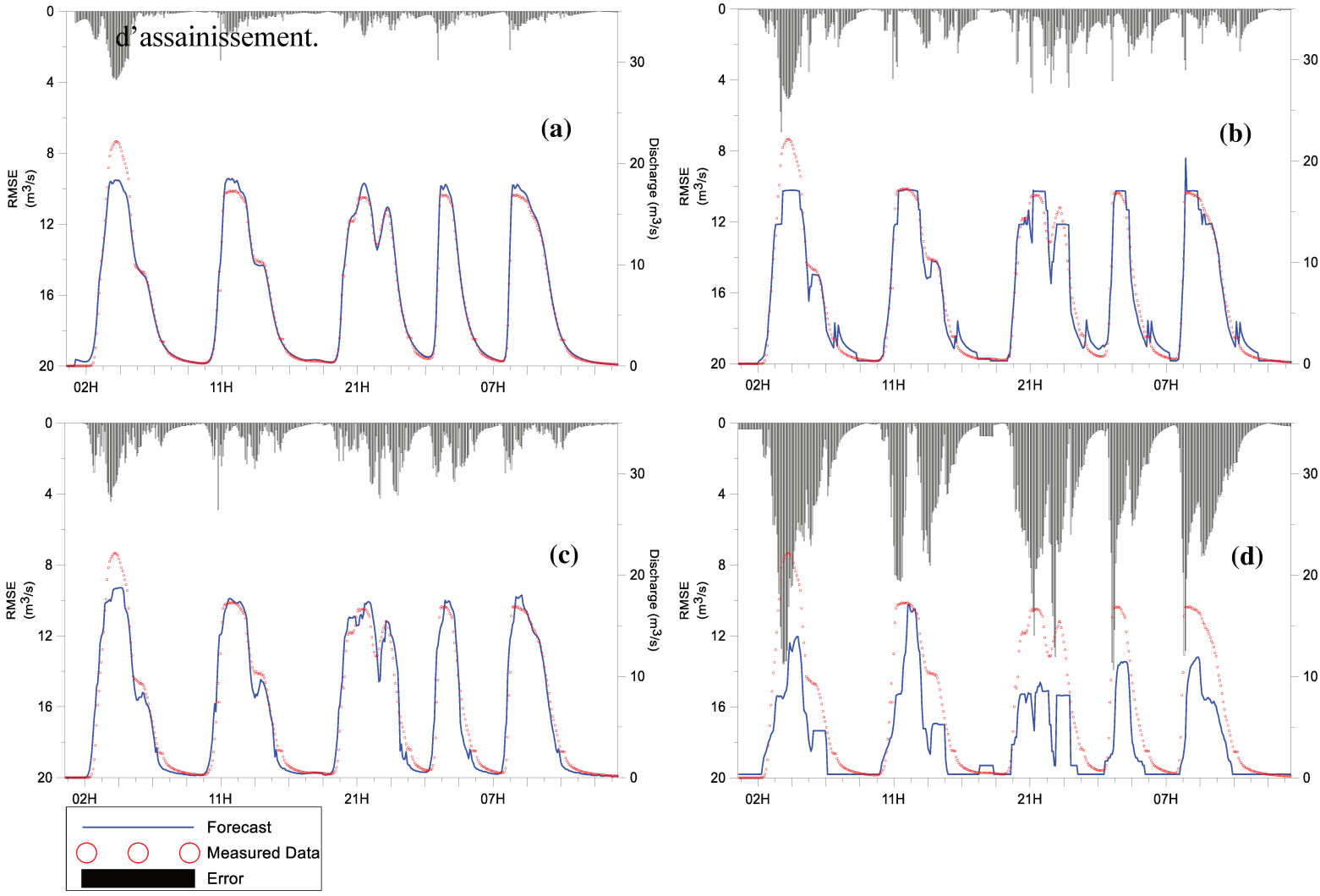

Résultats de prévisions des débits (a) NARX; (b) M5T; (c) RF; (d) ANFIS-PSO

La dernière partie de ce travail a consisté au développement d'un modèle prédictif de contrôle (MPC) basé sur le WWFFM et le SWFM pour la prévision des débits et un algorithme génétique pour optimiser le fonctionnement du réseau d'assainissement de Casablanca.

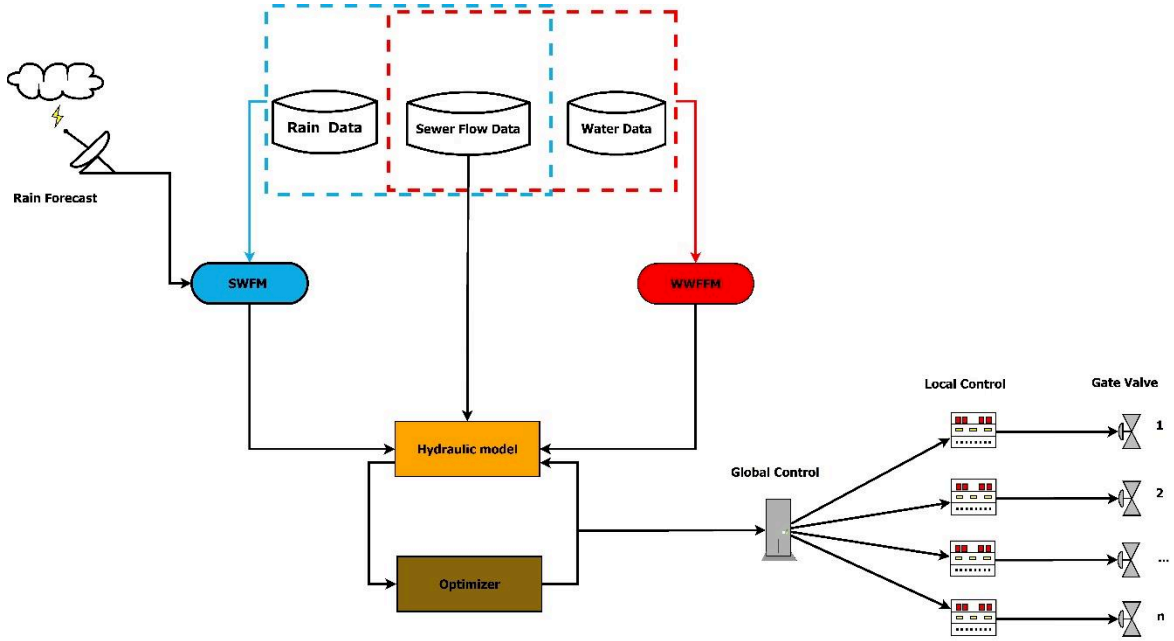

Architecture du MPC

Dans le cadre de ce travail, nous avons déterminé la meilleure taille de population et le meilleur nombre de générations qui présentent un compromis entre les performances de l'algorithme pour trouver une solution optimale et le temps de calcul. La parallélisation des calculs a permis de réduire considérablement le temps de calcul et améliorer la proactivité du MPC. Le MPC a démontré une grande efficacité dans la réduction des RUPT vers le milieu récepteur en générant des stratégies de contrôle dynamiques optimales et variées dans le temps et l'espace des vannes du système d'interception. Le MPC proposé dans le cadre de cette thèse peut profiter aux municipalités pour une gestion durable et intelligente des systèmes d'assainissement.

(a)

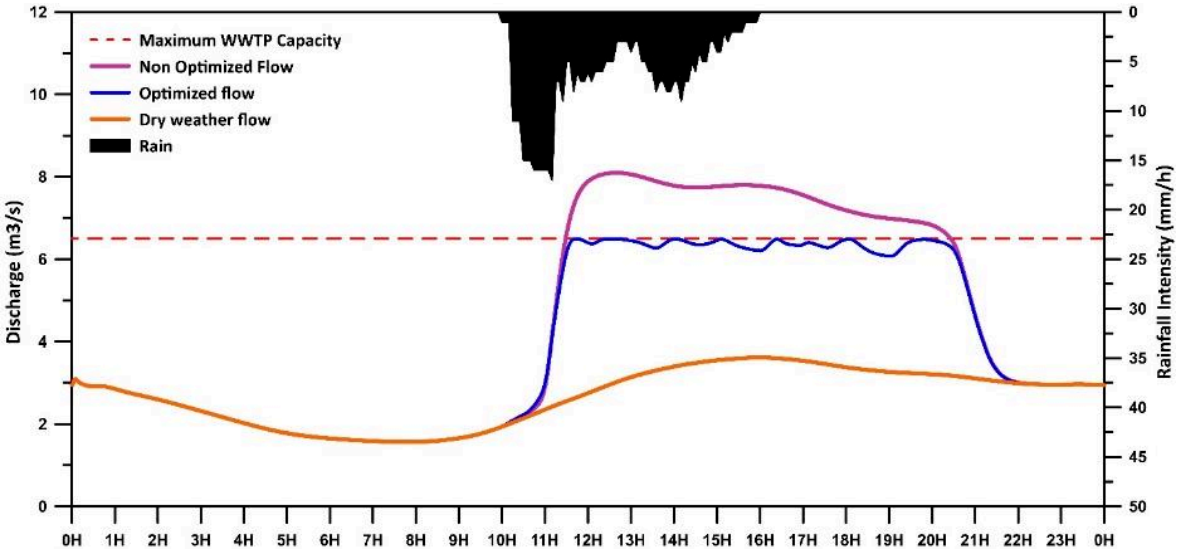

(b)

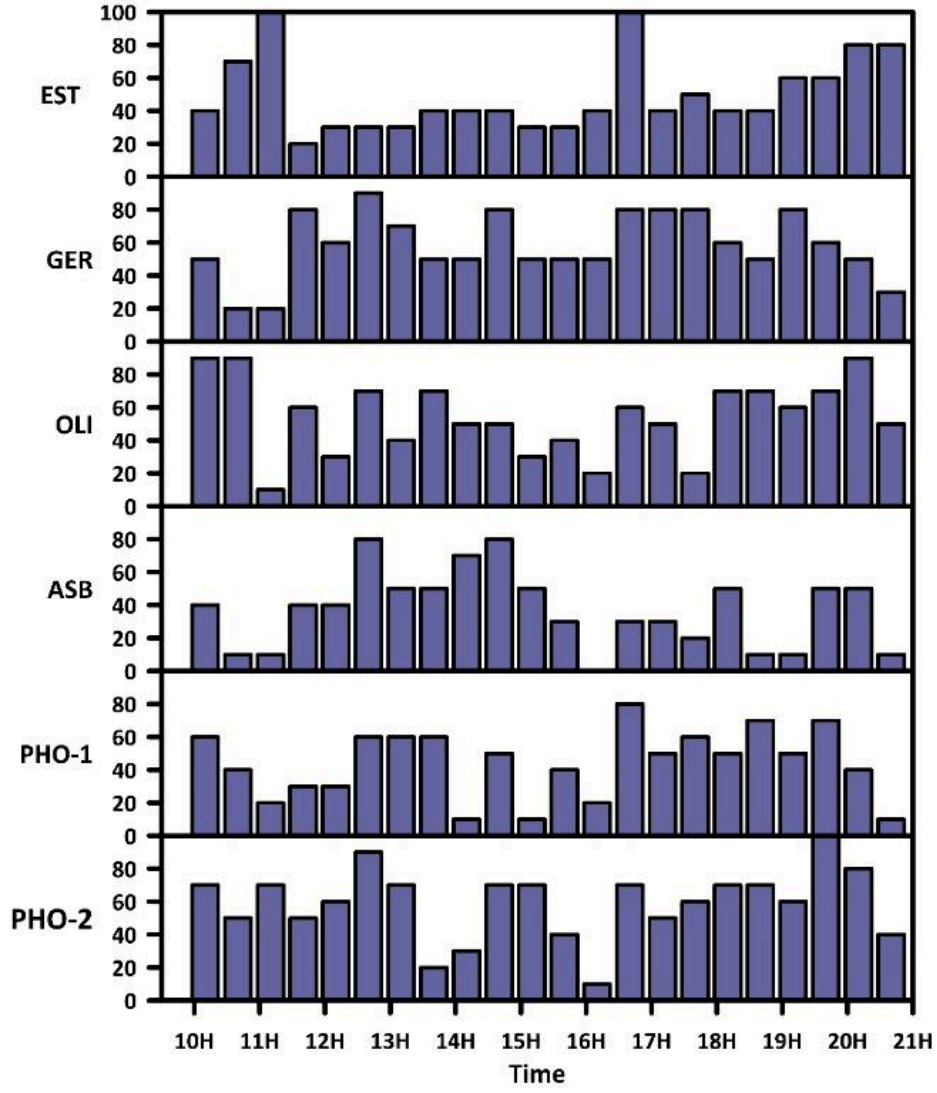

Résultats du MPC : (a) Maximisation des volumes traités et (b) planning des vannes généré par le MPC

ACKNOWLEDGMENT

First, I would like to express my deep and sincere gratitude to my Ph.D. supervisors, Dr. Jamal EL KHATTABI " Professor at Lille University ", Dr. Aziz SOULHI " Professor at Ecole Nationale Supérieure des Mines de Rabat ", who gave me the opportunity and the orientation to achieve this project.

I would like to express my deep and sincere gratitude to Dr. Isam SHAHROUR " Professor at Université de Lille " for giving me the opportunity to do research at the LGCGE. It was a great privilege and honor to work under his guidance.

I would like also to express my special thanks to all my committee members, Dr. Lahcen ZOUHRI " Professor at Unilasalle ", Dr. Ahmed MOUHSEN " Professor at Faculté des Sciences et Techniques Settat ", Dr. Oras ABBAS "Director of the control laboratory - Trescal Groupe", Dr. Mounia EL HAJI "Professor at Ecole Nationale Supérieure d'Electricité et Mécanique ", Dr. Toufik CHERRADI " Professor at Ecole Mohammadia d'Ingénieurs ", for evaluating my thesis work

My thanks go to all people who helped either directly or indirectly to finish this work.

Finally, and above all, I would like to thank my family. My parents for their love and sacrifices. My wife for her support, patience understanding, and encouragement during these past few years. My brother, his wife, and my nephew who offered invaluable support and humor over the years.

TABLE OF CONTENTS

LIST OF FIGURES

LIST OF TABLES

LIST OF ABBREVIATIONS

- A.I: Artificial intelligence
- ANFIS: Adaptive Neuro-Fuzzy Inference System
- ANN: Artificial Neural Network
- ARIMA: Autoregressive Integrated Moving Average
- BIF: Base Infiltration Flow
- CSOs: Combined sewer overflows
- DMA: District Metering Area
- DWF: dry-weather flow
- GA: Genetic algorithm
- LM: Linear Model
- LMBP: Levenberg-Marquardt Back-Propagation
- LSM: Least Square Method
- M5T: M5 Model Tree
- MBR: Membrane Bioreactor
- MLP: Multilayer Perceptron
- MPC: Model Predictive Control
- MSE: Mean Squared Error
- NARX-NN: Nonlinear Auto Regressive with eXogenous inputs neural network
- NSE Nash-Sutcliffe Efficiency (NSE)
- ObjFun: Objective Function
- PSO: Particle Swarm Optimization

- RF: Random Forest
- RTC: Real-time control
- RMSE: Root Mean Square Error
- RP: Return Period
- SS: Separate Sewer
- SWFM: Storm Water Forecasting Model
- SWMM: Storm Water Management Model
- UDS: Urban Drainage System
- WWFFM: WasteWater Flow Forecasting Model
- WWTP: WasteWater Treatment Plant (WWTP)
- YRP: Year Return Period

Introduction

World agglomerations are facing major environmental issues, particularly related to floods and pollution that impact water bodies, due to urbanization and climate change. In many cities, the existing combined sewer systems cannot convey all the polluted water to wastewater treatment plants during rain events, thereby leading to frequent combined sewer overflows (CSOs). The pollution released by sewer networks can significantly impact the ecosystem by unbalancing its kinetics.

Several control strategies have been implemented to minimize urban CSOs and improve the flood resilience of cities. Green infrastructures play a significant role in limiting runoff volumes, peak flows, and pollution, and they relieve the downstream sewer network by regulating the flow or infiltrating water. Storage basins allow storing a large volume of polluted water during rain events and release it back to sewer networks once the rainfall events are over. However, these solutions remain difficult to achieve because of the lack of construction space maintenance costs in high-density urbanized areas. One of the emerging ways to reduce CSOs is by performing the advanced real-time control (RTC) of sewer networks based on model predictive control (MPC) systems.

This thesis aimed to develop an MPC system that can set optimal control strategies for sewer network gate valves to minimize the environmental impact of CSOs during the rainy season.

The first chapter of this thesis presents and describes the role of the sewer system, the processes of pollution generation in urban watersheds, and the techniques used to minimize the impact of CSOs on the receiving environment.

The second chapter discusses the drinking water distribution and sanitation systems of Casablanca, Morocco, which served as an experimental site for this research work.

Forecasting flows in sewer networks constitutes a significant uncertainty for operators due to the nonlinear relationship between causal variables and predicted flows. These forecasts are a key component and a principal input for every MPC system.

The third chapter attempts to fill the wastewater flow forecasting research gaps across the world by proposing a novel wastewater flow forecasting model (WWFFM) based on the nonlinear autoregressive with exogenous input neural network (NARX-NN), real-time, and forecasted water consumption.

The fourth chapter exhibits the development of a storm water forecasting model (SWFM) through a comparative study on four data-driven modeling techniques in forecasting urban drainage stormwater discharge on the basis of rainfall prediction. The NARX-NN, M5 model tree (M5T), random forest (RF), and adaptive neuro-fuzzy inference system (ANFIS) are employed for stormwater forecasting.

The last chapter displays the development of an MPC system based on neural networks for predicting flows and a genetic algorithm for optimizing the operating of the sewer system of Casablanca to reduce the impact of CSOs on the receiving environment. The MPC system generates optimal temporally and spatially varied dynamic control strategies of the gate valves of the sewer system.

Chapter 1

Urban Drainage Systems: State of the Art

1.1. Evolution of the sewer system

The relationship between water and cities is ancient and complex. Over the centuries, humankind has always sought to build cities near rivers or water plans so that they can easily exploit and benefit from these resources. Regional planning then has become one of the human being concerns. Urbanization and industrialization have also become more prevalent with the increase of population. Accordingly, and since the origin of habitats, various techniques have been conceptualized to allow humans to control their environment to improve water management and quality. Urban sanitation is one of those techniques that have continued to evolve over the centuries.

From the earliest sedentary civilizations, when the first cities have been built, sewage disposal has become a matter of concern throughout history. Evacuating effluents far from cities has been imperative to avoid epidemics. In Harappa and Mohenjo Daro (−2500 to −1500 BC), wastewater was collected from small brick-lined pits located at the bottom of the walls of houses (Figure 1-1-a) before being routed by a network of pipes dug under the pavement of streets and covered with hard bricks (Figure 1-1-b). These pipes led to a more extensive system of covered sewers, which drained the wastewater out of the inhabited areas of the cities (Webster. 1962; Jansen. 1989; Angelakis. 2014).

(a)

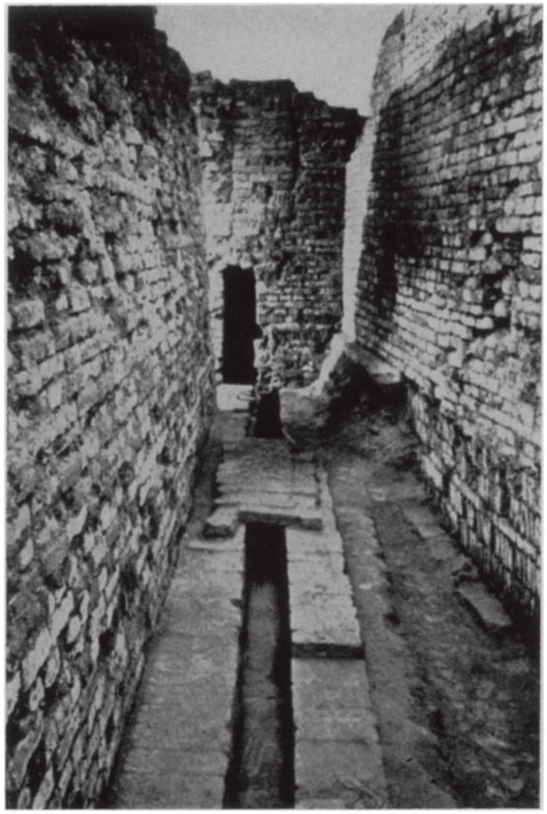

(b)

Figure 1-1| (a) Sewer outlet from a house, (b) typical street sewer with removed cover part (Webster 1962)

In Europe, the first sewerage network was built in Rome to drain and flush away the Forum Valley wastewater. The “Cloaca Maxima” or the “great sewer” (Figure 1-2) was built in the 6th century BC to drain water from swamps before being turned into a real sewer four centuries later (Marsalek 2005; Hopkins 2007). Unfortunately, following the fall of the Roman Empire, this type of public equipment was abandoned. For more than 1,500 years, wastewater in Europe was discharged directly into the street, thereby causing frequent epidemics. This situation persisted until the 19th century when plague, cholera, and typhus epidemics killed hundreds of thousands of people across Europe. Furthermore, the public health findings of that time demonstrated the need and urgency for sanitation. It was not until the 19th century that a modern conception of sanitation

was finally developed. The first modern sewerage networks appeared in Hamburg and London.

Figure 1-2| Cloaca Maxima (Hopkins 2007)

Thereafter, sewer networks evolved, thereby encompassing components such as pipes, manholes, storage basins, weirs, pumping stations, and wastewater treatment plants (WWTPs). We can distinguish two major types of sewer systems. The first type is the combined sewer (CS) system that discharges sewage water together with excess precipitation. The sewage water produced by homes and industries is called DWF. The CS system collects DWFs and stormwater flows, and the storage capacity of a CS system is limited. Outfalls are constructed at specific locations to prevent streets and adjacent areas from being flooded by polluted water when the storage capacity is reached in part of or in the entire sewer system. This overflow is called CSO. Some outfalls can be controlled, but most of them are fixed. In exceptional situations, the discharge capacity of the sewer system to the outfalls may become too low. Sewers flooding streets may be the undesirable result of such undercapacities.

The second type is the separate sewer (SS) system that involves two separate pipes. One drains DWFs, and the other drains excess precipitation water from impervious or semi-impervious surfaces, such as roofs, streets, and parking lots, and discharges it onto water bodies. The adoption of an SS system prevents CSOs because DWFs are conveyed by different conduits (Mannina & Viviani. 2009). However, the quality of stormwater discharges to surface water is generally still poor because the catchment areas from where precipitation is collected can be rather polluted. Additionally, mistakes in connecting houses to rainwater sewers are a continuous source of surface water pollution.

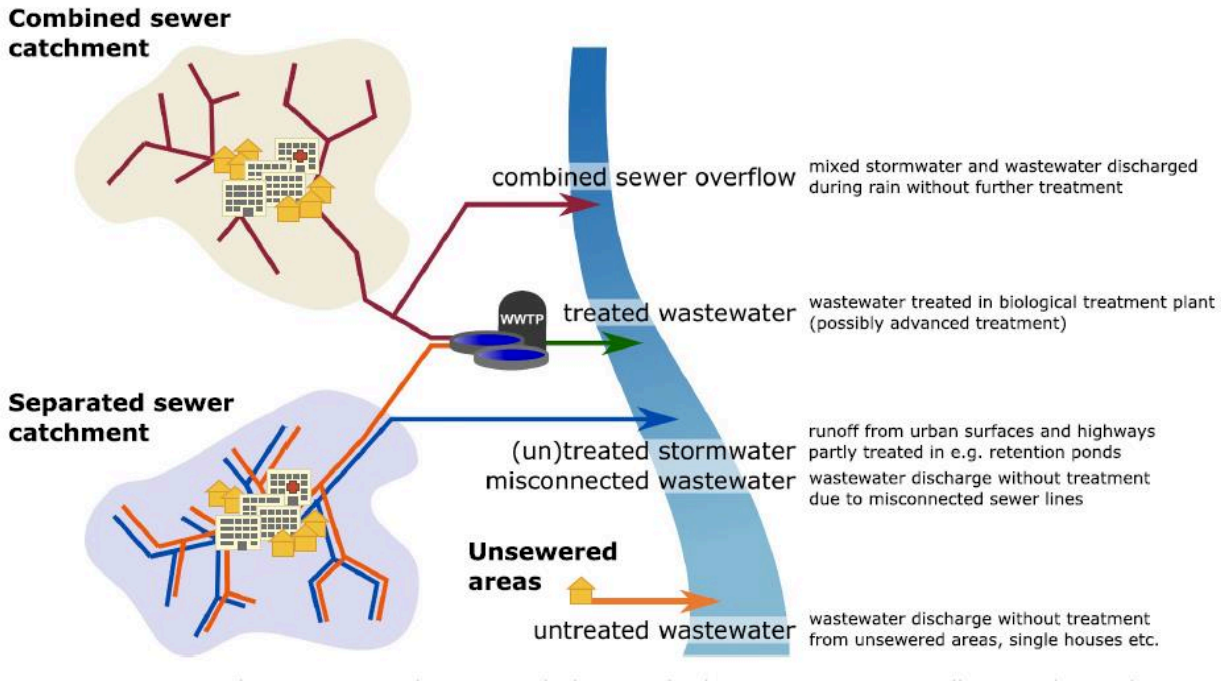

Figure 1-3| Combined vs. separate sewer systems (Bollmann et al. 2019)

1.2. Pollution sources in urban catchments:

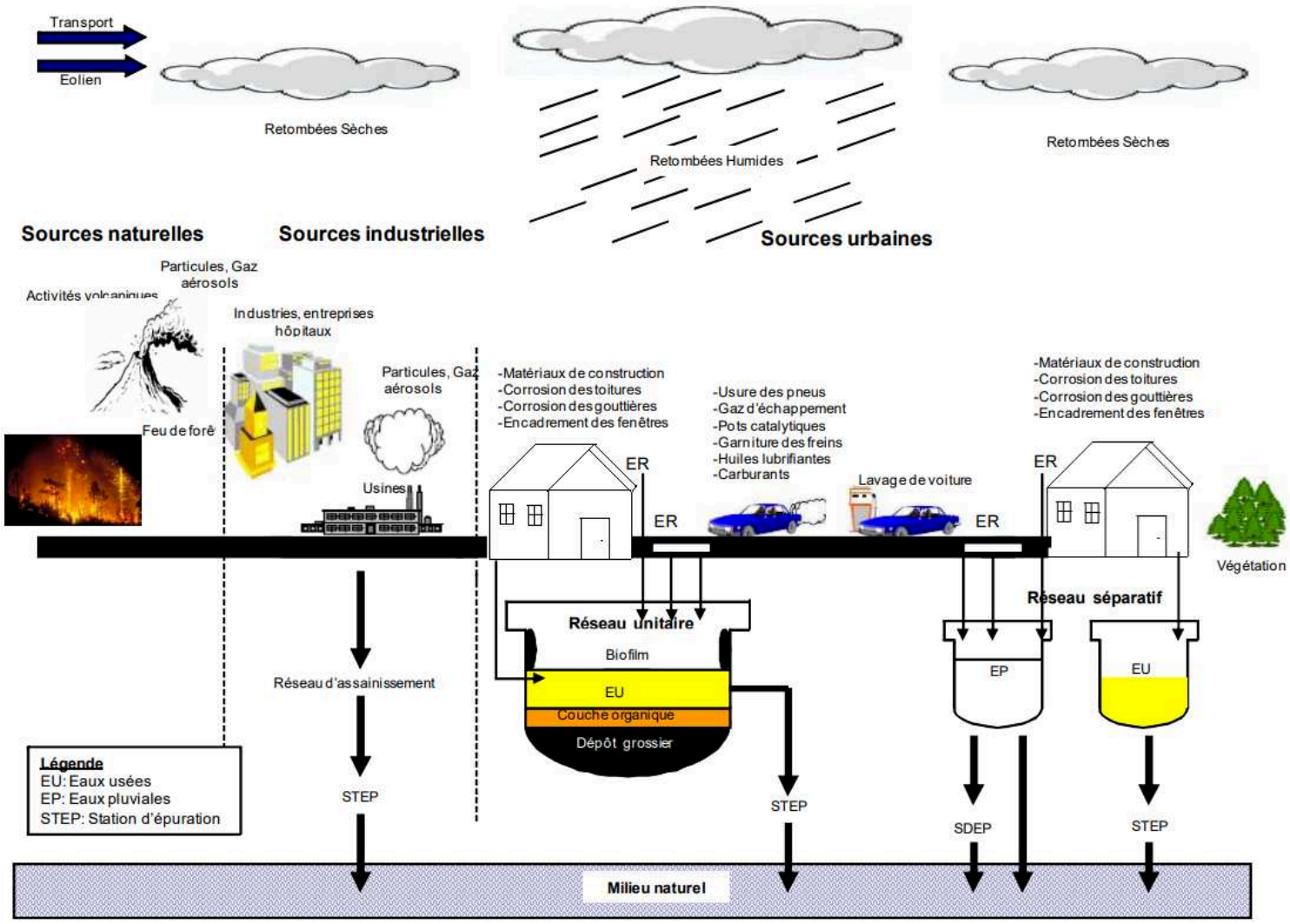

Figure 1-4| Sources of pollution in urban catchments (Zgheib 2011)

Two main mechanisms contribute to stormwater pollution, namely, air pollution and runoff.

Air pollution results from emissions from various sources such as industries, heating, and exhaust from vehicle combustion engines. Emitted pollution includes gases, such as carbon monoxide, sulfur dioxide, nitrogen oxide, hydrocarbons, and various particles. Carbon oxides, sulfur, and nitrogen are partially transformed into sulfuric and nitric acids by oxidation and cause the decrease of the pH of water vapor. This is the phenomenon of "acid rain" that can partially dissolve dust in the atmosphere. In addition, all air pollution

ends up falling to the ground or on vegetation either through precipitation or direct deposition. The pollution of discharges brought by atmospheric pollution during rainy weather constitutes approximately 20% to 25% (except for heavy metals where it could reach 70% to 75%). Thus, reducing air pollution can have an effect on heavy metals contained in rainwater (Valiron et al. 1992).

Stormwater runoff is a major vector for transporting particles and contaminants in urban watersheds (Good et al. 2014). This phenomenon is complex and is related to several elements, such as the energy of water drops, the speed of flows, and the cohesion between deposits. These elements interfere with parameters related to soil, particularly slopes, the importance of deposits, and the nature of soil (Zgheib. 2009). The pollution carried by runoff depends on the type of soil.

- In the presence of vegetation, rainfall washes the vegetation of the formed deposits that fall on the ground and resumes its runoff that carries plant detritus, pesticides, fertilizers, and soil particles.
- Case of impervious floors: they mainly comprise roads, sidewalks, and parking lots. These surfaces contain the following pollutants: soil and sludge, various waste, mineral elements, sand, hydrocarbons (oil and gasoline), lead, rubber (tire wear), nitrogen oxide (gas exhaust), and diverse metals from tires (zinc, cadmium, and copper) and metal parts (titanium, chromium, and aluminum). We can also add to this the products necessary for the servicing of roads during the winter season with the use of sand and de-icing salts (Nacl, CaCl2 and Kcl), which often contain different additives, such us chromates, cyanides, and ethylene glycol) (Chocat 1997).
- Case of roofing: it is generally considered that roof water is not polluted. Nonetheless, the runoff from these waters is loaded with several pollutants (Abbassi et al. 2011). Pollution linked to roofs is estimated at 15% to 30% (the rest being caused by roads, sidewalks, and parking lots) of suspended matter depending on the nature of the roof and gutter materials used (Valiron et al. 1992).

These pollutants comprise, for the most part, metals and heavy metals, particularly zinc, cadmium, and lead. Their concentrations depend on the age of roofs and the proximity to industrial areas (Akintola et al. 2013; Khayan et al. 2019).

Palliative solutions and measures to prevent this pollution

Several types of conventional solutions (systems and maintenance operations) are available to limit and avoid pollution:

- Upstream of the network: cleaning of roadways and retention basins. Retention basins reduce turbidity and suspended solids by decantation. This operation may concern up to 85% of the suspended matter depending on the particle size of solids. Nevertheless, given that retention basins are located in the network upstream, they only concern a small part of pollution.
- Structures of the network: for example, sand traps, oil separators, screens, and storm spillways.
- Treatment stations: their role is to purify water in such a way that the discharges are compatible with the targeted quality.

Other techniques are also employed to reduce the impact of rainwater discharges on the natural environment depending on the type of network (unitary or separate), such as green infrastructures or storage for flow lamination. Performing the advanced real-time control of UDSs is another emerging technique to reduce CSOs.

1.3. RTC systems

The challenge of RTC systems is to solve practical water control problems that arise while attempting to meet the objectives of numerous and sometimes conflicting interests in the water-related environment, such as preventing flooding or minimizing operational

costs. RTC concept is not new and has existed from very early humanity ages. By no later than 4,000 BC, the region of Babylonia became a quintessential hydraulic society where the natives had discovered the essential of control. Moreover, Babylonians utilized the principle of feedback control on the rivers of Euphrates and Tigris to irrigate and transform the desert floodplain into fertile cropland. One of the native challenges during the irrigation process was the use of regulating control to avoid flooding neighbor fields at the risk of a penalty that had been prescribed and codified among the 282 laws of King Hammurabi. Ancient Egypt also was a hydraulic society centered on a desert floodplain where Egyptians operated a largely decentralized irrigation system less complex than the Babylonian one (Ellickson & Thorland. 1995). Nowadays, more emphasis is being given to automatic and advanced control systems.

In UDSs, an RTC system is a combination of components (Figure 1-5) that are interconnected in a configuration designed to provide a specified system behavior aiming to optimize the operation of the collection system by rainy weather to best use the storage structures to limit polluted CSOs to the natural environment, regulate the flow at the inlet of WWTPs, and protect public and private properties and facilities against floods.

An RTC system acts on regulating components (e.g., pumps and valves) also called as actuators, which are used to physically influence the process and force the system to produce the desired setpoint output using information from measurement sensors or control commands.

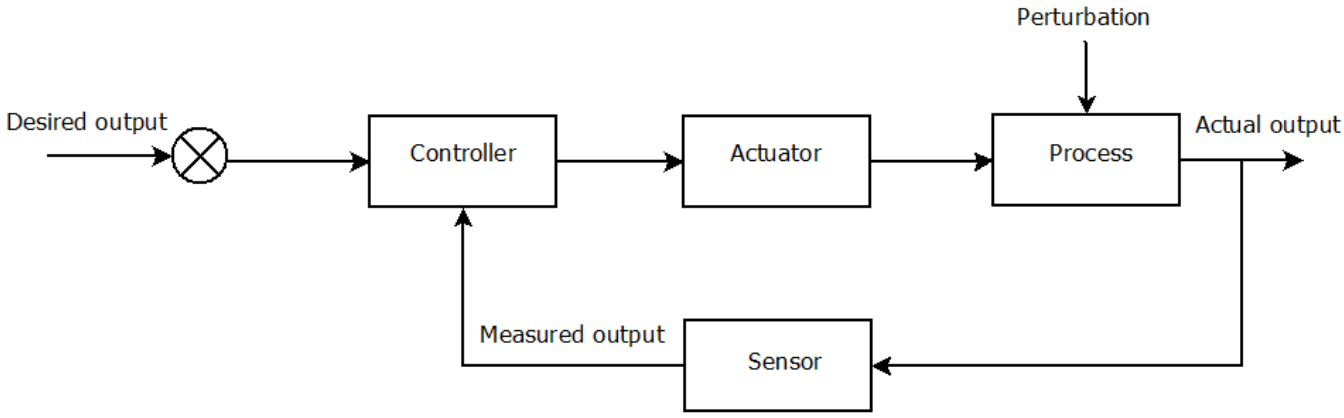

Figure 1-5| Components of a control system

Lobbrecht (2020) classified control systems with respect to where control decisions are made (Figure 1-6). According to this classification, we speak about local and central controls. Local control is when the control of a single regulated structure is executed on the basis of gathered monitoring data that influence the functioning of this structure. Furthermore, local control does not depend on communication with other facilities or other parts of the water system. This form of control is applied in pumping stations that control surface water levels and weirs that control upstream water levels.

In central control, control actions are taken either manually or automatically at a remote location different from the location of various regulating structures that must be controlled. Central control also involves one or more regulating structures and is executed on the basis of data from more than one location in the water system. Several subsystems can be included in central control. Additionally, central control has the advantage over local control because a global water system state can be determined, thereby avoiding unnecessary or contradictory local control actions.

A special case of central control is dynamic control, in which control actions are based on the time-varying requirements of interests in a water system, the water system load, and the dynamic processes in the water system. Dynamic control incorporates a mechanism that allows the continuous weighing of interests that enables available system capacities to be employed optimally under normal and extreme conditions.

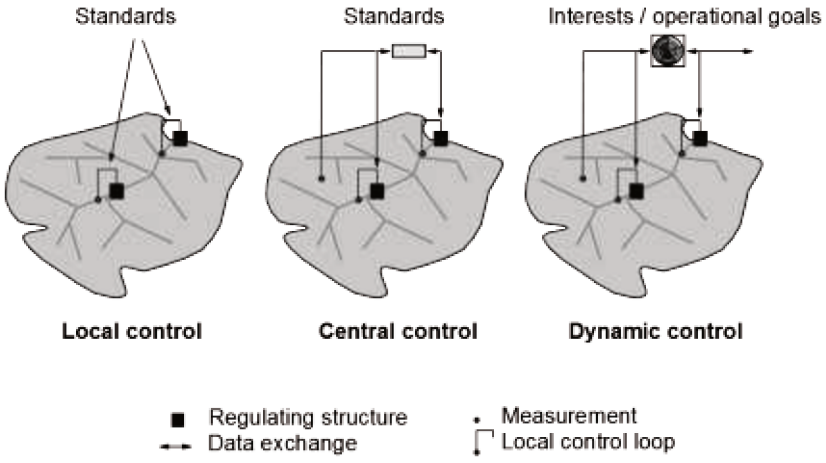

Figure 1-6| Representation of local, central and dynamic control (Lobbrecht. 2020)

The control objective varies according to UDS characteristics and operator preferences (Van der Werf et al. 2021) and can take various forms, such as pollution load reduction (Ly et al. 2019; Rathnayake and Faisal Anwar 2019; Sun et al. 2020), environmental impact minimization (Langeveld et al. 2013; Vezzaro et al. 2014), or energy use optimization (Kroll et al. 2018; Bonamente et al. 2020).

Several implementations of RTC systems have been deployed around the world. A dynamic management system has been deployed in Vejle, Denmark. Vejle is located at the junction of two rivers, thereby making it particularly prone to flooding. The implemented solution based on coupled models for groundwater, rivers, and urban storm drainage, combined with radar data and forecasted water levels, determines the best operational rules for managing flood control structures.

In Quebec, Canada, MPC is utilised to control UDSs. The MPC system has the ability to learn from past events using the gained information to elevate its efficiency to become more reactive to most of the rain scenarios.

Moreover, in Bordeaux, France, the RAMSES system has been deployed to limit flooding and CSOs by rainy weather by determining the best control strategies. The RAMSES system also uses field measurements (flow, rainfall, and valve positions), weather forecasts, tidal forecasts, information about treatment capacity, and pumping status to achieve these strategies. These data are used as input for real-time hydraulic modeling to provide operators with the future hydraulic states of the sewer system for three hours of forecasting horizons (Abbas 2015).

The RAMSES system has exhibited good performance in the management of large thunderstorms in recent years. On July 27, 2013, Bordeaux experienced a thunderstorm with a high peak intensity (over five minutes) equivalent to a rain of 250 mm/h where it rained 70 mm in 40 minutes.

The RAMES system allowed the management of this rain episode using the maximum storage capacity of the 30 retention basins with very limited flooding and a few circumscribed overflows.

1.4. Conclusion

Despite the evolution of sanitation networks and technological progress, cities are still subject to pollution problems linked to discharges from sanitation networks and the risk of flooding. The application of control systems worldwide has exhibited a real interest in these solutions for smart and sustainable cities. However, considering that the reaction time in urban sewer systems is usually short, for UDSs with many decision variables, such as a high number of gate valves or flow-regulating structures, the MPC algorithm running time coupled to hydraulic models may be very long and unsuitable for real-time control purposes.

This work aims to fill the gap in the MPC research field by presenting the development and investigation of the performance of MPC based on robust genetic algorithms (GAs) and neural networks that have the advantage of performing fast calculations that fit the needs of such systems. Further, it aims to demonstrate the benefits of MPC associated with parallel computing that offers a sufficient lead time to define the global optimal control strategies of weir gate valves to reduce CSOs in smart and durable cities.

1.5. References

Abbas O. 2015 Systèmes intelligents pour une gestion durable des réseaux d'assainissement. PhD thesis, University of Lille, Lille, France.

Abbasi T. & Abbasi, S. A. 2011 Sources of Pollution in Rooftop Rainwater Harvesting Systems and Their Control. Critical Reviews in Environmental Science and Technology, 41(23), 2097–2167.

Akintola O. A., Sangodoyin A. Y., & Agunbiade F. O. 2013 Evaluation of environmental pollution effects on domestic roof-harvested rainwater in Southern part of Nigeria using impact indices. Water Practice and Technology, 8(2), 244–255.

Angelakis A. N. 2014 Evolution of Sanitation and Wastewater Technologies through the Centuries. Water Intelligence Online, 13.

Bollmann U. E., Simon M., Vollertsen J., & Bester K. 2019 Assessment of input of organic micropollutants and microplastics into the Baltic Sea by urban waters. Marine Pollution Bulletin, 148, 149–155.

Bonamente E., Termite L. F., Garinei A., Menculini L., Marconi M., Piccioni E., Biondi L. & Rossi G. 2020 Run-time optimisation of sewer remote control systems using genetic algorithms and multi-criteria decision analysis: CSO and energy consumption reduction. Civil Engineering and Environmental Systems, 37(1–2), 62–79.

Chocat B. 1997 Encyclopédie de l'hydrologie urbaine et de l'assainissement, Tec & doc-Lavoisier. 529–543.

Ellickson R. C. & Thorland C. D. 1995 Ancient Land Law: Mesopotamia, Egypt, Israel. 71, 94.

Good J., O'Sullivan A., Wicke D., & Cochrane T. 2014 Ph buffering in stormwater infiltration systems—sustainable contaminant removal with waste mussel shells. Water Air Soil Pollut. 225 (3), 1885.

Hopkins J. N. N. (2007) The cloaca maxima and the monumental manipulation of water in archaic Rome. (4), 15.

Jansen M. 1989 Water supply and sewage disposal at Mohenjo-Daro. World Archaeology, 21(2), 177–192.

Khayan K., Husodo A. H., Astuti I., Sudarmadji S., & Djohan T. S. 2019 Rainwater as a Source of Drinking Water: Health Impacts and Rainwater Treatment. Journal of Environmental and Public Health, 11.

Kroll S., Weemaes M., Van Impe J., & Willems P. 2018 A Methodology for the Design of RTC Strategies for Combined Sewer Networks. Water, 10(11), 1675.

Langeveld J. G., Benedetti L., de Klein J. J. M., Nopens I., Amerlinck Y., van Nieuwenhuijzen A., Flameling T., van Zanten O., & Weijers, S. 2013 Impact-based integrated real-time control for improvement of the Dommel River water quality. Urban Water Journal, 10(5), 312–329.

Lobbrecht A. H. 2020 Dynamic Water-System Control: Design and Operation of Regional Water-Resources Systems, CRC Press.

Ly D. K., Maruéjouls T., Binet G., & Bertrand-Krajewski, J.-L. 2019 Application of stormwater mass–volume curve prediction for water quality-based real-time control in sewer systems. Urban Water Journal, 16(1), 11–20.

Mannina G., & Viviani G. 2009 Separate and combined sewer systems: a long-term modelling approach. Water Science and Technology, 60(3), 555–565.

Marsalek J. 2005 Evolution of urban drainage: from Cloaca Maxima to environmental sustainability. 22.

Rathnayake U. & Faisal Anwar A. H. M. 2019 Dynamic control of urban sewer systems to reduce combined sewer overflows and their adverse impacts. Journal of Hydrology, 579, 124150.

Sun C., Romero L., Joseph-Duran B., Meseguer J., Muñoz E., Guasch R., Martinez M., Puig V., & Cembrano, G. 2020 Integrated pollution-based real-time control of sanitation systems. Journal of Environmental Management, 269, 110798.

Valiron F. & Tabuchi J. P. 1992 Maîtrise de la pollution urbaine par temps de pluie: état de l'art, Tec & Doc - Lavoisier.

Van der Werf J. A., Kapelan Z., & Langeveld J. 2021 Quantifying the true potential of Real Time Control in urban drainage systems. Urban Water Journal, 1–12.

Webster C. 1962 The Sewers of Mohenjo-Daro. Journal (Water Pollution Control Federation), 34(2), 116–123.

Zgheib S. 2009 Flux et sources des polluants prioritaires dans les eaux urbaines en lien avec l'usage du territoire.

Van der Werf J. A., Kapelan Z., & Langeveld J. 2021 Quantifying the true potential of Real Time Control in urban drainage systems. Urban Water Journal, 1–12.

Vezzaro L., Christensen M. L., Thirsing C., Grum M., & Mikkelsen, P. S. 2014 Water Quality-based Real Time Control of Integrated Urban Drainage Systems: A Preliminary Study from Copenhagen, Denmark. Procedia Engineering, 70, 1707–1716.

Chapter 2

General presentation and site description: Region of Grand Casablanca

This chapter includes a general presentation of the Grand Casablanca region, which served as an experimental site for this research work.

The Grand Casablanca region is located on the Atlantic coast in the center-west of Morocco. The Atlantic Ocean bounds it to the west, the region of Chaouia-Ourdigha to the north, the province of Settat to the east and south, and the province of Ben Slimane to the north. Furthermore, the Grand Casablanca region has 35 municipalities covering 1,226 km².

Figure 2-1| Region of Grand Casablanca

The Greater Casablanca region, which is the first economic pole and the most populated region of Morocco, has undergone significant spatial transformations with the emergence of secondary urban centers. In 1980, urbanized areas covered approximately 100 km^2, while urbanized areas of today cover 240 km^2, which represents an average urbanization

rate of around 350 ha per year. The areas open to urbanization and that remain to be urbanized are estimated at 26,000 ha (Figure 2-2).

The Grand Casablanca population is estimated to comprise 4.3 million inhabitants and to exceed 5.1 million inhabitants in 2030.

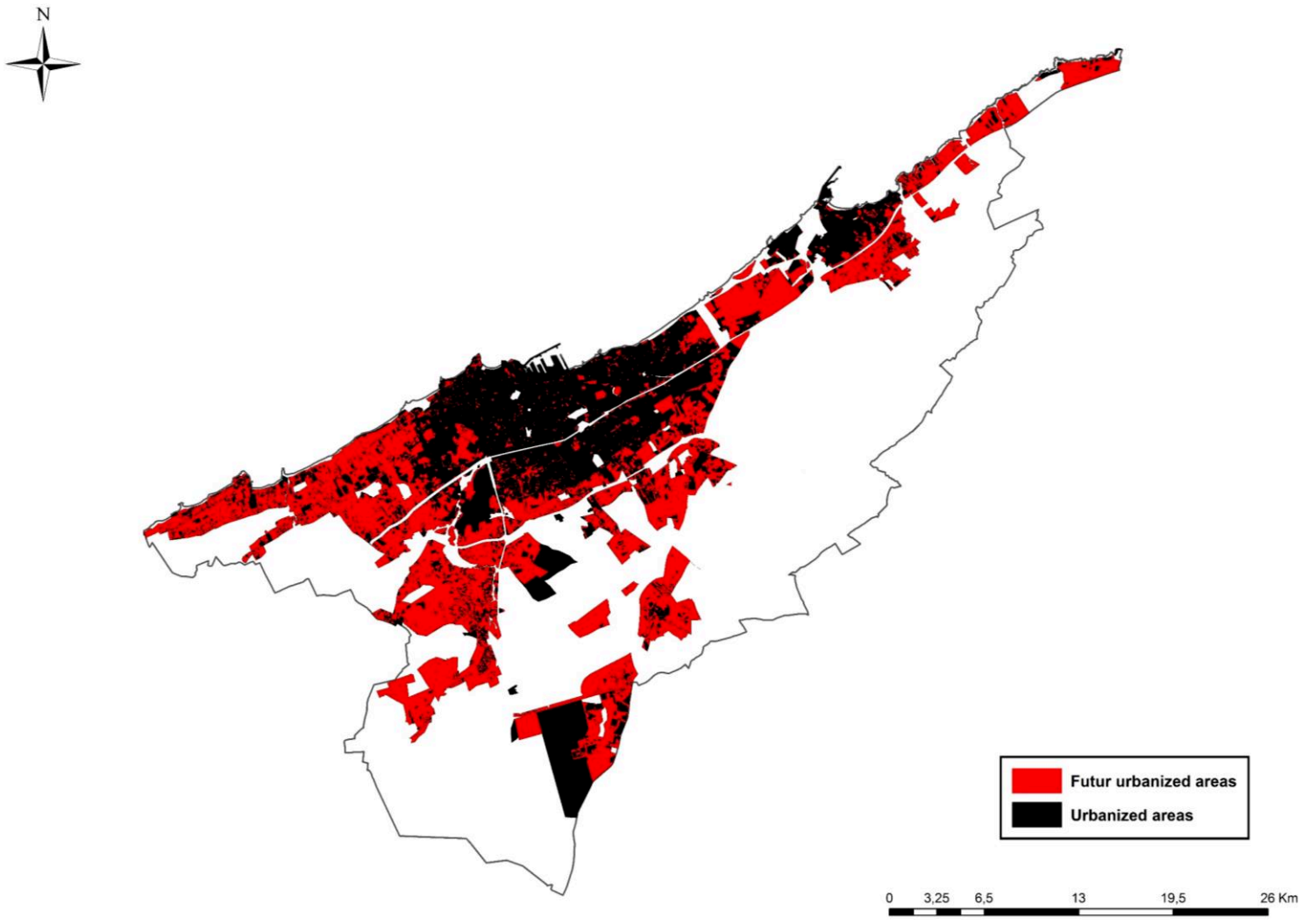

Figure 2-2| Urbanization of the Grand Casablanca region

2.1. Drinking water supply of the region of Grand Casablanca

The urban development and the evolution of the population create pressure on resources. The urban development of the Grand Casablanca region has been accompanied over time by constructing different trunk mains serving distinct altitudes.

- From 1912 to 1920, the drinking water boreholes of Tit Mellil were sufficient to supply Casablanca and its several thousand inhabitants with daily demands varying between 2,800 and 3,700 m^3.
- In 1920, additional sources were captured in the valleys of Oued El Maleh and Oued Hassar. The cumulative daily volume of approximately 12,000 m^3 was sufficient to supply Casablanca until around 1930. Water supply restrictions were frequent.
- After 1930, the works for the supply of water from Fouarat (from the Maamora forest to the east of Rabat) were launched simultaneously as the supply of water from the dam created in Oued El Maleh. The cumulative flow of the resource available for Casablanca reached nearly 40,000 m^3/d and was sufficient until 1945.
- In 1952, the water supply from the Oum Er R'bia to Casablanca with an initial capacity of 100,000 m^3/d made it possible to remedy the water shortages and cuts.
- The trunk main from Bou Regreg was initiated in 1969 and reinforced in 1975, 1983, and 2017.
- The trunk main from Daourat was put into service in 1983 and reinforced in 1991 and 1998.

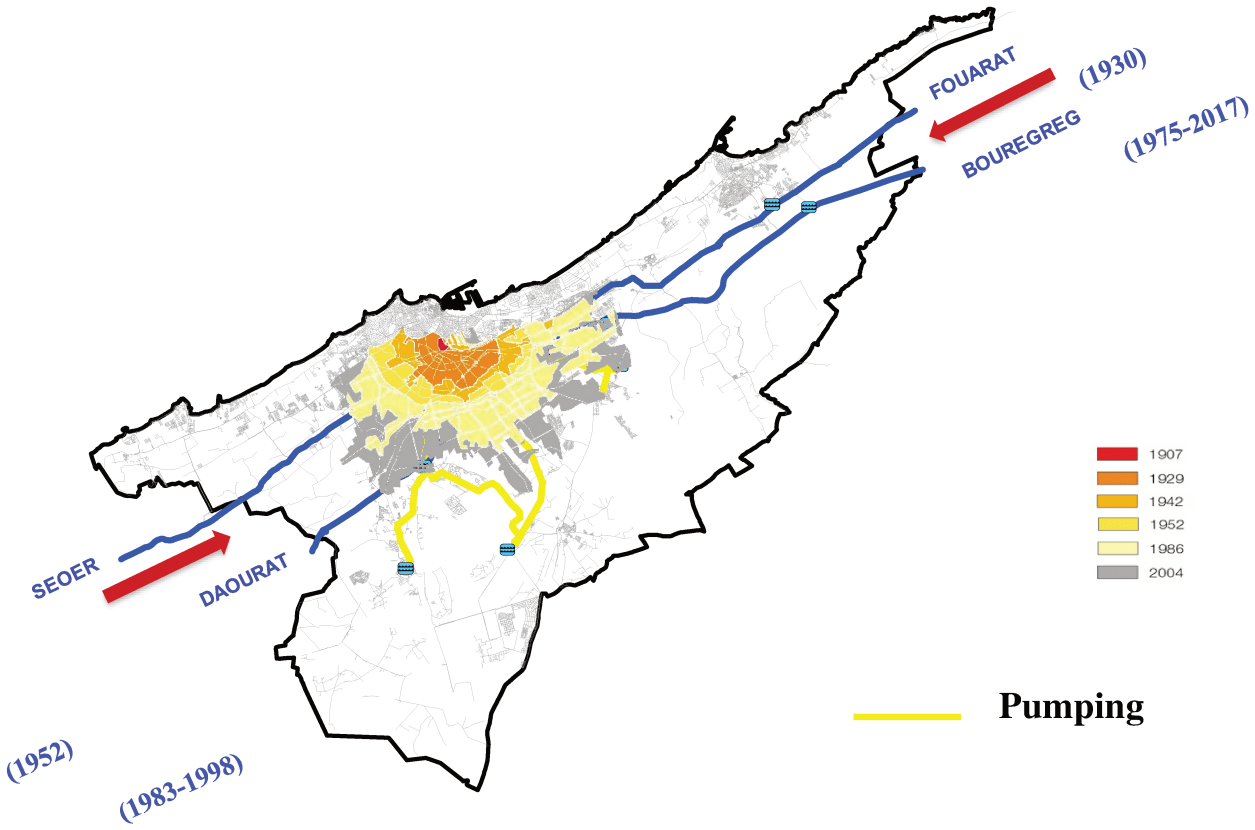

Figure 2-3| Trunk mains of the Grand Casablanca region

From the trunk main arrival points, water is distributed through reservoirs and pumping stations, allowing transfer between delivery points located at lower altitudes (85 m NGM) and areas at higher altitudes (240 m NGM).

The water distribution system of Grand Casablanca comprises the following:

- 6,570 km of pipe networks, made up mainly of plastic pipes (Figure 2-4) and diameters ranging between 26 and 1,000 mm (Table 2-1);
- 33 reservoirs with a storage capacity 667,130 m^3, ensuring 29-h water supply autonomy; and
- 19 pumping stations and 20 boosters.

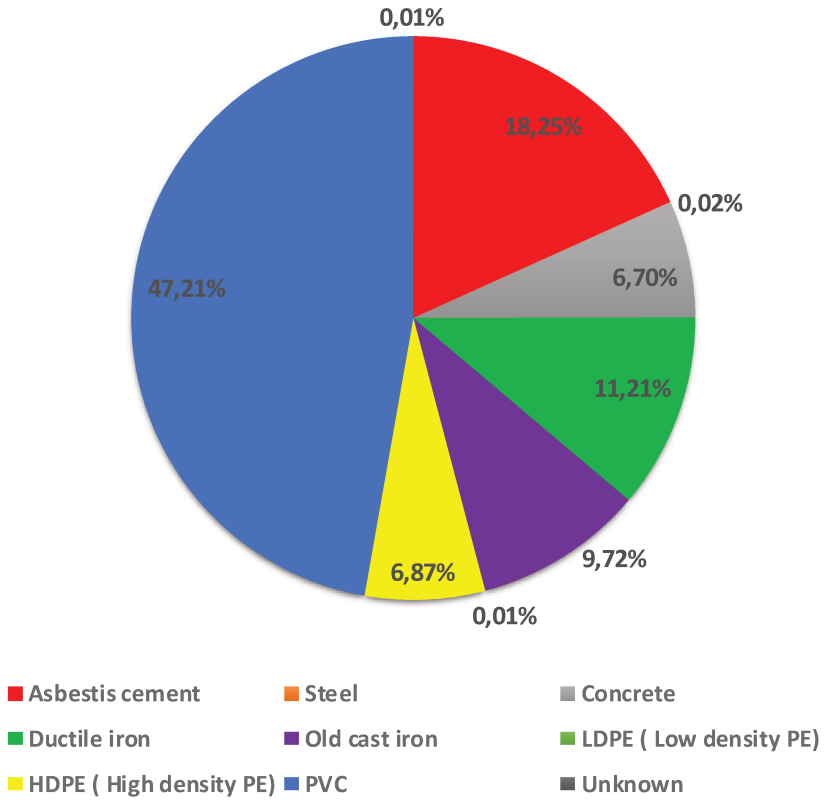

Figure 2-4| Percentage of pipes by material

Water distribution pipes	Length (km)
Primary distribution pipes ϕ ≥ 315 mm	
315 - 450	342
450 - 500	3
500 -1400	286
Secondary distribution pipes ϕ < 315 mm	
< 160	4529
160 - 315	1410
Total (km)	**6570**

Table 2-1| Distribution of pipes by diameter

Monitoring of the drinking water system

The drinking water network is equipped with the following:

- more than 413 sectorization meters to monitor the flows distributed in the hydraulic zones and the minimum nightly flows,
- 123 pressure measurement points for monitoring pressures across the entire drinking water network,
- acoustic sensors for leak detection, and
- sensors for monitoring water quality.

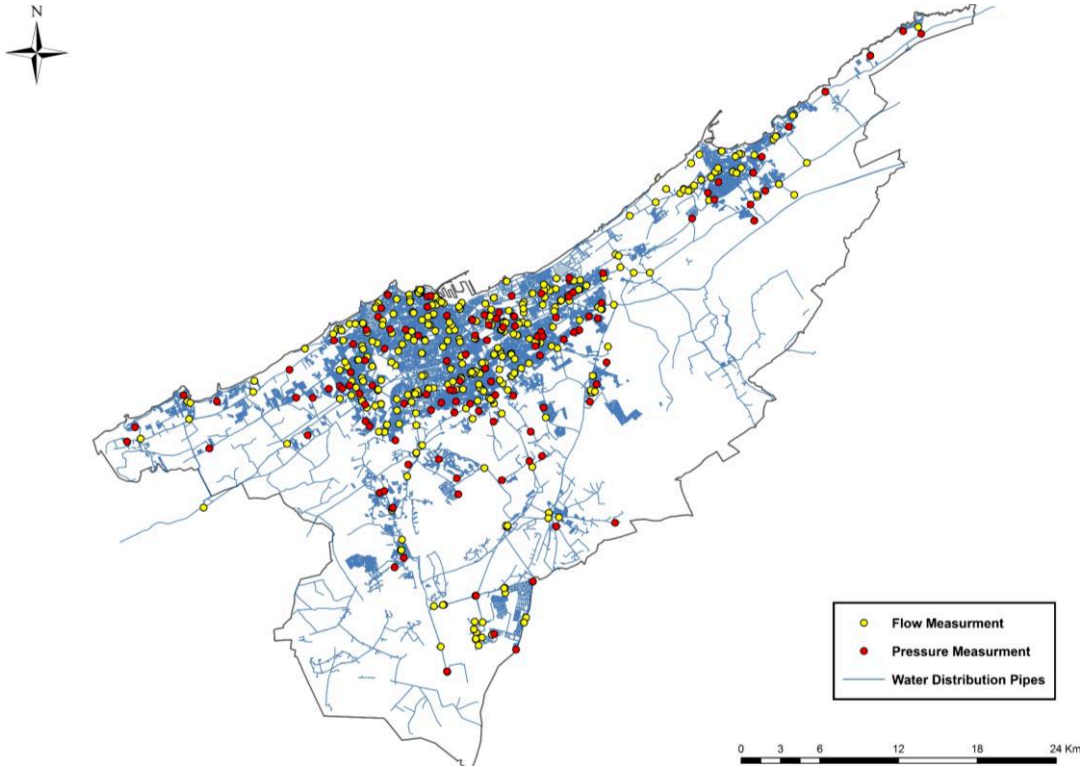

Figure 2-5| Pressure and flow measurement points in the Grand Casablanca region

2.2. Sewer system of the Grand Casablanca region

Historically, the Grand Casablanca sewer network was a combined system. Since the 1990s, the new extensions of the drainage network had been done in separative mode to limit stormwater flows, such as not saturating the downstream combined network.

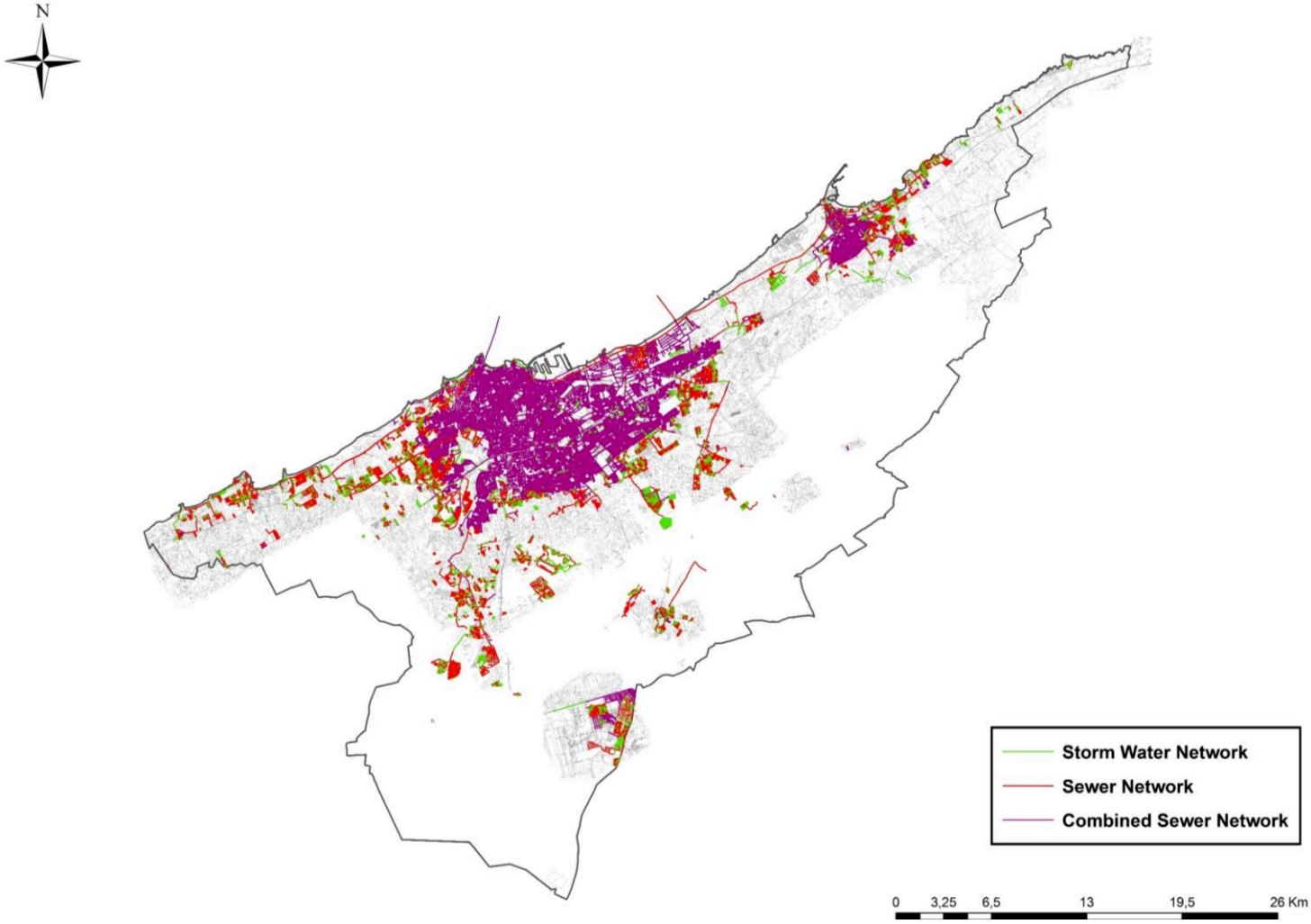

Figure 2-6| Sewer system of the Grand Casablanca region

The sewer system of Grand Casablanca consists of 6,155 km of pipe networks (1,552 km of a wastewater network, 1,605 km of a stormwater network, and 2,997 km of a combined network), 122 pumping stations, and 107 storage basins.

The wastewater treatment of Grand Casablanca is based on two systems:

- The first system is for areas far from the two large interception systems of Casablanca. The wastewater collected within this system benefits from advanced treatment before being released into water bodies.

- The second system is based on interceptors that convey wastewater to treatment plants, where it is pre-treated and released to the ocean via an emissary.

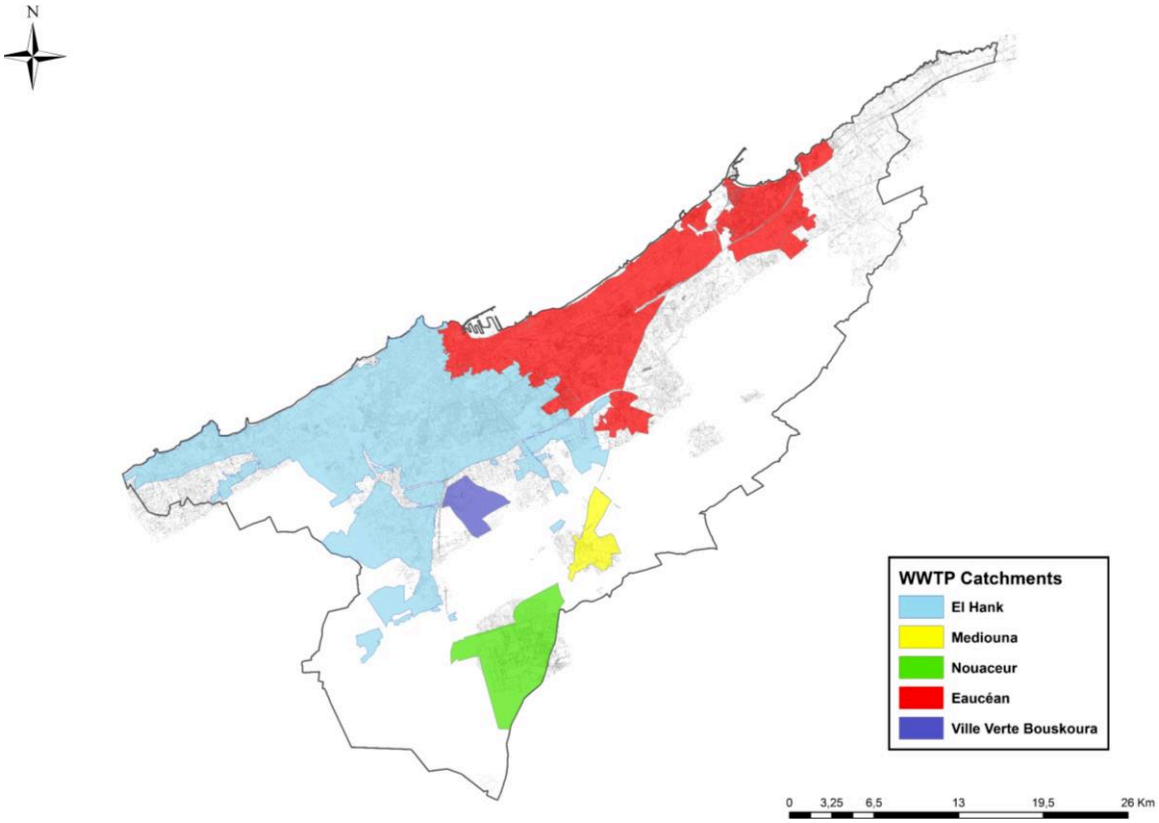

Figure 2-7| Major wastewater catchments in the Grand Casablanca region

2.2.1. Wastewater plants with advanced treatment:

- **Nouaceur "ONDA" wastewater treatment plant:**

  With a capacity of 50,400 equivalent inhabitants, the Nouaceur "ONDA" WWTP treats approximately 5,040 m^3/d of raw water. Equipped with "activated sludge" technology, the "ONDA" WWTP is composed of two treatment lines: one domestic for the treatment of domestic wastewater and another industrial for the treatment of industrial wastewater.

- **Mediouna wastewater treatment plant:**

With a capacity of 40,000 population equivalents, the Mediouna WWTP is equipped with membrane bioreactor (MBR) technology and treats approximately 3,800 m^3/d of raw water.

- **Ville Verte Bouskoura wastewater treatment plant:**

The Bouskoura WWTP is sized for a nominal capacity of 8,000 m³/d (equivalent to 50,000 inhabitants) and equipped with activated sludge technology.

2.2.2. Wastewater interception and pre-treatment systems:

- **West interception system:**

The wastewater collected from the western watersheds of Casablanca is pre-treated at EL Hank WWTP. The pre-treated volume is 200,000 m^3 per day by dry weather conditions and 500,000 m^3 per day on rainy days. Once pre-treated, the water is released to the sea via an emissary of 2.1 m diameter and 3,600 m long.

- **The East interception system:**

This antipollution system receives 45% of the wastewater of the Grand Casablanca region. It also allows the depollution of the 24-km coastline between Casablanca and Mohammedia thanks to two coastal interceptors. These underground collectors convey the flows to the Eaucéan WWTP to be pre-treated and then evacuated 2,200 m away from the coast via a marine emissary of 2.1 m diameter.

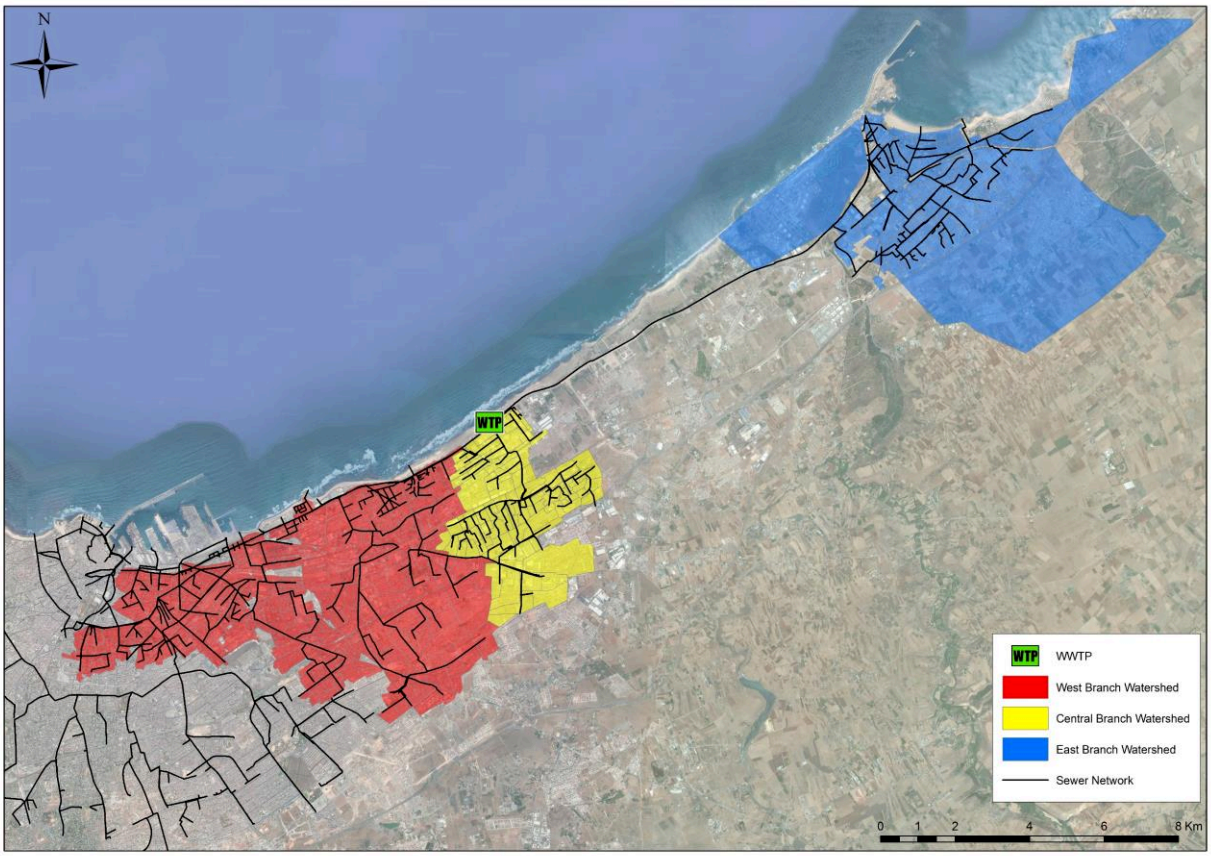

Figure 2-8| Branches and watersheds of the East antipollution system

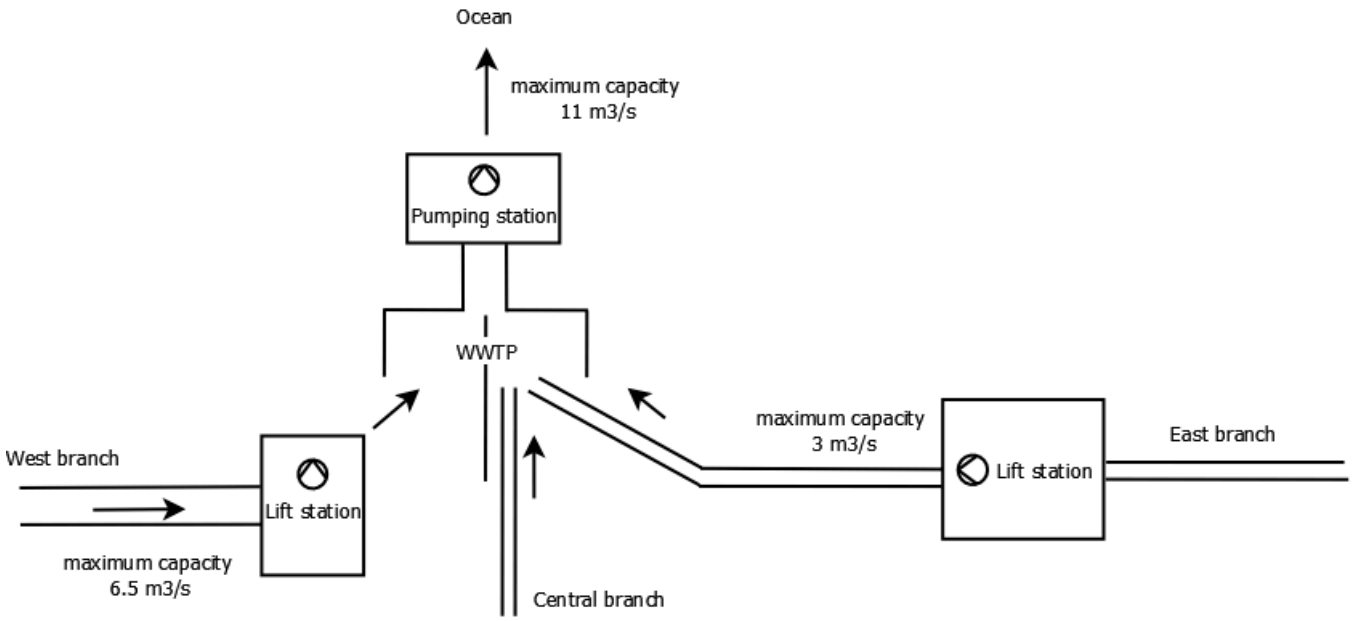

Figure 2-9| Branches of the East antipollution system

The East antipollution system comprises the following three main branches:

- an eastern branch between Mohammedia and Ben Yekhlef toward Sidi Bernoussi (15-km pipes) and a lifting station with a maximum capacity of 3 m^3/s;
- a central branch draining the sewer flows of a watershed of 3,315 ha, which covers Tit Mellil, Sidi Moumen, and Sidi Bernoussi; and
- a western branch that intercepts the sewer flows of parallel watersheds with an area of 41.6 km^2 via interception structures (Figure 2-10) consisting of the following:
    - weir structure (frontal or side) that allows the overflow of the exceeding discharge and
    - a controllable gate valve that controls the flow diverted to the WWTP
- A marine emissary downstream of the Eaucean pre-treatment plant has a discharge capacity of 11 m^3/s.

However, by rainy weather and in the absence of control strategies, gate valves are closed, and the polluted water is discharged directly into the sea, thus reducing the benefits of such a structure.

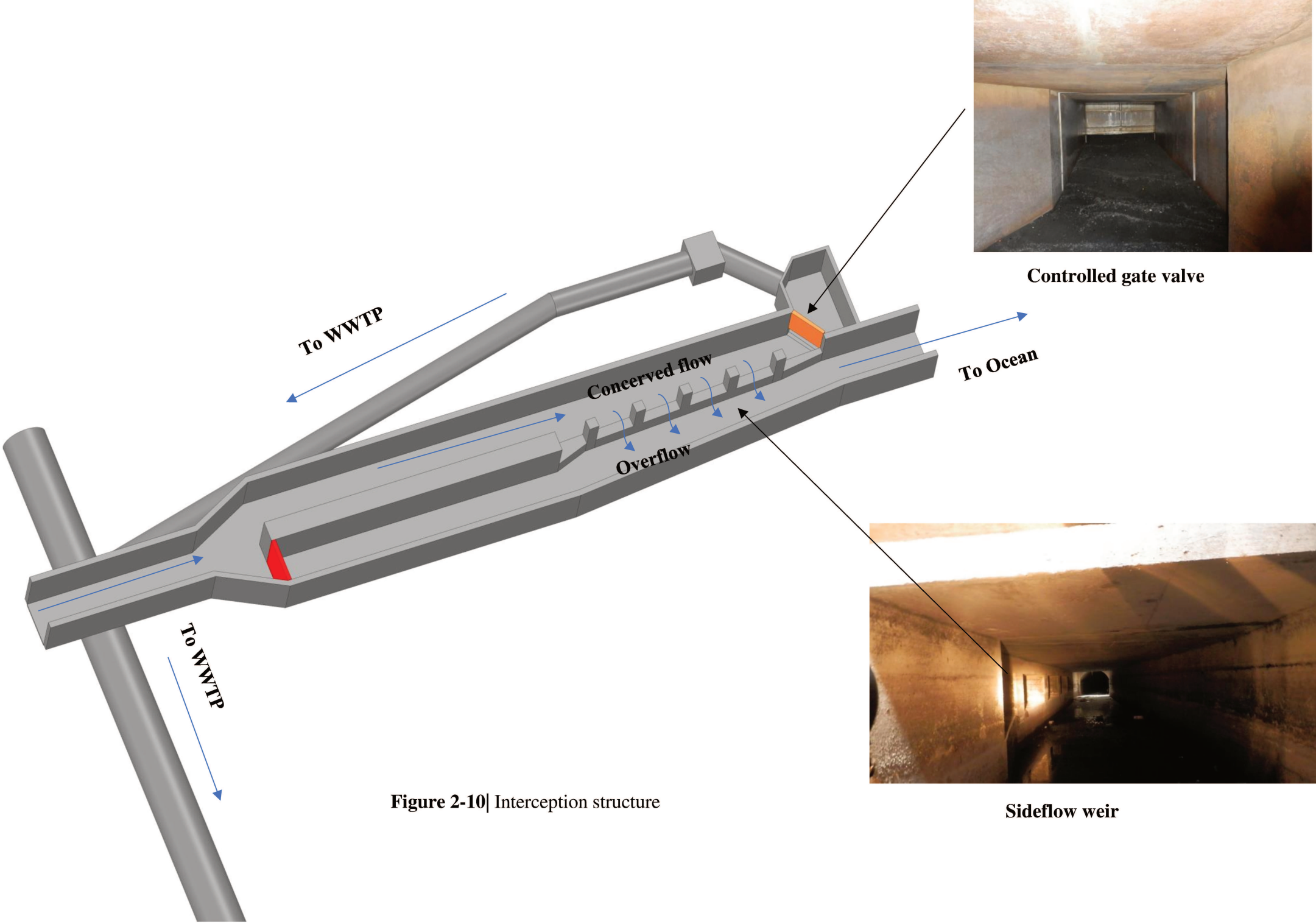

Figure 2-10| Interception structure

Chapter 3

Nonlinear Auto Regressive with eXogenous neural network (NARX) for forecasting wastewater flows in urban drainage systems

Wastewater flow forecasts are key components in the short- and long-term management of sewer systems. Forecasting flows in sewer networks constitutes a considerable uncertainty for operators due to the nonlinear relationship between causal variables and wastewater flows. This work aimed to fill the gaps in the wastewater flow forecasting research by proposing a novel wastewater flow forecasting model (WWFFM) based on the nonlinear autoregressive with exogenous inputs neural network (NARX-NN), real-time, and forecasted water consumption with an application to the sewer system of Casablanca in Morocco. Furthermore, this research compared the two approaches of the forecasting model. The first approach consists of forecasting wastewater flows on the basis of real-time water consumption and infiltration flows, and the second approach considers the same input in addition to water distribution flow forecasts. The results indicate that both approaches show accurate and similar performances in predicting wastewater flows, while the forecasting horizon does not exceed the watershed lag time. For prediction horizons that exceed the lag time value, the WWFFM with water distribution forecasts provided more reliable forecasts for long time horizons. The proposed WWFFM could benefit operators by providing valuable input data for predictive models enhance sewer system efficiency.

3.1. Introduction

Wastewater flow forecasts are key components in the short- and long-term management of sewer systems. In wastewater treatment plants (WWTPs), a wastewater flow forecasting model (WWFFM) could benefit operators by providing valuable input data for predictive models to simulate plant behavior and optimize performances and costs through the control of biological processes (Fernandez et al. 2009). For pumping stations, selecting the best pump scheduling configuration and running the pumps with an appropriate adjustment of rotation speed could help save energy (Wei et al. 2013). These forecasts could also enhance the performance and cost-effectiveness of real-time chemical dosing controllers, thereby preventing hydrogen sulfide formation (Chen et al. 2014).

Several models based on data-driven modeling for forecasting wastewater flows have been developed to address these challenges during the last decade. Wei et al. (2013) developed a multilayer perceptron (MLP) neural network model for the short-term prediction of influent flow rates in WWTPs. This model takes influent flow rate, rainfall rate, and radar reflectivity as inputs and returns an accurate flow forecast with a prediction horizon of up to 180 min. Boyd et al. (2019) proposed a model based on an autoregressive integrated moving average (ARIMA) for daily influent flow forecasts tested at five WWTPs across North America and was completed with a multilayer perceptron neural network (MLPNN) proposed by Zhang et al (2019). These models rely only on historical data with no external inputs. Although these models are efficient, they remain limited in their approach. In fact, for forecasting wastewater flows, these models only consider sewer flow historical data. Moreover, they do not integrate drinking water consumption, which is the main causal variable that may influence forecasted flows in the case of a water shutdown in a sector or water consumption variation due to a given event.

The current work aimed to fill the gaps in the wastewater flow forecasting research by proposing a novel WWFFM based on the nonlinear autoregressive with exogenous inputs neural network (NARX-NN), real-time, and forecasted water consumption with an application to the sewer system of Casablanca in Morocco.

3.2. Materials and Methods

The WWFFM aims at predicting instantaneous dry weather flows at specific points of watersheds. Dry weather flow usually corresponds to flows with no rainfall influence or at a maximum rainfall intensity of 0.3 mm and without inflows (Staufer et al. 2012). Given that the wastewater flow production function is nonlinear and depends on the spatial and temporal variations of water consumption through watersheds, using a model that can handle nonlinear problems for forecasting purposes is important. The proposed WWFFM is based on the NARX that has shown its efficiency through various nonlinear times series forecasting applications (Abou Rjeily et al. 2017; Koschwitz et al. 2018; Wunsch et al. 2018; Marcjasz et al. 2019; Di Nunno et al. 2021). The WWFFM considers

real-time water consumption and previous infiltration flow records as inputs and predicted wastewater flows with forecast horizons that vary from 30 to 240 min as outputs. These periods offer a sufficient lead time to real-time and predictive control models to process and apply optimal control strategies.

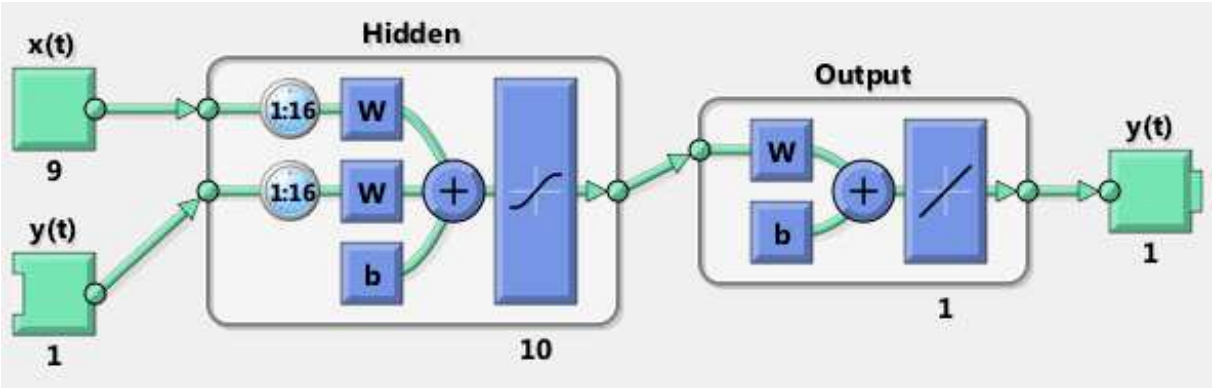

Figure 3-1| Neural network architecture

The proposed architecture of the network includes two layers, namely, a hidden layer and an output layer (Figure 3-1). The inputs were weighted with appropriate weights (w), and the sum of the weighted inputs and biases forms the input to the transfer function. A nonlinear transfer function, the tan-sigmoid function bounded between -1 and 1 and described by Equation (3-1), was used in the hidden layer. An unbounded linear transfer function depicted by Equation (3-2) was employed in the output layer due its ability to extrapolate to a certain extent beyond the training data range (Solomatine & Khada 2003).

$$tansig(x) = \frac{1}{1+ e^{-2x}} - 1 \quad \textbf{(3-1)}$$

$$purelin\ (x) = x \quad \textbf{(3-2)}$$

The NARX-NN is considered a black box containing the information to be learned. In the beginning, the neural network architecture is composed of layers and nodes without any information or knowledge of the simulated phenomenon. During the learning stage, the weights and biases were adjusted according to an optimization algorithm to minimize the error of the neural network output and measured data. In addition, the Levenberg–Marquardt back-propagation (LMBP) function was utilized to train the artificial neural

network as it demonstrated its ability to speed up the convergence rate of neural networks with MLP architectures (Hagan & Menhaj. 1994). The Levenberg–Marquardt algorithm described by Equation (3-3) combines the gradient descent method that updates the parameters in the steepest descent direction to reduce the sum of the squared quadratic errors. Additionally, the Gauss–Newton method reduces the sum of squared errors assuming that the least squares function is quadratic in the parameters and finding the minimum of this quadratic:

$$\Delta\omega = \left[J^T(\omega)J(\omega) + \lambda I\right]^{-1} J^T(\omega)e(\omega), \quad \textbf{(3-3)}$$

where ω is the weight vector, J is the Jacobian matrix, J^T is the transpose matrix of J, λ is a learning parameter, I is the identity matrix, and e is the vector of the network error.

The early stopping method for improving generalization was used, and the divide block method was employed to split the dataset into three subsets. The first subset representing 70% of the data is the training set, which was utilized to compute the gradient and update the network weights and biases to find the model parameters. The second subset is the validation set (15%). The error in the validation set was monitored during the training process to avoid the increase of errors in the validation set and overfitting. When a validation error increases for a specified number of iterations (six iterations in our case), the training is stopped, and the weights and biases at the minimum of the validation error are returned. Further, the total number of allowed epochs was set to 1,000. The remaining 15% of the dataset was employed as a test set to assess the generalization error in the final model.

The NARX trained in its open-loop form (Figure 3-2-a) also called series-parallel architecture, given by Equation (3-4), efficiently predicts a time series value for a one-time step ahead. In the open-loop form, the predicted value $\hat{y}(t)$ of the target time series $y(t)$ is predicted from the past values of $u(t)$ and the past measured values of $y(t)$ with the appropriate tapped delay line (TDL).

$$\hat{\boldsymbol{y}}(\boldsymbol{t}+\mathbf{1}) = \boldsymbol{f}\left(\boldsymbol{y}(\boldsymbol{t}), \boldsymbol{y}(\boldsymbol{t}-\mathbf{1}), \ldots, \boldsymbol{y}(\boldsymbol{t}-\boldsymbol{n_y}), \boldsymbol{u}(\boldsymbol{t}+\mathbf{1}), \boldsymbol{u}(\boldsymbol{t}), \boldsymbol{u}(\boldsymbol{t}-\mathbf{1}), \ldots, \boldsymbol{u}(\boldsymbol{t}-\boldsymbol{n_u})\right) \quad (3\text{-}4)$$

Once the training process is over, the NARX is turned to its closed-loop form (Figure 3-2-b), which is called the parallel architecture given by Equation (3-5) to perform multistep-ahead time series forecasting. The closed-loop form takes the past and present values of $x(t)$ and the $y(t)$ previous predicted values as inputs.

$$\hat{\boldsymbol{y}}(\boldsymbol{t}+\mathbf{1}) = \boldsymbol{f}\left(\hat{\boldsymbol{y}}(\boldsymbol{t}), \hat{\boldsymbol{y}}(\boldsymbol{t}-\mathbf{1}), \ldots, \hat{\boldsymbol{y}}(\boldsymbol{t}-\boldsymbol{n_y}), \boldsymbol{u}(\boldsymbol{t}+\mathbf{1}), \boldsymbol{u}(\boldsymbol{t}), \boldsymbol{u}(\boldsymbol{t}-\mathbf{1}), \ldots, \boldsymbol{u}(\boldsymbol{t}-\boldsymbol{n_u})\right) \quad (3\text{-}5)$$

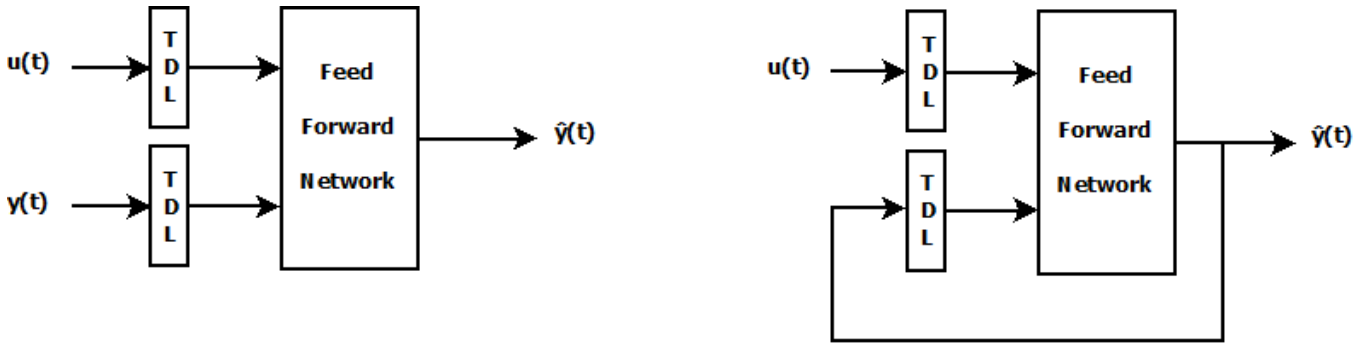

Figure 3-2| (a) Series-parallel architecture, (b) parallel architecture

Two statistical metrics were used in this study to assess the efficiency of the model. The Nash–Sutcliffe efficiency (NSE) given by Equation (3-6), where a value is closed to 1, represents a perfect fit between the observed and forecasted data. And root mean square errors (RMSEs) given by Equation (3-7), where low RMSEs are preferred for model validation:

$$\boldsymbol{NSE} = \mathbf{1} - \frac{\sum_{i=1}^{n}(\boldsymbol{Q_o^i} - \boldsymbol{Q_f^i})^2}{\sum_{i=1}^{n}(\boldsymbol{Q_o^t} - \overline{\boldsymbol{Q_o^t}})^2}, \quad \textbf{(3-6)}$$

$$\boldsymbol{RMSE} = \sqrt{\frac{\sum_{i=1}^{n}(\boldsymbol{Q_o^i} - \boldsymbol{Q_f^i})^2}{\boldsymbol{n}}}, \quad \textbf{(3-7)}$$

where Q_o^i is the observed flow at time step i, Q_f^i is the forecasted flow at time step I, $\overline{Q_o^t}$ is the mean observed value, and n is the number of observations.

In the present work, two approaches of the forecasting model were compared (Figure 3-3):

- The first approach consists of forecasting wastewater flows on the basis of real-time water distribution flows for eight district metering areas (DMAs) and infiltration flows.
- The second approach comprises forecasting wastewater flows according to infiltration flow, water demand flow, and short-term water demand forecasts for the eight DMAs. The water consumption forecasting model is based on a feed-forward back-propagation neural network. The input dataset is composed of historical temperature, water consumption, and days of specification data.

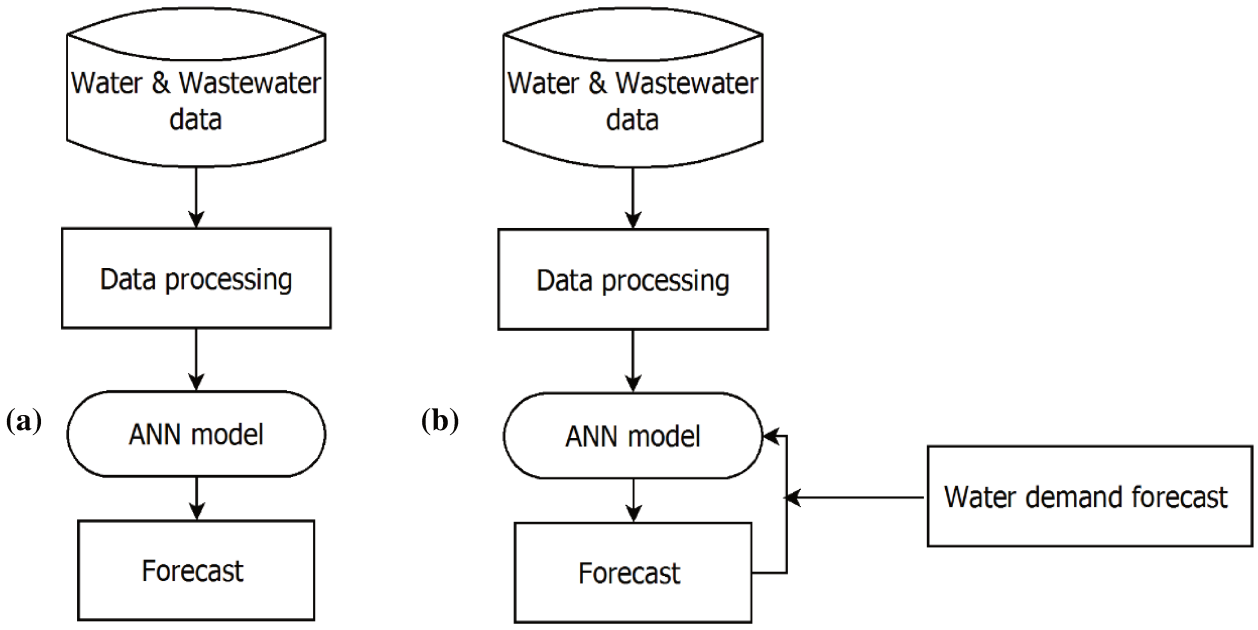

Figure 3-3| Process overview of the operation of the WWFFM: (a) without water demand forecasts and (b) with water demand forecasts

The water consumption forecasting model is based on a feed-forward back-propagation neural network that has shown its efficiency in forecasting water consumption on the campus of Lille University (Farah et al. 2019). The input dataset comprises historical

temperature, water consumption, and days of specification data. The model gives as output, and water demand forecasts are used as inputs for the WWFFM.

In the model, days of specifications are represented as vectors containing information about the following:

- Day of the week (i.e., Monday to Sunday, where values range from 1 to 7).
- Holidays and special days (New Year's Day and religious celebrations such as Aid El-Adha) are represented with a vector where the values are either 0 or 1.
- Special consumption periods as Ramadan, where consumption patterns differ from normal consumption ones. The vector values are either 0 or 1, where 1 corresponds to the Ramadan period.
- The daily time is represented with 288 five-minute timesteps, where values range between 1 and 288.

3.3. Experimental data

3.3.1. Site description

The data were collected from a watershed of 3315 ha, which covers the townships of the Eastern part of Casablanca (Figure 3-4). The urbanization of the area is fairly heterogeneous and comprises industrial and residential areas. The urban drainage system (UDS) is a combined system in the historical part of the townships with a separate sewer system in the new urbanized areas.

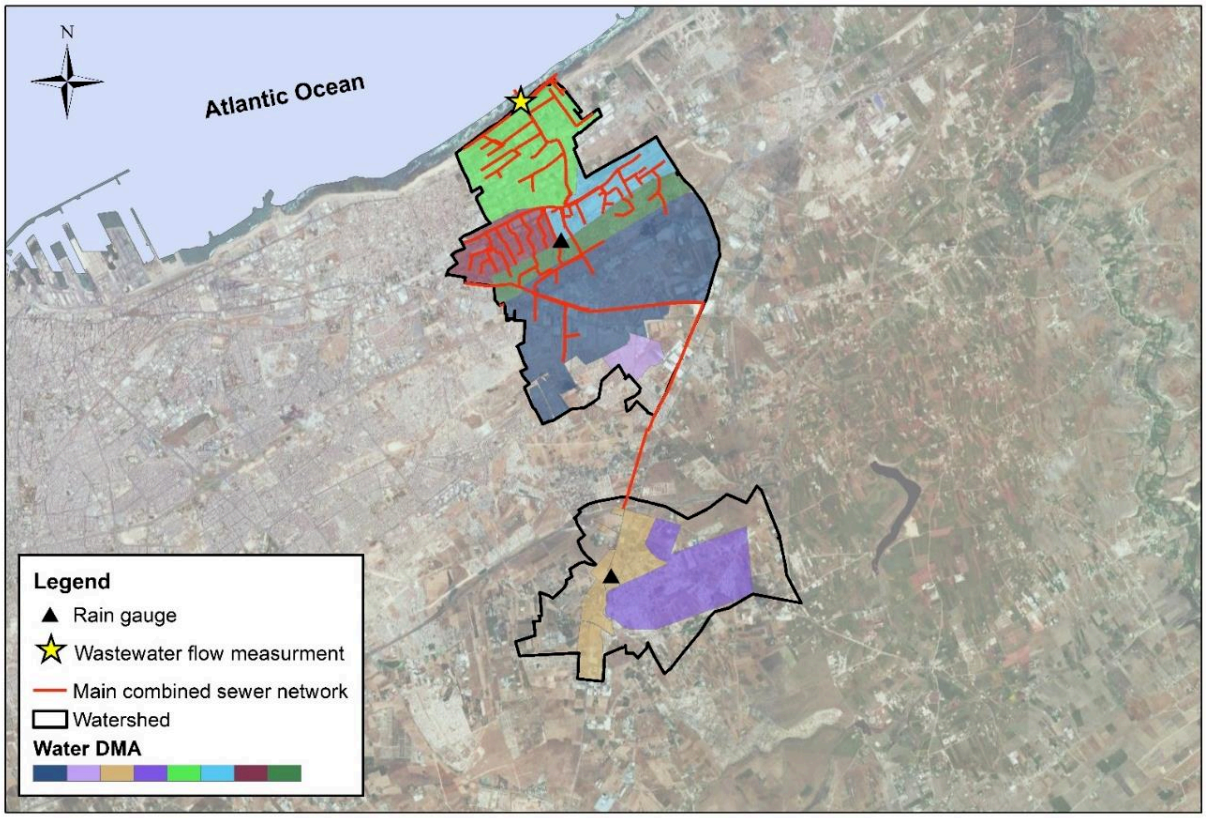

Figure 3-4| Sewer system and district metering areas of the studied area

3.3.2. Data collection and processing

The area is equipped with a monitoring system based on quantitative sensors that measure sewer flows at the watershed outlet and water consumption at the eight DMAs. The monitoring system of the DMAs is composed of insertion and electromagnetic flowmeters that conduct measurements at a five-minute time step. The UDS is equipped with a depth meter to measure the water level and a flow meter to measure the discharge at the watershed outlet. The measurement for the UDS is conducted at a fifteen-minute time step.

In the framework of the current study, wastewater flow (Qw), precipitation (P), water consumption (Wc), and temperature (T) data were collected for three years between March 2014 and July 2017.

The mean dry weather flow rate pattern presented in Figure 3-5 shows that wastewater flows vary between 390 l/s for the minimum night flow (MNF) and 900 l/s for the peak flow that occurs around 12:00 pm. Figure 3-6 illustrates the diurnal patterns for days of the week, average diurnal, seasonal patterns, and special diurnal patterns for specific periods. For normal days, the flow rates of water consumption vary from 270 l/s to 1100 l/s with an average flow rate of 650 l/s and can reach a value of 1600 l/s during the Aid El-Adha Celebration. Furthermore, Figures 6 a and b display the similar variations of the diurnal patterns for each day of the week and each season, with a rise of the MNF in summer of approximately 70 l/s and the peak flow of nearly 150 l/s. For all the consumption patterns, the peak flow is recorded between 11:00 am and 12:00 pm and decreases to reach the MNF between 2:00 am and 4:00 pm. However, the water consumption diurnal pattern trend changes during Ramadan, where we observe an increase in water consumption during the night with a peak flow around 4:00 am before the beginning of the fast and a MNF that shifts to 6:00 am. We can also observe a fast drop and variation in water consumption roughly 7:00 pm, which corresponds to the fast break time.

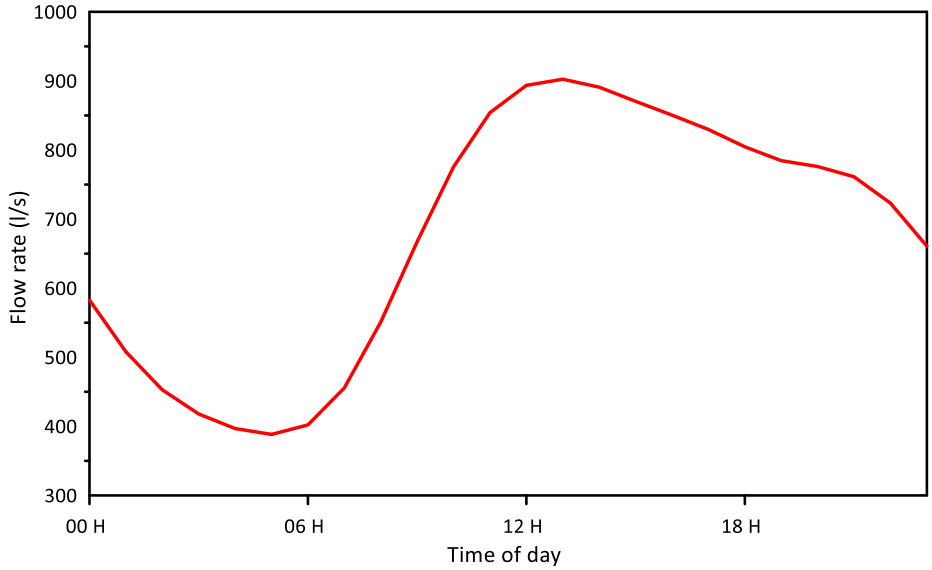

Figure 3-5| Diurnal pattern of the mean dry wastewater flow rate

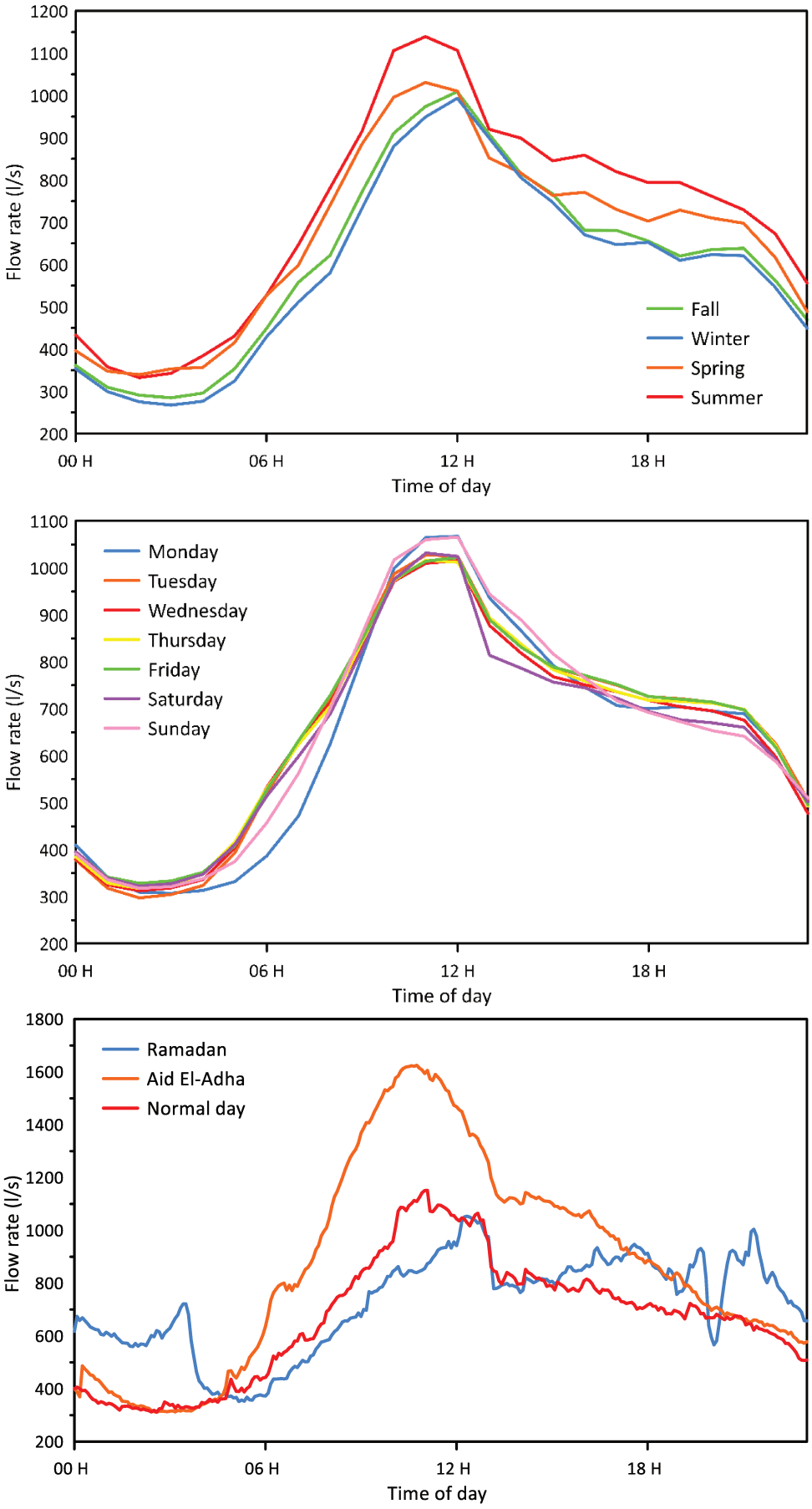

Figure 3-6| Diurnal patterns of water consumption flow rate for the seasons of the year (a), the days of the week (b), special periods (c)

However, given that the main sewer system was combined, the first step consisted of identifying rainy days on the basis of the rainfall records of the rain gauges and removing the corresponding data to keep only dry weather flows in the dataset.

For model predictive control systems and forecasting models, missing data constitute a major issue that does not fulfill the requirements of algorithms (Yuri et al. 2016). These problems could result from several factors, such as a power outage or a communication failure between the remote terminal units and the SCADA system (Walski et al. 2003). Many filling methods were proposed and could be found in the literature (Li et al. 2006; Qin et al. 2009; Fan et al. 2012), such as artificial filling, average value filling, special value filling, and regression. The reconstitution of the missing values of the dataset was performed through a linear interpolation.

In addition to missing values, data from field measurements usually include noise (Ruiz et al. 2016) that can affect the efficiency of machine learning algorithms (Lucas 2010; Munawar et al. 2011). The LOESS nonparametric regression method proposed by Cleveland (1979) and further developed by Cleveland et al. (1988, 1991, 1992) was employed to smooth the collected data (Figure 3-7).

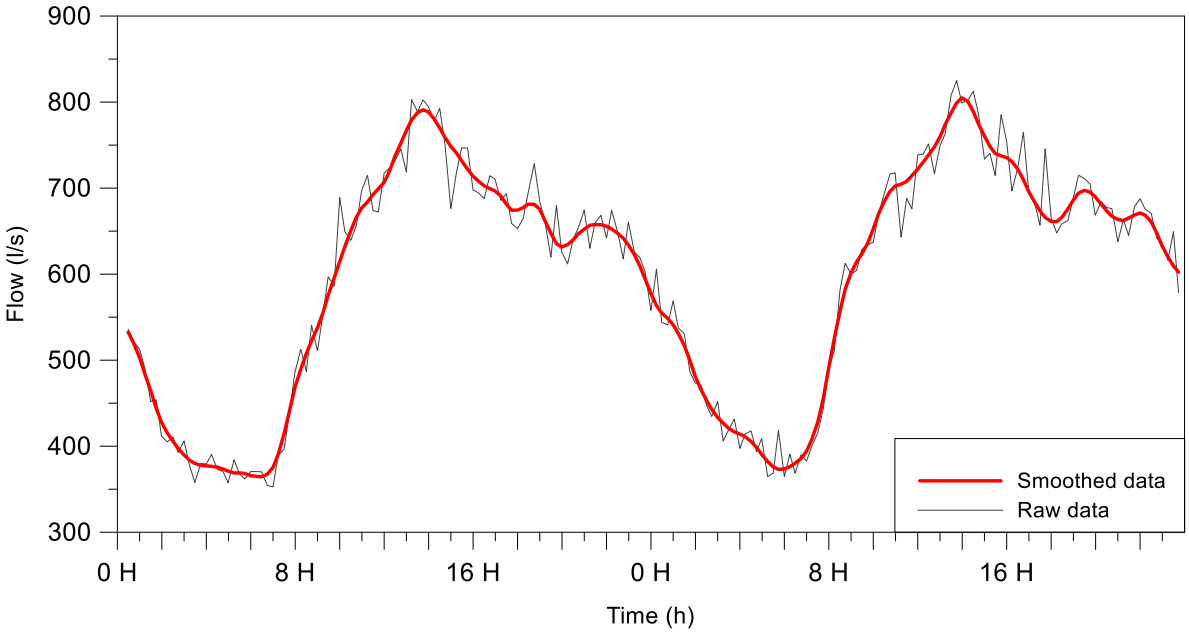

Figure 3-7| Smoothed data with the LOESS method

Dry weather flows in sewer networks consist of strict wastewater flows and infiltration flows (Figure 3-8). The origin of infiltration water or "parasite water" commonly corresponds to diffuse groundwater infiltration or seawater. This water enters the network through leaky joints, cracks, and defective manholes. Therefore, considering infiltration rate variation as an input for our model and decomposing the hydrogram components into strict wastewater and infiltration are essential. Many studies have developed and applied methods for the quantification and detection of infiltration water and could be found in the literature (Weiss et al. 2002; Ertl et al. 2002; Mitchell et al. 2006; Ertl et al. 2008; Staufer et al. 2012; WSAA 2013; USEPA 2014; Water NZ 2015; Hey et al. 2016). There are two common methods for quantifying the base infiltration flow (BIF), namely, the flow rate method based on daily flow monitoring and the tracer method based on natural tracers or pollutant load mass balance (Hey et al. 2016). The infiltration rate was determined on the basis of the flow rate method according to Equation (3-8):

$$BIF = \overline{\mathrm{MWF}} - (MNF\ (1 - RL)RC), \textbf{(3-8)}$$

where $\overline{MWF}$ is the average MNF on the last three dry weather days, *MNF* is the minimum water consumption flow, *RL* is the real loss percentage where values range between 23 and 25 %, and *RC* is a restitution coefficient equal to 80% and corresponding to the fraction of consumed water released back to the sewer network.

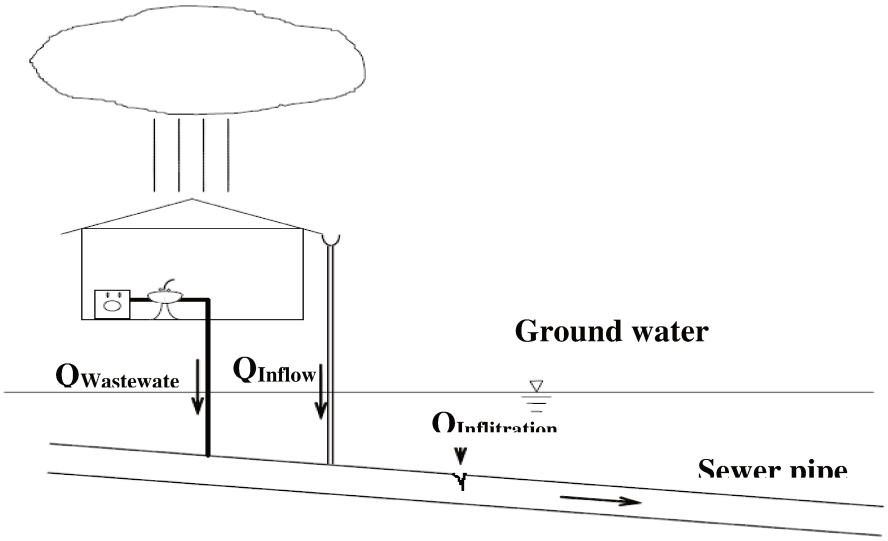

Figure 3-8| Flow components in sewer networks

3.3.3. Data analysis

The visualization of the total distributed water and the wastewater flows (Figure 3-9) shows that the maximum lag time between the peaks of these two variables is around 80 min. Additional lag time analysis was performed using the cross-correlation analysis between distribution water and wastewater flows (Figure 3-10). The analysis results show a high correlation between these two variables because the lag is less than 80 min. Above this value, the correlation starts decreasing under 80%, exhibiting a weaker relation between both variables. Thus, the lag value for the NARX model is considered to be 80 min, corresponding to 16-time step delays for the NARX.

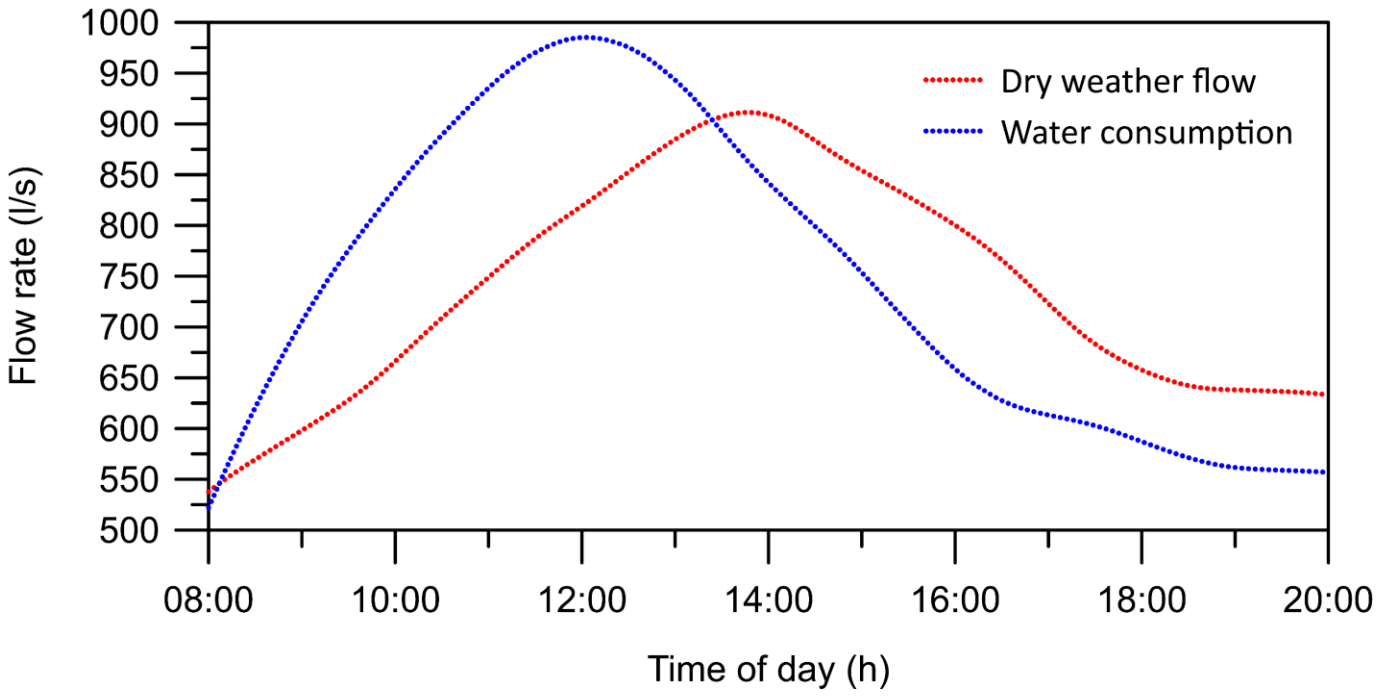

Figure 3-9| Plot of water consumption and wastewater flow peaks

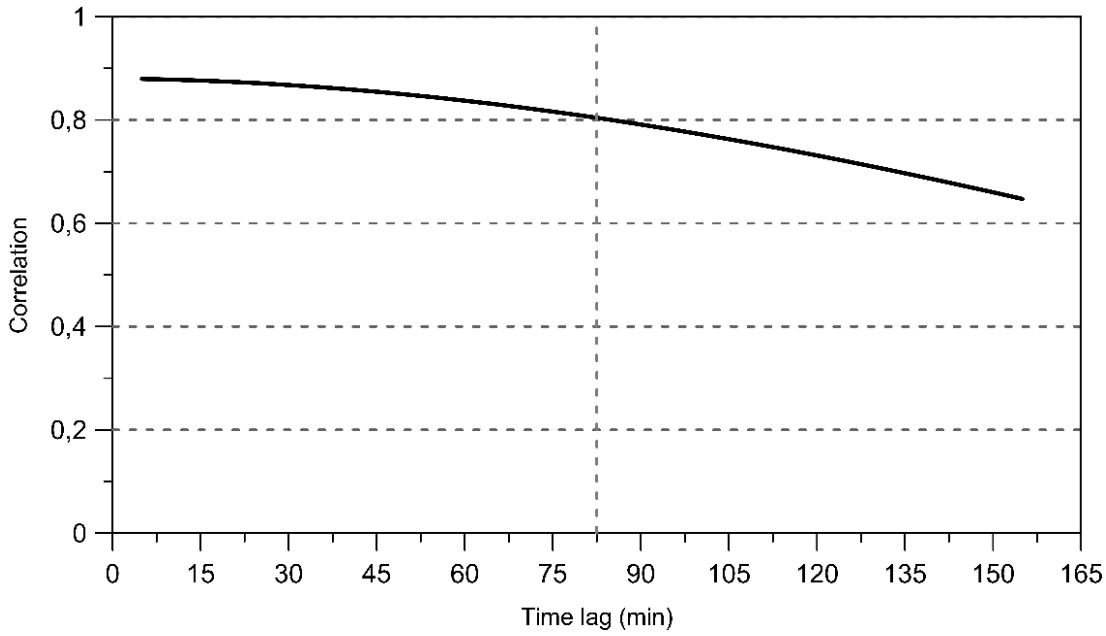

Figure 3-10| Cross correlation analysis

3.4. Results

During the training stage, the NARX neural network minimizes the error between the model results and the real observed data. A different number of neurons were tested and, after several trials, the best training, testing, and validation results were obtained with a hidden layer with 10 neurons allowing the reduction of the mean squared error (MSE) that decreases from 10^5 at the beginning of the training stage to 0.17 after 302 iterations. Tables 1 and 2 present the performance statistics of the NARX-NN architectures. The presented results show that increasing the number of neurons increases the efficiency of the model. However, increasing the number of neurons to more than ten results in poor performances in multi-step ahead forecasts. Figure 3-11 shows the performance of the trained ANN in the training, validation, and testing sets. In addition, Figure 3-12 highlights that the efficiency of the trained network presented by high regression values (R) of 0.999 is presented for the training, validation, and testing parts.

	Q_{t+6}	Q_{t+9}	Q_{t+12}	Q_{t+15}	Q_{t+18}	Q_{t+24}	Q_{t+48}
1 neuron	0.397	6.311	4.119	2.287	8.081	24.108	35.447
5 neurons	0.6181	5.809	3.823	2.180	7.676	17.659	25.646
10 neurons	1.828	5.603	4.828	1.729	7.238	16.922	17.868
15 neurons	1.495	4.727	1.762	6.413	14.678	29.529	29.528

Table 3-1| RMSE for different number of neurons

	Q_{t+6}	Q_{t+9}	Q_{t+12}	Q_{t+15}	Q_{t+18}	Q_{t+24}	Q_{t+48}
1 neuron	0.9998	0.9934	0.9918	0.9989	0.9852	0.8348	0.6881
5 neurons	0.9999	0.9944	0.9933	0.9990	0.9866	0.9113	0.8367
10 neurons	0.9995	0.9948	0.9957	0.9994	0.9806	0.9756	0.9207
15 neurons	0.9997	0.9963	0.9924	0.9916	0.9511	0.7521	0.7835

Table 3-2| NSE for different number of neurons

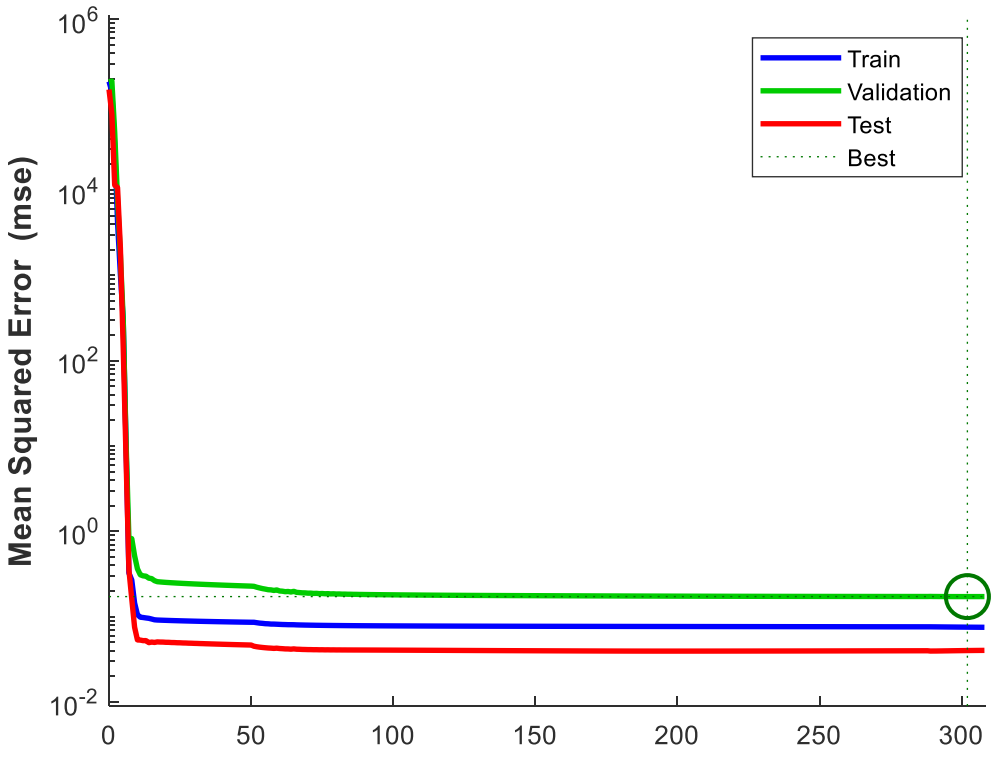

Figure 3-11| Performance evaluation of the trained neural network

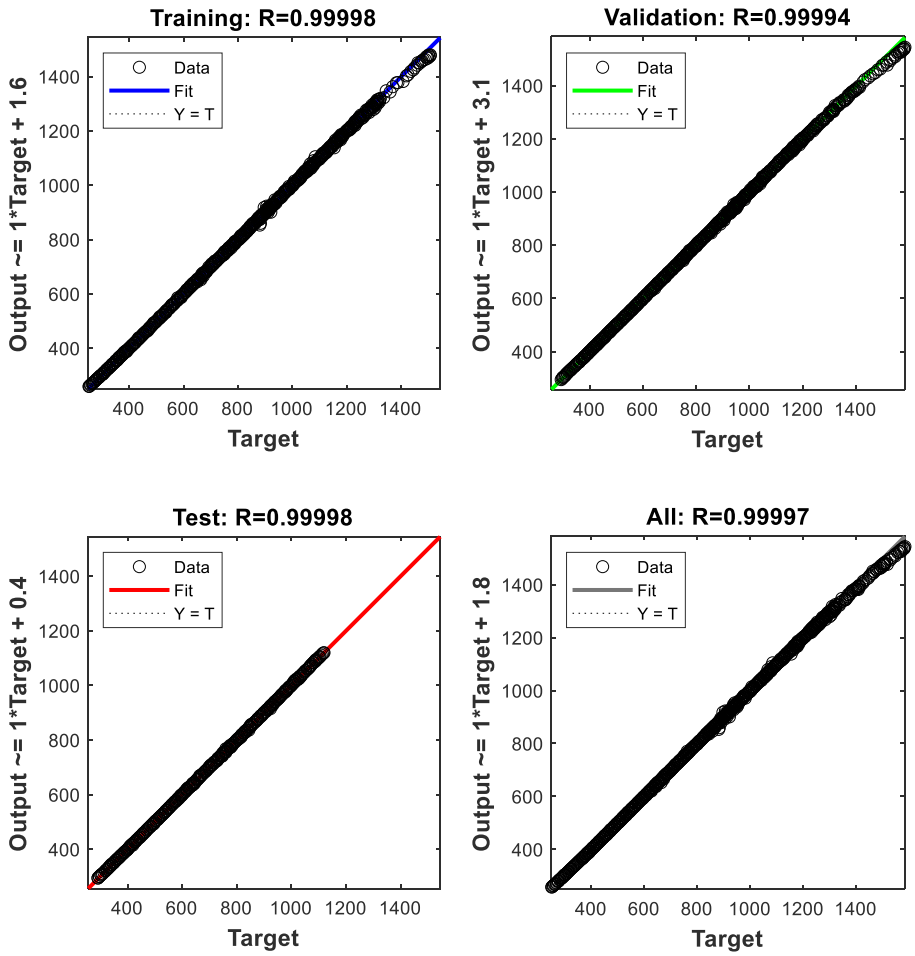

Figure 3-12| Regression results of the trained NARX-NN

Once the model had been trained, further validation of the accuracy of the WWFFM was performed through multi-step ahead predictions for 5 days, from September 8, 2016 to September 12, 2016, with hidden data not used during the training process. Figure 3-13 exhibits the water consumption of the eight DMAs and BIF employed for forecasting wastewater flows for a five-day period. During this period, high water consumption was recorded on September 12, and corresponded to Aid El-Adha celebration day. The predictions of the WWFFM were conducted for different horizons Q_{t+k}. Where Q_t designates the wastewater flow at timestep t, while Q_{t+k} stands for the wastewater flow at timestep t+k (k = 6, 9, 12, 15, 18, 24, and 48) with a five-minute time step.

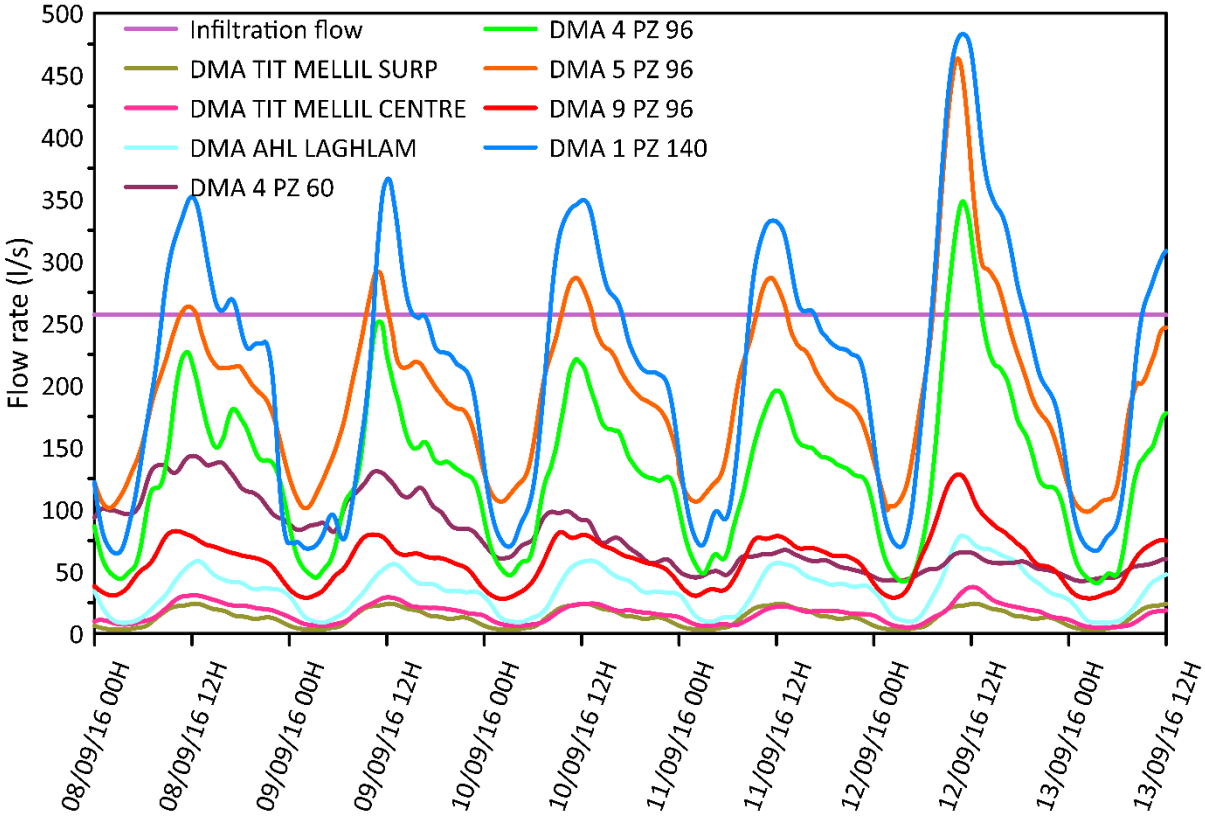

Figure 3-13| Plot of water consumption of the eight DMAs and BIF

Tables 3 and 4 present the performance statistics of the WWFFM without water demand forecasts and the WWFFM with water demand forecasts, respectively. Figures 14 (a), (b), (c), (d), (e), (f), and (g) depict the predicted and observed flows for both approaches.

	Q_{t+6}	Q_{t+9}	Q_{t+12}	Q_{t+15}	Q_{t+18}	Q_{t+24}	Q_{t+48}
RMSE ($m^3 s^{-1}$)	3.300	5.492	10.383	16.166	18.918	43.487	82.855
NSE	0.999	0.999	0.998	0.995	0.993	0.967	0.881

Table 3-3| Performance statistics of the WWFFM without water demand forecasts

	Q_{t+6}	Q_{t+9}	Q_{t+12}	Q_{t+15}	Q_{t+18}	Q_{t+24}	Q_{t+48}
RMSE ($m^3 s^{-1}$)	3.504	4.367	4.135	4.7915	11.711	11.888	12.017
NSE	0.999	0.999	0.999	0.999	0.997	0.997	0.997

Table 3-4| Performance statistics of the WWFFM with water consumption forecast

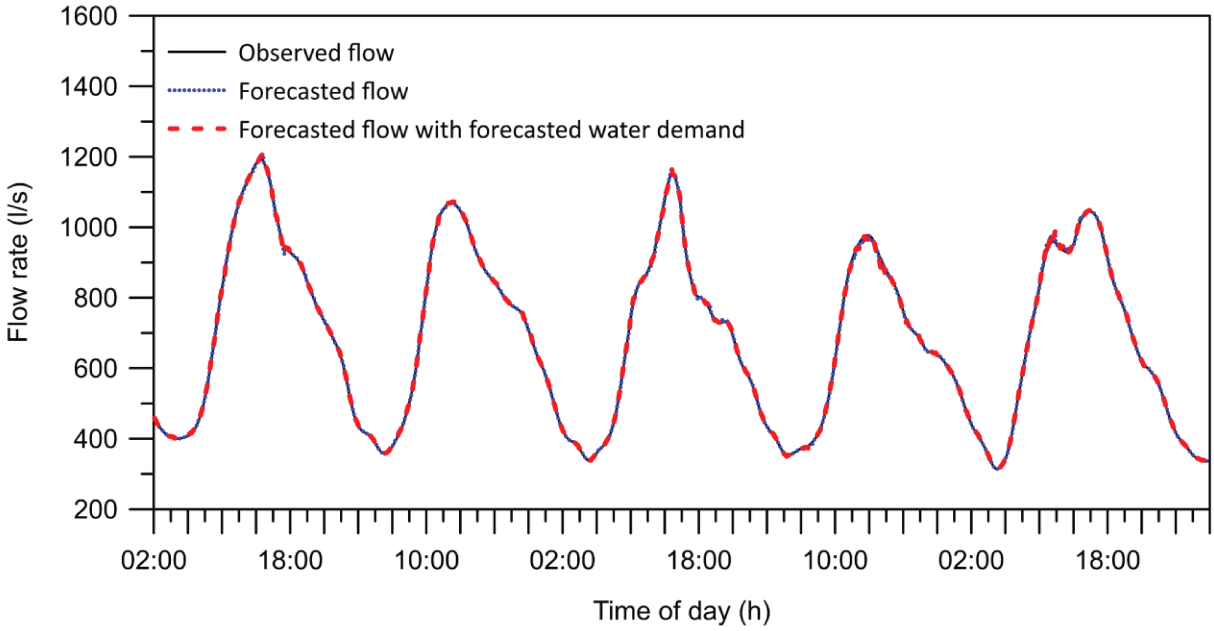
Observed flow
Forecasted flow
Forecasted flow with forecasted water demand
Flow rate (l/s)
1600
1400
1200
1000
800
600
400
200
02:00
18:00
10:00
02:00
18:00
10:00
02:00
18:00
Time of day (h)

(a)

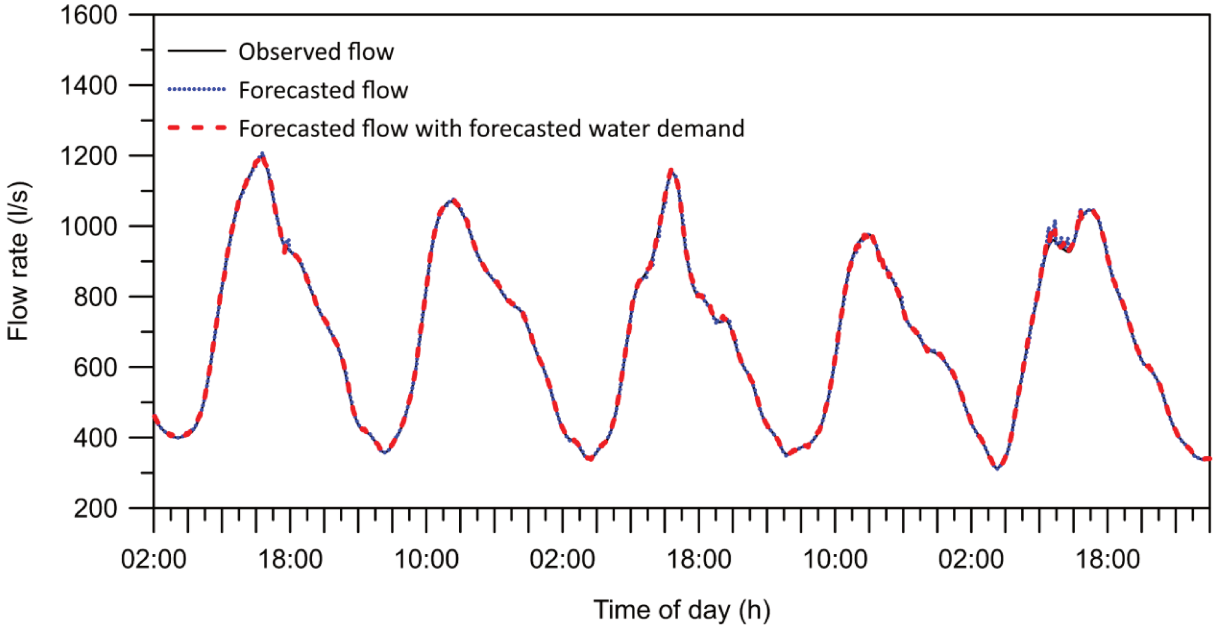
Observed flow
Forecasted flow
Forecasted flow with forecasted water demand
Flow rate (l/s)
1600
1400
1200
1000
800
600
400
200
02:00
18:00
10:00
02:00
18:00
10:00
02:00
18:00
Time of day (h)

(b)

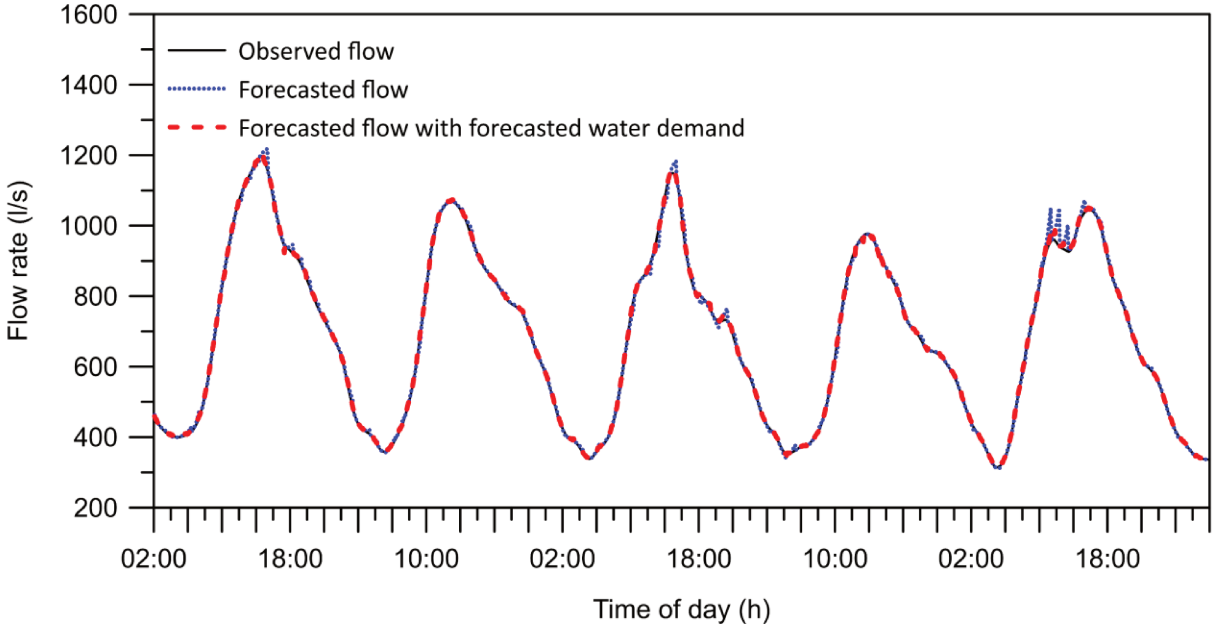
Observed flow
Forecasted flow
Forecasted flow with forecasted water demand
Flow rate (l/s)
1600
1400
1200
1000
800
600
400
200
02:00
18:00
10:00
02:00
18:00
10:00
02:00
18:00
Time of day (h)

(c)

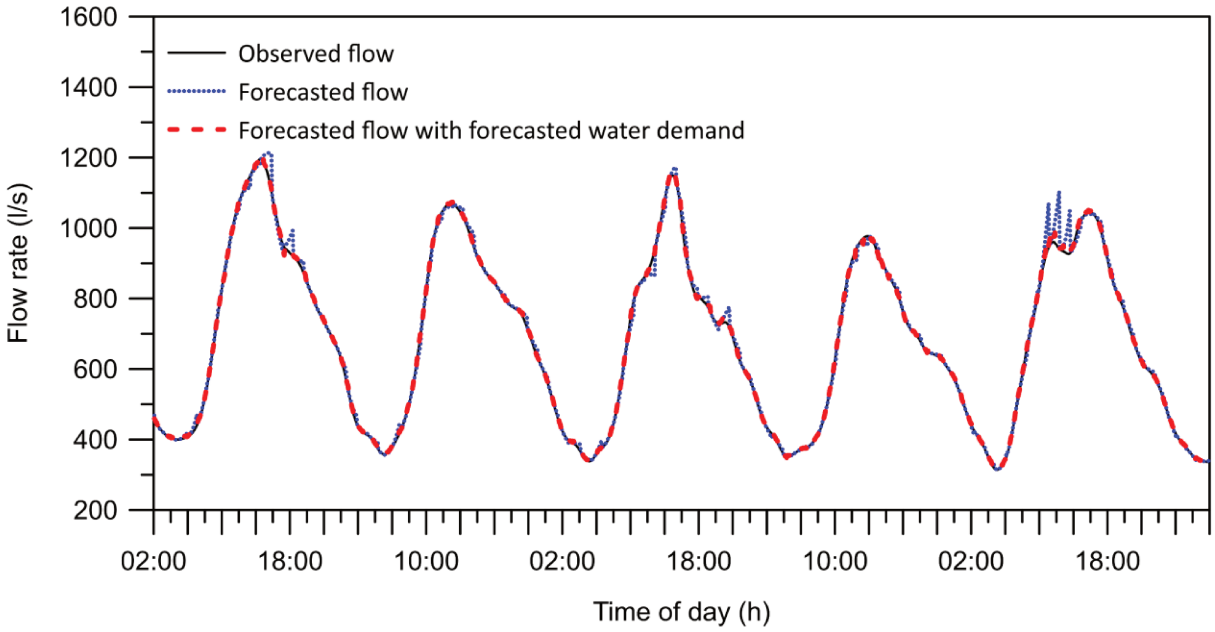
Observed flow
Forecasted flow
Forecasted flow with forecasted water demand
Flow rate (l/s)
1600
1400
1200
1000
800
600
400
200
02:00
18:00
10:00
02:00
18:00
10:00
02:00
18:00
Time of day (h)

(d)

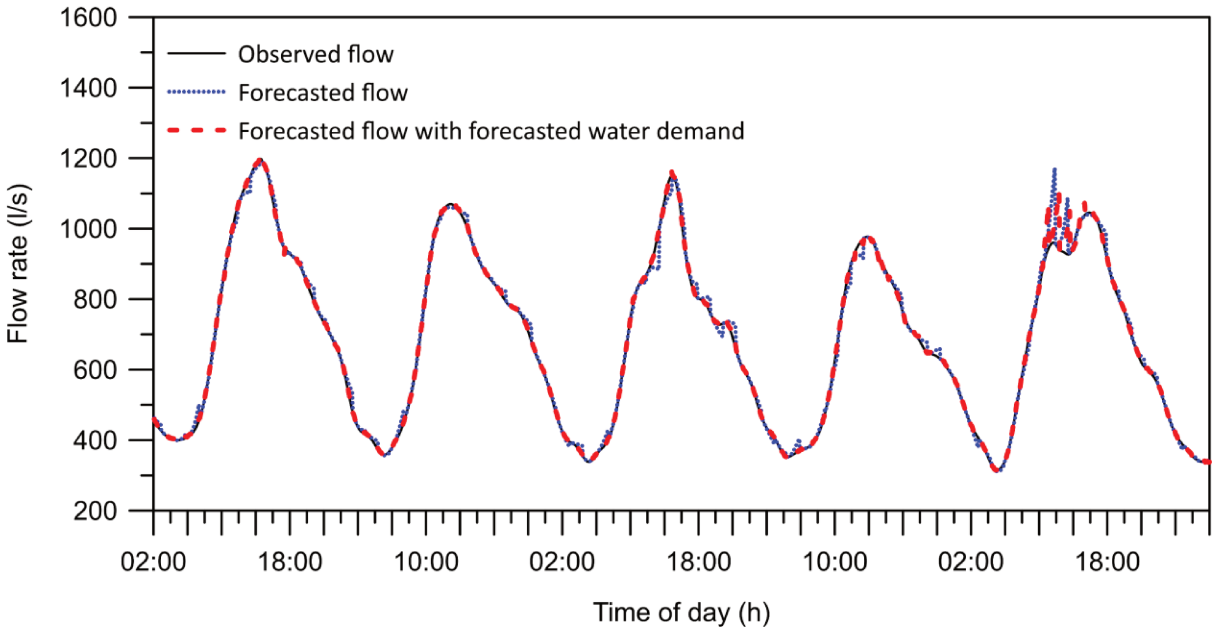
Observed flow
Forecasted flow
Forecasted flow with forecasted water demand
Flow rate (l/s)
1600
1400
1200
1000
800
600
400
200
02:00
18:00
10:00
02:00
18:00
10:00
02:00
18:00
Time of day (h)

(e)

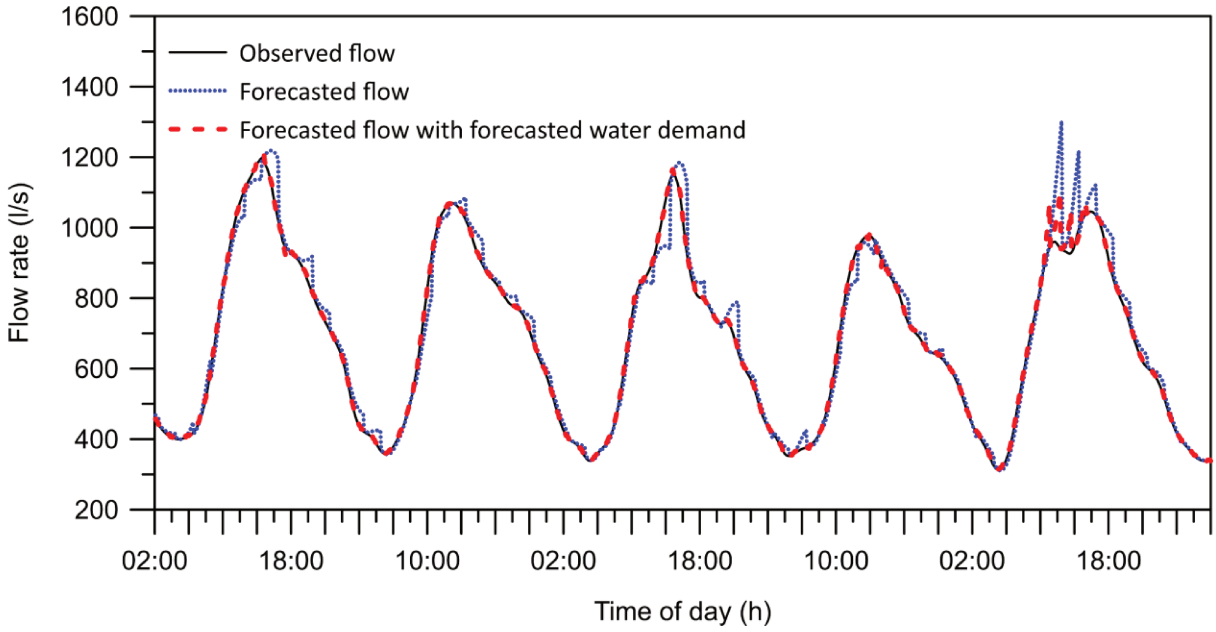
Observed flow
Forecasted flow
Forecasted flow with forecasted water demand
Flow rate (l/s)
1600
1400
1200
1000
800
600
400
200
02:00
18:00
10:00
02:00
18:00
10:00
02:00
18:00
Time of day (h)

(f)

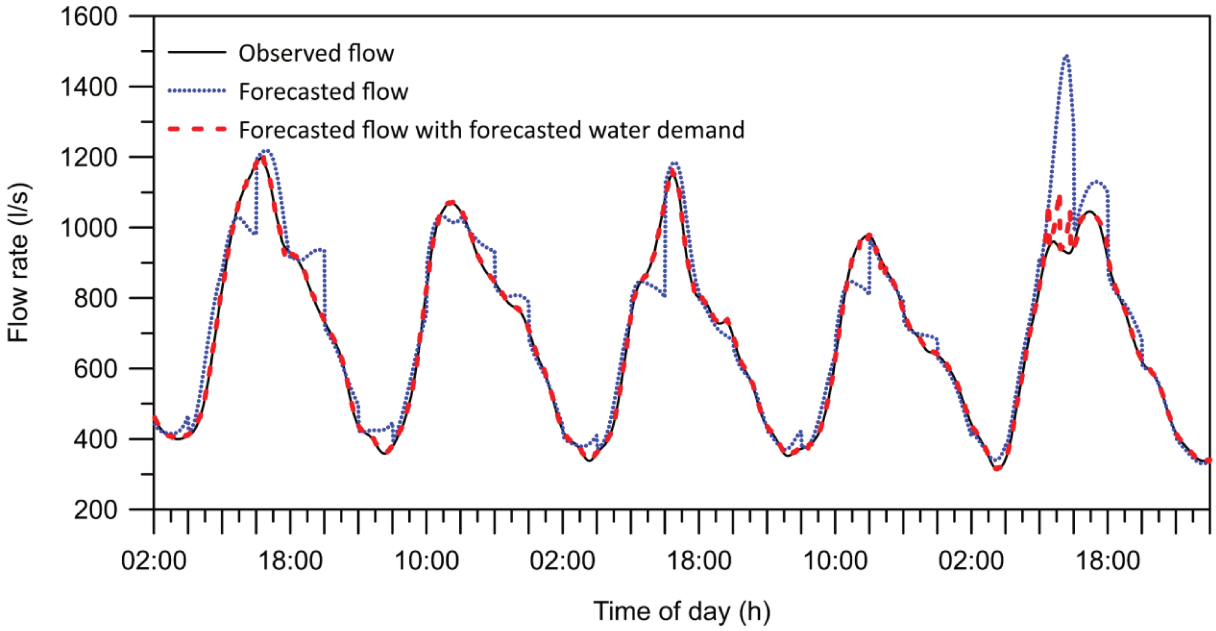

(g)

Figure 3-14| Prediction of (a) Q_t+6; (b) Q_t+9; (c) Q_t+12; (d) Q_t+15; (e) Q_t+18; (f) Q_t+24; (g) Q_t+48; using NARX-NN.

The analysis of the error statistical results in Figure 3-14 demonstrates that the WWFFM model with both approaches shows good performances in forecasting dry weather flow as long as the lag time remains less than 80 min. The forecast results are highly accurate, with a RMSE ranging between 3.3 and 16.16 and a NSE ranging between 0.995 and 0.999. Nonetheless, for prediction horizons exceeding 80 min, the WWFFM without water distribution forecasts has a poor performance that decreases with the increase of the forecasting horizon that fails to predict peak, especially for September 12, where the NARX-NN overestimate the peak flow of more than 550 l/s. Conversely, the WWFFM with water distribution forecasts enables the forecast of long-time horizons with a slight variation of the RMSEs over the different forecasting horizons ranging between 3.5 and 12.

3.5. Discussion

The current study explored a new approach for predicting instantaneous dry weather flows in the UDS on the basis of the NARX-NN and drinking water consumption, and such an approach was tested on a part of the sewer system of Casablanca, which comprises approximately five million people. The construction of the model required essential steps to reconstitute data through linear interpolation because most modeling techniques cannot deal with missing values and cast out the whole instance value if one of the variable values is missing. In addition, the LOESS nonparametric regression method was used to smooth the data lying far from the bulk of the data range, and a cross-correlation analysis was also conducted to assess the suitable lagged information of the model.

The findings of this study validate that both tested approaches of the WWFFM display accurate results and similar performances in predicting dry weather flows with low RMSEs less than 16.16 and high NSEs as long as the forecasting horizon does not exceed 80 min. Nonetheless, the results further confirm that for prediction horizons that exceed 80 min, the WWFFM without water distribution forecasts presents poor performances that decrease with the increase of the forecasting horizon due to the lack of appropriate causal input variables, thereby making it unsuitable for long time horizon forecasts for model predictive system use. Conversely, the WWFFM with water distribution forecasts is continuously updated with appropriate lagged input data, thereby enabling it to perform highly accurate forecasts for long time horizons though representing all the flow ranges. The findings also highlight the importance of the WWFFM that could benefit operators and water engineers, thereby providing valuable input data for predictive model control to enhance the efficiency of sewer systems.

To our knowledge, this is the first study that has explored this new approach of forecasting dry weather flows on the basis of real-time water consumption and the BIF, which thus improves the knowledge of and complements previous research works in forecasting dry weather flows. The currently known models proposed in the literature

(Wei et al. 2013; Boyd et al. 2019; Zhang et al. 2019) rely only on historical data with no external inputs. Additionally, they do not integrate drinking water consumption, which is the main causal variable that may influence forecasted flows in case of a water shutdown in a sector or water consumption variation due to a given event.

The limitation of the proposed WWFFM model lies in its use of real-time data, which can pose a problem in the event of data unavailability due to a sensor failure or a communication problem. Therefore, ensuring the good maintenance of the flow meters and continuous data transmissions for the needs of the NARX-NN is essential. Moreover, defining strategies for filling in data in case of communication failures would be interesting. In the meantime, the proposed model only integrates the forecasts of wastewater flows, and it is planned in the perspective of future works to develop the model by integrating the forecasts of combined sewer flows considering the fraction of stormwater flows.

3.6. Conclusion

The present work aims to fill the gaps in the wastewater flow forecasting research across the world by proposing a novel WWFFM based on the NARX. The proposed model considers real-time and forecasted water consumption as the main causal variable input of wastewater flow production. This study differs from the approaches presented through the literature that remain limited considering the only sewer flow historical data and that would fail to forecast sewer flows in the case of a water shutdown in a sector or water consumption variation due to a given event. This research compares the two approaches of the forecasting model. The first approach consists of forecasting wastewater flows on the basis of real-time water consumption and infiltration flows, and the second approach considers the same input in addition to the water distribution flow forecasts. Consequently, both approaches display accurate results and similar performances in predicting wastewater flows, while the forecasting horizon does not exceed 80 min. Nonetheless, for prediction horizons that exceed 80 min, the WWFFM without water distribution forecasts presents poor performances that decrease with the increase of the

forecasting horizon. Conversely, the WWFFM with water distribution forecasts is continuously updated with the appropriate lagged input data, thereby making it able to perform highly accurate forecasts for long time horizons. Hence, the WWFFM developed in this study could benefit operators and water engineers, providing valuable input data for predictive model control and thus enhancing UDS efficiency.

3.7. References

Abou Rjeily Y., Abbas O., Sadek M., Shahrour I. & Hage Chehade F. 2017 Flood forecasting within urban drainage systems using NARX neural network. Water Sci Technol, 76(9), 2401–2412.

Boyd G., Na D., Li Z., Snowling S., Zhang Q. & Zhou P. 2019 Influent forecasting for wastewater treatment plants in North America. Sustainability, 11(6), 1764.

Chen J., Ganigue R., Liu Y. & Yuan Z. 2014 Real-time multi-step prediction of sewer flow for online chemical dosing control. ASCE J. Environ. Eng.

Cleveland W. S. 1979 Robust locally weighted regression and smoothing scatterplots. Journal of the American Statistical Association, 74(368), 829–836.

Cleveland W. S., Devlin S. J. & Grosse E. 1988 Regression By Local Fitting Journal of Econometrics, 37, 87–114.

Cleveland W. S. & Grosse E. 1991 Computational Methods for Local Regression. Statistics and Computing, 1, 47–62.

Cleveland W. S., Grosse E. & Ming-Jen S. 1992 A Package of C and Fortran Routines for Fitting Local Regression Models. Unpublished paper.

Di Nunno F., Granata F., Gargano R. & Marinis G. 2021 Prediction of spring flows using nonlinear autoregressive exogenous (NARX) neural network models. Environ Monit Assess, 193, 350.

Ertl T. W., Dlauhy F. & Haberl L. 2002 Investigations of the amount of infiltration inflow in to a sewage system. Proceedings of the 3rd "Sewer Processes and Networks". International Conference, Paris, France, 15–17.

Ertl T., Spazierer G. & Wildt S. 2008 Estimating groundwater infiltration into sewerages by using the moving minimum method — a survey in Austria. 11th International Conference on Urban Drainage, Edinburgh, Scotland, UK.

Fan B., Zhang G. & Li H. 2012 Multiple models fusion for pattern classification on noise data. ,*2012 International Conference on System Science and Engineering (ICSSE)*, 64–68.

Farah E., Abdallah A. & Shahrour I. 2019 Prediction of water consumption using Artificial Neural Networks modelling (ANN). MATEC Web of Conferences, 295, 01004.

Fernandez F. J., Seco A., Ferrer J. & Rodrigo M. A. 2009 Use of neurofuzzy networks to improve wastewater flow-rate forecasting. Environmental Modelling & Software, 24(6), 686–693.

Gavin B., Dain N., Zhong Li., Spencer S., Qianqian Z. & Pengxiao Z. 2019 Influent forecasting for wastewater treatment plants in North America. Sustainability 11, 6, 1764. https://doi.org/10.3390/su11061764

Hagan M. T. & Menhaj M. B. 1994 Training feed-forward networks with the Marquardt algorithm. IEEE Transactions on Neural Networks, 5, 989–993.

Hey G., Jonsson K. & Mattsson A. 2016 The Impact of Infiltration and Inflow on Waste Water Treatment Plants: a Case Study in Sweden.

Koschwitz D., Frisch J. & Van Treeck J. C. 2018 Data-driven heating and cooling load predictions for non-residential buildings based on support vector machine regression and NARX recurrent neural network: a comparative study on district scale. Energy, 165, 134–142.

Li J., Li P. & Shu K. 2006 RMINE: a rough set based data mining prototype for the reasoning of incomplete data in condition-based fault diagnosis. J Intell Manuf, 1, 163–76.

Lucas A. 2010 Corporate data quality management: from theory to practice. Ind Electron Appl.

Marcjasz G., Uniejewski B. & Weron R. 2019 On the importance of the long-term seasonal component in day-ahead electricity price forecasting with NARX neural networks. International Journal of Forecasting, 35(4), 1520–1532.

Mitchell P., Stevens P. & Nazaroff A. 2006 Determining base infiltration in sewers. A Comparison of Empirical Methods and Verification Results, 1–13.

Munawar M., Salim N. & Ibrahim R. 2011 Towards data quality into the data warehouse development. Int J Electr Power Energy Syst.

Qin Y., Zhang S. & Zhu X. 2009 Pop algorithm: kernel-based imputation to treat missing data in knowledge discovery from databases. Expert Syst Appl, 2, 2794–804.

Ruiz L. G. B., Cuéllar M. P., Calvo-Flores M. D. & Jiménez M. D. C. P. 2016 An application of non-linear autoregressive neural networks to predict energy consumption in public buildings. Energies, 9, 684.

Solomatine D. P. & Khada N. D. 2003 Model trees as an alternative to neural networks in rainfall–runoff modelling. Hydrological Sciences Journal, 48(3), 399–411.

Staufer P., Scheidegger A. & Rieckermann J. 2012 Assessing the performance of sewer rehabilitation on the reduction of infiltration and inflow. Water Research, 46(16), 5185–5196.

Walski T., Chase D. V., Savic D.A., Grayman W. M., Beckwith S. & Edmundo K. 2003 Advanced Water Distribution Modeling and Management, 244–248.

Water NZ 2015 Infiltration and Inflow Control Manual, 1 & 2.

WSAA 2013 Good Practice Guidelines for Management of Wastewater System Inflow and Infiltration, 1 & 2.

Wei X., Kusiak A. & Sadat H. R. 2013 Prediction of Influent Flow Rate: Data-Mining Approach.

Weiss G., Brombach H. & Haller B. 2002 Infiltration and inflow in combined sewer systems: long-term analysis. Water Science & Technology, 45, 227–230.

Wunsch A., Liesch T. & Broda S. 2018 Forecasting groundwater levels using nonlinear autoregressive networks with exogenous input (NARX). Journal of Hydrology, 567, 743–758.

Yuri A. W., Shardt, X. Y. & Steven X. D. 2016 Quantisation and data quality: implications for system identification. Journal of Process Control, 40, 13–23.

Zhang Q., Li Z., Snowling S., Siam A. & El-Dakhakhni W. 2019 Predictive models for wastewater flow forecasting based on time series analysis and artificial neural network. Water Sci Technol, 80(2), 243–253

Chapter 4

Comparison of M5 model tree, nonlinear autoregressive with exogenous inputs (NARX) neural network, random forest, ANFIS-PSO models for urban stormwater discharge modeling

4.1. Introduction

Major cities are facing urban flood issues due to urbanization and climate change. RTC systems improve the performances of sewer networks by controlling different network components and optimizing storage within retention ponds and main collectors (Beeneken et al. 2014). The essential input parameters in RTC systems are rain and flow forecasts. Artificial intelligence (AI) techniques have shown good performances in nonlinear modeling systems with a considerable reduction in computing time compared with hydrologic and hydraulic models (Abou Rjeily et al. 2017). Four AI techniques, namely, NARX neural network, M5T, RF, and ANFIS, have been discussed in several applications, such as sediment transport modeling (Bhattacharya et al. 2007), river flow forecast (Solomatine & Dulal 2003), evaporation estimation (Rahimikhoob 2014), wastewater treatment plant inflow prediction (Zhou et al. 2019), and monthly potential evapotranspiration prediction (Mohammadrezapour et al. 2019).

This chapter presents an extension to urban drainage application through a comparative study on four data-driven modeling techniques in forecasting urban drainage stormwater discharge on the basis of rainfall prediction. The NARX-NN, M5T, RF, and ANFIS are utilized for stormwater forecasting.

4.2. Methodology

The hydraulic modeling of large sewer networks with conventional software may be time-consuming. The SWFM model has the advantage of performing fast calculations and providing quick and accurate stormwater discharge inputs for anticipatory models. Moreover, this model takes real-time rainfall forecasts as inputs and returns as output stormwater discharge. The following sections present the machine learning models used for building and evaluating the SWFM. The NARX neural networks have already been presented in Chapter 3 and will not be presented in this section anymore.

4.2.1. M5T

The M5 model is based on information theory (Quinlan 1992; Solomatine & Dulal 2003), and it can also handle nonlinear problems by splitting them into multiple linear ones. The M5T is similar to conventional decision trees, but instead of predicting classes through a classifier, it predicts continuous variables through linear regression functions at the leaves. The construction of the M5T is conducted in two stages (Solomatine & Xue 2004; Rahimikhoob et al. 2014). In the first stage, the M5T is constructed by a divide-and-conquer method that splits the multidimensional data space into several subspaces on the basis of a splitting criterion (Figure 4-1) that treats the standard deviation of the class values that reach a node as a measure of the error at that node and computes the expected reduction in the error by testing each attribute at that node.

The splitting operation stops when the values of the instances reach a node with a slight variation, or just few instances remain (Goyal & Ojha 2014).

The formula employed to calculate the standard deviation reduction is given by the following (Solomatine & Dulal 2003; Pal & Deswal 2009; Goyal & Ojha 2014; Singh et al. 2016):

$$\boldsymbol{SDR} = \boldsymbol{sd}(\boldsymbol{T}) - \sum \frac{|\boldsymbol{T_i}|}{|\boldsymbol{T}|} \boldsymbol{sd}(\boldsymbol{T_i}), \quad (2)$$

where *T* is the set of examples that reaches the node; *Ti* is the subset of examples that have the *i*th outcome of the potential set; and *sd* is the standard deviation.

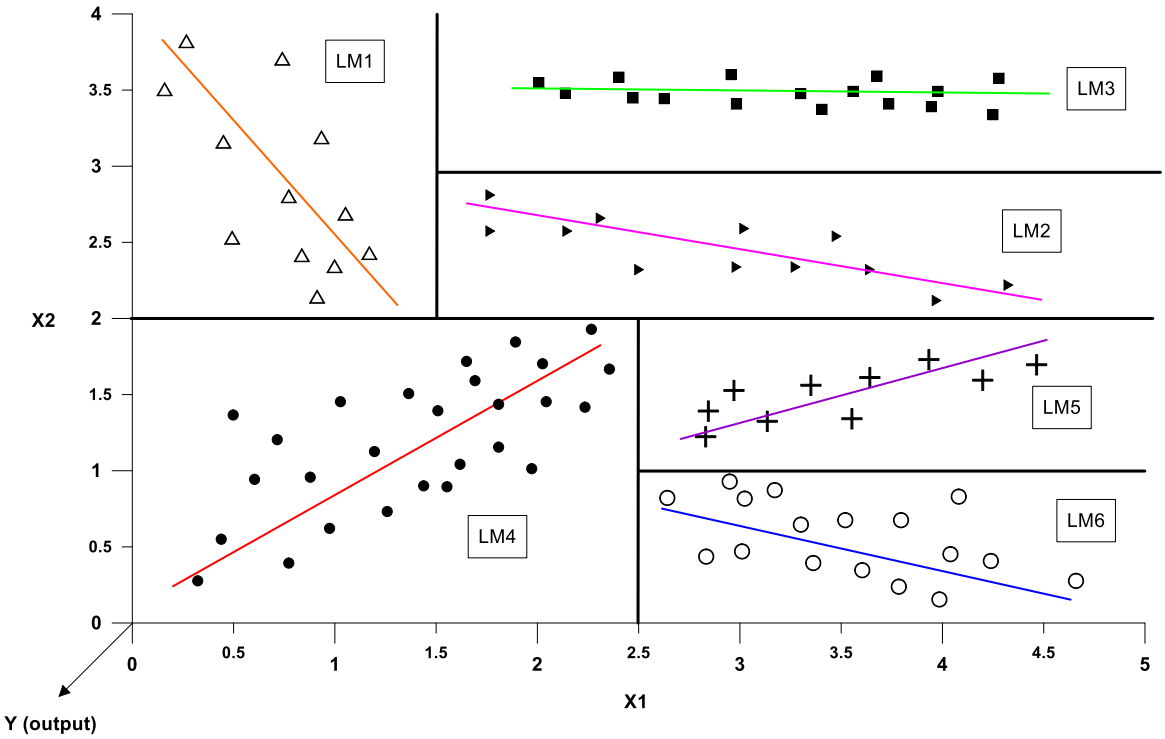

Figure 4-1| Splitting the input space (X1×X2) by the M5 model tree algorithm

The splitting result is a tree with splitting rules at the nodes with expert linear models (LMs) at the leaves (Figure 4-2). The combination of LMs can be observed as a committee machine (Haykin 1999).

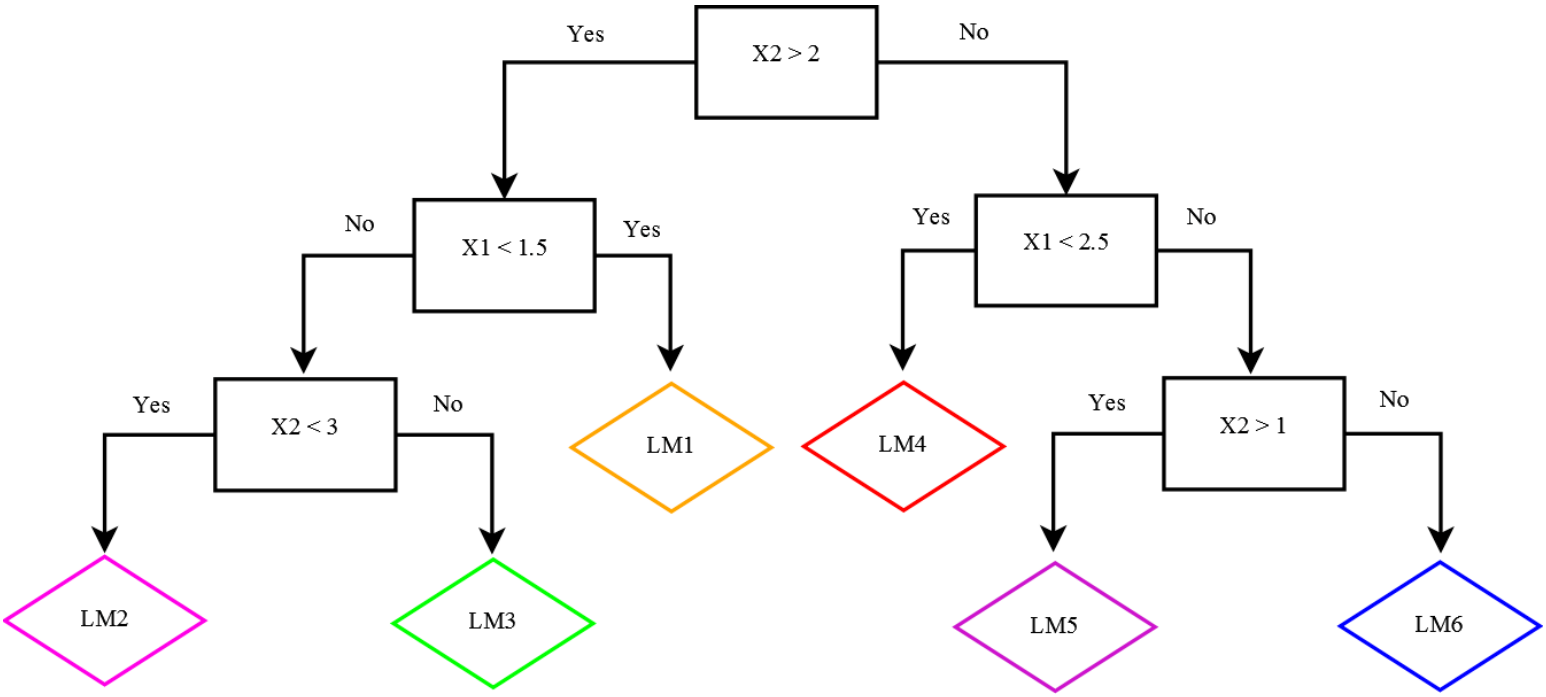

Figure 4-2| Diagram of the M5 model tree with six linear regression models at the leaves

The generated tree is generally large and difficult to analyze and may lead to overfitting. In the second stage, a pruning operation is necessary to overcome this problem by replacing a subset with a leaf. In addition, the smoothing is performed to compensate the discontinuities that can occur between the adjacent LMs at the pruned leaves of the tree.

4.2.2. Random Forest Regression

RF is an ensemble model tree introduced by Breiman (2001), and it lies on an ensemble of tree models (Breiman et al. 1984) that can perform classification and regression capable of performing regression and classification tasks.

RF starts with a bootstrap sampling process that involves a random sampling of subsets of data with replacement from the original training dataset, and a regression tree is created on the bootstrap samples. The final predicted values are produced by the aggregation of the results of all the individual trees that make up the forest.

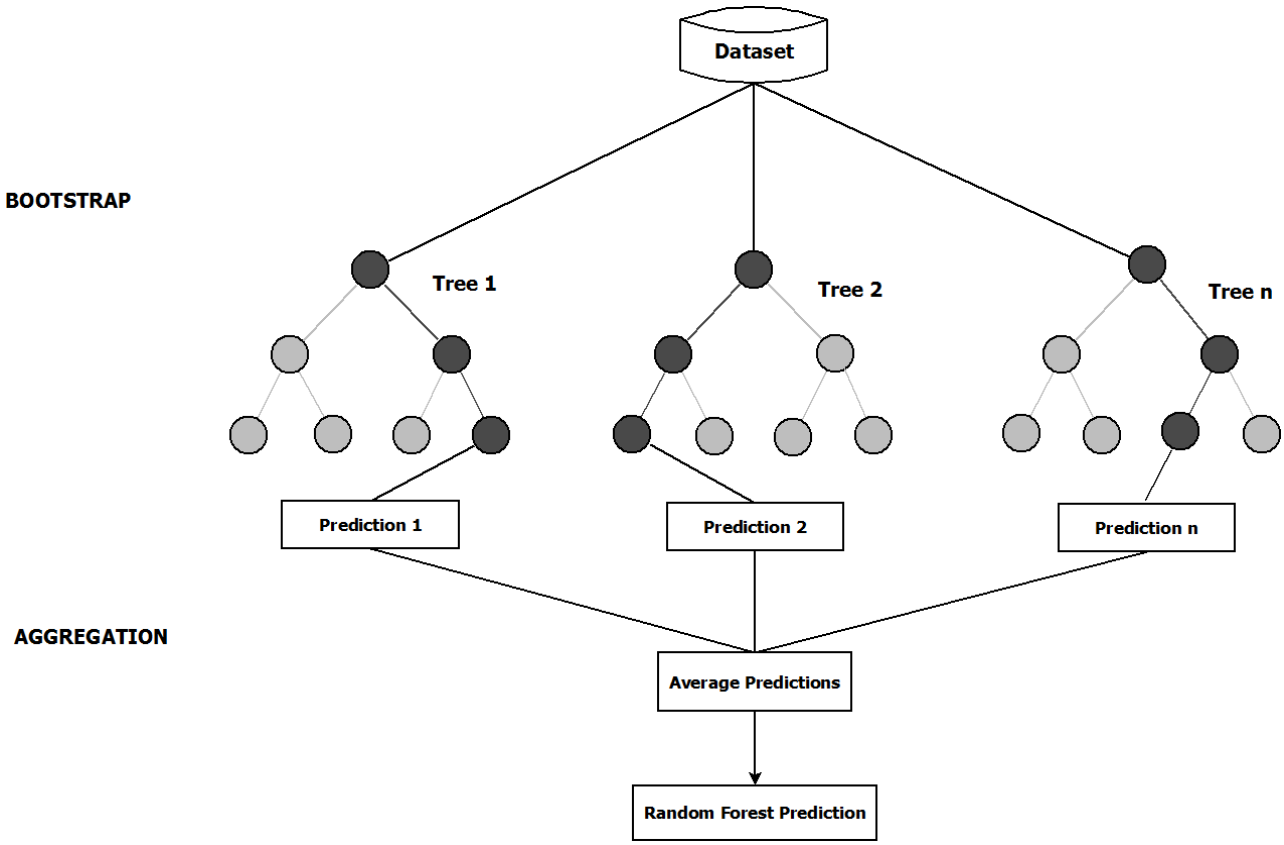

Figure 4-3| RF process

4.2.3. ANFIS

The ANFIS or adaptive network-based fuzzy inference system was developed by Jang (1993). It combines an adaptive neural network and a Takagi–Sugeno fuzzy inference system.

The ANFIS has also been widely utilized in many applications for modeling water systems (Azad et al. 2018; Tien Bui et al. 2018; Azad et al. 2019), and it can approximate nonlinear functions (Abraham 2005). Additionally, it simulates the relationship between the input and the output of a given process through hybrid learning based on the fuzzy IF-THEN rules to determine the optimal distribution of the membership functions.

ANFIS architecture

The following five layers compose the ANFIS model:

- The first layer, called the fuzzification layer, determines the membership functions.
- The second layer generates the firing strengths for the rules.
- The third layer normalizes the computed firing strengths by dividing each value by the sum of all firing strength rules.
- The fourth layer or the defuzzification layer takes the consequence parameter set and the normalized values as inputs.
- This fifth layer proceeds to the summation of the defuzzificated outputs.

The figure below represents the architecture of the model built in MATLAB. This model takes a single input (rain data) with six rules and bell-shaped membership functions and returns a single output (storm discharge).

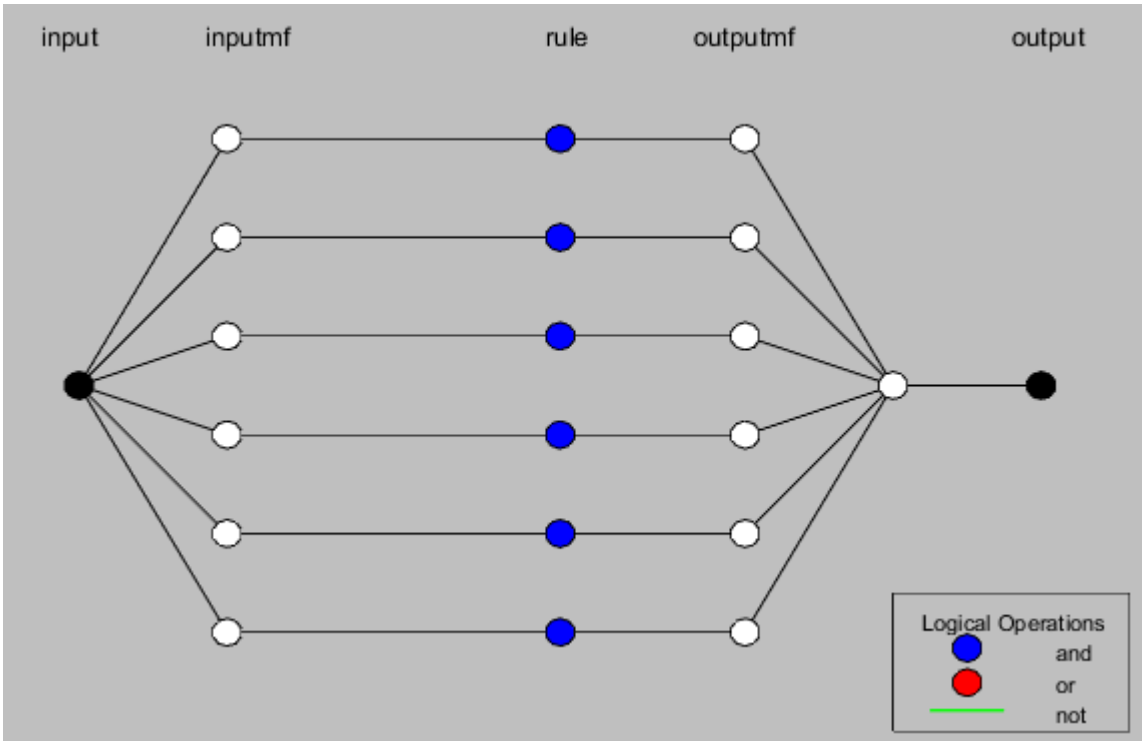

Figure 4-4| ANFIS architecture built in Matlab

Learning of the ANFIS

The adjustment of ANFIS parameters is conducted during the learning phase. For this, a set of data combining inputs and outputs is essential. For performing this phase, the hybrid learning algorithm is used. It is a combination of the error gradient descent and least squares estimation methods. The error gradient descent method adjusts the premises, while the least square ,method (LSM) adjusts the linear parameters (consequent or conclusions).

Learning is iterative until the stop criterion is met, and this criterion could be either the number of iterations or the average error between the desired and generated output values.

One of the most important steps for generating the structure of ANFIS neuro-fuzzy networks is establishing fuzzy inference rules. With the use of an inference mechanism, the rules are defined as combinations of membership functions of various input variables. The input variables are split into a limited number of linguistic values (label), with each

being characterized by a membership function (and their combinations lead to numerous fuzzy inference rules).

ANFIS optimization with the PSO algorithm

Meta-heuristics are optimization methods that allow the acquisition of an approximate value of an optimal solution, where exact optimization techniques fail to give satisfying results. A particular interest is brought to the particle swarm optimization (PSO) method to find optimized membership function parameters. The PSO proposed by Kennedy and Russel Eberhart (1995) was employed in different studies to optimize ANFIS parameters (Alarifi et al. 2019; Shamshirband et al. 2019; Yang et al. 2020).

The algorithm is based on "social interactions" between agents called particles, inspired by the operation of birds seeking food (Shamshirband et al. 2019) to achieve a given objective in a common research space where each particle has a capacity for memorizing and processing information.

In PSO, a mathematical equation modeled social behavior allows guiding particles during their displacement process. The displacement of a particle is influenced by the following three components: inertia, cognitive, and social.

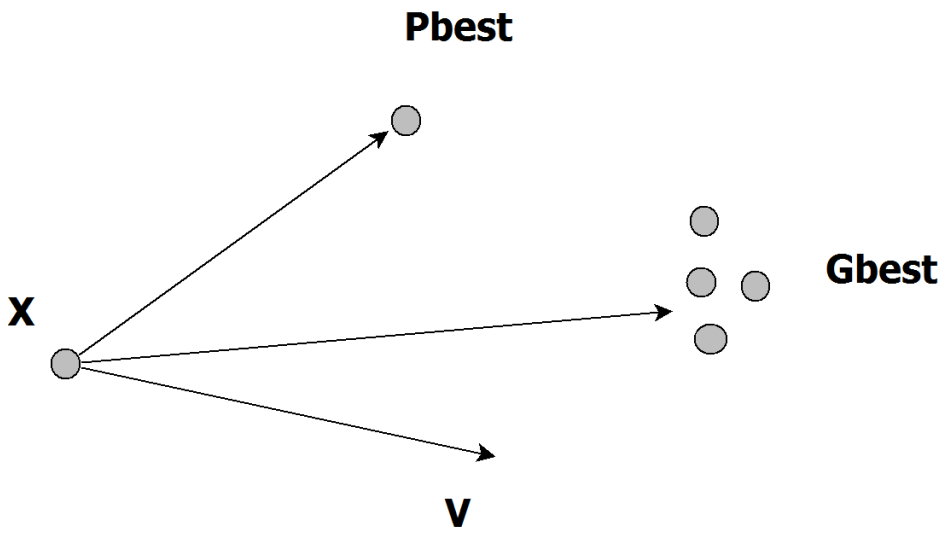

Figure 4-5| Particle displacement

The position and pathway of each particle are described by the following formulas:

$$\boldsymbol{v(t+1) = v(t) + c1.r1.\left(pbest(t) - x(t)\right) + c2.r2.\left(gbest(t) - x(t)\right)},$$

$$\boldsymbol{x(t+1) = x(t) + v(t+1)},$$

where:

vector *x* (the inertia component) represents the current place of a particle;

vector *v* (the cognitive component) stands for the current speed;

vector *pbest* (the social component) means the best placement found by the particle;

gbest represents the optimal solution found by the swarm;

*c*1 and *c*2 stand for the learning constants;

*r*1 and *r*2 are random numbers that range between 0 and 1; and

pbest and *gbest* are updated at each iteration and the process is repeated until the stop criterion is satisfied.

The flowchart below describes the different steps of the optimization process.

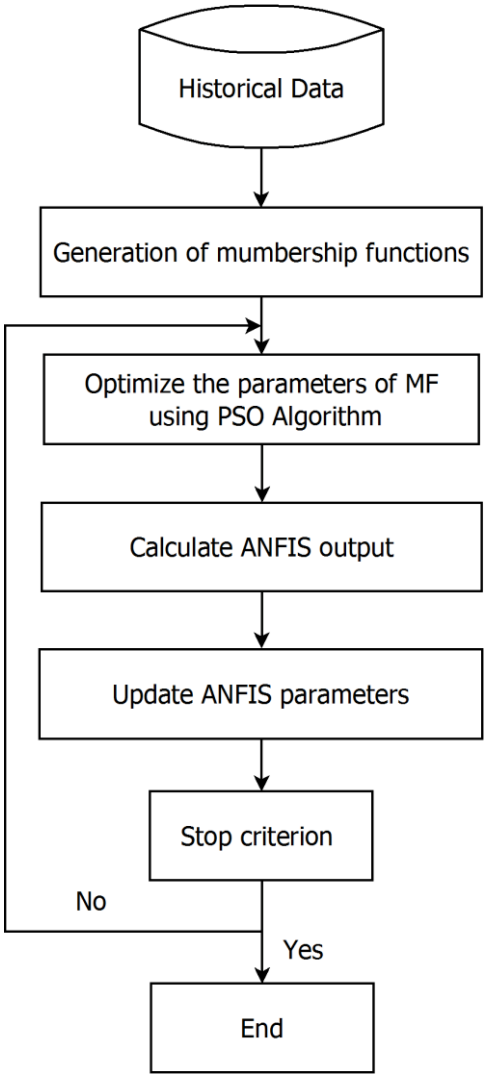

Figure 4-6| Particle swarm optimization process

4.3. Experimental data and site description

Site description

The study area concerns the 3,315-ha watershed, which covers the townships of Tit Mellil, Sidi Moumen, and Sidi Bernoussi (Figure 4-7).

The UDS is equipped with a depth meter and a flow meter at the watershed outlet. The measurements for UDS are recorded at a 15-min time interval, and a rain gauge is located in the watershed to record the rain intensity at a 5-min time interval.

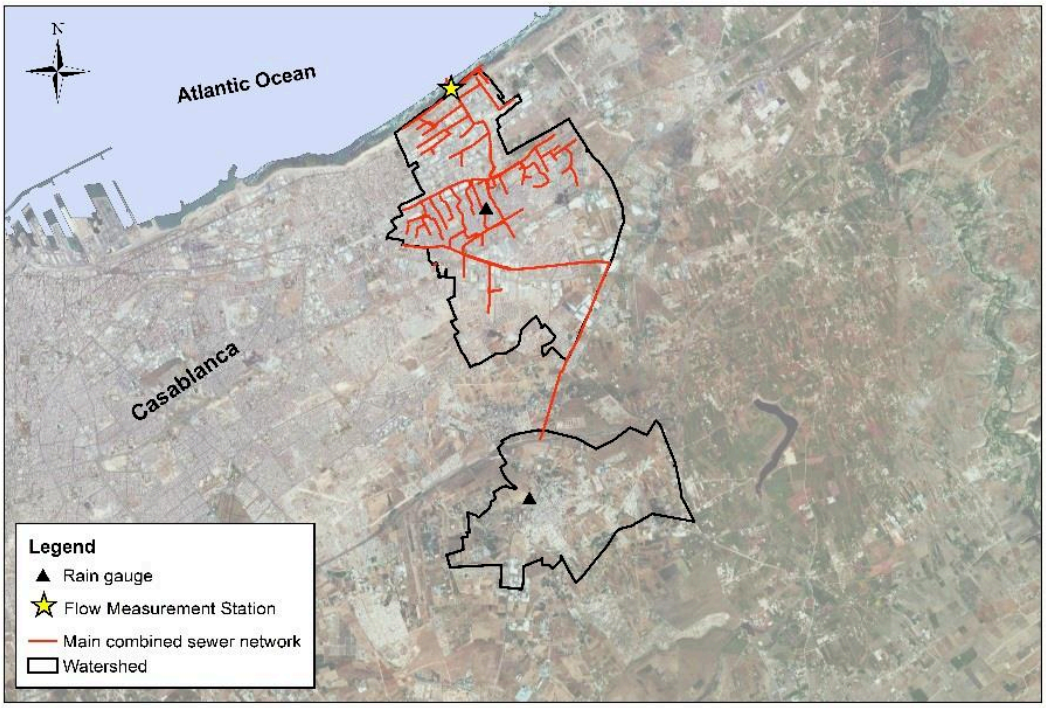

Figure 4-7| Study area, Casablanca

Data collection

The data were extracted from the database for 4 years (January 2015–January 2019). Given that the main sewer system is combined, dry weather flows were removed to keep only the data related to rain flows.

The return periods (RPs) of the dataset were characterized according to intensity–duration curves that relate rainfall intensity with its duration and frequency of occurrence (Figure 4-8).

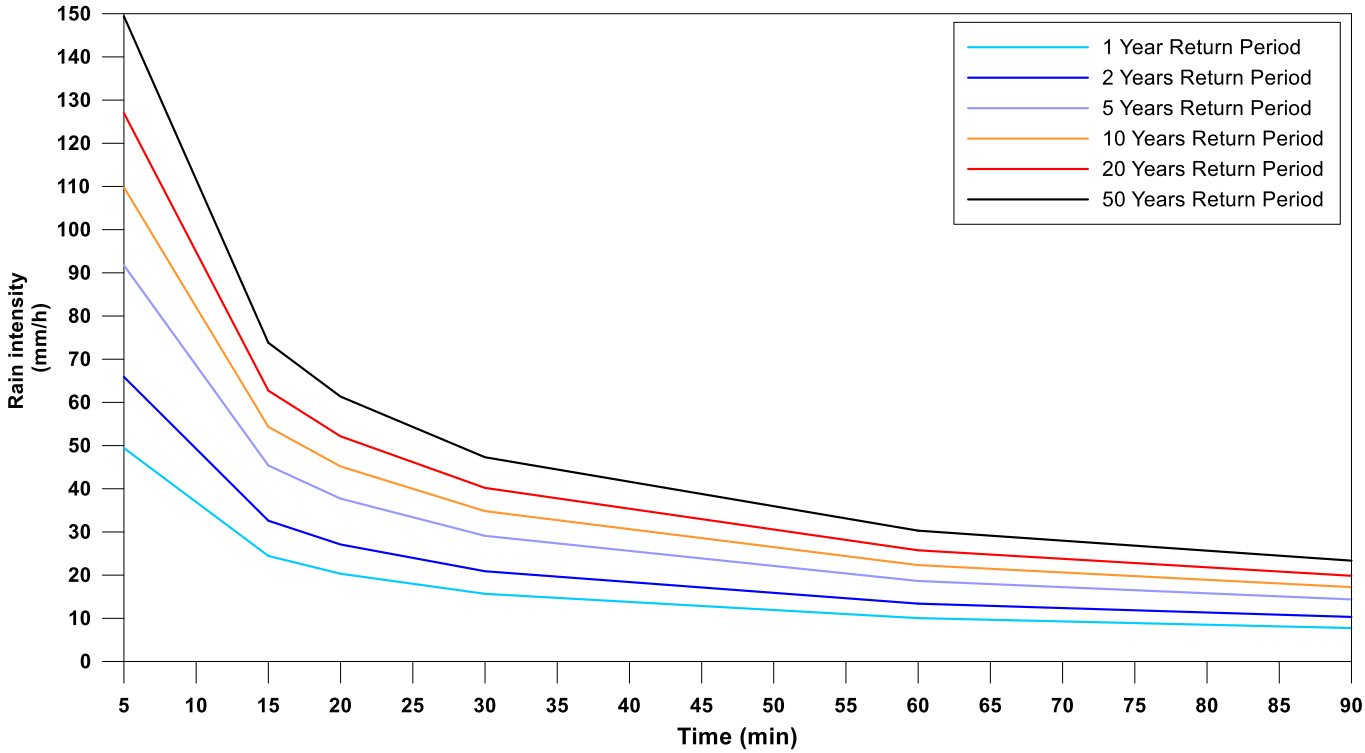

Figure 4-8| Intensity-duration-frequency curves

The rain dataset used in this present work was characterized by RPs summarized in Table 4-1, which shows a dominance of low to medium rains in the dataset representing 90% of the dataset.

Return Period	Percentage of the sample
1 year	58%
2 year	18%
5 year	14%
10 year	2%
20 year	4%
50 year	4%

Table 4-1| Statistics of return periods (RP) of the rain dataset

4.4. Application

The NARX, M5T, RF, and ANFIS-PSO were utilized to predict the stormwater flow at the watershed outlet. The data used in the model construction were rain and strict stormwater flows. All the models were trained on the same 4-year data sample.

A sample of five rain events with different intensities and RPs was used to evaluate the performances of the AI models in predicting stormwater flows for distinct meteorological conditions.

The rainfall RPs used for testing the models are as follows: 10 year RPs (YRPs), 50 YRPs, 2 YRPs, 5 YRPs, and 5 YRPs.

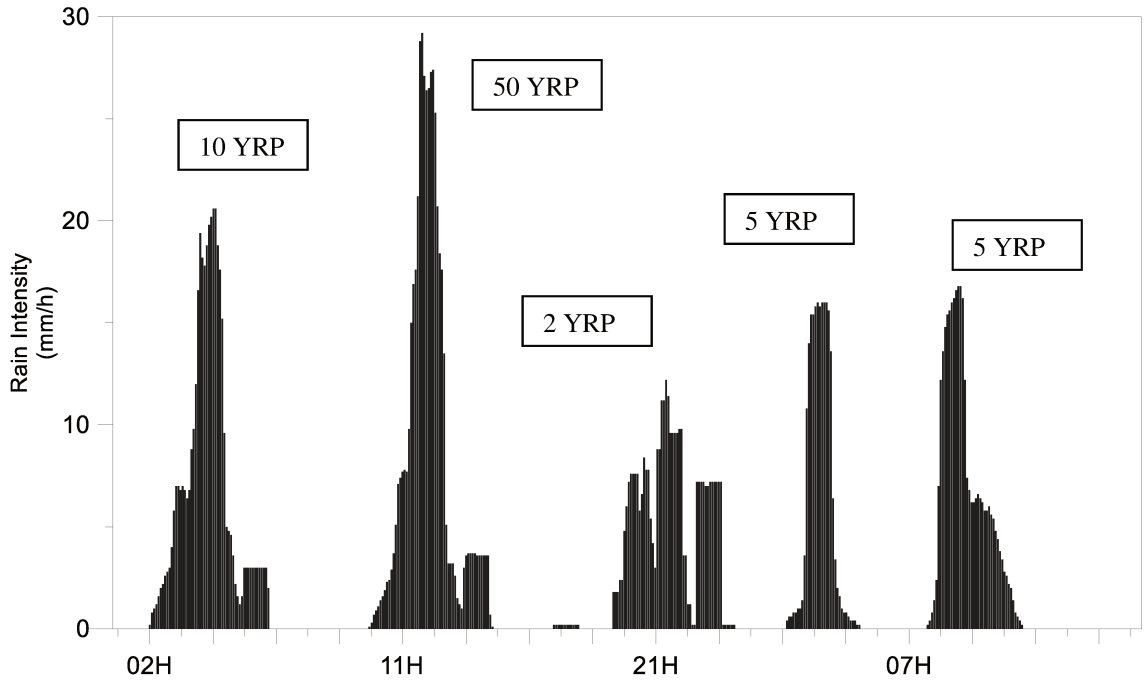

Figure 4-9| Rain dataset used for the stormwater forecast

The model efficiency was examined through a comparison of results and measurements with a Nash–Sutcliffe efficiency and root mean square error calculation.

4.5. Results and discussion

Stormwater forecast for low to medium rainfall intensities:

For the forecasts of stormwater flows for low to medium rainfall intensities, the results in Table 4-2 exhibit the good performances of NARX, M5T, and RF models with a low RMSE and a high NSE where ANFIS-PSO fails, giving satisfying results. Figure 4-10 shows that the NARX model represents better the flow hydrograph with a slight overestimation of the peak flow (nearly 10%) compared with M5T and RF, which gives better results in predicting peak flows.

Stormwater forecast for high rainfall intensities:

For the forecasts of stormwater flows for high rainfall intensities, the results in Table 3 display the poor performance of the ANFIS-PSO model, with a low NSE (0.66) and a high RMSE (3.38m^3 s^{-1}). The NARX, M5T, and RF models show good performances with an NSE greater than 0.95 and an RMSE lower than 1.23 m^3 s^{-1}.

Nonetheless, the analysis of Figure 4-10 affirms that the AI models underestimate the peak flows (roughly 20%) for the 10 YRP rainfall. This underestimation is mainly due to the non-representativeness of the sample of the 10 YRP rainfall events, which barely represents 2% of the dataset.

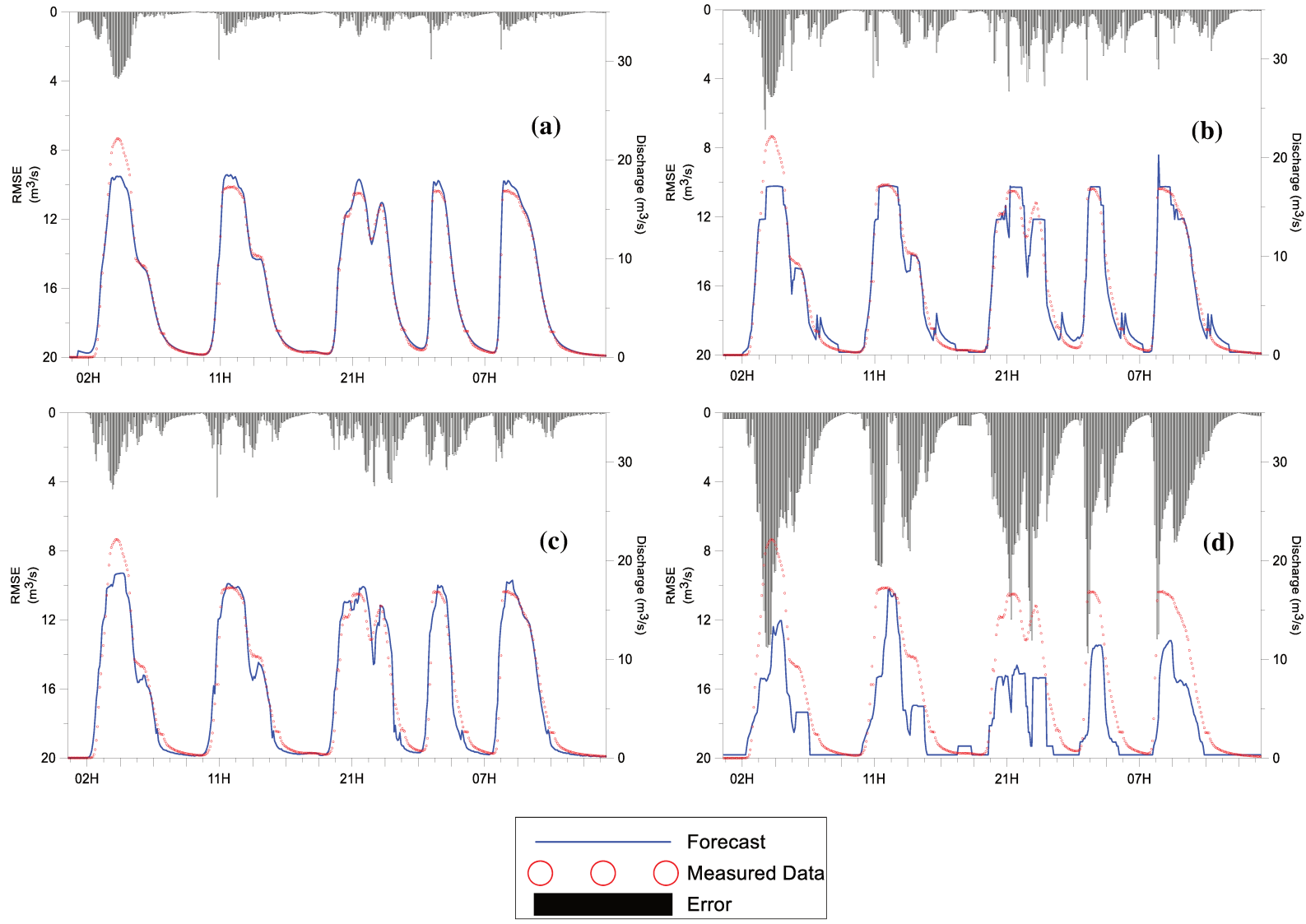

Figure 4-10| Prediction of storm waterflow (a) NARX; (b) M5T; (c) RF; (d) ANFIS-PSO.

	NARX	M5T	RF	ANFIS-PSO
RMSE ($m^3 s^{-1}$)	0,406	1,066	1,291	3,835
NSE	0,996	0,970	0,956	0,611

Table 4-2| Performance statistics of the models for low rainfall events

	NARX	M5T	RF	ANFIS-PSO
RMSE ($m^3 s^{-1}$)	0,831	1,236	1,121	3,380
NSE	0,978	0,952	0,961	0,642

Table 4-3| Performance statistics of the models for high rainfall events

4.6. Conclusion

This chapter presents the use of four AI techniques, namely, NARX, M5T, RF, and ANFIS-PSO, for forecasting urban drainage stormwater discharge using rainfall predictions. They were tested and compared on the data collected from the 3,315-ha watershed area located in Casablanca. The results validate that the NARX, M5T, and RF models provide good results where ANFIS-PSO fails, giving satisfying results. The NARX model shows good performances in modeling all the ranges of flows with a slight overestimation of peak values for low to medium intensities compared with M5T and RF models, which provide good results in peak flow forecasting. The NARX, M5T, ANFIS, and RF models underestimate the peak flows for the 10 YRP rainfalls. This underestimation is mainly due to the non-representativeness of the sample of the 10 YRP rainfall events, which barely represents 2% of the dataset. Over time, the underestimation will be resolved with a larger rainfall dataset and continuous learning of AI models. The efficiency of the SWFM for 10 YRPs can also be improved by training the SWFM models on the hydraulic modeling results of synthetic high-intensity rainfalls.

The SWFM based on the NARX, M5T, and RF models could be easily implemented for practical use in urban drainage systems. The SWFM coupled to a WWFFM can be an efficient tool for predicting flows in combined sewer networks.

4.7. References

Abou Rjeily Y., Abbas O., Sadek M., Shahrour I. and Hage Chehade F. (2017) Flood forecasting within urban drainage systems using NARX neural network, Water Science & Technology

Abraham A. 2005 Adaptation of fuzzy inference system using neural learning. In: Fuzzy Systems Engineering. Studies in Fuzziness and Soft Computing, Nedjah N, de Macedo Mourelle L(eds.), Berlin, Heidelberg, Springer Berlin Heidelberg, 181, 53–83.

Alarifi I. M., Nguyen H. M., Naderi Bakhtiyari A. & Asadi A. 2019 Feasibility of ANFIS-PSO and ANFIS-GA models in predicting thermophysical properties of Al2O3-MWCNT/oil hybrid nanofluid. Materials, 12, 3628.

Azad A., Karami H. & Farzin S. 2018 Prediction of water quality parameters using ANFIS optimized by intelligence algorithms (case study: Gorganrood River). KSCE J. Civ. Eng., 22, 2206–2213.

Azad A., Karami H., Farzin S., Mousavi S. F. & Kisi O. 2019 Modeling river water quality parameters using modified adaptive neuro fuzzy inference system. Water Sci.

Beeneken T., Erbe V., Messmer A., Reder C., Rohlfing R., Scheer M., Schuetze M., Schumacher B., Weilandt M. & Weyand M. 2014 Real time control (RTC) of urban drainage systems — a discussion of the additional efforts compared to conventionally operated systems. Urban Water Journal 10.

Bhattacharya B., Price R. K. & Solomatine D. P. 2007 Machine learning approach to modeling sediment transport. J. Hydraul. Eng., 133(4), 440–450.

Breiman L. 2001 Random forests. Machine Learning, 45, 5–32.

Breiman L., Friedman J., Olshen R. & Stone C. 1984 Classification and regression trees. Statistics/Probability Series. Wadsworth & Brooks/Cole Advanced Books & Software.

Goyal M. K. & Ojha C. S. P. 2014 Evaluation of rule and decision tree induction algorithms for generating climate change scenarios for temperature and pan evaporation on a lake basin. Journal of Hydrologic Engineering, 19(4), 828–835.

Haykin S. 1999 Neural Networks: A Comprehensive Foundation. Prentice-Hall, Englewood Cliffs, N.J.

Jang J. S. R. 1993 ANFIS: adaptive-network-based fuzzy inference system. IEEE Transactions on Systems, Man and Cybernetics, 23(3), 665–685.

Kennedy J. and Eberhart R. 1995 Particle Swarm Optimization. Proceedings of the IEEE International Conference on Neural Networks, 1942-1948.

Mohammadrezapour O., Piri J. & Kisi O. 2019 Comparison of SVM, ANFIS and GEP in modeling monthly potential evapotranspiration in an arid region (case study: Sistan and Baluchestan Province, Iran). Water Supply, 19(2), 392–403.

Pal M. & Deswal S. 2009 M5 model tree based modelling of reference evapotranspiration. Hydrol Process, 23, 1437–1443.

Quinlan J. R. 1992 Learning with continuous classes. In: Proceedings of Australian Joint Conference on Artificial Intelligence, World Scientific Press: Singapore, pp. 343–348.

Rahimikhoob A. 2014 Comparison between M5 model tree and neural networks for estimating reference evapotranspiration in an arid environment. Water Resour. Manage., 28, 657–669.

Shamshirband S., Hadipoor M., Baghban A., Mosavi A., Bukor J. & Várkonyi-Kóczy A. R. 2019 Developing an ANFIS-PSO model to predict mercury emissions in combustion flue gases. Mathematics, 7, 965.

Singh G., Sachdeva S.N. & Pal M. 2016 M5 model tree based predictive modeling of road accidents on non-urban sections of highways in India. Accid. Anal. Prev., 96, 108–117.

Solomatine D. P. & Dulal K. N. 2003 Model trees as an alternative to neural networks in rainfall–runoff modelling. Hydrological Sciences Journal, 48(3), 399–411.

Solomatine D.P. & Xue Y. 2004 M5 model trees compared to neural networks: application to flood forecasting in the upper reach of the Huai River in China. J Hydr Engrg 9(6), 491–501.

Tien Bui D., Khosravi K., Li S., Shahabi H., Panahi M., Singh V. P., Chapi K., Shirzadi A., Panahi S., Chen W. & Bin Ahmad B. 2018 New hybrids of ANFIS with several optimization algorithms for flood susceptibility modeling. Water, 10, 1210.

Yang H., Hasanipanah M. & Tahir M. M. 2020 Intelligent prediction of blasting-induced ground vibration using ANFIS optimized by GA and PSO. Nat. Resour. Res., 29, 739–750.

Zhou P., Li Z. & Snowling S. 2019 A random forest model for inflow prediction at wastewater treatment plants. Stoch Environ Res Risk Assess, 33, 1781–1792.

Chapter 5

Model Predictive Control based on Artificial Intelligence and EPA-SWMM model to reduce CSOs impacts in sewer systems

Urbanization and an increase in precipitation intensities due to climate change, in addition to limited urban drainage systems (UDS) capacity, are the main causes of combined sewer overflows (CSOs) that cause serious water pollution problems in many cities around the world. Model predictive control (MPC) systems offer a new approach to mitigate the impact of CSOs by generating optimal temporally and spatially varied dynamic control strategies of sewer system actuators. This chapter presents a novel MPC based on neural networks for predicting flows, a stormwater management model (SWMM) for flow conveyance, and a genetic algorithm for optimizing the operation of sewer systems and defining the best control strategies. The proposed model was tested on the sewer system of the city of Casablanca in Morocco. The results have shown the efficiency of the developed MPC to reduce CSOs while considering short optimization time thanks to parallel computing.

5.1. Introduction

As results of urbanization and climate change, world agglomerations are facing major environmental issues, particularly those related to pollution that impacts waterbodies. In many cities, the existing combined sewer systems cannot convey all the polluted water to wastewater treatment plants during rain events (Zhao et al. 2019), leading to frequent combined sewer overflows (CSOs). The pollution released by sewer networks can significantly impact the ecosystem by unbalancing its kinetics through the increase of the concentrations of microbiological, mineral, and organic pollutants, thereby leading to oxygen depletion and eutrophication rise (Chocat 1997; McLellan et al. 2007; Weyrauch et al. 2010; Passerat et al. 2011; Phillips et al. 2012; Brokamp et al. 2017). Climatic factors, such as the quantity and intensity of precipitation, are key factors that determine the severity of CSO discharges (Botturi et al. 2020). According to future meteorological projection scenarios, a substantial increase in storm intensities and frequencies will be recorded, thereby causing more frequent CSOs (Yazdanfar & Sharma 2015; Alves et al. 2016; Jean et al. 2018).

Multiple research studies have discussed the impact of CSOs on ecosystems. Viviano et al. (2017) demonstrated through a complete monitoring scheme based on caffeine and turbidity that more than 50% of the total phosphorus of the Lambro River is due to sewer network overflows by rainy weather. Studies conducted by Phillips et al. (2012) and Launay et al. (2016) affirmed that even if the volume of CSOs represents a small part of the annual volume of wastewater, their impact is not negligible and can contribute up to 95% of the annual pollution caused by various pollutants.

Several actions can minimize CSOs and improve the receiving environment quality. Green infrastructures play a significant role in limiting peak flows and pollution, and they also relieve the downstream sewer network by regulating the flow or infiltrating water. Storage basins allow the storage of a large volume of polluted water during rain events and release it back to sewer networks once the rainfall events are over. However, the construction of basins remains complicated because of the lack of space, construction, and maintenance costs (Garofalo et al. 2017). One of the emerging ways to reduce CSOs is by performing the advanced real-time control of urban drainage systems (UDS) based on model predictive control (MPC), which computes optimal control strategies on the basis of deterministic rain forecasts. MPC has exhibited the efficient and cost-effective management of sewer systems to reduce pollution and energy consumption through several research case studies. Lund et al. (2020) used an integrated stormwater inflow control to mitigate CSOs in Copenhagen by dynamically controlling stormwater inflow to the combined sewer system in real-time. This control was performed with a MPC on the basis of convex optimization including a linear internal surrogate. The MPC was tested on 18 rainfalls that have caused CSOs. Four of the 18 events were avoided, and the total CSO volume was reduced by 98.4% of the potential reducible volume. In addition, Bonamente et al. (2020) demonstrated through a study conducted on a sewer system that a MPC based on the NSGA II optimization algorithm can save energy consumption up to 32% and an overflow of approximately 10%. Rathnayake and Faisal Anwar (2019) also successfully applied a MPC to the combined sewer network of Liverpool in the

United Kingdom using the NSGA II and SWMM models. The proposed model minimized the pollution load in the receiving water body and wastewater treatment and pumping costs in the sewer system. Although the proposed algorithm produced satisfactory results, the solution algorithm could not be applied to real-time control due to the simulation time needed to be improved. Considering that the reaction time in urban sewer systems is usually short, for UDS with many decision variables, such as a high number of gate valves or flow-regulating structures, the algorithms running time may be very long and unsuitable for real-time control purposes.

This work aims to fill the gap in the MPC research field by presenting the development and investigation of the performance of a MPC, based on robust genetic algorithms (GAs) and neural networks that have the advantage of performing fast calculations that fit the needs of such systems. Further, it aims to demonstrate the benefits of MPC associated with parallel computing that offers a sufficient lead time to define the global optimal control strategies of weir gate valves to reduce CSOs in smart and durable city.

5.2. Material and Methods

The control of sewer networks is based on regulated structures (e.g., gates and pumps), most of the time controlled locally, and does not depend on communication with other facilities or the other parts of the sewer system. Local control strategies may represent a good solution in the case of one actuator, but in the case of complex sewer systems where many actuators must operate jointly, a dynamic global control system becomes necessary. In dynamic systems, control actions are based on the time-varying requirements of interests in a sewer system, the water system load, and the watershed dynamic processes.

The current work aims to develop a robust dynamic MPC system for implementing global control strategies aiming at reducing CSOs through the dynamic management of gate valves. The MPC system combines a supervisory control and data acquisition (SCADA) that receives information and measures from monitoring sensors and implements control actions, hydraulic modeling software for flow conveyance, and artificial intelligence

algorithms for forecasting and control optimization purposes. MPC is based on the following three main parts (Figure 5-1):

- The first part concerns the forecast of wastewater and rainwater flows at watershed outlets representing strategic control points.
- The second part comprises real-time modeling to better represent the network state at any time.
- The third part is about predictive modeling and optimization.

.

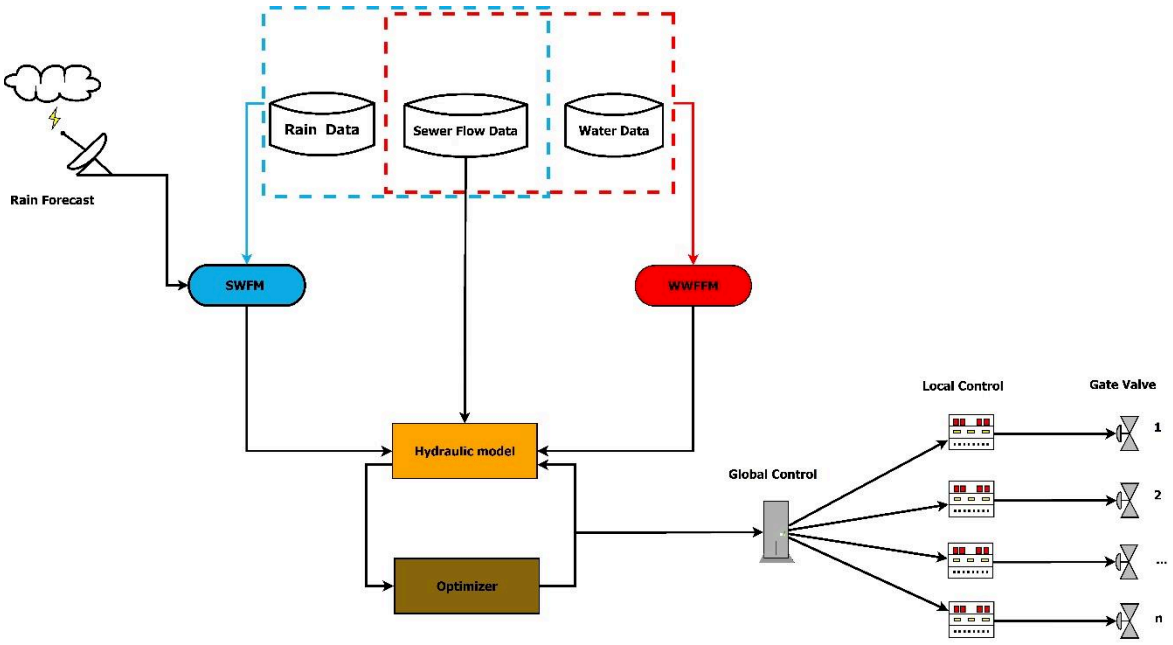

Figure 5-1| Model Predictive Control architecture

5.2.1. Flow forecasting in sewer networks

Without a robust model, forecasting flows in sewer networks constitute significant uncertainties for operators. Short-term forecasts are an essential component for any MPC system and significantly improve the reaction time. Nevertheless, given that the main sewer system is combined and considering the spatial variation of rainfalls, having a flow forecast of dry and rainy weather flows is necessary. The forecasting of stormwater discharges is performed with a stormwater forecasting model (SWFM) based on the

NARX neural networks that have the advantage of performing fast calculations and providing quick and accurate stormwater discharges for anticipatory models (El Ghazouli et al. 2019). This model takes rainfall forecasts as inputs once available and returns as output stormwater discharges. Given that a nowcasting method based on extrapolation gives reasonable values for short-term (0–180 min) rainfall forecasts (Bowler et al. 2006; Berenguer et al. 2011), the SWFM will run with the latest updated rainfall forecasts every hour.

Instantaneous dry weather flows at watershed outlets are predicted with a wastewater flow forecasting model (WWFFM). The WWFFM is an artificial neural network (ANN) black-box model that handles nonlinear problems taking real-time water consumption, and previous wastewater flow records as inputs (El Ghazouli et al. 2021). The output of the model is a 5-h forecasted wastewater flow time series. The combination of the SWFM and the WWFFM gives combined sewer discharge inputs for the SWMM model for flow conveyance and optimization purposes.

5.2.2. Real-time modeling

The MPC system uses the EPA SWMM engine to compute flow conveyance on the basis of a simplified model that comprises the main branches of the interception system of the sewer networks of Casablanca, as can be seen in Figure 5-2. The model is connected to a SCADA and continuously updated with real-time data. Flow rates at the outlet of the watersheds and orifice opening status are automatically set to the same values as those observed in the field. Moreover, the real-time model is automatically updated every hour with the last few hours data. At the end of each model run, a Hotstart file containing the system boundary conditions is generated and will be employed for the next simulation with stormwater and dry weather flow forecasts as inputs.

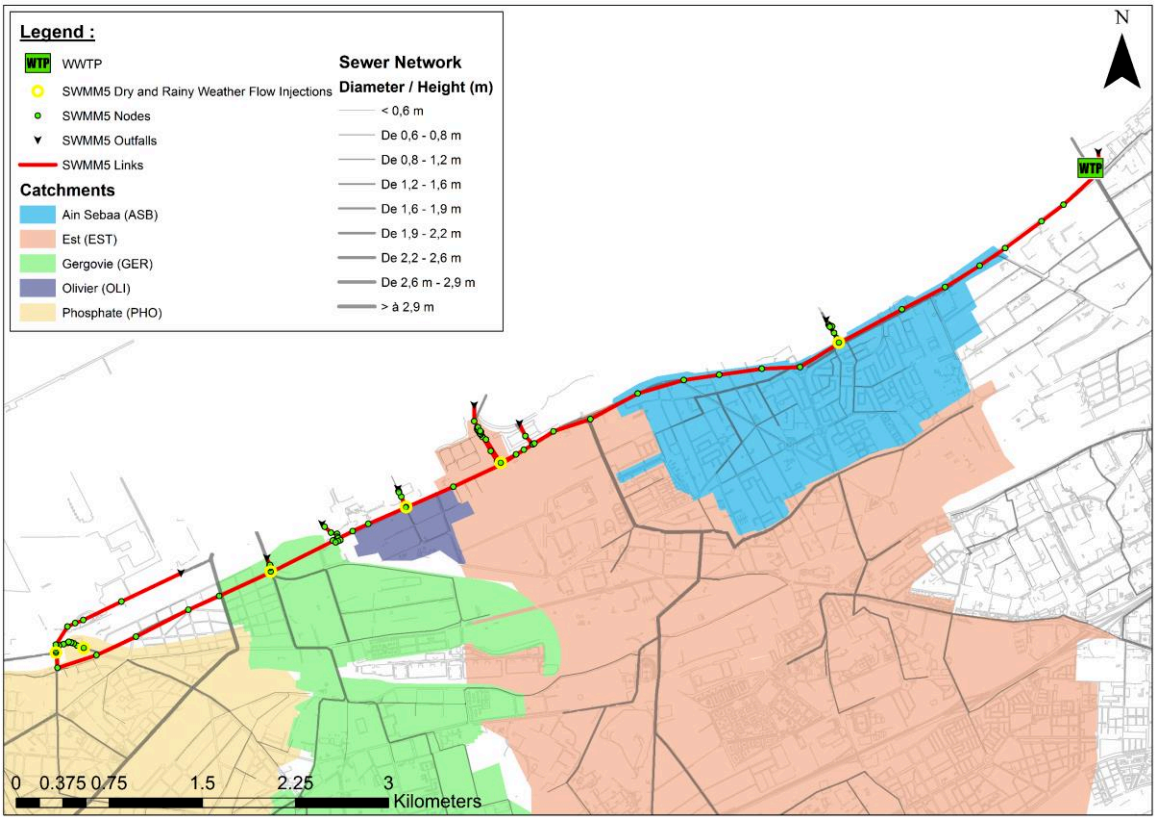

Figure 5-2| Architecture of the Simplified SWMM Model

5.2.3. Optimization of the operational system

The optimization section consists of algorithms able to set optimal operating control strategies while considering various constraints, e.g., the maximum flow of the wastewater treatment plant (WWTP). GAs are widely utilized and present their efficiency to solve many optimization problems in many fields, specifically in water. We can cite the works of Tayfur et al (2009) for predicting peak flows, Li et al. (2020) for water resource management, Bostan et al. (2019) for the optimal design of shock dampers, Montes et al. (2020) for predicting bedload sediment transport in sewer networks, and Hassan et al. (2020) for the optimal design of sewer networks. Therefore, GAs are chosen to optimize the sewer system operating as part of this work. GAs are inspired by the evolution theory of Darwin (1859) and, more specifically, natural selection, reproduction, and the survival of the fittest. In addition, they belong to the larger class of evolutionary algorithms. They were also developed by Holland (1962) in the 1970s and were

popularized in the late 1980s and the early 1990s (Davis 1987; Goldberg 1989; Alliot & Schiex 1993; Forrest 1993).

The MPC is designed to be robust enough to define optimal strategies for managing the sewer system. The optimization of the objective function that we seek to minimize is reducing CSOs by maximizing the treated volume of polluted water at the WWTP. The optimization work involves adjusting the system decision variables that correspond to gate valve opening status at each time of the simulation horizon during different generations considering the operation of constraints, which are mainly the maximum flow capacities at the entrance of the WWTP, by applying a succession of operators to population individuals. The flow chart below describes the distinct steps of GAs.

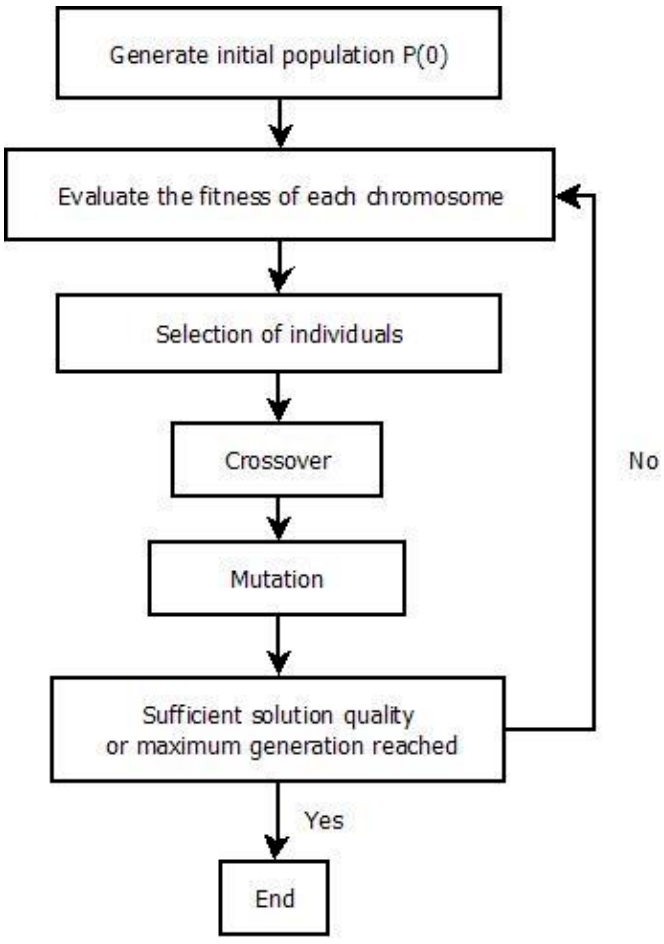

Figure 5-3| Flow Chart of Genetic Algorithms

First, an initial population (P (0)) of gate valve status is generated. This population contains chromosomes distributed in the solution space with varied genetic material defined in a given interval. The choice of the initial population strongly conditions the algorithm's convergence. The fitness of each chromosome is evaluated, and the best individuals are selected for reproduction. Multiple selection methods exist in the literature. We can cite the roulette wheel, tournament, and ranking methods. Once the selection operation is conducted for the current population (P (t)), the crossover operator is then applied. The crossover operation used by GAs is the computer transposition of the mechanism, which allows, in nature, the production of chromosomes that partially inherit the characteristics of parents. Its fundamental role is to enrich the population diversity by manipulating the structure of chromosomes through the recombination of information present in the genetic heritage of individuals.

The newly generated individuals are then submitted to the mutation operator. This operator allows GAs to better search the space of solutions by changing the allelic value of the gene with a very low mutation probability, which is generally between 0.01 and 0.001 (Fogel et al. 2000).

The last step in the iterative process is to incorporate new solutions into the current population. The new solutions are added to the current population, thereby replacing the old solutions. Usually, the best solutions replace the worst ones and improve the population. This process (Figure 5-3) is repeated until a stop criterion is met, and this criterion can be a determined number of generations or a particular value of the objective function.

5.2.4. Application on the sewer network of Casablanca (Morocco)

The sewer network of the eastern part of Casablanca is used to implement and evaluate the proposed MPC. The total area of the studied sector is approximately 41.6 km² (Figure 5-4). It comprises parallel watersheds with combined sewer networks.

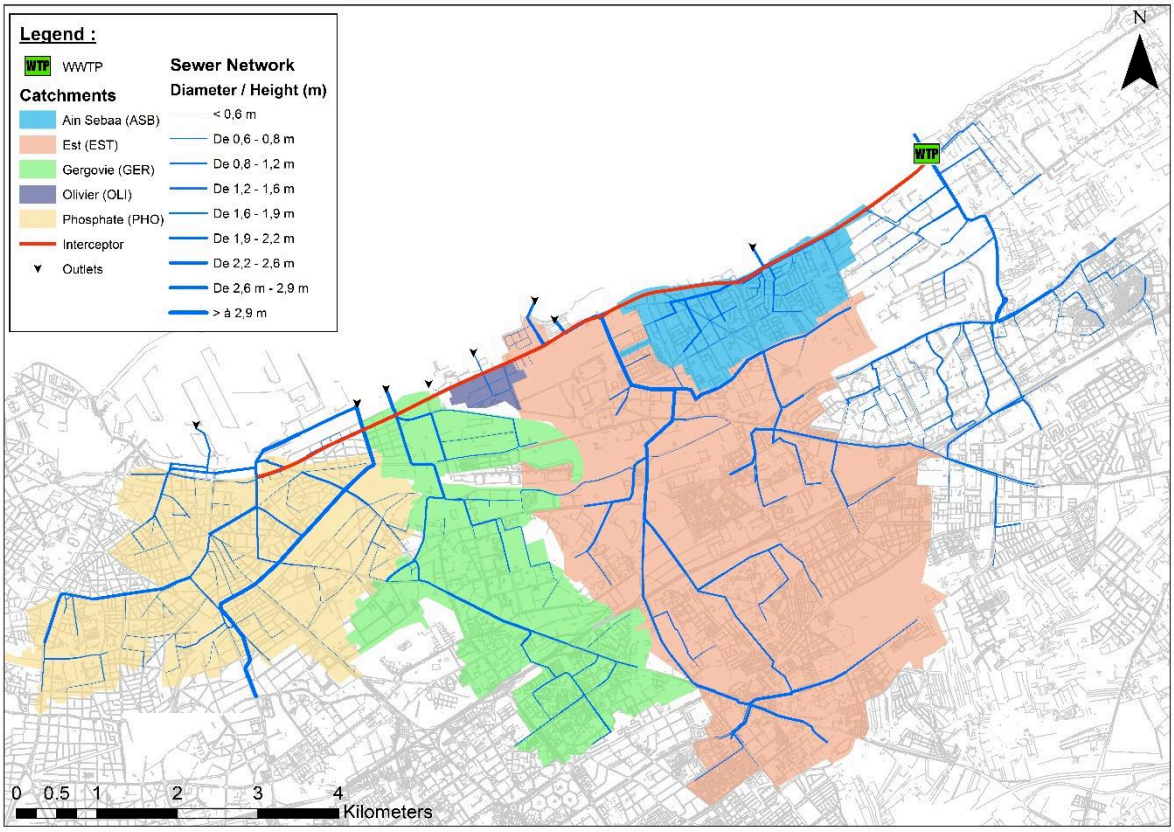

Figure 5-4| Sewer network of the eastern part of Casablanca

The main sewer network outlets of these watersheds are historically discharged into the sea. An interceptor has been designed to convey dry weather flows to the treatment plant and discharges the excess water into the sea by rainy weather via frontal or side weirs. Additionally, it consists of a pipe of 9.5 km with a maximum capacity constrained by the capacity of a lift station (6.5 m^3/s) downstream at the entrance of the WWTP. The interception system (Figure 5-5) at each branch level is equipped with gate valves that control the flow diverted to the WWTP. These valves are modeled as orifices in our SWMM model. Today, by rainy weather and in the absence of control strategies, the gate valves are closed, and the polluted water is discharged directly into the sea.

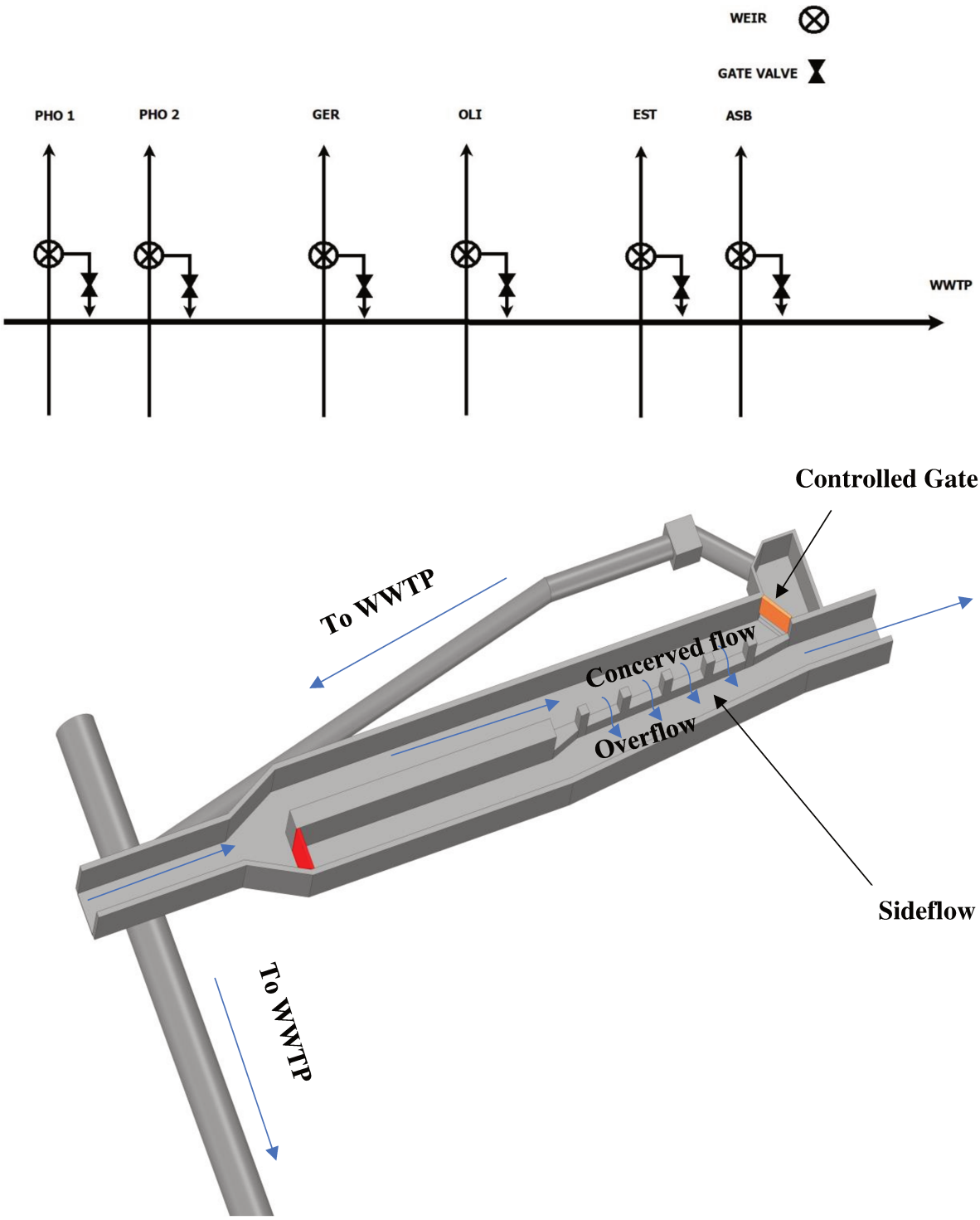

Figure 5-5| Interception system

The developed algorithm on the sewer network of Casablanca considers one objective function (Obj*Fun*) that is formulated to minimize CSOs by maximizing the total treated

volume. The mathematical expression of the objective function is given in Equation (5-1):

$$\mathbf{Obj}\boldsymbol{Fun} = -\sum_{i=1}^{n}\left(\boldsymbol{V}_{x;i}\right), \textbf{(5-1)}$$

where V is the intercepted volume at branch x at a given timestep (i).

The above-mentioned objective function is under a set of nonlinear constraints. A constraint is set such that the instantaneous flow rate at the WWTP entrance should not exceed its maximum capacity. The mathematical expression of the constraint is given in Equation (5-2):

$$\boldsymbol{Qt} \leq \boldsymbol{Qmax}, \textbf{(5-2)}$$

where Qt and $Qmax$ are the flow rates at the entrance of the WWTP at timestep t.

The number of decision variables (n) corresponds to the different states (St) of the orifices for the simulation duration. The decision variable values are bounded between 0, which corresponds to a closed valve, and 1, which represents a totally opened valve. They can take a value among the following ones [0 0.1 0.2 0.3 0.4 0.5 0.6 0.7 0.8 0.9 1]. The MPC result is an optimal gate valve control schedule with a 30-min timestep that reduces CSOs in the ocean.

The MPC is initially run on the basis of a one-year return period (YRP) double-triangle rainfall hyetograph with a total duration of 1 h, an intense duration of 10 min, and a simulation time of 3 h. To evaluate the performance of GA and guide the choice of the population size to obtain an accurate solution in reasonable computational time, the optimization calculations are first performed in serial computing for different population sizes composed of 10, 20, 40, 60, 80, and 100 individuals over 100 generations. This optimization problem comprises 36 decision variables corresponding to the states of six orifices for a simulation horizon of 3 h with six timesteps of 30 min.

Once the suitable numbers of population and generation are chosen, MPC is then evaluated on a real rainfall event recorded on 11 December 2017. The event has been marked by two successive rainfalls with a return period of 5 years, a cumulative rain of 38 mm, and a total duration of 6 h. For this event, MPC runs a simulation every 2 h with a 5-h simulation horizon. For this problem, the number of decision variables for every run is equal to 60 and corresponds to the states of the orifices over the simulation time.

For problems with a high number of decision variables, the running time of the algorithm may be very long. Parallel computation is a technique that reduces computational time by distributing the population and evaluating their fitness over several workers. Parallelization tasks are conducted for this event, and a comparison of the performance times according to a different number of threads (workers) is performed. All the simulations are performed on the same desktop PC (CPU: AMD Ryzen Threadripper 3970X 4.5 GHz, RAM: 128 GB).

5.3. Results and discussion

5.3.1. Serial computing

Simulation results for distinct population sizes (Table 5-1 and Figure 5-6) applied to one YRP rainfall event validate that the MPC demonstrates its ability to reduce CSOs into the sea by maximizing the volume treated without exceeding the maximum flow at the WWTP. We can notice that population size significantly impacts the final solution determined by GAs.

Population size	10	20	40	50	60	80	100
Treated water volume (m^3)	53,978	53,674	55,110	55,153	54,707	54,950	54,950

Table 5-1| Optimized Flow for Different Population Sizes

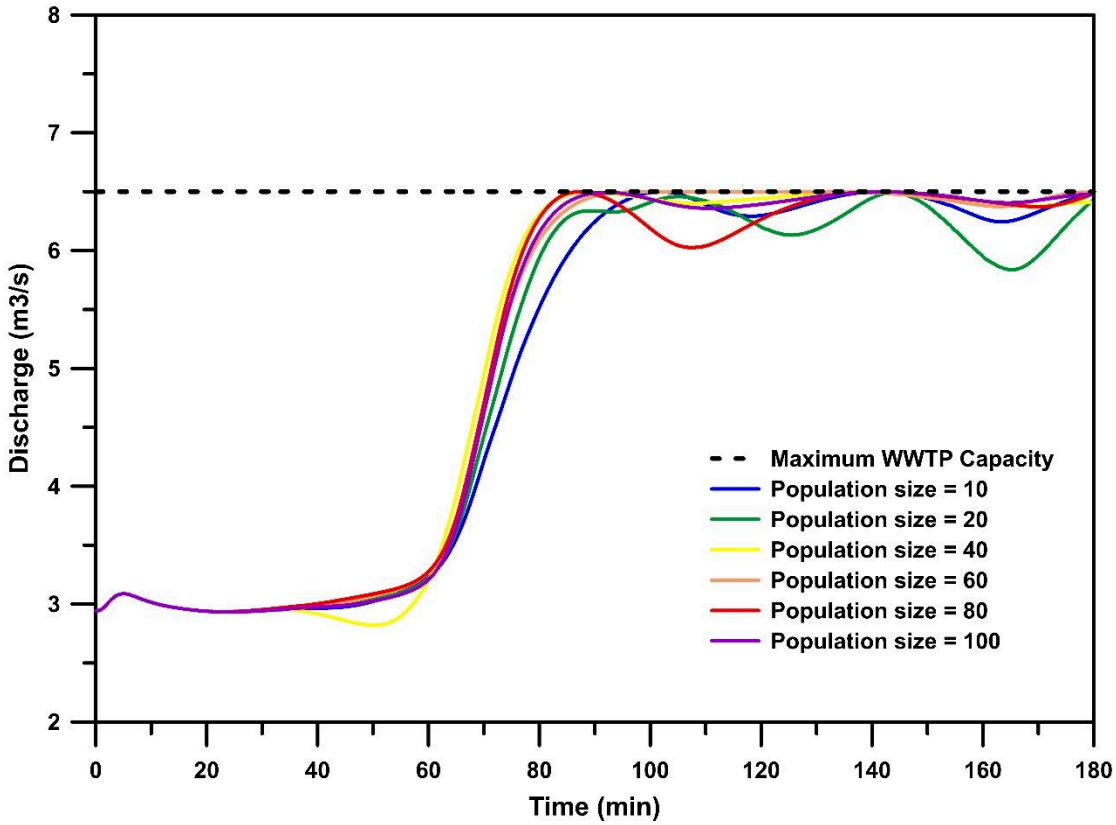

Figure 5-6| Optimized Flow for Different Population Sizes

The analysis of Figure 5-7, which presents the evolution of fitness according to generation numbers, verifies that the larger the population size, the more the algorithm converges toward an optimal solution in the first iterations of the calculation. We can also observe that the number of generations becomes negligible on the convergence as soon as we exceed the generation equal to 60.

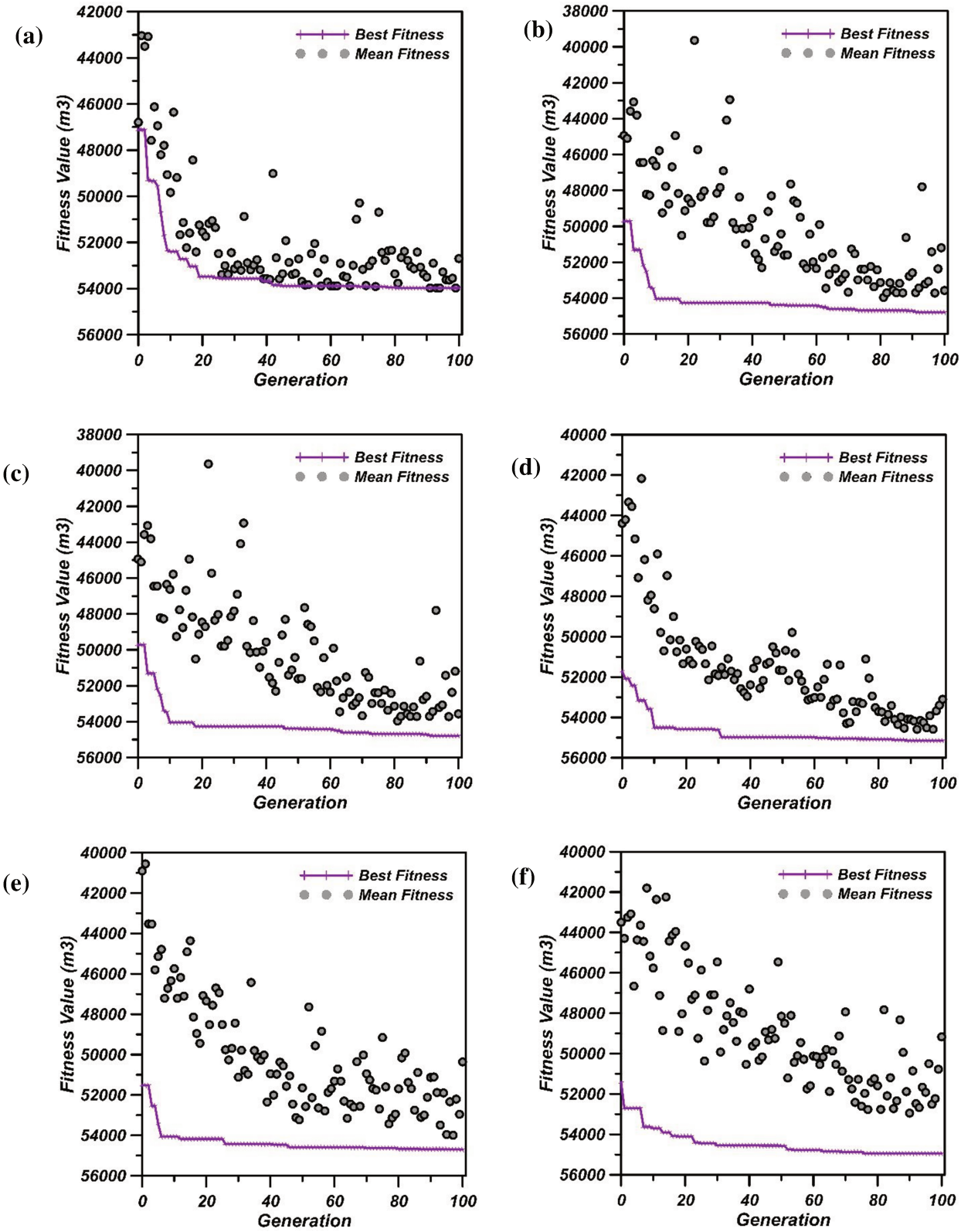

Figure 5-7| Fitness with Populations Equal to (a) 10; (b) 20; (c) 40; (d) 60; (e) 80; and (f) 100

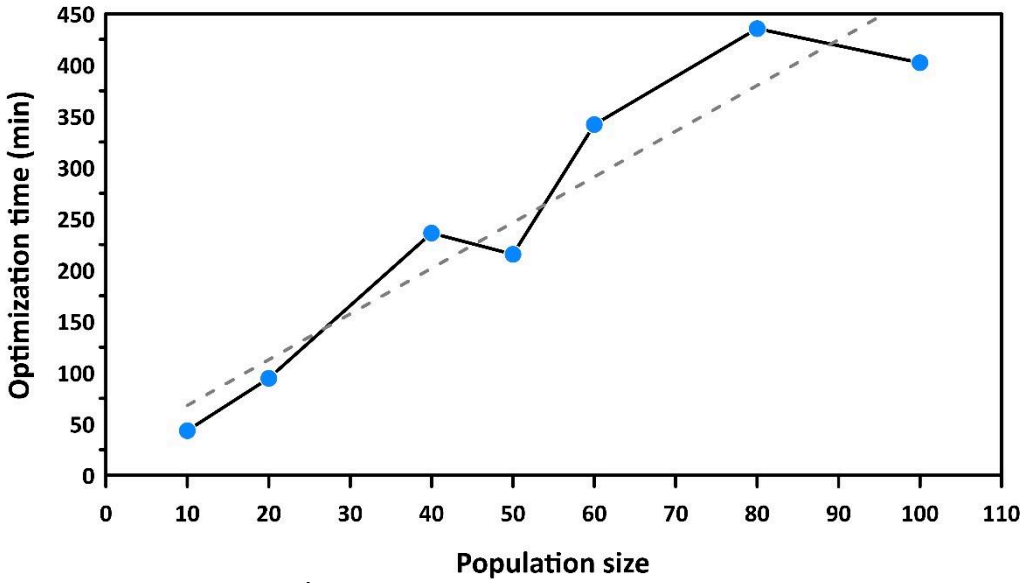

Figure 5-8| Optimization Time Versus Population Size

Figure 5-8 depicts the linear relationship between the computation time and the population size. Computation time is a critical component in MPC systems, and it must be reduced. The analysis of the various results confirms that population size and a generation number equal to 60 appear to be a good compromise between the algorithm performance in finding an optimal solution and the computation time. Hence, population size and a number of generations equal to 60 are applied for the parallel calculation for the 11 December 2017 rainfall event. The detailed performances and the valves sceduels are reported in appendice 1 for the different population sizes.

5.3.2. Parallel computing

For the 11 December 2017 rainfall event, the MPC performed four runs with a 5-h simulation horizon. These simulations are updated every 2 h to consider recent and accurate sewer network states, boundary conditions, and rainfall forecasts, allowing to define an operating schedule for the various control valves over 5 h with a 30-min timestep for each simulation (Figure 5-9).

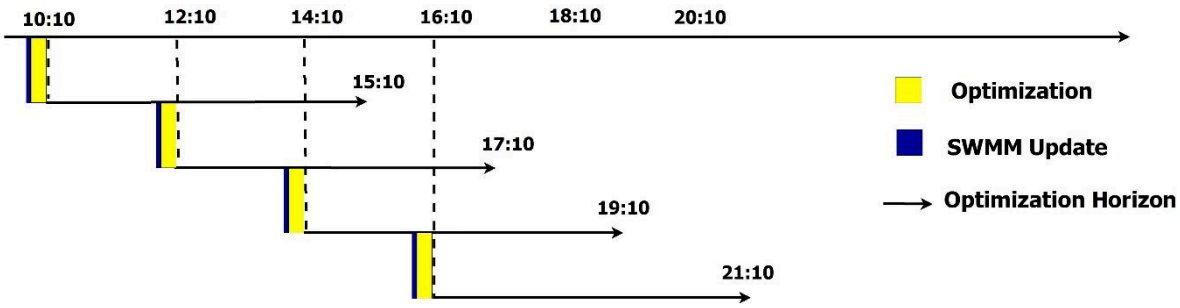

Figure 5-9| Process of the MPC Strategy

For the rainfalls of 11 December 2017, a comparison of the performance times according to the different numbers of threads (workers) is performed. Figure 5-10 illustrates that parallel computing can significantly reduce computing time from 4 092 s for four threads to 890 s for 64 threads on the same processor. However, parallel computing performance decreases exponentially as a function of the number of threads employed in the simulation. Above 32 threads, the number of threads has no significant impact on the solution time. Moreover, for more proactivity, the computation time could be reduced further by parallelizing computation on several processors.

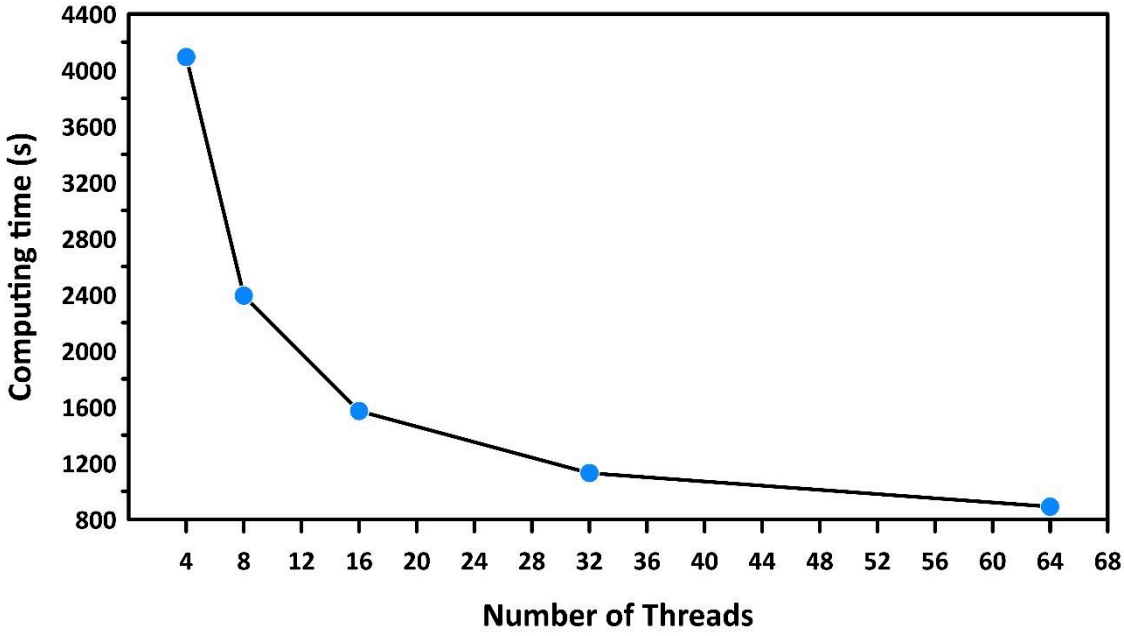

Figure 5-10| Computation time Versus Number of Threads

Figure 5-11 exhibits that the MPC developed as part of this work gives good results and enhances the efficiency of the sewer system of Casablanca, thereby allowing to convey to the WWTP in addition to strict wastewater a volume of 146 830 m3 of polluted rainwater without exceeding the maximum flow of the WWTP. The MPC managed the rainy event of 11 December 2017 by generating a schedule (Figure 5-12) for controlling the gate valves at the interception structures. Furthermore, we can notice that a lack of a control strategy would cause disturbances and flooding at the lifting station at the entrance of the treatment plant with a peak flow rate exceeding 8.5 m^3 /s.

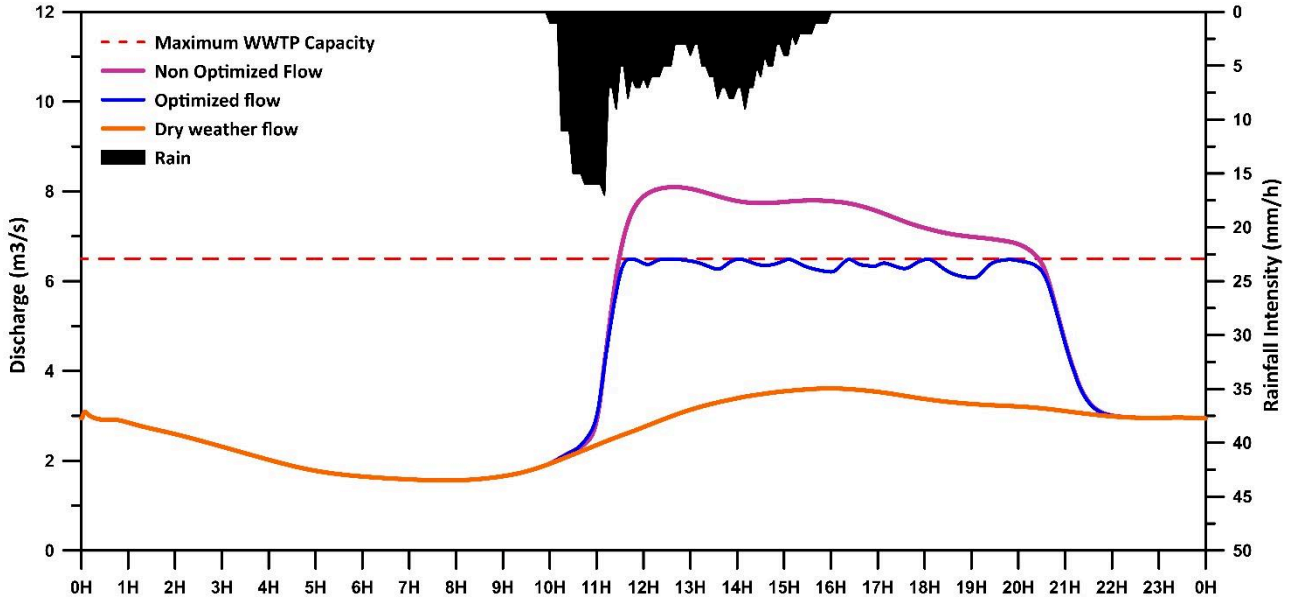

Figure 5-11| Optimized Flow for the Rainfalls of 11 December 2017

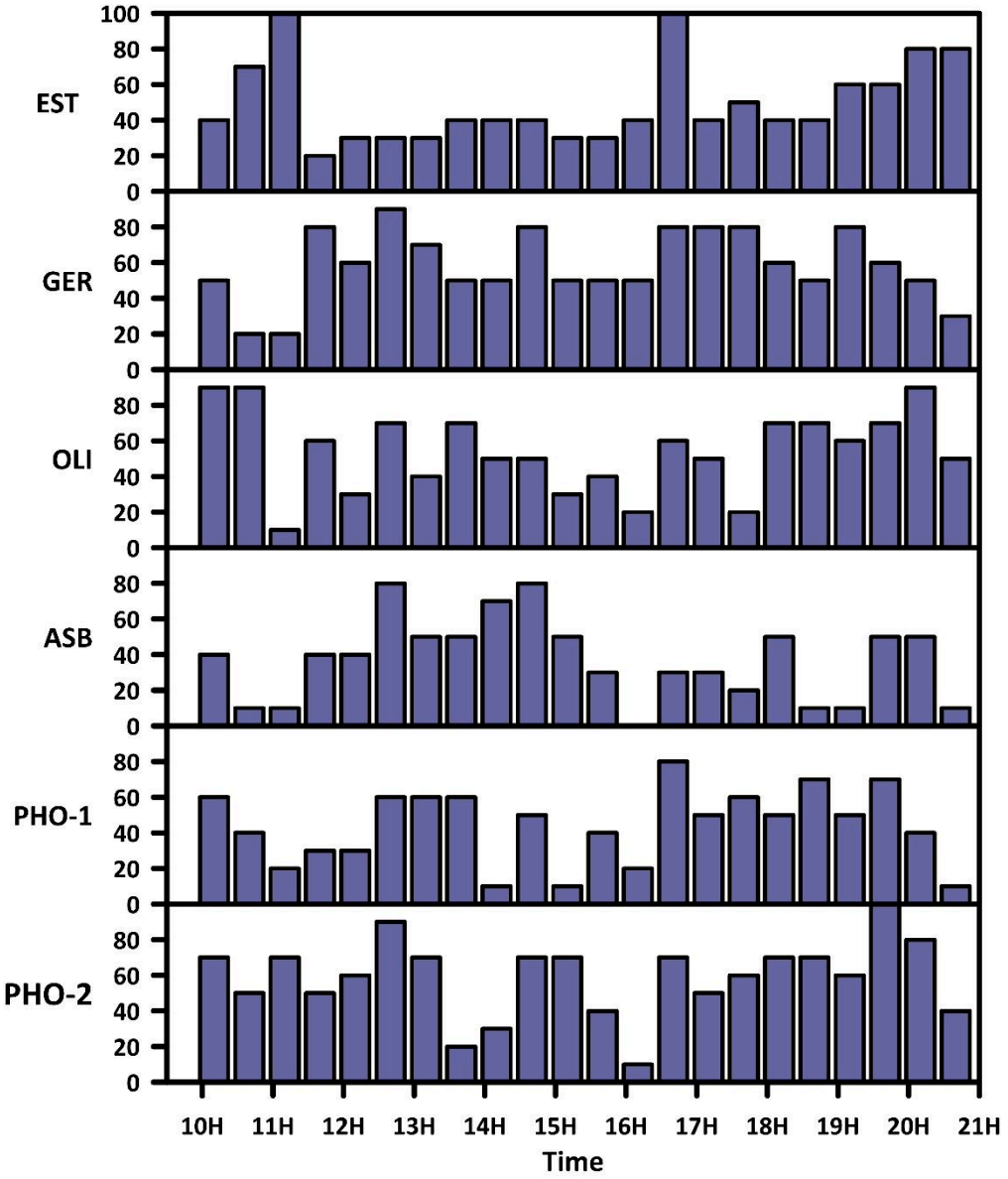

Figure 5-12| Gate Valves Percentage Opening Schedules for the Rainfalls of 11 December 2017

5.4. Conclusions

This chapter presented a novel MPC based on neural networks for predicting flows and a GA for optimizing the operation of the sewer system of Casablanca. The MPC demonstrates high efficiency in reducing CSOs in the receiving environment by generating optimal temporally and spatially varied dynamic control strategies of the gate valves of the sewer system. This MPC could benefit municipalities around the world

facing environmental issues and their consequences, such as CSOs and floods. As part of this work, we determined the best population size and the generation number that present a compromise between the algorithm performance in finding an optimal solution and the computation time. The parallelization of calculations allows the reduction of the computation time considerably and makes the MPC more proactive. However, since the MPC relies on weather forecasts, handling the uncertainty is required to successfully introduce the use of rainfall forecasts in operational management systems. Long-term verification analysis is needed to assess the quality of the forecasts for a particular sewer system. If this is satisfactory, a verification analysis is needed to test the decision rules and control strategies, given the forecasts, so that operators can see the effect of potential management strategies and avoid disasters.

In the continuity of this work, a pollution measurement campaign will be conducted at the outlet of each watershed to determine the impact of CSOs on the natural environment and will be completed by two-dimensional hydraulic modeling of the dispersion of pollution into the sea. Thus, on the basis of these future results, the objective function will be adapted by weighting the volumes intercepted at the level of each branch according to the identified impact risk.

5.5. References

Alliot J. M. & Schiex T. 1993 Intelligence artificielle et informatique théorique. *Toulouse. Cepadues.*

Alves A., Sanchez A., Vojinovic Z., Seyoum S., Babel M. & Brdjanovic D. 2016 Evolutionary and holistic assessment of green-grey infrastructure for CSO reduction. *Water*, **8**(9), 402.

Berenguer M., Sempere-Torres D. & Pegram G. G. S. 2011 SBMcast — an ensemble nowcasting technique to assess the uncertainty in rainfall forecasts by Lagrangian extrapolation. *Journal of Hydrology*, **404**(3–4), 226–240.

Bonamente E., Termite L. F., Garinei A., Menculini L., Marconi M., Piccioni E., Biondi L. & Rossi G. 2020 Run-time optimisation of sewer remote control systems using genetic algorithms and multi-criteria decision analysis: CSO and energy consumption reduction. *Civil Engineering and Environmental Systems*, **37**(1–2), 62–79.

Bostan M., Akhtari A. A., Bonakdari H. & Jalili F. 2019 Optimal design for shock damper with genetic algorithm to control water hammer effects in complex water distribution systems. *Water Resources Management*, **33**(5), 1665–1681.

Botturi A., Ozbayram E. G., Tondera K., Gilbert N. I., Rouault P., Caradot N., Gutierrez O., Daneshgar S., Frison N., Akyol Ç., Foglia A., Eusebi A. L. & Fatone F. 2020 Combined sewer overflows: a critical review on best practice and innovative solutions to mitigate impacts on environment and human health. *Critical Reviews in Environmental Science and Technology*, **51**(15), 1585–1618.

Bowler N. E., Pierce C. E. & Seed A. W. 2006 STEPS: a probabilistic precipitation forecasting scheme which merges an extrapolation nowcast with downscaled NWP. *Quarterly Journal of the Royal Meteorological Society*, **132**(620), 2127–2155.

Brokamp C., Beck A. F., Muglia L. & Ryan P. 2017 Combined sewer overflow events and childhood emergency department visits: a case-crossover study. *Science of the Total Environment*, **607–608**, 1180–1187.

Chocat B. 1997 *Encyclopédie de l'hydrologie urbaine et de l'assainissement*, Tec & doc-Lavoisier, Paris, pp.529–543.

Darwin C. 1859 *On the Origin of Species by Means of Natural Selection or the Preservation of Favoured Races in the Struggle for Life*. J. Murray, London.

Davis L. 1987 *Genetic Algorithms and Simulated Annealing*. Morgan Kaufmann Publishers, Pitman, London.

El Ghazouli K., El Khattabi J., Shahrour I. & Soulhi A. 2019 Comparison of M5 model tree and nonlinear autoregressive with exogenous inputs (NARX) neural network for urban stormwater discharge modelling. *MATEC Web of Conferences*, **295**, 02002. https://doi.org/10.1051/matecconf/201929502002

El Ghazouli K., El Khattabi J., Shahrour I. & Soulhi A. 2021 Wastewater flow forecasting model based on the nonlinear autoregressive with exogenous inputs (NARX) neural network. *H2Open Journal*. https://doi.org/10.2166/h2oj.2021.107

Fogel D. B., Bäck T. & Michalewicz Z. 2000 *Evolutionary Computation: Basic Algorithms and Operators*. Institute of Physics Publishing , Bristol and Philadelphia.

Forrest S. 1993 Genetic algorithms: principles of natural selection applied to computation. *Science*, **261**, 872–878.

Garofalo G., Giordano A., Piro P., Spezzano G. & Vinci A. 2017 A distributed real-time approach for mitigating CSO and flooding in urban drainage systems. *Journal of Network and Computer Applications*, **78**, 30–42.

Goldberg, D. E. 1989 *Genetic Algorithms in Search, Optimization, and Machine Learning*. Addison-Wesley Publishing Company, Boston, Massachusetts, USA.

Hassan W. H., Attea Z. H. & Mohammed S. S. 2020 Optimum layout design of sewer networks by hybrid genetic algorithm. *Journal of Applied Water Engineering and Research*, **8**(2), 108–124.

Holland J. H. 1962 Outline for a logical theory of adaptive systems. *Journal of the ACM*, **9**(3), 297–314.

Jean M. È., Duchesne S., Pelletier G. & Pleau M. 2018 Selection of rainfall information as input data for the design of combined sewer overflow solutions. *Journal of Hydrology*, **565**, 559–569.

Launay M. A., Dittmer U. & Steinmetz H. 2016 Organic micropollutants discharged by combined sewer overflows — characterisation of pollutant sources and stormwater-related processes. *Water Research*, **104**, 82–92.

Li M., Zhang J., Cheng X. & Bao Y. 2020 Application of the genetic algorithm. In: *Water Resource Management*, M. Atiquzzaman, N. Yen & Z. Xu (eds.), Big Data Analytics for Cyber-Physical System in Smart City, Singapore, Springer Singapore, pp. 1681–1686.

Lund, N. S. V., Borup, M., Madsen, H., Mark, O., & Mikkelsen, P. S. 2020 CSO reduction by integrated model predictive control of stormwater inflows: A simulated proof of concept using linear surrogate models. *Water Resources Research*, **56**(8), 1-15.

McLellan S. L., Hollis E. J., Depas M. M., Van Dyke M., Harris J. & Scopel C. O. 2007 Distribution and fate of Escherichia coli in Lake Michigan following contamination

with urban stormwater and combined sewer overflows. *Journal of Great Lakes Research*, **33**(3), 566.

Montes C., Berardi L., Kapelan Z. & Saldarriaga J. 2020 Predicting bedload sediment transport of non-cohesive material in sewer pipes using evolutionary polynomial regression — multi-objective genetic algorithm strategy. *Urban Water Journal*, **17**(2), 154–162.

Passerat J., Ouattara N. K., Mouchel J. M., Rocher V. & Servais P. 2011 Impact of an intense combined sewer overflow event on the microbiological water quality of the Seine River. *Water Research*, **45**(2), 893–903.

Phillips P. J., Chalmers A. T., Gray J. L., Kolpin D. W., Foreman W. T. & Wall G. R. 2012 Combined sewer overflows: an environmental source of hormones and wastewater micropollutants. *Environmental Science & Technology*, **46**(10), 5336–5343.

Rathnayake U. & Faisal Anwar A. H. M. 2019 Dynamic control of urban sewer systems to reduce combined sewer overflows and their adverse impacts. *Journal of Hydrology*, **579**, 124150.

Tayfur, G., Barbetta, S., and Moramarco, T. 2009 Genetic algorithm-based discharge estimation at sites receiving lateral inflows. *Journal of Hydrologic Engineering*, **14**(5), 463–474.

Viviano G., Valsecchi S., Polesello S., Capodaglio A., Tartari G. & Salerno F. 2017 Combined use of caffeine and turbidity to evaluate the impact of CSOs on river water quality. *Water, Air, & Soil Pollution*, **228**(9), 330.

Weyrauch P., Matzinger A., Pawlowsky-Reusing E., Plume S., von Seggern D., Heinzmann B., Schroeder K. & Rouault P. 2010 Contribution of combined sewer overflows to trace contaminant loads in urban streams. *Water Research*, **44**(15), 4451–4462.

Yazdanfar Z. & Sharma A. 2015 Urban drainage system planning and design — challenges with climate change and urbanization: a review. *Water Science and Technology*, **72**(2), 165–179.

Zhao W., Beach T. H. & Rezgui Y. 2019 Automated model construction for combined sewer overflow prediction based on efficient LASSO algorithm. *IEEE Transactions on Systems, Man, and Cybernetics: Systems*, **49**(6), 1254–1269.

.

General conclusion

As a result of urbanization and climate change, the agglomerations of the world are facing major environmental issues, particularly related to floods and pollutions that impact waterbodies. In many cities, the existing CS systems cannot convey all the polluted water to WWTPs during rain events, thereby leading to frequent CSOs. The pollution released by sewer networks can significantly impact the ecosystem by unbalancing its kinetics.

This thesis aimed to develop an MPC system that can set optimal control strategies for sewer network gate valves to minimize CSO environmental impact by rainy weather. Data forecasts are a key component for every MPC system. The first step of this work comprises the development of two flow forecasting models, namely, the WWFFM to forecast DWFs and the SWFM to predict stormwater flows in sewer networks. These models provide valuable input data and sufficient lead time for predictive model control systems to enhance efficiency in UDSs and reduce CSOs.

The proposed WWFM based on the nonlinear autoregressive with exogenous neural network provides wastewater flow forecasts for a four-hour horizon at a five-minute timestep. This model has been tested on a watershed of 3,315 ha in Casablanca. The WWFFM with water distribution forecasts has displayed accurate results and high performances predicting wastewater flows.

Four data-driven models, namely, NARX, M5T, RF, and ANFIS-PSO, have been tested and compared with forecast urban drainage stormwater discharge using rainfall prediction on the same watershed as the WWFFM. Performance results validate that the NARX, M5T, and RF models provide good results in forecasting stormwater flows based on rainfall data input where ANFIS-PSO fails to give satisfying results. Nonetheless, the NARX, M5T, ANFIS, and RF models underestimate peak flows for 10 YRP rainfalls. This underestimation is mainly due to the sample's non-representativeness of the 10 YRP rainfall events, which barely represent 2% of the dataset. Over time, the underestimation will be resolved with a larger rainfall dataset and continuous learning of artificial intelligence models. The efficiency of the SWFM for 10 YRP can also be improved by training the SWFM on the hydraulic modeling results of synthetic high-intensity rainfalls.

The SWFM based on the NARX, M5T, and RF models could be easily implemented for practical use in UDSs. The SWFM coupled to the WWFFM can be an efficient tool for predicting flows in CS networks.

The last part of this work comprises the development of MPC based on the WWFFM and the SWFM for predicting flows and a genetic algorithm for optimizing the operation of the sewer system of Casablanca. As part of this work, we determined the best population size and generation number that present a compromise between the performance of the algorithm in finding an optimal solution and the computation time. The parallelization of calculations allowed the reduction of the computation time considerably and made MPC more proactive. MPC demonstrates high efficiency in reducing CSOs to the receiving environment by generating the optimal temporally and spatially varied dynamic control strategies of the gate valves of the sewer system. This MPC could benefit municipalities worldwide that are facing environmental issues and their consequences, such as CSOs and floods.

In continuation of this work, an analysis of the sewer network will be conducted to evaluate the potential inline storage by looking for suitable gate valve locations to reduce CSOs through the dynamic management of the system.

A field measurement campaign will also be performed to measure the pollution at the outlet of different watersheds with risk-based analysis to integrate the pollution risk as a decision criterion in the optimization of the MPC system. The desired follow-up to this study is to deploy the MPC system in Casablanca after the theoretical development of the method.

Appendices

Appendix 1: Model Predictive Control performance and valve gates schedule for different population sizes

MPC performance and valve gates schedule for a population size equal to 10

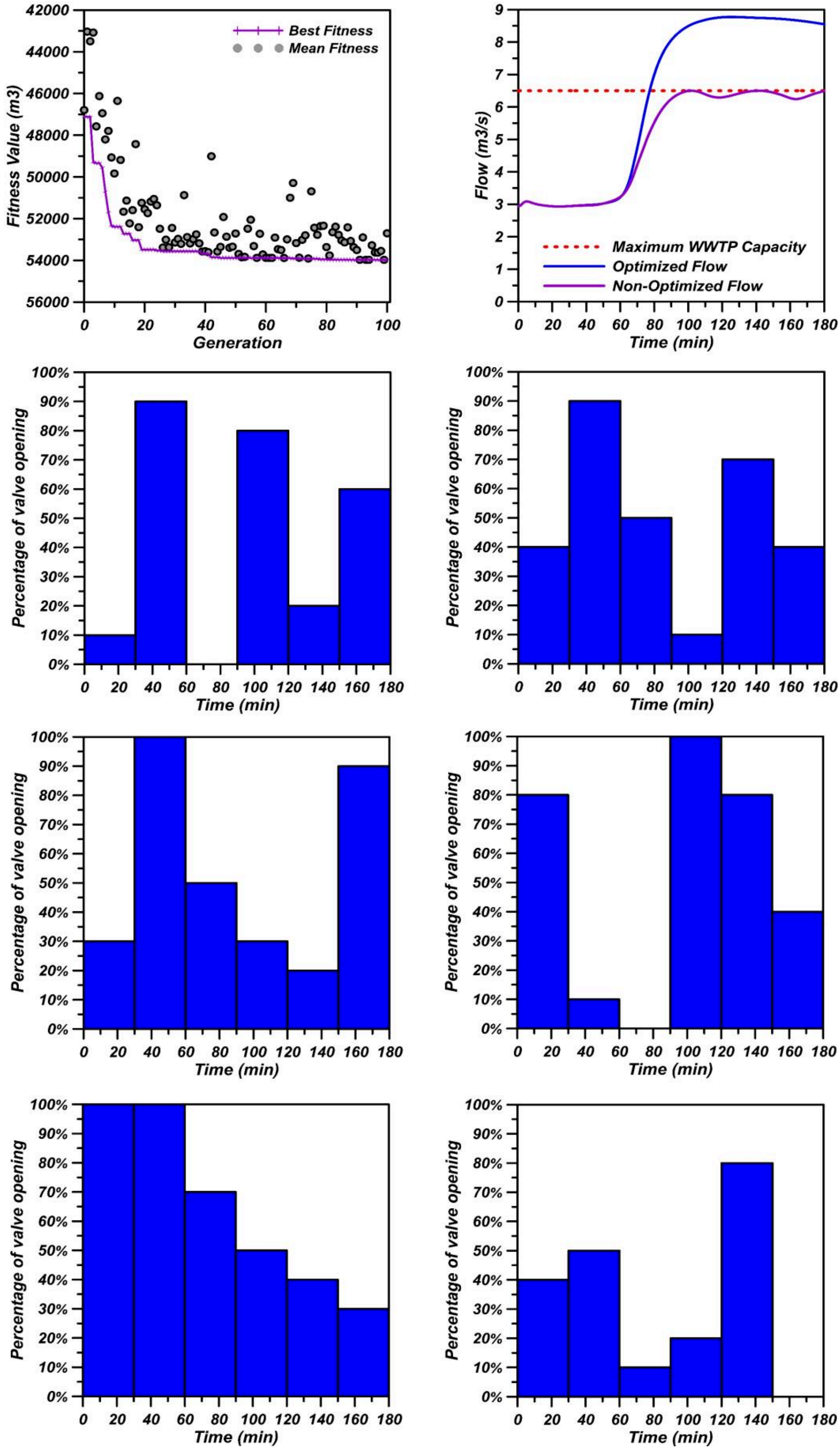

MPC performance and valve gates schedule for a population size equal to 20

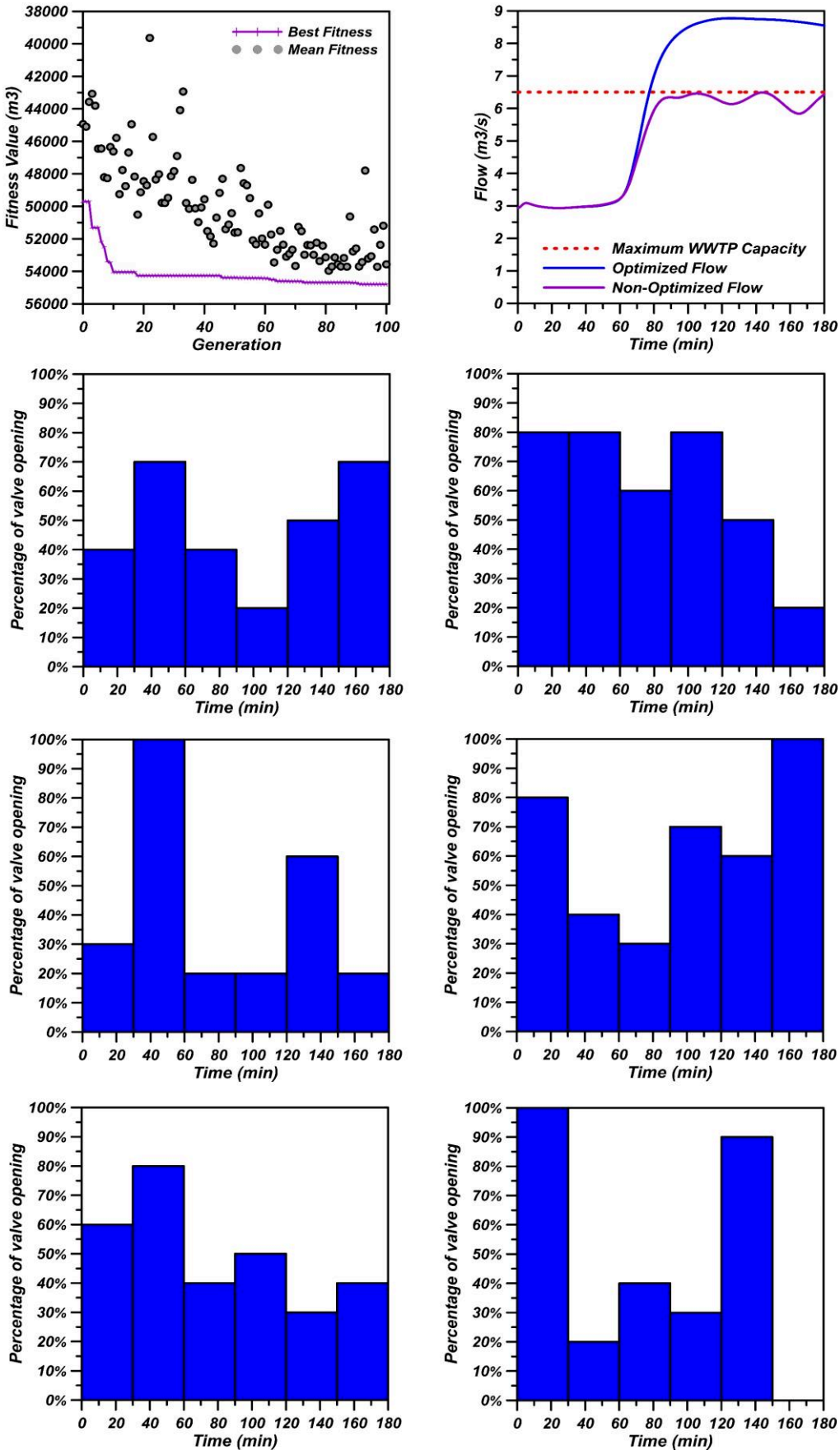

MPC performance and valve gates schedule for a population size equal to 40

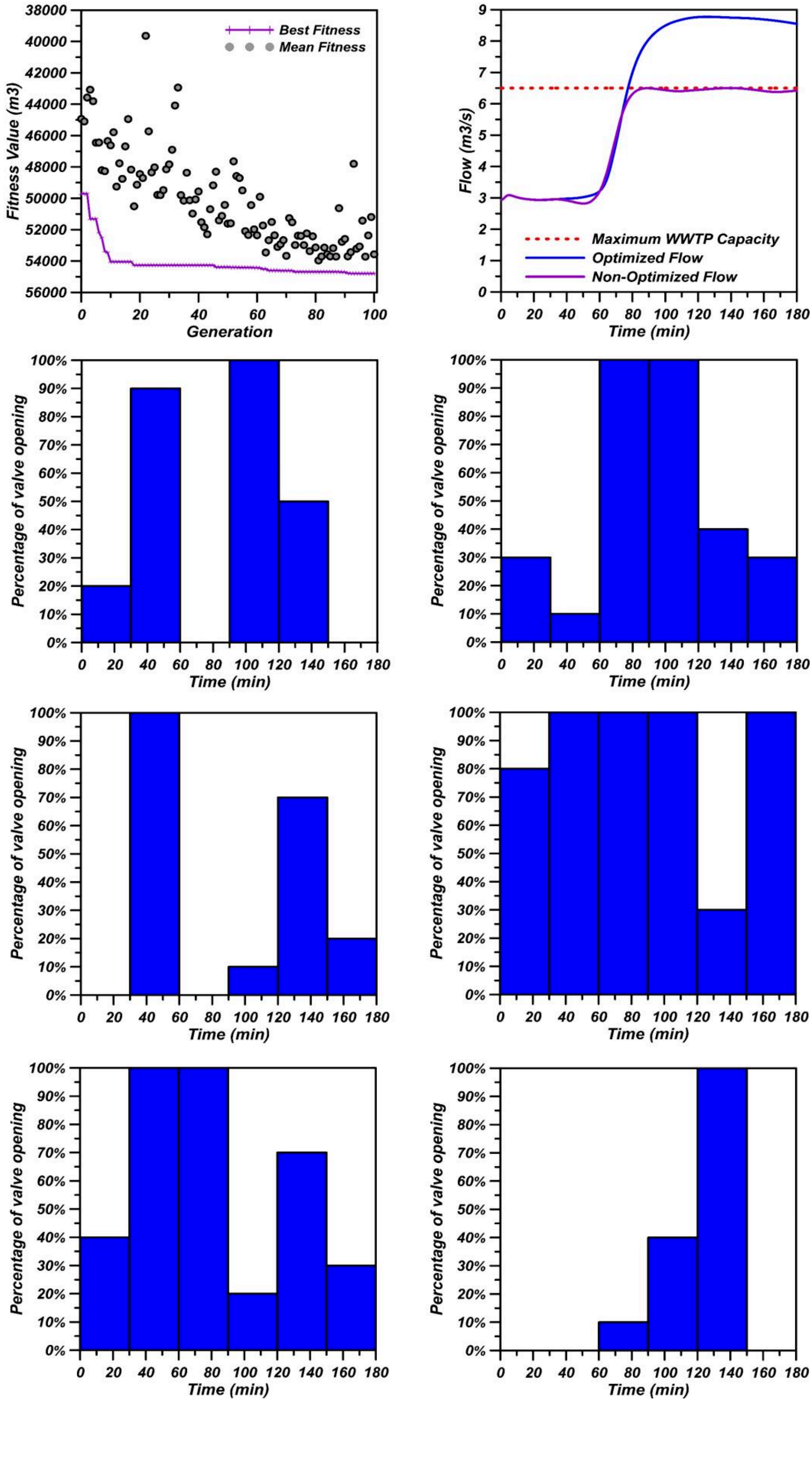

MPC performance and valve gates schedule for a population size equal to 60

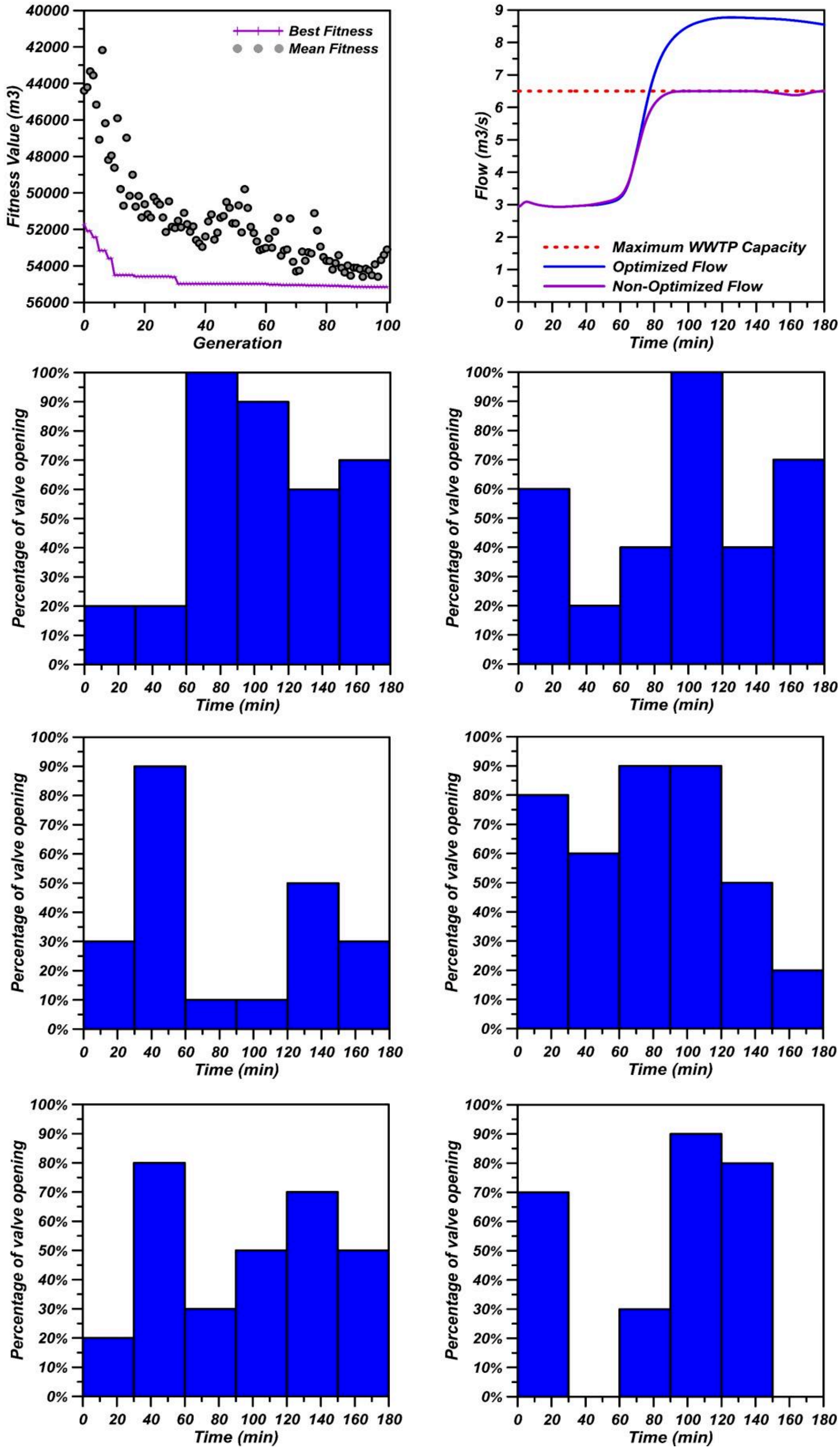

MPC performance and valve gates schedule for a population size equal to 80

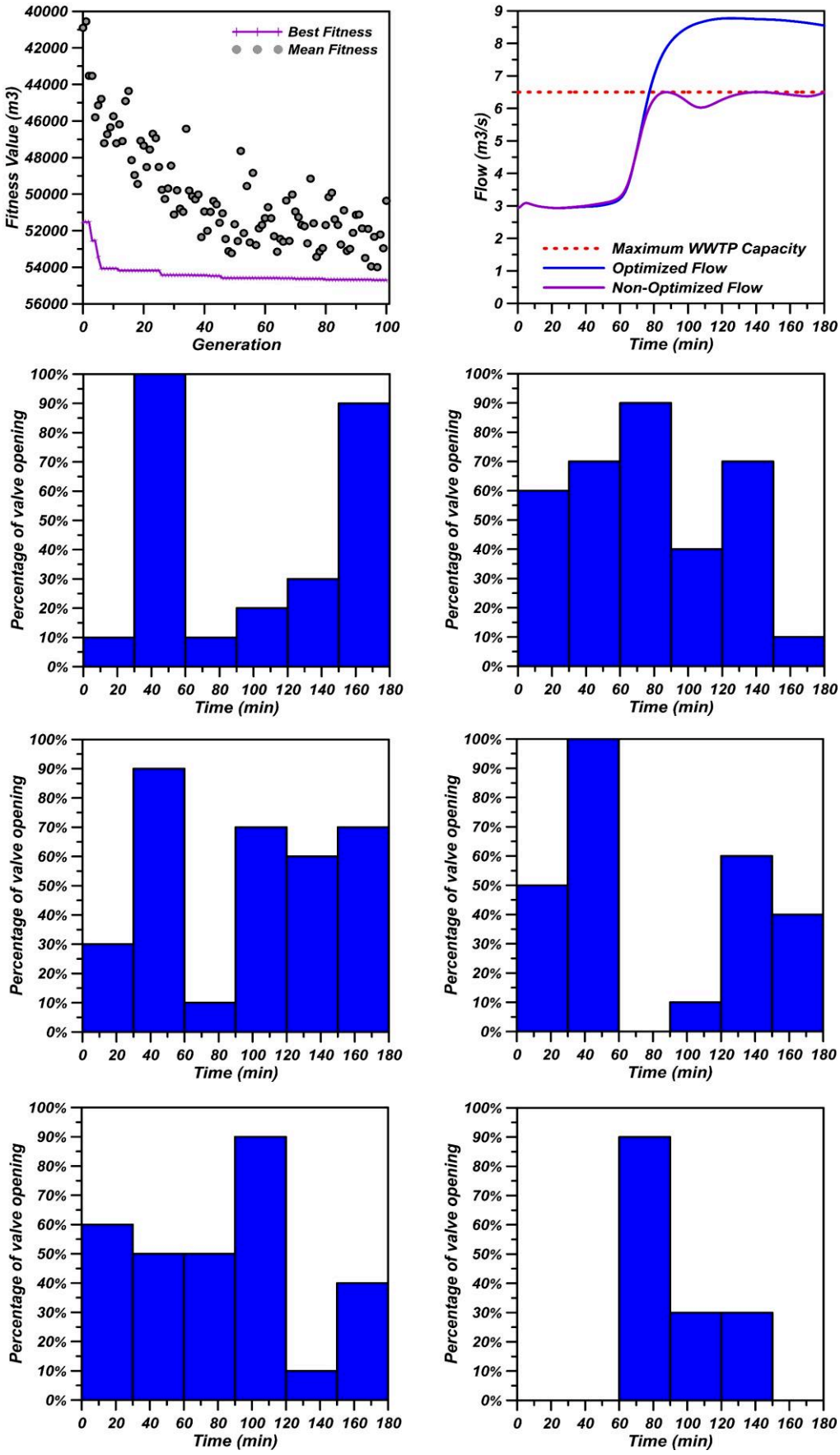

MPC performance and valve gates schedule for a population size equal to 100

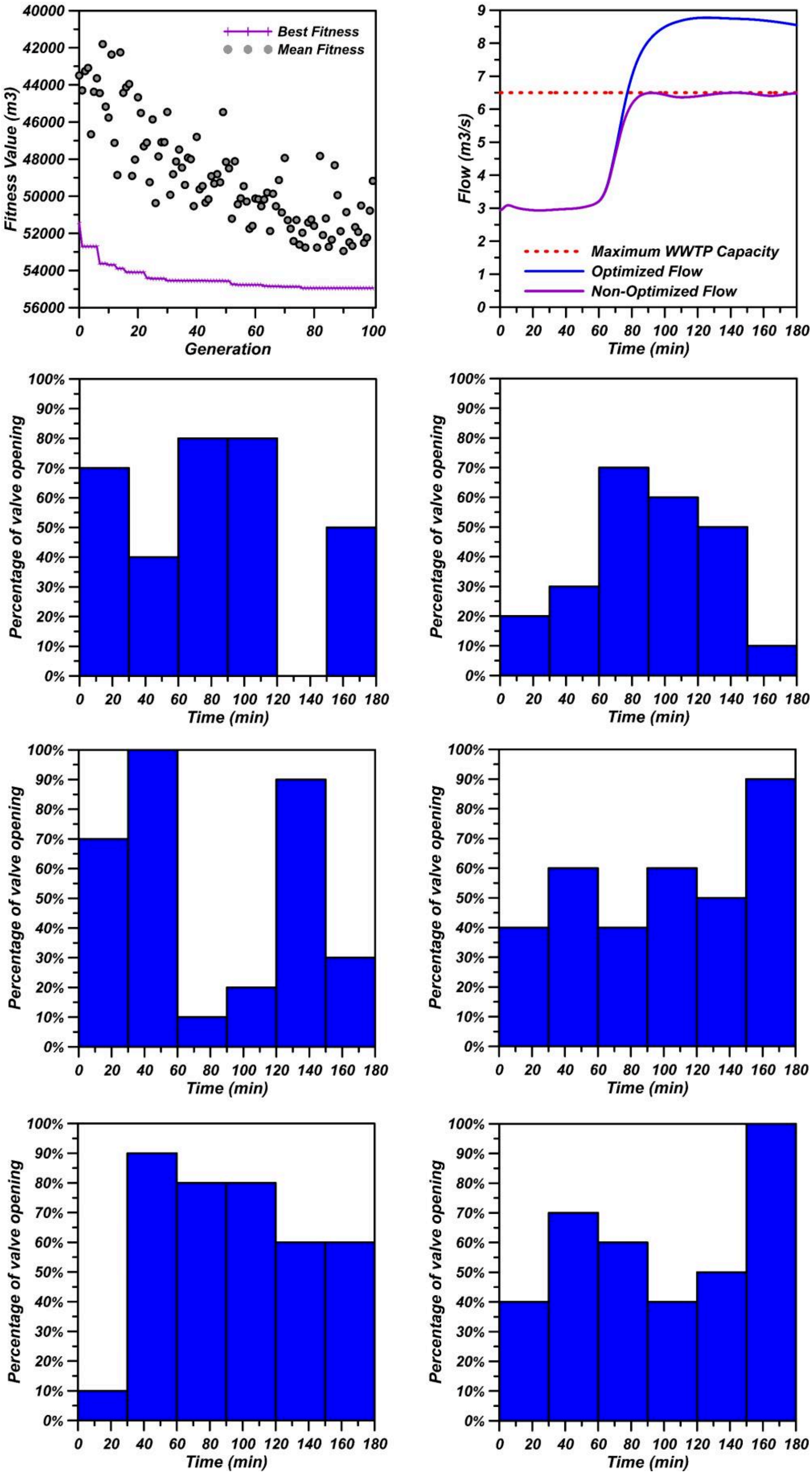

Appendix 2: Publications

Comparison of M5 Model Tree and Nonlinear Autoregressive with eXogenous inputs (NARX) Neural Network for urban stormwater discharge modelling

EL GHAZOULI Khalid[1,2], EL KHATABI Jamal[1], SHAHROUR Isam[1] and SOULHI Aziz[3]

1 Laboratoire de Génie Civil et géo-Environnement, Université de Lille, 5900 Lille, France

2 Laboratoire d'Analyse des Systèmes, Traitement de l'Information et Management Industriel, Université Mohammed V, Rabat, Morocco

3 National Higher School of Mines, Agdal Rabat, Morocco

Abstract. This paper presents a comparative study of two data-driven modelling techniques in forecasting urban drainage stormwater discharge based on rainfall prediction. Both M5T and NARX (Nonlinear Autoregressive with eXogenous inputs) Neural Network are used for 30 minutes storm water forecasting. Data are collected from watershed area of 3315 ha, located in the city of Casablanca in Morocco. The results show that both models provide good results, but however with better performances of the NARX model.

1. Introduction

Major cities are facing urban flood issues due to urbanization and climate change. Real time control (RTC) systems allow an improvement in the performances of sewer networks through the control of the different network components and the optimization of storage within retention ponds and main collectors (Beeneken et al., 2014). The essential input parameters in RTC systems are rain and flow forecasts. Artificial intelligence techniques had shown good performances in modelling nonlinear systems with a considerable reduction in computing time compared to hydrologic and hydraulic models (Abou Rjeily et al. 2017). Two artificial intelligence techniques, namely, neural networks and M5 Model Tree were discussed in several applications such as sediment transport modeling (Bhattacharya et al. 2007), river flow forecast (Solomatine and Khada. 2003), evaporation estimation (Rahimikhoob. 2014). This paper presents an extension of this comparison to urban drainage application.

2. Methodology and material

2.1. Methododology

Artificial Neural Networks

Neural networks are commonly used in artificial intelligence techniques. They showed good performances in nonlinear system simulation and time series prediction (stock forecasts (Pang, X et al 2018) and urban flood prediction (Berkhahn et al 2019)). They are considered as black box containing the information to be learned. In the beginning, the architecture of the neural network is composed of layers and nodes without any information or knowledge of the simulated phenomenon. During the learning stage, the weights of the neurons that connect the different nodes are determined according to an optimization algorithm to minimize the error of the output of the neural network and measured data.

The Nonlinear Autoregressive with eXogenous inputs (NARX) neural network given by equation (1) is used in this research:

$$\boldsymbol{y(t) = f\left(y(t-1), y(t-2), \ldots, y(t-n_y), u(t-2), \ldots, u(t-n_u)\right)} \quad (1)$$

where y(t): output time series, u(t): input time series, ny and nu: are the time delays representing the phenomenon dynamic behavior.

Two types of architectures of NARX are generally used. The first one is efficient in forecasting a time series value one-time step ahead and it's called series-parallel or open loop. The second one is called parallel architecture or closed-loop and it is efficient for multistep-ahead prediction.

M5T

The M5 model is based on the principle of information theory (Quinlan 1992, Solomatine and Khada. 2003). It can handle nonlinear problem by splitting it into multiple linear ones. The M5T is similar to conventional decision trees, but instead of predicting classes through a classifier it predicts continuous variables through linear regression functions at the leaves. The construction of the M5 model tree is done in two stages (Solomatine and Xue. 2004, Rahimikhoob et al. 2013). First, the M5 model tree is constructed by a divide-and-conquer method that splits the multidimensional data space into several subspaces based on a splitting criterion (Figure 1) that treats the standard deviation of the class values that reach a node as a measure of the error at that node and computes the expected reduction in the error by testing each attribute at that node . The splitting operation stops when the values of the instances reaches a node with slight variation or just few instances remain (Goyal and Ojha 2014)
The formula used to calculate the standard deviation reduction is given by (Solomatine and Khada. 2003, Pal and Deswal, 2009. Goyal and Ojha. 2014, Gyanendra et al 2016):

$$\boldsymbol{SDR = sd(T) - \sum \frac{|T_i|}{|T|} sd(T_i)} \quad (2)$$

where T is the set of examples that reaches the node; Ti is the subset of examples that have the ith outcome of the potential set; and sd is the standard deviation

.

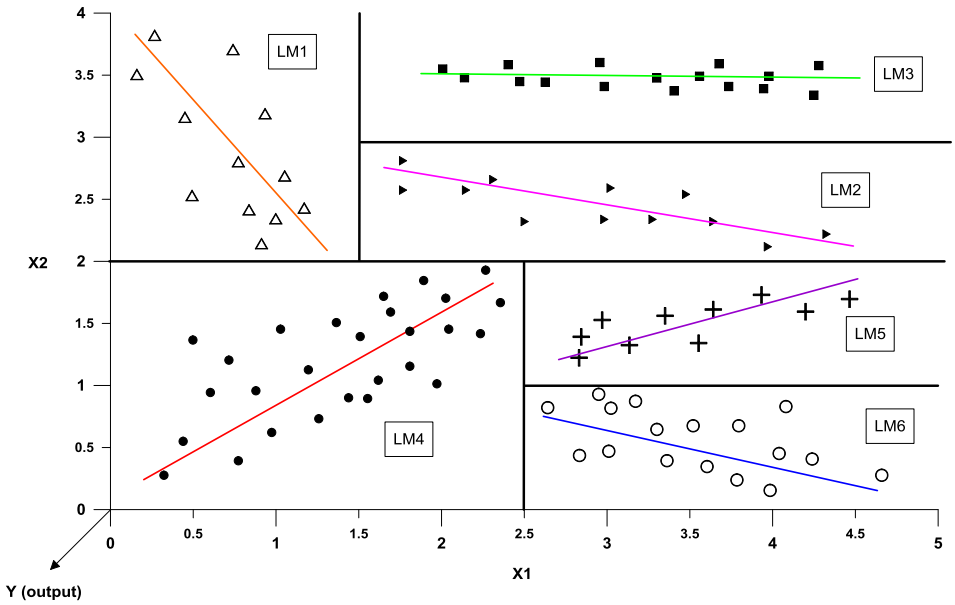

Figure 1: Splitting the input space (X1×X2) by M5 model tree algorithm

The result of the splitting is a tree with splitting rules at the nodes with expert linear models (LM) at the leaves (Figure 2). The combination of linear models can be seen as committee machine (Haykin. 1999).

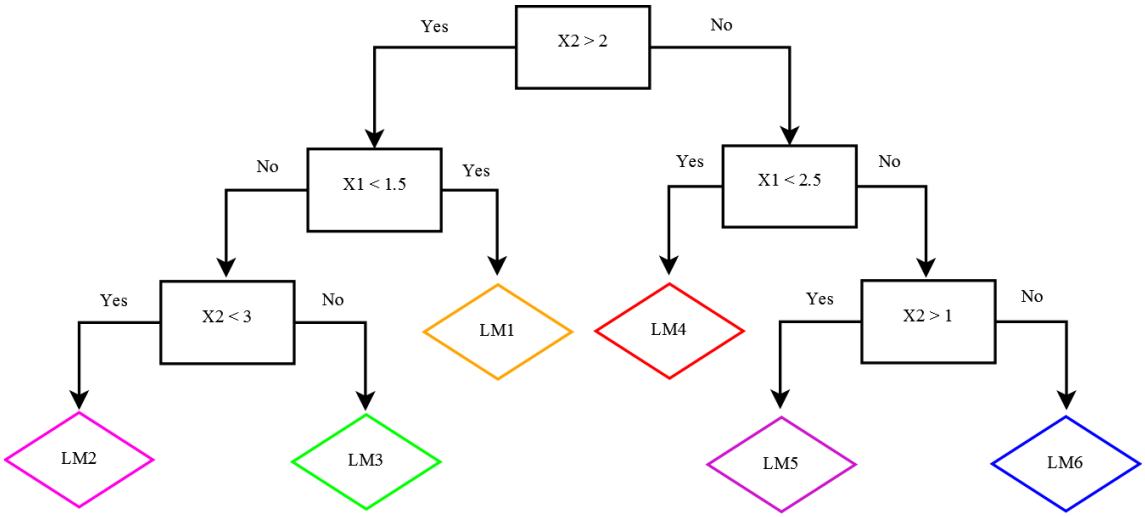

Figure 2: Diagram of the M5 model tree with six linear regression models at the leaves

The generated tree is often large and difficult to analyze and may lead to overfitting. In the second stage a pruning operation is needed to overcome this problem by replacing a subset with a leaf. In addition to this, the smoothing is performed to compensate the discontinuities that can occur between the adjacent linear models at the pruned leaves of the three.

2.2. Site description

The study area concerns a watershed of 3315 ha located in the city of Casablanca in Morocco.
The urban drainage system (UDS) in this area is composed of 485 km of both combined and separate networks (Figure 3).
The UDS is equipped with a depth meter and flow meter the outlet of the watershed. The measurements for UDS are recorded at 15 minutes time interval. A rain gauge is located in the watershed to record the rain intensity at a 5 minutes time interval.

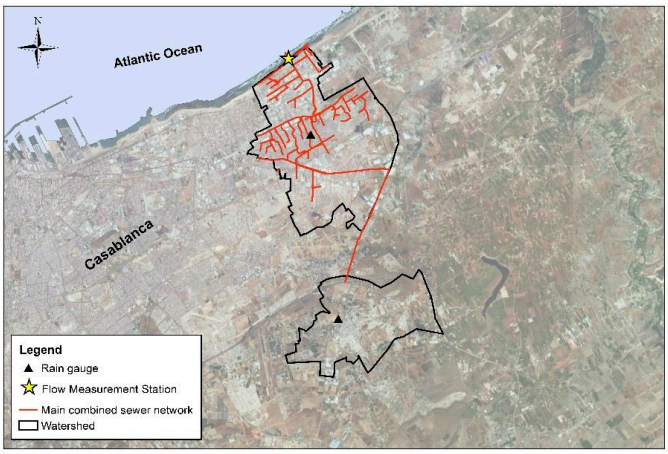

Figure 3: Area used in this study, Casablanca

2.3. Data collection

Data had been extracted from the database for a period of 4 years (January 2015 – January 2019). Since the main sewer system at the outlet of the watershed is a combined one dry weather flow had been removed to keep only data related to rain flows.
The rain dataset used in this present work is characterized by return periods summarized in table 1, which shows a dominance of low to medium rains in the dataset.

Return Period	Percentage of the sample
1 year	58%
2 year	18%
5 year	14%
10 year	2%
20 year	4%
50 year	4%

Table 1: Statistics of return periods (RP) of the rain dataset

3. Application

Both M5T and NARX were used to predict the stormwater flow at 30 minutes. Data used in the construction of the two models are the appropriate data that contribute in the stormwater flow Qt_{+30min}.
These Data are the previous rainfall data (Ret_{-80min}, …, Ret_{-5min}, Ret) and the previous measured discharge (Qt-10min, Qt-5min and Qt). Both models were trained on a data sample of 4 years.
In order to evaluate the performances of both models in predicting Qt_{+30min} for different meteorological conditions, a sample of 4 rain events with various intensities and different return period was used.
These rainfall return periods used for testing the models are: 50YRP (Year Return Period), 2 YRP, 5YRP and 5YRP.

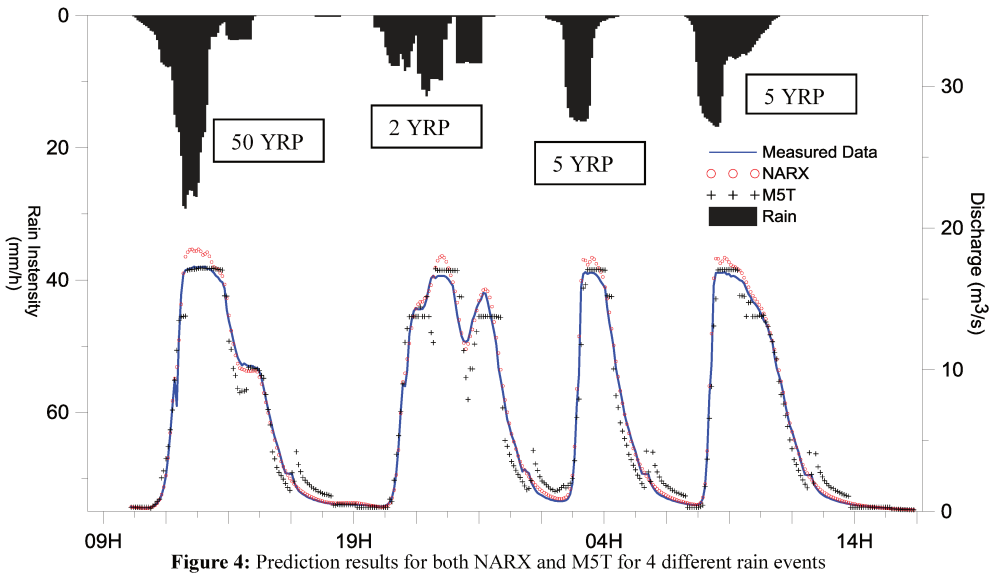

Figure 4: Prediction results for both NARX and M5T for 4 different rain events

	NARX	M5T
RMSE (m3 s)	0.726	1.330
NSE	0.988	0.959

Table 2: Performance statistics of NARX and M5 model tree

The efficiency of the models was examined through results and measurements comparison with a Nash Sutcliffe Efficiency (NSE) and Root Mean Square Error (RMSE) calculation.
Results in table 2, show a good performance of both models with a small RMSE and a high NSE. Figure 4 shows that the NARX model represents better the flow hydrograph with a slight overestimation of the peak flow (about 10%) compared to M5T, which gives better results in predicting peak flows.

4. Conclusion

This paper presented the use of two artificial intelligence techniques, namely NARX and M5T for forecasting urban drainage stormwater discharge using rainfall predictions. Both of these models could be easily implemented for practical use. They were tested and compared on data collected from watershed area of 3315 ha, located in the city of Casablanca. Results show that both models provide good results. The NARX model shows good performances in modelling all the ranges of flow with slight overestimation of peak values compared to M5T Model, which provides good results in peak flows forecasting.

References

1. Y. Abou Rjeily, O. Abbas, M. Sadek, I. Shahrour and F. Hage Chehade (2017) Flood forecasting within urban drainage systems using NARX neural network , Water Science & Technology
2. Bhattacharya, B., Price, R. K., and Solomatine, D. P. (2007). "Machine learning approach to modeling sediment transport." J. Hydraul. Eng., 133(4), 440–450
3. Beeneken, T., Erbe, V., Messmer, A., Reder, C., Rohlfing, R.,Scheer, M., Schuetze, M., Schumacher, B., Weilandt, M. & Weyand, M. (2014). Real time control (RTC) of urban drainage systems – A discussion of the additional efforts compared to conventionally operated systems. UrbanWater Journal 10
4. Berkhahn S, Fuchs, L., Neuweiler I. An ensemble neural network model for real-time prediction of urban floods.(2019) Journal of hydrology- Volume 575,~~Volume 575,~~ Pages 743-754
5. Goyal MK, Ojha CSP (2014) Evaluation of rule and decision tree induction algorithms for generating climate change scenarios for temperature and pan evaporation on a Lake Basin. ASCE J Hydrol Eng 10.1061/(ASCE)HE. 1943–5584.0000615
6. Singh G, Sachdeva SN, Pal M (2016) M5 model tree based predictive modeling of road accidents on non-urban sections of highways in India. Accid Anal Prev 96:108–117
7. Haykin, S. _1999_. Neural networks: A comprehensive foundation,Prentice-Hall, Englewood Cliffs, N.J.
8. Pal M, Deswal S (2009) M5 model tree based modelling of reference evapotranspiration. Hydrol Process 23:1437–1443
9. Pang, X.; Zhou, Y.; Wang, P.; Lin, W.; Chang, V. (2018). An innovative neural network approach for stock market prediction. J. Supercomput, 1–21.
10. Quinlan, J.R., (1992). Learning with continuous classes. In: Proceedings of ustralianJoint Conference on Artificial Intelligence, World Scientific Press: Singapore,pp. 343–348.
11. Rahimikhoob, A. (2014). Comparison between M5 model tree and neural networks for estimating reference evapotranspiration in an arid environment. Water Resour. Manage. 28, 657–669.
12. Solomatine, D. P. & Dulal, K. N. (2003) Model trees as an alternative to neural networks in rainfall–runoff modelling. Hydrological Sciences Journal. 48(3), 399–411.
13. Solomatine DP, Xue Y (2004) M5 model trees compared to neural networks: application to flood forecasting in the upper reach of the Huai River in China. J Hydr Engrg 9(6):491–501

H2Open Journal

IWA PUBLISHING

H2Open Journal Vol 4 No 1, 276 doi: 10.2166/h2oj.2021.107

Wastewater flow forecasting model based on the nonlinear autoregressive with exogenous inputs (NARX) neural network

Khalid El Ghazouli [a,b,*], Jamal El Khattabi [a], Isam Shahrour [a] and Aziz Soulhi [c]

[a] ULR 4515 - LGCgE, Laboratoire de Génie Civil et géo-Environnement, Université de Lille, IMT Lille Douai, Université d'Artois, Yncrea Hauts-de-France, F-59000 Lille, France
[b] Laboratoire d'Analyse des Systèmes, Traitement de l'Information et Management Industriel, Université Mohammed V, Rabat, Morocco
[c] Ecole Nationale Supérieure des Mines de Rabat, Rabat, Morocco
*Corresponding author. E-mail: elghazouli.khalid@gmail.com

KEG, 0000-0002-3078-055X; JEK, 0000-0002-9046-4399; IS, 0000-0001-7279-8005; AS, 0000-0003-1904-513X

ABSTRACT

Wastewater flow forecasts are key components in the short- and long-term management of sewer systems. Forecasting flows in sewer networks constitutes a considerable uncertainty for operators due to the nonlinear relationship between causal variables and wastewater flows. This work aimed to fill the gaps in the wastewater flow forecasting research by proposing a novel wastewater flow forecasting model (WWFFM) based on the nonlinear autoregressive with exogenous inputs neural network, real-time, and forecasted water consumption with an application to the sewer system of Casablanca in Morocco. Furthermore, this research compared the two approaches of the forecasting model. The first approach consists of forecasting wastewater flows on the basis of real-time water consumption and infiltration flows, and the second approach considers the same input in addition to water distribution flow forecasts. The results indicate that both approaches show accurate and similar performances in predicting wastewater flows, while the forecasting horizon does not exceed the watershed lag time. For prediction horizons that exceed the lag time value, the WWFFM with water distribution forecasts provided more reliable forecasts for long-time horizons. The proposed WWFFM could benefit operators by providing valuable input data for predictive models to enhance sewer system efficiency.

Key words: artificial intelligence, NARX neural network, sewer network, urban drainage system, wastewater flow forecast

HIGHLIGHTS

- Implementation of a novel wastewater flow forecasting model based on the NARX neural network.
- New tool for flow forecasting in urban drainage catchments.
- The wastewater flow forecasting model provides accurate input data for predictive modeling.

INTRODUCTION

Wastewater flow forecasts are key components in the short- and long-term management of sewer systems. In wastewater treatment plants (WWTPs), a wastewater flow forecasting model (WWFFM) could benefit operators by providing valuable input data for predictive models to simulate plant behavior and optimize performances and costs through the control of biological processes (Fernandez *et al.* 2009). For pumping stations, selecting the best pump scheduling configuration and running the pumps with an appropriate adjustment of rotation speed could help save energy (Wei *et al.* 2013). These forecasts could also enhance the performance and cost-effectiveness of real-time chemical dosing controllers, thereby preventing hydrogen sulfide formation (Chen *et al.* 2014).

Several models based on data-driven modeling for forecasting wastewater flows have been developed to address these challenges during the last decade. Wei *et al.* (2013) developed a multilayer perceptron (MLP) neural network model for the short-term prediction of influent flow rates in WWTPs. This model takes influent flow rate, rainfall rate, and radar reflectivity as inputs and returns an accurate flow forecast with a prediction horizon of up to 180 min. Boyd *et al.* (2019) proposed a model based on an autoregressive integrated moving average for daily influent flow forecasts tested at five WWTPs across North America and was completed with a multilayer perceptron neural network proposed by Zhang *et al.* (2019). These models rely only on historical data with no

external inputs. Although these models are efficient, they remain limited in their approach. In fact, for forecasting wastewater flows, these models only consider sewer flow historical data. Moreover, they do not integrate drinking water consumption, which is the main causal variable that may influence forecasted flows in the case of a water shutdown in a sector or water consumption variation due to a given event.

The current work aimed to fill the gaps in the wastewater flow forecasting research by proposing a novel WWFFM based on the nonlinear autoregressive with exogenous inputs neural network (NARX-NN), real-time, and forecasted water consumption with an application to the sewer system of Casablanca in Morocco.

MATERIALS AND METHODS

The WWFFM aims at predicting instantaneous dry weather flows at specific points of watersheds. Dry weather flow usually corresponds to flows with no rainfall influence or at a maximum rainfall intensity of 0.3 mm and without inflows (Staufer *et al.* 2012). Given that the wastewater flow production function is nonlinear and depends on the spatial and temporal variations of water consumption through watersheds, using a model that can handle nonlinear problems for forecasting purposes is important. The proposed WWFFM is based on the NARX that has shown its efficiency through various nonlinear times-series forecasting applications (Abou Rjeily *et al.* 2017; Koschwitz *et al.* 2018; Wunsch *et al.* 2018; Marcjasz *et al.* 2019; Di Nunno *et al.* 2021). The WWFFM considers real-time water consumption and previous infiltration flow records as inputs and predicted wastewater flows with forecast horizons that vary from 30 to 240 min as outputs. These periods offer a sufficient lead time to real-time and predictive control models to process and apply optimal control strategies.

The proposed architecture of the network includes two layers, namely, a hidden layer and an output layer (Figure 1). The inputs were weighted with appropriate weights (w), and the sum of the weighted inputs and biases forms the input to the transfer function. A nonlinear transfer function, the tan-sigmoid function bounded between -1 and 1 and described by Equation (1), was used in the hidden layer. An unbounded linear transfer function depicted by Equation (2) was employed in the output layer due to its ability to extrapolate to a certain extent beyond the training data range (Solomatine & Khada 2003):

$$\text{tansig}(x) = \frac{1}{1+e^{-2x}} - 1 \tag{1}$$

$$\text{purelin}(x) = x \tag{2}$$

The NARX-NN is considered a black box containing the information to be learned. In the beginning, the neural network architecture is composed of layers and nodes without any information or knowledge of the simulated phenomenon. During the learning stage, the weights and biases were adjusted according to an optimization algorithm to minimize the error of the neural network output and measured data. In addition, the Levenberg–Marquardt back-propagation function was utilized to train the artificial neural network, as it demonstrated its ability to speed up the convergence rate of neural networks with MLP architectures (Hagan & Menhaj 1994). The Levenberg–Marquardt algorithm described by Equation (3) combines the gradient descent method that updates the parameters in the steepest descent direction to reduce the sum of the squared quadratic errors. Additionally, the Gauss–Newton method reduces the sum of squared errors, assuming that the least-squares

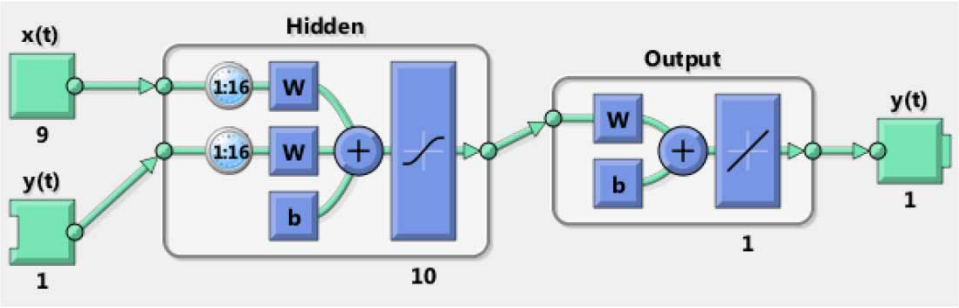

Figure 1 | Neural network architecture.

function is quadratic in the parameters and finding the minimum of this quadratic:

$$\Delta\omega = [J^T(\omega)J(\omega) + \lambda I]^{-1}J^T(\omega)e(\omega) \tag{3}$$

where ω is the weight vector, J is the Jacobian matrix, J^T is the transpose matrix of J, λ is a learning parameter, I is the identity matrix, and e is the vector of the network error.

The early stopping method for improving generalization was used, and the divide block method was employed to split the dataset into three subsets. The first subset representing 70% of the data is the training set, which was utilized to compute the gradient and update the network weights and biases to find the model parameters. The second subset is the validation set (15%). The error in the validation set was monitored during the training process to avoid the increase of errors in the validation set and overfitting. When a validation error increases for a specified number of iterations (six iterations in our case), the training is stopped, and the weights and biases at the minimum of the validation error are returned. Furthermore, the total number of allowed epochs was set to 1,000. The remaining 15% of the dataset was employed as a test set to assess the generalization error in the final model.

The NARX trained in its open-loop form (Figure 2(a)) also called series-parallel architecture, given by Equation (4), efficiently predicts a time-series value for a one-time step ahead. In the open-loop form, the predicted value $\hat{y}(t)$ of the target time series $y(t)$ is predicted from the past values of $u(t)$ and the past measured values of $y(t)$ with the appropriate tapped delay line:

$$\hat{y}(t+1) = f(y(t), y(t-1), \ldots, y(t-n_y), u(t+1), u(t), u(t-1), \ldots, u(t-n_u)) \tag{4}$$

Once the training process is over, the NARX is turned to its closed-loop form (Figure 2(b)), which is called the parallel architecture given by Equation (5) to perform multistep-ahead time-series forecasting. The closed-loop form takes the past and present values of $x(t)$ and $y(t)$ previously predicted values as inputs:

$$\hat{y}(t+1) = f(\hat{y}(t), \hat{y}(t-1), \ldots, \hat{y}(t-n_y), u(t+1), u(t), u(t-1), \ldots, u(t-n_u)) \tag{5}$$

Two statistical metrics were used in this study to assess the efficiency of the model. The Nash–Sutcliffe efficiency (NSE) given by Equation (6), where a value is close to 1, represents a perfect fit between the observed and forecasted data. And the root-mean-square error (RMSE) is given by Equation (7), where low RMSEs are preferred for model validation:

$$\mathrm{NSE} = 1 - \frac{\sum_{i=1}^{n}(Q_o^i - Q_f^i)^2}{\sum_{i=1}^{n}(Q_o^t - \overline{Q_o^t})^2} \tag{6}$$

$$\mathrm{RMSE} = \sqrt{\frac{\sum_{i=1}^{n}(Q_o^i - Q_f^i)^2}{n}} \tag{7}$$

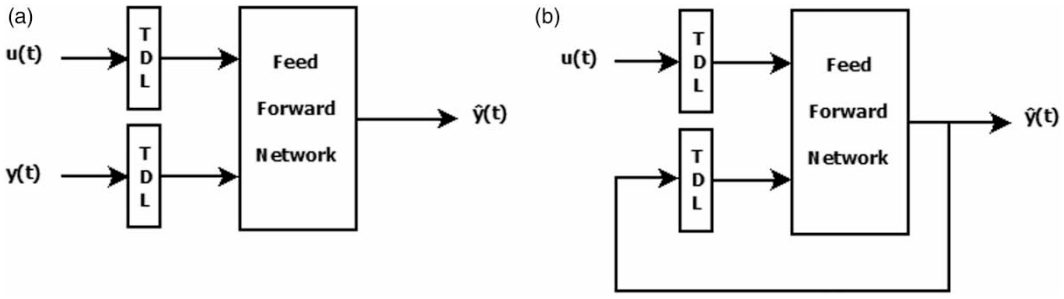

Figure 2 | (a) Series-parallel architecture and (b) parallel architecture.

where Q_o^i is the observed flow at time step i, Q_f^i is the forecasted flow at time step I, $\overline{Q_o^i}$ is the mean observed value, and n is the number of observations.

In the present work, two approaches of the forecasting model were compared (Figure 3):

- The first approach consists of forecasting wastewater flows on the basis of real-time water distribution flows for eight district metering areas (DMAs) and infiltration flows.
- The second approach comprises forecasting wastewater flows according to infiltration flow, water demand flow, and short-term water demand forecasts for the eight DMAs. The water consumption forecasting model is based on a feed-forward back-propagation neural network. The input dataset is composed of historical temperature, water consumption, and days of specification data.

The water consumption forecasting model is based on a feed-forward back-propagation neural network that has shown its efficiency in forecasting water consumption on the campus of Lille University (Farah *et al.* 2019). The input dataset comprises historical temperature, water consumption, and days of specification data. The model gives as output, and water demand forecasts are used as inputs for the WWFFM.

In the model, days of specifications are represented as vectors containing information about the following:

- Day of the week (i.e., Monday to Sunday, where values range from 1 to 7).
- Holidays and special days (New Year's Day and religious celebrations such as Aid El-Adha) are represented with a vector where the values are either 0 or 1.
- Special consumption periods as Ramadan, where consumption patterns differ from normal consumption ones. The vector values are either 0 or 1, where 1 corresponds to the Ramadan period.
- The daily time is represented with 288 5-min timesteps, where values range between 1 and 288.

EXPERIMENTAL DATA

Site description

The data were collected from a watershed of 3,315 ha, which covers the townships of the Eastern part of Casablanca (Figure 4). The urbanization of the area is fairly heterogeneous and comprises industrial and residential areas. The urban drainage system (UDS) is a combined system in the historical part of the townships with a separate sewer system in the new urbanized areas.

Data collection and processing

The area is equipped with a monitoring system based on quantitative sensors that measure sewer flows at the watershed outlet and water consumption at the eight DMAs. The monitoring system of the DMAs is composed of insertion and electromagnetic flowmeters that conduct measurements at a 5-min time step. The UDS is

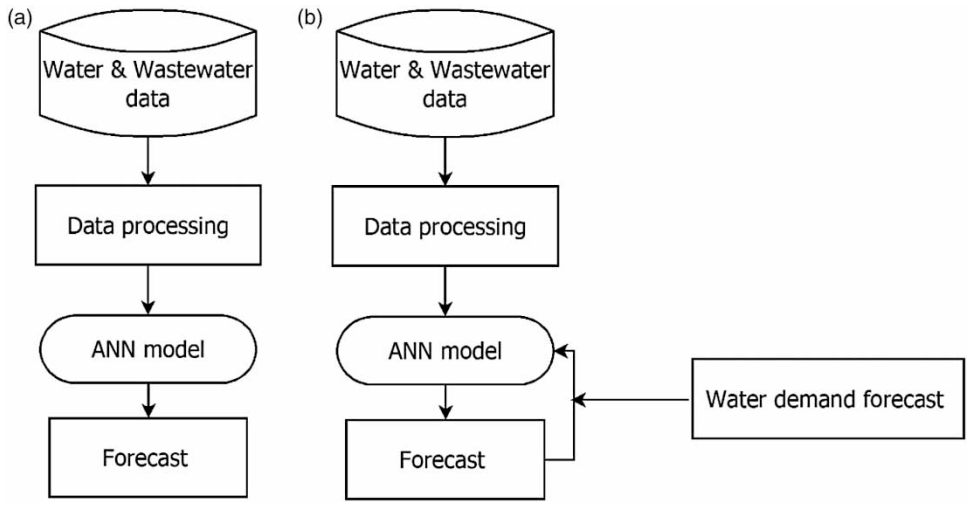

Figure 3 | Process overview of the operation of the WWFFM: (a) without water demand forecasts and (b) with water demand forecasts.

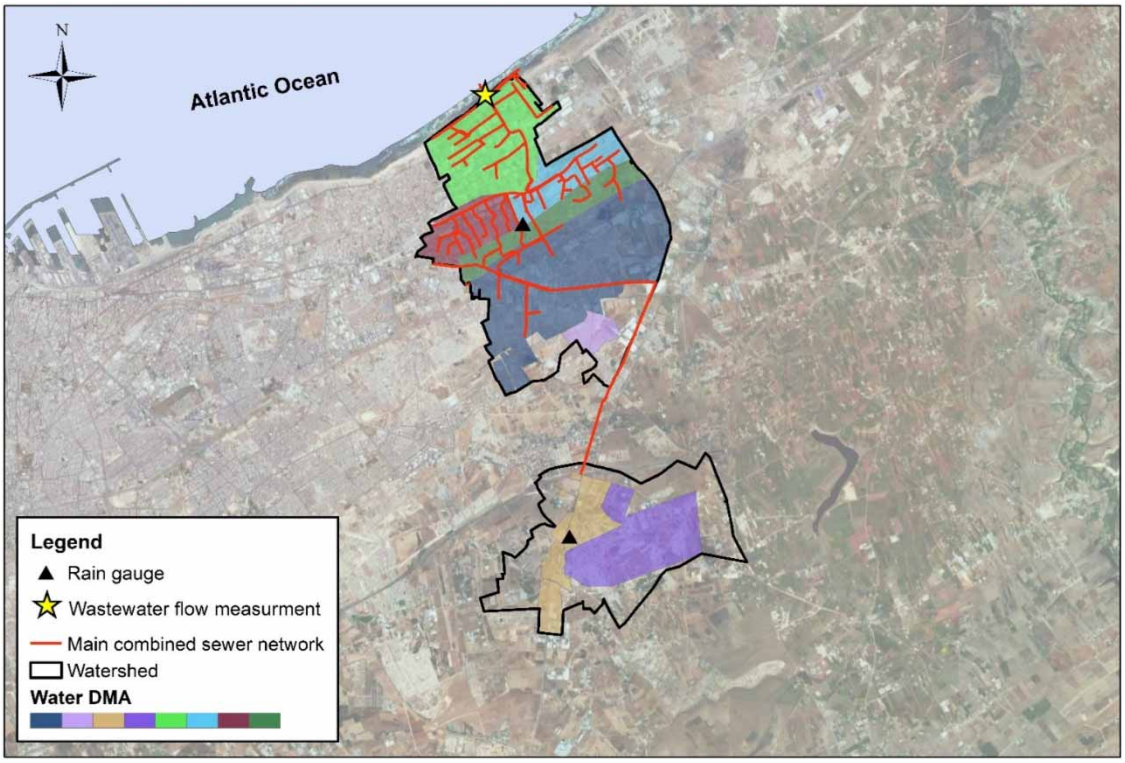

Figure 4 | Sewer system and DMAs of the studied area.

equipped with a depth meter to measure the water level and a flow meter to measure the discharge at the watershed outlet. The measurement for the UDS is conducted at a 15-min time step.

In the framework of the current study, wastewater flow (Q_w), precipitation (P), water consumption (W_c), and temperature (T) data were collected for 3 years between March 2014 and July 2017.

The mean dry weather flow rate pattern presented in Figure 5 shows that wastewater flows vary between 390 L/s for the minimum night flow (MNF) and 900 L/s for the peak flow that occurs around 12:00 pm. Figure 6 illustrates the diurnal patterns for days of the week, average diurnal, seasonal patterns, and special diurnal patterns for specific periods. For normal days, the flow rates of water consumption vary from 270 to 1,100 L/s

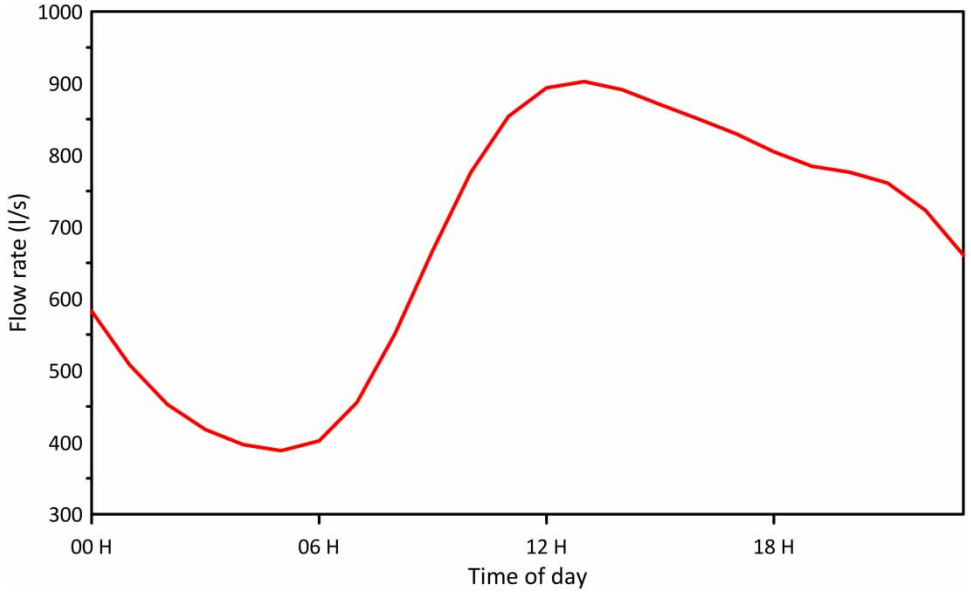

Figure 5 | Diurnal pattern of the mean dry wastewater flow rate.

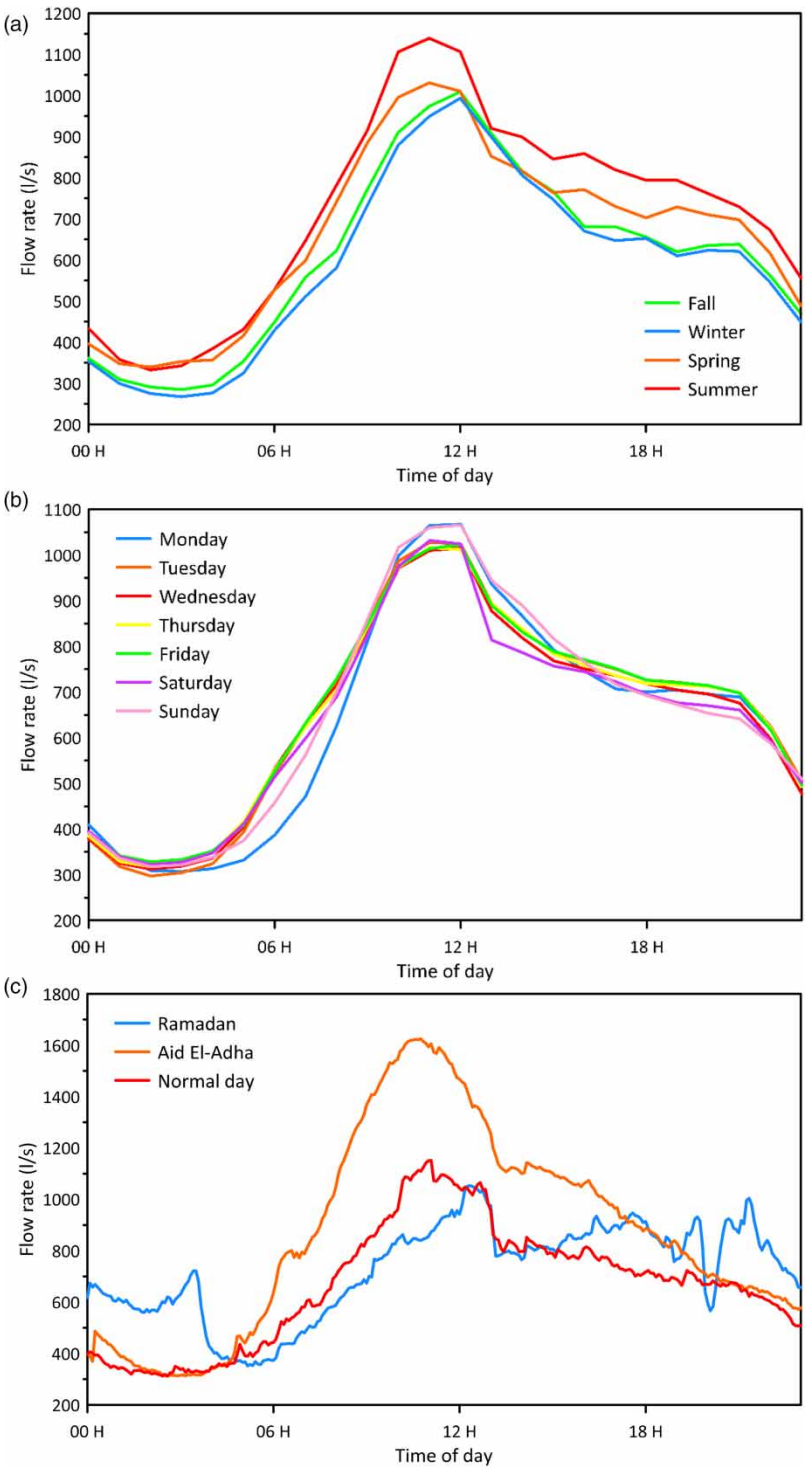

Figure 6 | Diurnal patterns of water consumption flow rate for the seasons of the year (a), the days of the week (b), and special periods (c).

with an average flow rate of 650 L/s and can reach a value of 1,600 L/s during the Aid El-Adha celebration. Furthermore, Figure 6(a) and 6(b) displays the similar variations of the diurnal patterns for each day of the week and each season, with a rise of the MNF in summer of approximately 70 L/s and the peak flow of nearly 150 L/s. For all the consumption patterns, the peak flow is recorded between 11:00 am and 12:00 pm and decreases to reach the MNF between 2:00 am and 4:00 pm. However, the water consumption diurnal pattern trend changes during Ramadan, where we observe an increase in water consumption during the night with a peak flow around 4:00 am

before the beginning of the fast and an MNF that shifts to 6:00 am. We can also observe a fast drop and variation in water consumption roughly 7:00 pm, which corresponds to the fast break time.

However, given that the main sewer system was combined, the first step consisted of identifying rainy days on the basis of the rainfall records of the rain gauges and removing the corresponding data to keep only dry weather flows in the dataset.

For model predictive control systems and forecasting models, missing data constitute a major issue that does not fulfill the requirements of algorithms (Yuri *et al.* 2016). These problems could result from several factors, such as a power outage or a communication failure between the remote terminal units and the SCADA system (Walski *et al.* 2003). Many filling methods were proposed and could be found in the literature (Li *et al.* 2006; Qin *et al.* 2009; Fan *et al.* 2012), such as artificial filling, average value filling, special value filling, and regression. The reconstitution of the missing values of the dataset was performed through a linear interpolation.

In addition to missing values, data from field measurements usually include noise (Ruiz *et al.* 2016) that can affect the efficiency of machine learning algorithms (Lucas 2010; Munawar *et al.* 2011). The LOESS nonparametric regression method proposed by Cleveland (1979) and further developed by Cleveland *et al.* (1988), Cleveland & Grosse (1991), and Cleveland *et al.* (1992) was employed to smooth the collected data (Figure 7).

Dry weather flows in sewer networks consist of strict wastewater flows and infiltration flows (Figure 8). The origin of infiltration water or 'parasite water' commonly corresponds to diffuse groundwater infiltration or seawater. This water enters the network through leaky joints, cracks, and defective manholes. Therefore, considering infiltration rate variation as an input for our model and decomposing the hydrogram components into strict wastewater and infiltration are essential. Many studies have developed and applied methods for the

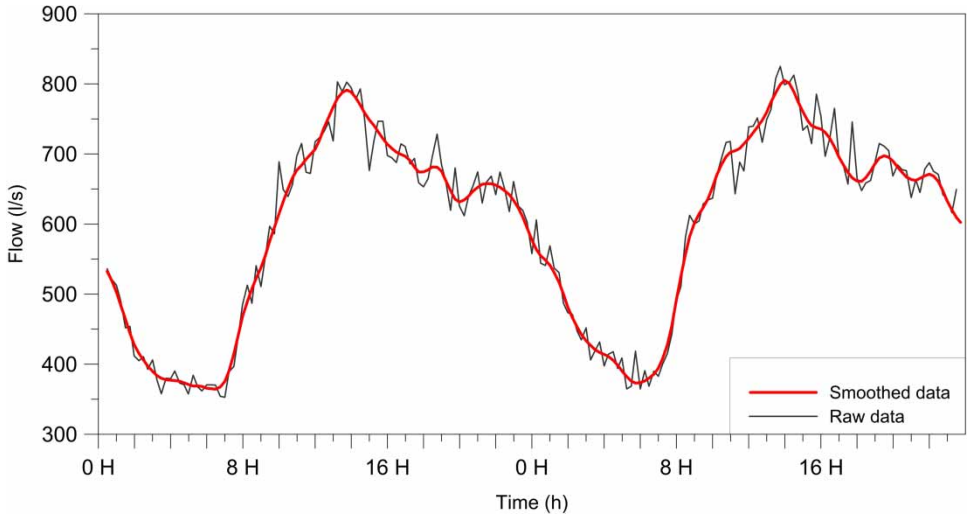

Figure 7 | Smoothed data with the LOESS method.

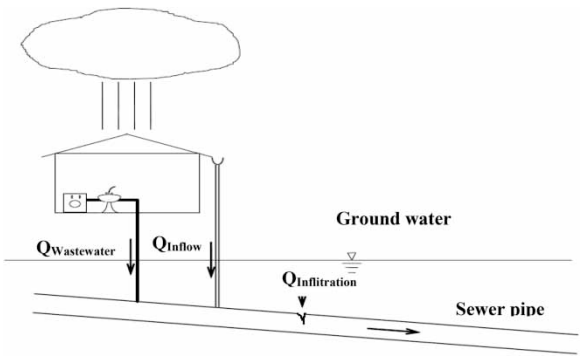

Figure 8 | Flow components in sewer networks.

quantification and detection of infiltration water and could be found in the literature (Ertl *et al.* 2002; Weiss *et al.* 2002; Mitchell *et al.* 2006; Ertl *et al.* 2008; Staufer *et al.* 2012; Water Services Association of Australia 2013; New Zealand Water and Wastes Association 2015; Hey *et al.* 2016). There are two common methods for quantifying the base infiltration flow (BIF), namely, the flow rate method based on daily flow monitoring and the tracer method based on natural tracers or pollutant load mass balance (Hey *et al.* 2016). The infiltration rate was determined on the basis of the flow rate method according to the following equation:

$$\mathrm{BIF} = \overline{\mathrm{MWF}} - (\mathrm{MNF}\,(1 - \mathrm{RL})\mathrm{RC}) \tag{8}$$

where $\overline{\mathrm{MWF}}$ is the average MNF on the last three dry weather days, MNF is the minimum water consumption flow, RL is the real loss percentage where values range between 23 and 25%, and RC is a restitution coefficient equal to 80% and corresponding to the fraction of consumed water released back to the sewer network.

Data analysis

The visualization of the total distributed water and the wastewater flows (Figure 9) shows that the maximum lag time between the peaks of these two variables is around 80 min. Additional lag time analysis was performed using the cross-correlation analysis between distribution water and wastewater flows (Figure 10). The analysis results show a high correlation between these two variables because the lag is less than 80 min. Above this value, the correlation starts decreasing under 80%, exhibiting a weaker relation between both variables. Thus, the lag value for the NARX model is considered to be 80 min, corresponding to 16-time step delays for the NARX.

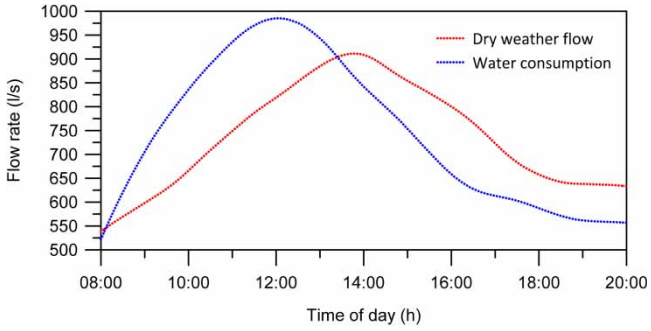

Figure 9 | Plot of water consumption and wastewater flow peaks.

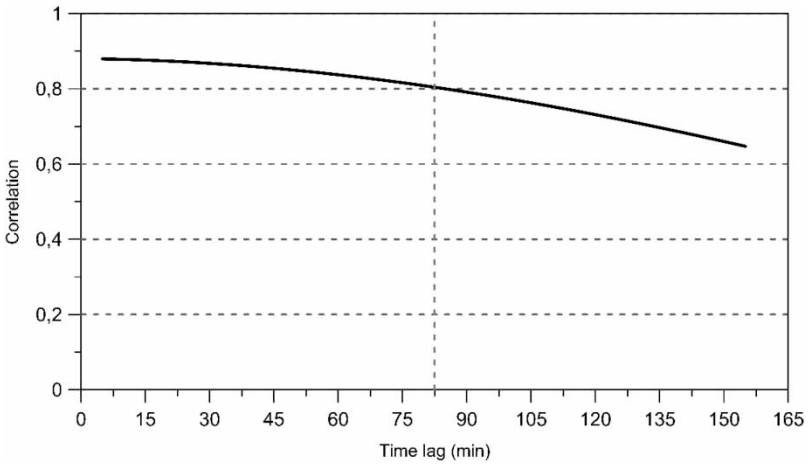

Figure 10 | Cross-correlation analysis.

RESULTS

During the training stage, the NARX neural network minimizes the error between the model results and the real observed data. A different number of neurons were tested and, after several trials, the best training, testing, and validation results were obtained with a hidden layer with 10 neurons allowing the reduction of the mean squared error (MSE) that decreases from 10^5 at the beginning of the training stage to 0.17 after 302 iterations. Tables 1 and 2 present the performance statistics of the NARX-NN architectures. The presented results show that increasing the number of neurons increases the efficiency of the model. However, increasing the number of neurons to more than 10 results in poor performances in multistep ahead forecasts. Figure 11 shows the performance of the trained ANN in the training, validation, and testing sets. In addition, Figure 12 highlights that the efficiency of the trained network presented by high regression values (R) of 0.999 is presented for the training, validation, and testing parts.

Once the model had been trained, further validation of the accuracy of the WWFFM was performed through multistep ahead predictions for 5 days, from September 8, 2016 to September 12, 2016, with hidden data not used during the training process. Figure 13 exhibits the water consumption of the eight DMAs and BIF employed for forecasting wastewater flows for a 5-day period. During this period, high water consumption was recorded on September 12 and corresponded to Aid El-Adha celebration day. The predictions of the WWFFM were

Table 1 | RMSE for the different number of neurons

	Q_{t+6}	Q_{t+9}	Q_{t+12}	Q_{t+15}	Q_{t+18}	Q_{t+24}	Q_{t+48}
1 neuron	0.397	6.311	4.119	2.287	8.081	24.108	35.447
5 neurons	0.6181	5.809	3.823	2.180	7.676	17.659	25.646
10 neurons	1.828	5.603	4.828	1.729	7.238	16.922	17.868
15 neurons	1.495	4.727	1.762	6.413	14.678	29.529	29.528

Table 2 | NSE for the different number of neurons

	Q_{t+6}	Q_{t+9}	Q_{t+12}	Q_{t+15}	Q_{t+18}	Q_{t+24}	Q_{t+48}
1 neuron	0.9998	0.9934	0.9918	0.9989	0.9852	0.8348	0.6881
5 neurons	0.9999	0.9944	0.9933	0.9990	0.9866	0.9113	0.8367
10 neurons	0.9995	0.9948	0.9957	0.9994	0.9806	0.9756	0.9207
15 neurons	0.9997	0.9963	0.9924	0.9916	0.9511	0.7521	0.7835

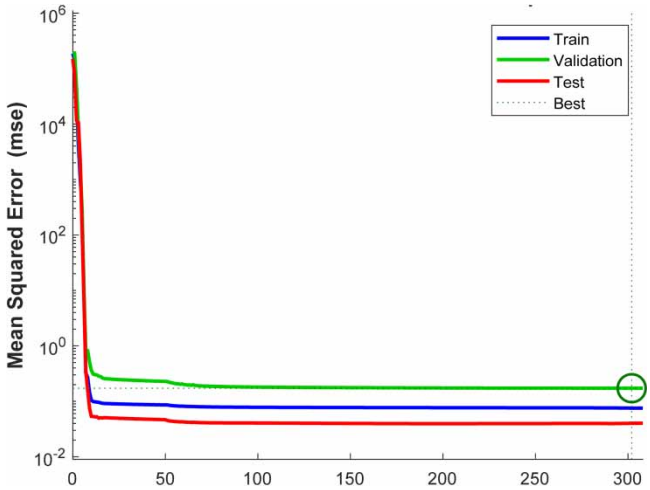

Figure 11 | Performance evaluation of the trained neural network.

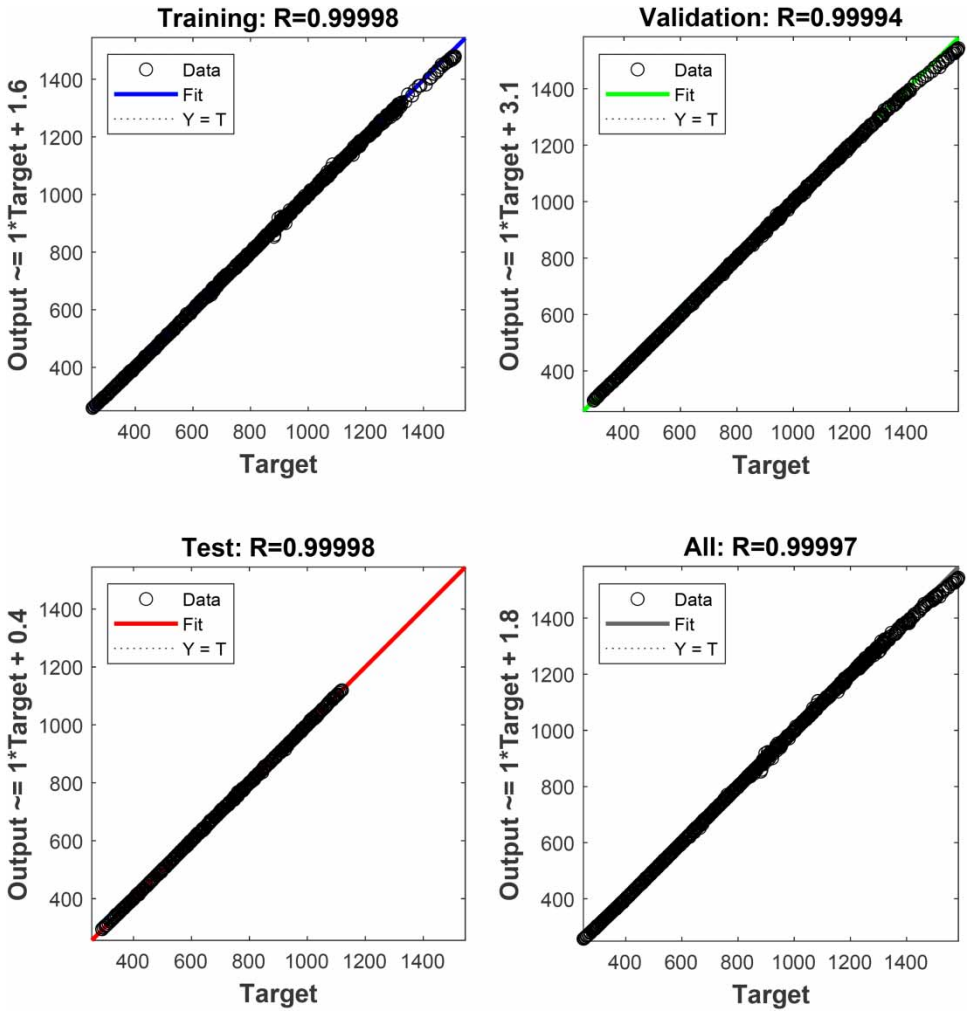

Figure 12 | Regression results of the trained NARX-NN.

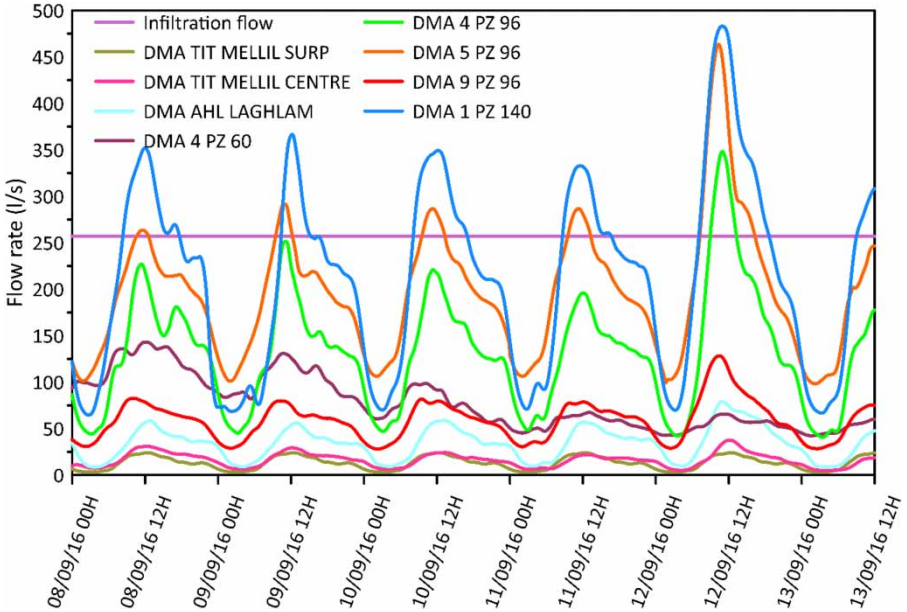

Figure 13 | Plot of water consumption of the eight DMAs and BIF.

conducted for different horizons Q_{t+k}. Where Q_t designates the wastewater flow at timestep t, while Q_{t+k} stands for the wastewater flow at timestep $t+k$ ($k = 6$, 9, 12, 15, 18, 24, and 48) with a 5-min time step.

Tables 3 and 4 present the performance statistics of the WWFFM without water demand forecasts and the WWFFM with water demand forecasts, respectively. Figure 14(a)–14(g) depicts the predicted and observed flows for both approaches.

The analysis of the error statistical results in Figure 14 demonstrates that the WWFFM model with both approaches shows good performances in forecasting dry weather flow as long as the lag time remains less than 80 min. The forecast results are highly accurate, with an RMSE ranging between 3.3 and 16.16 and an NSE ranging between 0.995 and 0.999. Nonetheless, for prediction horizons exceeding 80 min, the WWFFM without water distribution forecasts has a poor performance that decreases with the increase of the forecasting horizon that fails to predict peak, especially for September 12, where the NARX-NN overestimates the peak flow of more than 550 L/s. Conversely, the WWFFM with water distribution forecasts enables the forecast of long-time horizons with a slight variation of the RMSEs over the different forecasting horizons ranging between 3.5 and 12.

DISCUSSION

The current study explored a new approach for predicting instantaneous dry weather flows in the UDS on the basis of the NARX-NN and drinking water consumption, and such an approach was tested on a part of the sewer system of Casablanca, which comprises approximately five million people. The construction of the model required essential steps to reconstitute data through linear interpolation because most modeling techniques cannot deal with missing values and cast out the whole instance value if one of the variable values is missing. In addition, the LOESS nonparametric regression method was used to smooth the data lying far from the bulk of the data range, and a cross-correlation analysis was also conducted to assess the suitable lagged information of the model.

The findings of this study validate that both tested approaches of the WWFFM display accurate results and similar performances in predicting dry weather flows with low RMSEs less than 16.16 and high NSEs as long as the forecasting horizon does not exceed 80 min. Nonetheless, the results further confirm that for prediction horizons that exceed 80 min, the WWFFM without water distribution forecasts presents poor performances that decrease with the increase of the forecasting horizon due to the lack of appropriate causal input variables, thereby making it unsuitable for long-time horizon forecasts for model predictive system use. Conversely, the WWFFM with water distribution forecasts is continuously updated with appropriate lagged input data, thereby enabling it to perform highly accurate forecasts for long-time horizons though representing all the flow ranges. The findings also highlight the importance of the WWFFM that could benefit operators and water engineers, thereby providing valuable input data for predictive model control to enhance the efficiency of sewer systems.

To our knowledge, this is the first study that has explored this new approach of forecasting dry weather flows on the basis of real-time water consumption and the BIF, which thus improves the knowledge of and complements previous research works in forecasting dry weather flows. The currently known models proposed in the literature

Table 3 | Performance statistics of the WWFFM without water demand forecasts

	Q_{t+6}	Q_{t+9}	Q_{t+12}	Q_{t+15}	Q_{t+18}	Q_{t+24}	Q_{t+48}
RMSE ($m^3\ s^{-1}$)	3.300	5.492	10.383	16.166	18.918	43.487	82.855
NSE	0.999	0.999	0.998	0.995	0.993	0.967	0.881

Table 4 | Performance statistics of the WWFFM with water consumption forecast

	Q_{t+6}	Q_{t+9}	Q_{t+12}	Q_{t+15}	Q_{t+18}	Q_{t+24}	Q_{t+48}
RMSE ($m^3\ s^{-1}$)	3.504	4.367	4.135	4.7915	11.711	11.888	12.017
NSE	0.999	0.999	0.999	0.999	0.997	0.997	0.997

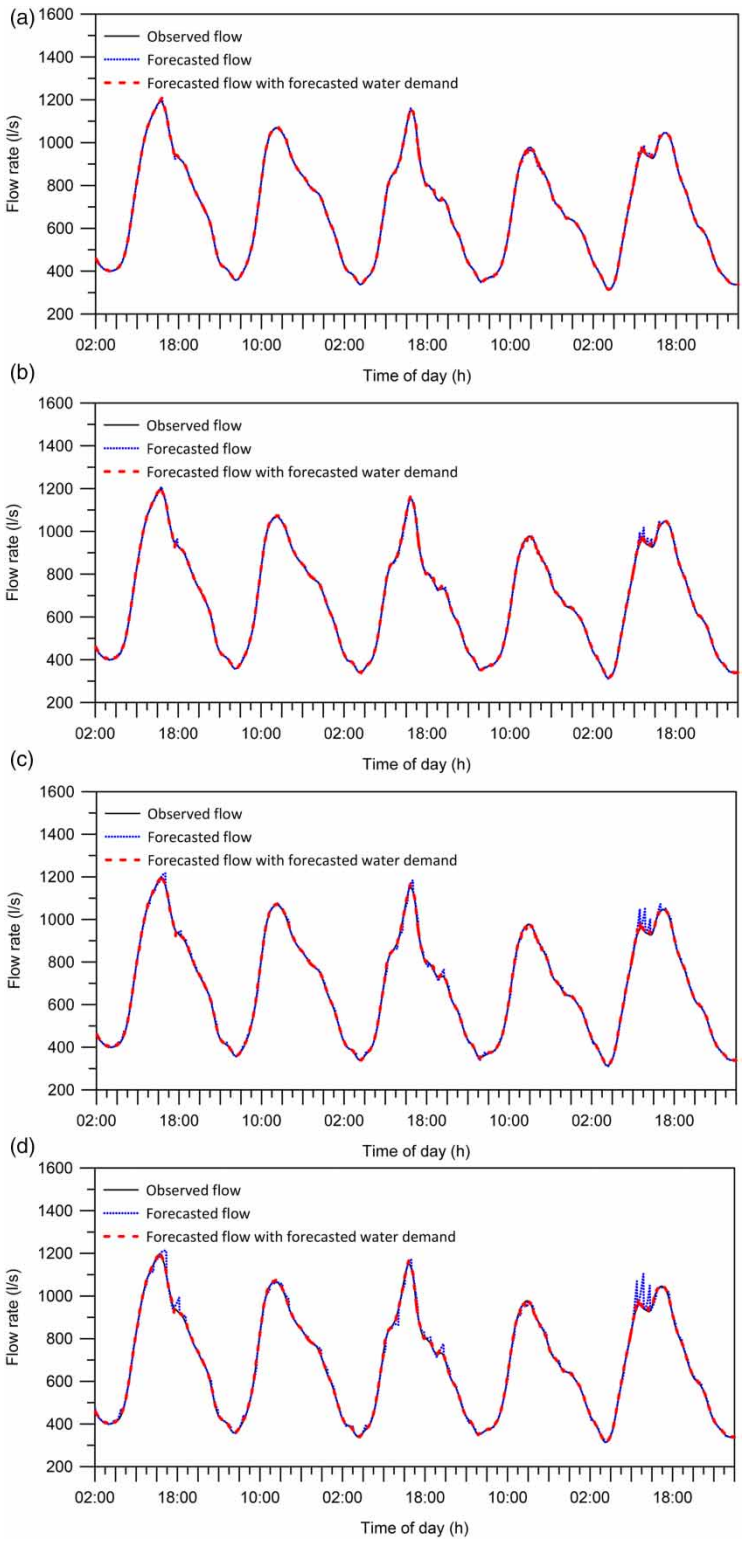

Figure 14 | Prediction of (a) $Q_t + 6$, (b) $Q_t + 9$, (c) $Q_t + 12$, (d) $Q_t + 15$, (e) $Q_t + 18$, (f) $Q_t + 24$, and (g) $Q_t + 48$, using the NARX-NN. *(continued.)*

(Wei *et al.* 2013; Boyd *et al.* 2019; Zhang *et al.* 2019) rely only on historical data with no external inputs. Additionally, they do not integrate drinking water consumption, which is the main causal variable that may influence forecasted flows in case of a water shutdown in a sector or water consumption variation due to a given event.

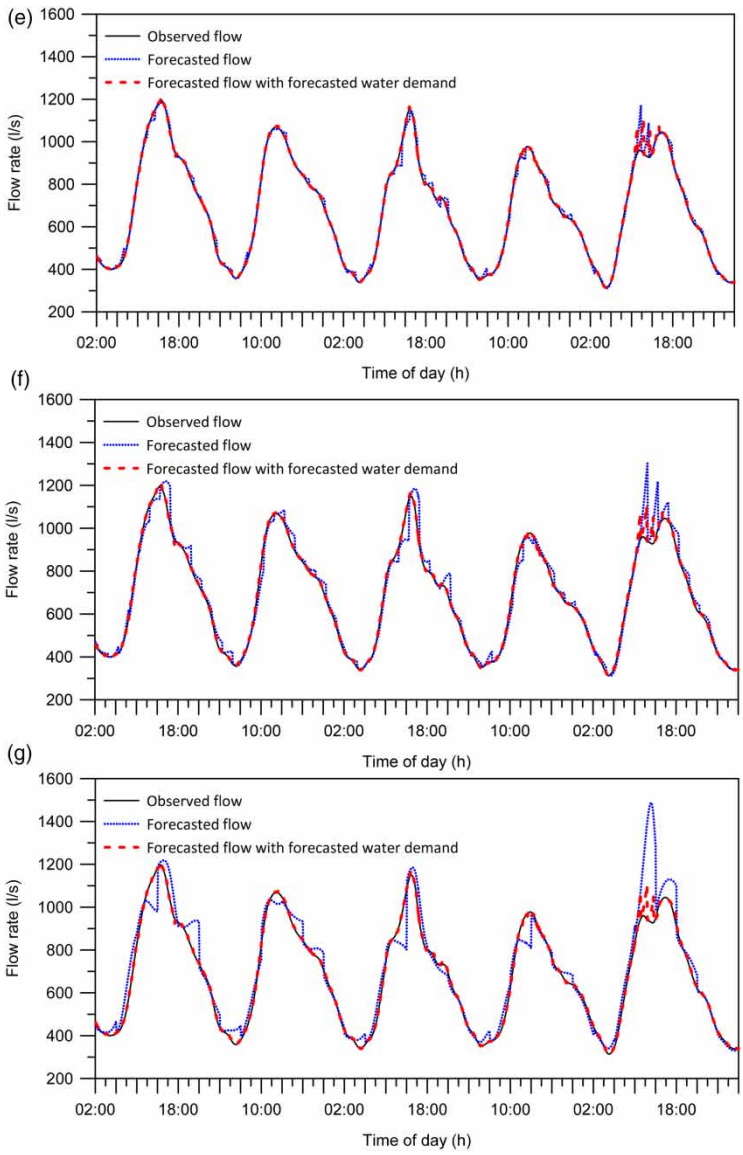

Figure 14 | Continued.

The limitation of the proposed WWFFM model lies in its use of real-time data, which can pose a problem in the event of data unavailability due to a sensor failure or a communication problem. Therefore, ensuring the good maintenance of the flow meters and continuous data transmissions for the needs of the NARX-NN is essential. Moreover, defining strategies for filling in data in case of communication failures would be interesting. In the meantime, the proposed model only integrates the forecasts of wastewater flows, and it is planned in the perspective of future works to develop the model by integrating the forecasts of combined sewer flows considering the fraction of stormwater flows.

CONCLUSION

The present work aims to fill the gaps in the wastewater flow forecasting research across the world by proposing a novel WWFFM based on the NARX. The proposed model considers real-time and forecasted water consumption as the main causal variable input of wastewater flow production. This study differs from the approaches presented through the literature that remain limited considering the only sewer flow historical data and that would fail to forecast sewer flows in the case of a water shutdown in a sector or water consumption variation due to a given event. This research compares the two approaches of the forecasting model. The first approach consists of forecasting wastewater flows on the basis of real-time water consumption and infiltration flows, and the second

approach considers the same input in addition to the water distribution flow forecasts. Consequently, both approaches display accurate results and similar performances in predicting wastewater flows, while the forecasting horizon does not exceed 80 min. Nonetheless, for prediction horizons that exceed 80 min, the WWFFM without water distribution forecasts presents poor performances that decrease with the increase of the forecasting horizon. Conversely, the WWFFM with water distribution forecasts is continuously updated with the appropriate lagged input data, thereby making it able to perform highly accurate forecasts for long-time horizons. Hence, the WWFFM developed in this study could benefit operators and water engineers, providing valuable input data for predictive model control and thus enhancing UDS efficiency.

DATA AVAILABILITY STATEMENT

Data cannot be made publicly available; readers should contact the corresponding author for details.

REFERENCES

Abou Rjeily, Y., Abbas, O., Sadek, M., Shahrour, I. & Hage Chehade, F. 2017 Flood forecasting within urban drainage systems using NARX neural network. *Water Science and Technology* **76** (9), 2401–2412.

Boyd, G., Na, D., Li, Z., Snowling, S., Zhang, Q. & Zhou, P. 2019 Influent forecasting for wastewater treatment plants in North America. *Sustainability* **11** (6), 1764.

Chen, J., Ganigue, R., Liu, Y. & Yuan, Z. 2014 Real-time multi-step prediction of sewer flow for online chemical dosing control. *ASCE Journal of Environmental Engineering* **140** (11), 04014037. https://dx.doi.org/10.1061/(ASCE)EE.1943-7870.0000860.

Cleveland, W. S. 1979 Robust locally weighted regression and smoothing scatterplots. *Journal of the American Statistical Association* **74** (368), 829–836.

Cleveland, W. S. & Grosse, E. 1991 Computational methods for local regression. *Statistics and Computing* **1**, 47–62.

Cleveland, W. S., Devlin, S. J. & Grosse, E. 1988 Regression by local fitting. *Journal of Econometrics* **37**, 87–114.

Cleveland, W. S., Grosse, E. & Ming-Jen, S. 1992 *A Package of C and Fortran Routines for Fitting Local Regression Models*. Unpublished paper.

Di Nunno, F., Granata, F., Gargano, R. & Marinis, G. 2021 Prediction of spring flows using nonlinear autoregressive exogenous (NARX) neural network models. *Environmental Monitoring and Assessment* **193**, 350.

Ertl, T. W., Dlauhy, F. & Haberl, L. 2002 Investigations of the amount of infiltration inflow in to a sewage system. In: *Proceedings of the 3rd 'Sewer Processes and Networks' International Conference*, Paris, France, pp. 15–17.

Ertl, T., Spazierer, G. & Wildt, S. 2008 Estimating groundwater infiltration into sewerages by using the moving minimum method – a survey in Austria. In: *11th International Conference on Urban Drainage*, Edinburgh, Scotland, UK.

Fan, B., Zhang, G. & Li, H. 2012 Multiple models fusion for pattern classification on noise data. In: *2012 International Conference on System Science and Engineering (ICSSE)*, pp. 64–68.

Farah, E., Abdallah, A. & Shahrour, I. 2019 Prediction of water consumption using artificial neural networks modelling (ANN). *MATEC Web of Conferences* **295**, 01004.

Fernandez, F. J., Seco, A., Ferrer, J. & Rodrigo, M. A. 2009 Use of neurofuzzy networks to improve wastewater flow-rate forecasting. *Environmental Modelling & Software* **24** (6), 686–693.

Hagan, M. T. & Menhaj, M. B. 1994 Training feed-forward networks with the Marquardt algorithm. *IEEE Transactions on Neural Networks* **5**, 989–993.

Hey, G., Jonsson, K. & Mattsson, A. 2016 *The Impact of Infiltration and Inflow on Waste Water Treatment Plants: A Case Study in Sweden*.

Koschwitz, D., Frisch, J. & Van Treeck, J. C. 2018 Data-driven heating and cooling load predictions for non-residential buildings based on support vector machine regression and NARX recurrent neural network: a comparative study on district scale. *Energy* **165**, 134–142.

Li, J., Li, P. & Shu, K. 2006 RMINE: a rough set based data mining prototype for the reasoning of incomplete data in condition-based fault diagnosis. *Journal of Intelligent Manufacturing* **1**, 163–176.

Lucas, A. 2010 *Corporate data quality management: from theory to practice*. In: *5th Iberian Conference on Information Systems and Technologies*, Santiago de Compostela, Spain, pp. 1–7.

Marcjasz, G., Uniejewski, B. & Weron, R. 2019 On the importance of the long-term seasonal component in day-ahead electricity price forecasting with NARX neural networks. *International Journal of Forecasting* **35** (4), 1520–1532.

Mitchell, P., Stevens, P. & Nazaroff, A. 2006 Determining base infiltration in sewers: a comparison of empirical methods and verification results. in *Pipelines* 1–13. https://doi.org/10.1061/40854(211)20.

Munawar, M., Salim, N. & Ibrahim, R. 2011 Towards data quality into the data warehouse development. *International Journal of Electrical Power and Energy Systems*. In: IEEE 9th International Conference on Dependable, Autonomic and Secure Computing. Sydney, Australia, IEEE 1199–1206.

New Zealand Water and Wastes Association 2015 *Infiltration and Inflow Control Manual*, Vols 1 & 2. Water New Zealand, Wellington. Available from: https://www.waternz.org.nz/Folder?Action=View%20File&Folder_id=394&File=II%

20Manual%20Volume%201.pdf and https://www.waternz.org.nz/Folder?Action=View%20File&Folder_id=394&File=II%20Manual%20Volume%202.pdf.

Qin, Y., Zhang, S. & Zhu, X. 2009 Pop algorithm: kernel-based imputation to treat missing data in knowledge discovery from databases. *Expert Systems with Applications* **2**, 2794–2804.

Ruiz, L. G. B., Cuéllar, M. P., Calvo-Flores, M. D. & Jiménez, M. D. C. P. 2016 An application of non-linear autoregressive neural networks to predict energy consumption in public buildings. *Energies* **9**, 684.

Solomatine, D. P. & Khada, N. D. 2003 Model trees as an alternative to neural networks in rainfall–runoff modelling. *Hydrological Sciences Journal* **48** (3), 399–411.

Staufer, P., Scheidegger, A. & Rieckermann, J. 2012 Assessing the performance of sewer rehabilitation on the reduction of infiltration and inflow. *Water Research* **46** (16), 5185–5196.

Walski, T., Chase, D. V., Savic, D. A., Grayman, W. M., Beckwith, S. & Edmundo, K. 2003 *Advanced Water Distribution Modeling and Management*. Haestad Press, Waterbury, CT, pp. 244–248.

Wei, X., Kusiak, A. & Sadat, H. R. 2013 *Prediction of Influent Flow Rate: Data-Mining Approach*.

Weiss, G., Brombach, H. & Haller, B. 2002 Infiltration and inflow in combined sewer systems: long-term analysis. *Water Science & Technology* **45**, 227–230.

Water Services Association of Australia (WSAA) 2013 *Good Practice Guidelines for Management of Wastewater System Inflow and infiltration*, Vol. 1 & 2. Prepared by GHD and Urban Water Solutions. Melbourne, Australia.

Wunsch, A., Liesch, T. & Broda, S. 2018 Forecasting groundwater levels using nonlinear autoregressive networks with exogenous input (NARX). *Journal of Hydrology* **567**, 743–758.

Yuri, A. W., Shardt, X. Y. & Steven, X. D. 2016 Quantisation and data quality: implications for system identification. *Journal of Process Control* **40**, 13–23.

Zhang, Q., Li, Z., Snowling, S., Siam, A. & El-Dakhakhni, W. 2019 Predictive models for wastewater flow forecasting based on time series analysis and artificial neural network. *Water Science and Technology* **80** (2), 243–253.

First received 19 June 2021; accepted in revised form 1 October 2021. Available online 12 October 2021

Water Science & Technology

Water Science & Technology Vol 00 No 0, 1 doi: 10.2166/wst.2021.511

Model predictive control based on artificial intelligence and EPA-SWMM model to reduce CSOs impacts in sewer systems

Khalid El Ghazouli [a,b], Jamal El Khatabi [a], Aziz Soulhi [c] and Isam Shahrour [a]

[a] Laboratoire de Génie Civil et géo-Environnement, Univ. Lille, IMT Lille Douai, Univ. Artois, Yncrea Hauts-de-France, ULR, 4515 - LGCgE, Lille F-59000, France
[b] Laboratoire d'Analyse des Systèmes, Traitement de l'Information et Management Industriel, Université Mohammed V, Rabat, Morocco
[c] National Higher School of Mines, Agdal Rabat, Morocco
*Corresponding author. E-mail: elghazouli.khalid@gmail.com

KEG, 0000-0002-3078-055X; JEK, 0000-0002-9046-4399; IS, 0000-0001-7279-8005

ABSTRACT

Urbanization and an increase in precipitation intensities due to climate change, in addition to limited urban drainage systems (UDS) capacity, are the main causes of combined sewer overflows (CSOs) that cause serious water pollution problems in many cities around the world. Model predictive control (MPC) systems offer a new approach to mitigate the impact of CSOs by generating optimal temporally and spatially varied dynamic control strategies of sewer system actuators. This paper presents a novel MPC based on neural networks for predicting flows, a stormwater management model (SWMM) for flow conveyance, and a genetic algorithm for optimizing the operation of sewer systems and defining the best control strategies. The proposed model was tested on the sewer system of the city of Casablanca in Morocco. The results have shown the efficiency of the developed MPC to reduce CSOs while considering short optimization time thanks to parallel computing.

Key words: artificial intelligence, combined sewer overflows, genetic algorithm, model predictive control, real-time control, sewer network

HIGHLIGHTS

- Model predictive control of smart sewer networks.
- Artificial Neural Networks and parallel computing enhance the proactivity of the MPC.
- Real-Time Control.
- Combined sewer overflows reduction.

INTRODUCTION

As results of urbanization and climate change, world agglomerations are facing major environmental issues, particularly those related to pollution that impacts waterbodies. In many cities, the existing combined sewer systems cannot convey all the polluted water to wastewater treatment plants during rain events (Zhao *et al.* 2019), leading to frequent combined sewer overflows (CSOs). The pollution released by sewer networks can significantly impact the ecosystem by unbalancing its kinetics through the increase of the concentrations of microbiological, mineral, and organic pollutants, thereby leading to oxygen depletion and a rise in eutrophication (Chocat 1997; McLellan *et al.* 2007; Weyrauch *et al.* 2010; Passerat *et al.* 2011; Phillips *et al.* 2012; Brokamp *et al.* 2017). Climatic factors, such as the quantity and intensity of precipitation, are key factors that determine the severity of CSO discharges (Botturi *et al.* 2020). According to future meteorological projection scenarios, a substantial increase in storm intensities and frequencies will be recorded, thereby causing more frequent CSOs (Yazdanfar & Sharma 2015; Alves *et al.* 2016; Jean *et al.* 2018).

Multiple research studies have discussed the impact of CSOs on ecosystems. Viviano *et al.* (2017) demonstrated through a complete monitoring scheme based on caffeine and turbidity that more than 50% of the total phosphorus of the Lambro River is due to sewer network overflows from rainy weather. Studies conducted by Phillips *et al.* (2012) and Launay *et al.* (2016) affirmed that even if the volume of CSOs represents a small part of the annual volume of wastewater, their impact is not negligible and can contribute up to 95% of the annual pollution caused by various pollutants.

Several actions can minimize CSOs and improve the receiving environment quality. Green infrastructures play a significant role in limiting peak flows and pollution, and they also relieve the downstream sewer network by regulating the flow or infiltrating water. Storage basins allow the storage of a large volume of polluted water during rain events and release it back to sewer networks once the rainfall events are over. However, the construction of basins remains complicated because of the lack of space, construction, and maintenance costs (Garofalo *et al.* 2017). One of the emerging ways to reduce CSOs is by performing the advanced real-time control of urban drainage systems (UDS) based on model predictive control (MPC), which computes optimal control strategies on the basis of deterministic rain forecasts. MPC has exhibited the efficient and cost-effective management of sewer systems to reduce pollution and energy consumption through several research case studies. Lund *et al.* (2020) used an integrated stormwater inflow control to mitigate CSOs in Copenhagen by dynamically controlling stormwater inflow to the combined sewer system in real time. This control was performed with an MPC on the basis of convex optimization including a linear internal surrogate. The MPC was tested on 18 rainfalls that have caused CSOs. Four of the 18 events were avoided, and the total CSO volume was reduced by 98.4% of the potential reducible volume. In addition, Bonamente *et al.* (2020) demonstrated through a study conducted on a sewer system that an MPC based on the NSGA II optimization algorithm can save energy consumption up to 32% and an overflow of approximately 10%. Rathnayake & Faisal Anwar (2019) also successfully applied an MPC to the combined sewer network of Liverpool in the United Kingdom using the NSGA II and SWMM models. The proposed model minimized the pollution load in the receiving water body and wastewater treatment and pumping costs in the sewer system. Although the proposed algorithm produced satisfactory results, the solution algorithm could not be applied to real-time control due to the simulation time needing to be improved. Considering that the reaction time in urban sewer systems is usually short, for UDS with many decision variables, such as a high number of gate valves or flow-regulating structures, the algorithm's running time may be very long and unsuitable for real-time control purposes.

This paper aims to fill the gap in the MPC research field by presenting the development and investigation of the performance of an MPC, based on robust genetic algorithms (GAs) and neural networks that have the advantage of performing fast calculations that fit the needs of such systems. Further, it aims to demonstrate the benefits of MPC associated with parallel computing that offers a sufficient lead time to define the global optimal control strategies of weir gate valves to reduce CSOs in the smart and durable city.

MATERIALS AND METHODS

The control of sewer networks is based on regulated structures (e.g., gates and pumps), most of the time controlled locally, and does not depend on communication with other facilities or the other parts of the sewer system. Local control strategies may represent a good solution in the case of one actuator, but in the case of complex sewer systems where many actuators must operate jointly, a dynamic global control system becomes necessary. In dynamic systems, control actions are based on the time-varying requirements of interests in a sewer system, the water system load, and the watershed dynamic processes.

The current work aims to develop a robust dynamic MPC system for implementing global control strategies aiming at reducing CSOs through the dynamic management of gate valves. The MPC system combines a supervisory control and data acquisition (SCADA) that receives information and measures from monitoring sensors and implements control actions, hydraulic modeling software for flow conveyance, and artificial intelligence algorithms for forecasting and control optimization purposes. MPC is based on the following three main parts (Figure 1):

1. The first part concerns the forecast of wastewater and rainwater flows at watershed outlets representing strategic control points.
2. The second part comprises real-time modeling to better represent the network state at any time.
3. The third part is about predictive modeling and optimization.

Flow forecasting in sewer networks

Without a robust model, forecasting flows in sewer networks constitute significant uncertainties for operators. Short-term forecasts are an essential component for any MPC system and significantly improve the reaction time. Nevertheless, given that the main sewer system is combined and considering the spatial variation of rainfalls, having a flow forecast of dry and rainy weather flows is necessary. The forecasting of stormwater discharges is performed with a stormwater forecasting model (SWFM) based on the NARX neural networks, which have the advantage of performing fast calculations and providing quick and accurate stormwater discharges for anticipatory models (El Ghazouli *et al.* 2019). This model takes rainfall

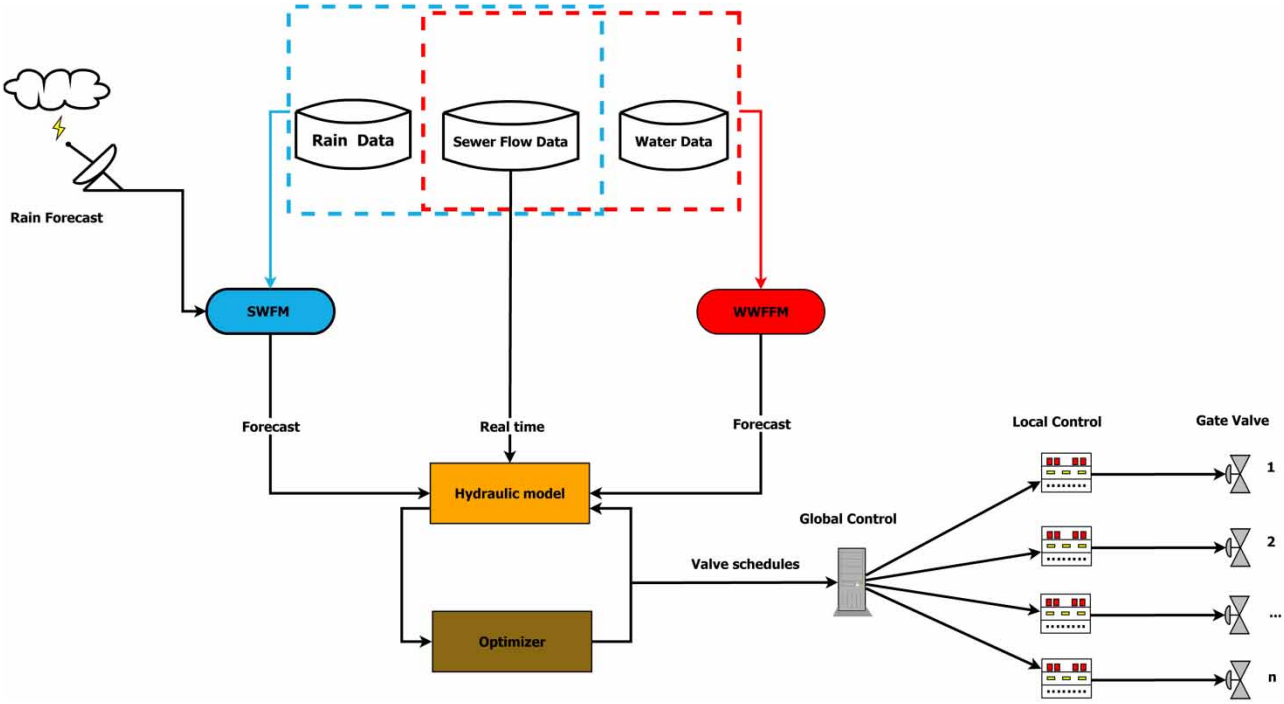

Figure 1 | Model predictive control architecture.

forecasts as inputs once available and returns as output stormwater discharges. Given that a nowcasting method based on extrapolation gives reasonable values for short-term (0–180 min) rainfall forecasts (Bowler *et al.* 2006; Berenguer *et al.* 2011), the SWFM will run with the latest updated rainfall forecasts every hour.

Instantaneous dry weather flows at watershed outlets are predicted with a wastewater flow forecasting model (WWFFM). The WWFFM is an artificial neural network (ANN) black-box model that handles nonlinear problems taking real-time water consumption and previous wastewater flow records as inputs (El Ghazouli *et al.* 2021). The output of the model is a 5-h forecasted wastewater flow time series. The combination of the SWFM and the WWFFM gives combined sewer discharge inputs for the SWMM model for flow conveyance and optimization purposes.

The architectures of the SWFM and the WWFFM neural networks include two layers; namely, a hidden layer and an output layer. The tan-sigmoid nonlinear transfer function was used in the hidden layer, and the unbounded linear transfer function that transforms the weighted sum inputs of the neurons to an output was employed in the output layer. During the learning phase, the weights and biases of the SWFM and the WWFFM ANN were adjusted according to the Levenberg–Marquardt back-propagation (LMBP) algorithm to minimize the error between the neural network output and measured data. In addition, the suitable lag parameter of the WWFFM was assessed through a cross-correlation analysis between the main causal variable and the output data. The lag parameter was defined as the concentration time of the watersheds for the SWFM, and the dataset was split into three subsets using the divide block method for the forecasting models. The first subset, representing 70% of the data, is the training set used to find the model parameters by computing the gradient and updating the network weights and biases, and the second subset, depicting 15% of the dataset, is the validation set. Additionally, during the training, the validation set error was monitored to prevent the increase of errors that leads to overfitting based on the early stopping method. The remaining 15% of the dataset was utilized as a test set to evaluate the performances and the generalization error in the final models. The SWFM and WWFFM NARX-NN were trained in their open-loop form and turned to their closed-loop form to perform multistep-ahead time series forecasting. Various neurons were tested, and the best training, testing, and validation results were obtained with a hidden layer with 10 neurons after several trials.

Real-time modeling

The MPC system uses the EPA SWMM engine to compute flow conveyance on the basis of a simplified model that comprises the main branches of the interception system of the sewer networks of Casablanca, as can be seen in Supplementary Material, Fig. S1. The model is connected to a SCADA and continuously updated with real-time data. Flow rates at the outlet of the watersheds and orifice opening status are automatically set to the same values as those observed in the field. Moreover,

the real-time model is automatically updated every hour with the last few hours of data. At the end of each model run, a Hot-start file containing the system boundary conditions is generated and will be employed for the next simulation with stormwater and dry weather flow forecasts as inputs.

Optimization of the operational system

The optimization section consists of algorithms able to set optimal operating control strategies while considering various constraints, such as the maximum flow of the wastewater treatment plant (WWTP). GAs are widely utilized and present their efficiency to solve many optimization problems in many fields, specifically in water. We can cite the works of Tayfur *et al.* (2009) for predicting peak flows, Li *et al.* (2020) for water resource management, Bostan *et al.* (2019) for the optimal design of shock dampers, Montes *et al.* (2020) for predicting bedload sediment transport in sewer networks, and Hassan *et al.* (2020) for the optimal design of sewer networks. Therefore, GAs are chosen to optimize the sewer system operating as part of this work. GAs are inspired by the evolution theory of Darwin (1859) and, more specifically, natural selection, reproduction, and the survival of the fittest. In addition, they belong to the larger class of evolutionary algorithms. They were also developed by Holland (1962) in the 1970s and were popularized in the late 1980s and the early 1990s (Davis 1987; Goldberg 1989; Alliot & Schiex 1993; Forrest 1993).

The MPC is designed to be robust enough to define optimal strategies for managing the sewer system. The optimization of the objective function that we seek to minimize is reducing CSOs by maximizing the treated volume of polluted water at the WWTP. The optimization work involves adjusting the system decision variables that correspond to gate valve opening status at each time of the simulation horizon during different generations considering the operation of constraints, which are mainly the maximum flow capacities at the entrance of the WWTP, by applying a succession of operators to population individuals. The flow chart below describes the distinct steps of GAs.

First, an initial population (P (0)) of gate valve status is generated. This population contains chromosomes distributed in the solution space with varied genetic materials defined in a given interval. The fitness of each chromosome is evaluated, and the best individuals are selected for reproduction. Once the selection operation is conducted for the current population (P (t)), the crossover operator is then applied. The fundamental role of the crossover operation is to enrich the population diversity by manipulating the structure of chromosomes through the recombination of information present in the genetic heritage of individuals. The newly generated individuals are then submitted to the mutation operator. This operator allows GAs to better search the space of solutions by changing the allelic value of the gene with a very low mutation probability, which is generally between 0.01 and 0.001 (Fogel *et al.* 2000). The last step in the iterative process is to incorporate new solutions into the current population. The new solutions are added to the current population, thereby replacing the old solutions. This process is repeated until a stop criterion is met, and this criterion can be a determined number of generations or a particular value of the objective function (Figure 2).

Application for the sewer network of Casablanca (Morocco)

The sewer network of the eastern part of Casablanca is used to implement and evaluate the proposed MPC. The total area of the studied sector is approximately 41.6 km² (Figure 3). It comprises parallel watersheds with combined sewer networks.

The main sewer network outlets of these watersheds are historically discharged into the sea. An interceptor has been designed to convey dry weather flows to the treatment plant and discharges the excess water into the sea by rainy weather via frontal or side weirs. Additionally, it consists of a pipe of 9.5 km with a maximum capacity constrained by the capacity of a lift station (6.5 m^3/s) downstream at the entrance to the WWTP. At each branch level, the interception system (Figure 4) is equipped with gate valves that control the flow diverted to the WWTP. These valves are modeled as orifices in the SWMM model. Today, by rainy weather and in the absence of control strategies, the gate valves are closed, and the polluted water is discharged directly into the sea.

The developed algorithm for the sewer network of Casablanca considers one objective function (Obj *Fun*) that is formulated to minimize CSOs by maximizing the total treated volume. The mathematical expression of the objective function is given in Equation (1):

$$\text{Obj}\,Fun = -\sum_{i=1}^{n} (V_{x;i}) \tag{1}$$

where V is the intercepted volume at branch x at a given timestep (i).

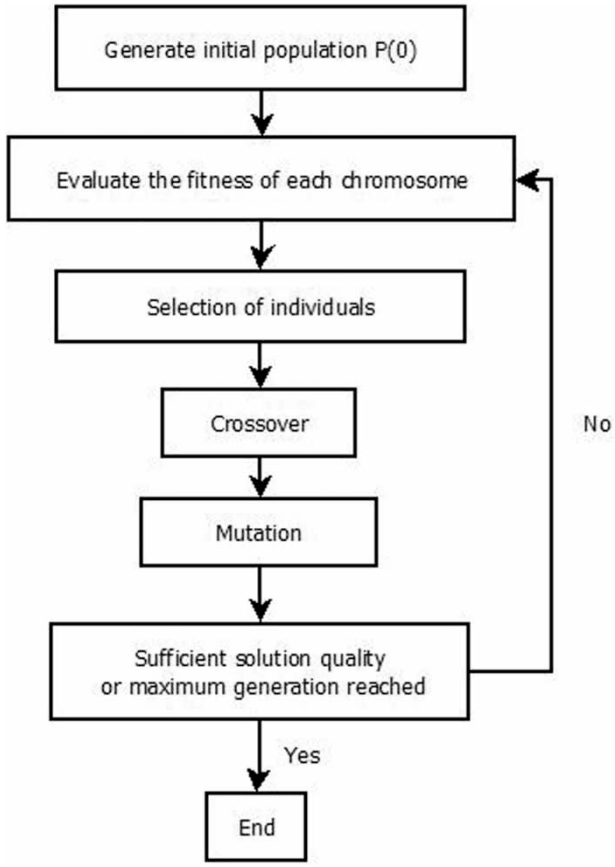

Figure 2 | Flow chart of genetic algorithms.

The above-mentioned objective function is under a set of nonlinear constraints. A constraint is set such that the instantaneous flow rate at the WWTP entrance should not exceed its maximum capacity. The mathematical expression of the constraint is given in Equation (2):

$$Qt \leq Qmax \tag{2}$$

where Qt and $Qmax$ are the flow rates at the entrance of the WWTP at timestep t.

The number of decision variables (n) corresponds to the states (St) of the orifices for the simulation duration. The decision variable values are bounded between 0, which corresponds to a closed valve, and 1 represents a totally opened valve. The MPC result is an optimal gate valve control schedule with a 30-min timestep.

The MPC was initially run on the basis of a one-year return period (YRP) double-triangle rainfall hyetograph with a total duration of 1 h, an intense duration of 10 min, and a simulation time of 3 h. The optimization calculations were first performed in serial computing for different population sizes composed of 10, 20, 40, 60, 80, and 100 individuals over 100 generations to choose the best population size. This optimization problem comprises 36 decision variables corresponding to the states of six orifices for a simulation horizon of 3 h with six timesteps of 30 min.

Once the suitable numbers of population and generation are chosen, MPC is then evaluated on a real rainfall event recorded on 11 December 2017. The event has been marked by two successive rainfalls with a return period of 5 years, a cumulative rain of 38 mm, and a total duration of 6 h. For this event, MPC runs a simulation every 2 h with a 5-h simulation horizon.

For problems with a high number of decision variables, the running time of the algorithm may be very long. Parallel computation is a technique that reduces computational time by distributing the population and evaluating their fitness over several workers. Parallelization tasks are conducted for this event, and a comparison of the performance times according

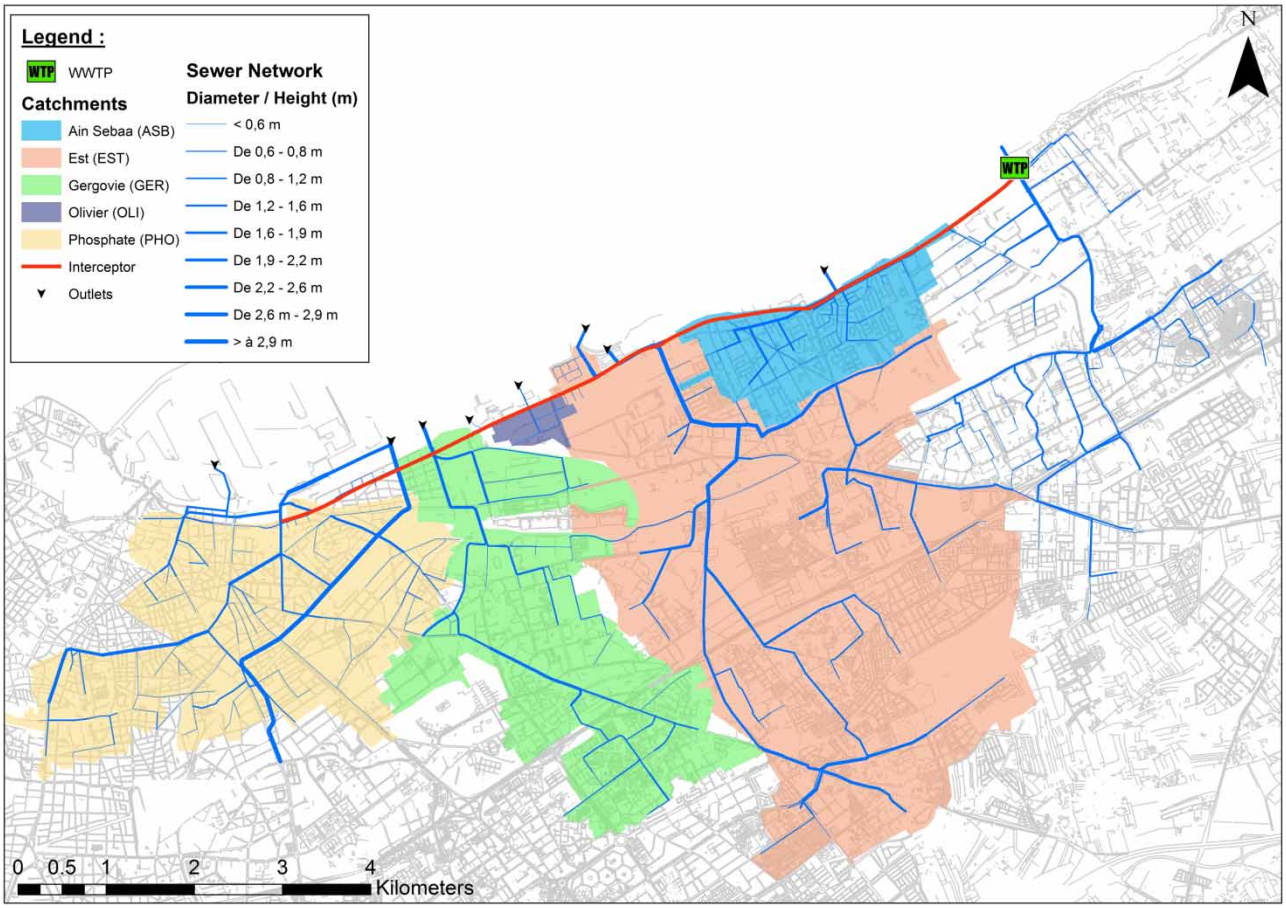

Figure 3 | Sewer network of the eastern part of Casablanca.

to a different number of threads (workers) is performed. All the simulations are performed on the same desktop PC (CPU: AMD Ryzen Threadripper 3970X 4.5 GHz, RAM: 128 GB).

RESULTS AND DISCUSSION

Serial computing

Simulation results for distinct population sizes (Table 1 and Figure 5) applied to one YRP rainfall event validate that the MPC demonstrates its ability to reduce CSOs into the sea by maximizing the volume treated without exceeding the maximum flow at the WWTP. We can notice that population size significantly impacts the final solution determined by GAs.

The analysis of Figure 6, which presents the evolution of fitness according to generation numbers, verifies that the larger the population size, the more the algorithm converges toward an optimal solution in the first iterations of the calculation. We can also observe that the number of generations becomes negligible on the convergence as soon as we exceed the generation equal to 60.

Computation time is a critical component in MPC systems, and it must be reduced. Supplementary Material, Fig. S2 depicts the linear relationship between the computation time and the population size. The analysis of the various results confirms that population size and a generation number equal to 60 appear to be a good compromise between the algorithm performance in finding an optimal solution and the computation time. Hence, population size and a number of generations equal to 60 are applied for the parallel calculation for the 11 December 2017 rainfall event.

Parallel computing

For the 11 December 2017 rainfall event, the MPC performed four runs with a 5-h simulation horizon. These simulations are updated every 2 h to consider recent and accurate sewer network states, boundary conditions, and rainfall forecasts, allowing definition of an operating schedule for the various control valves over 5 h with a 30-min timestep for each simulation (Figure 7).

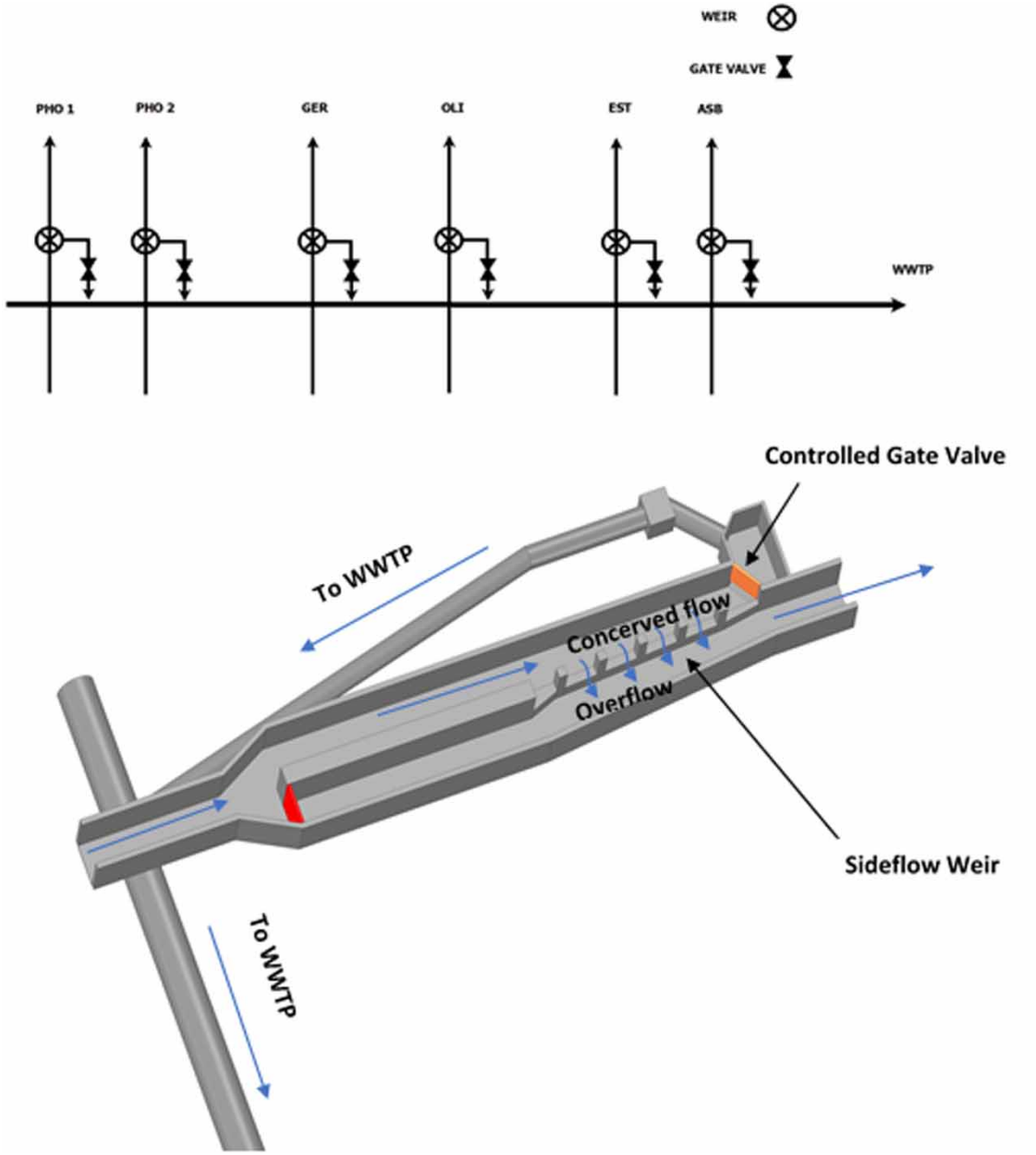

Figure 4 | Interception system.

For each run, the SWFM and the WWFFM generate accurate forecasted flows (Supplementary Material, Fig. S3) used as inputs for the SWMM model. The NARX-NN allows the MPC to benefit more proactively from the relatively fast computing time of neural networks within 2 sec compared with a conventional hydraulic model that takes approximately 6 min for each run.

For the rainfalls of 11 December 2017, a comparison of the performance times according to the divergent numbers of threads (workers) is performed. Supplementary Material, Fig. S4 illustrates that parallel computing can significantly reduce computing time from 4,092 s for four threads to 890 s for 64 threads on the same processor. However, parallel

Table 1 | Optimized flow for different population sizes

Population size	10	20	40	50	60	80	100
Treated water volume (m^3)	53,978	53,674	55,110	55,153	54,707	54,950	54,950

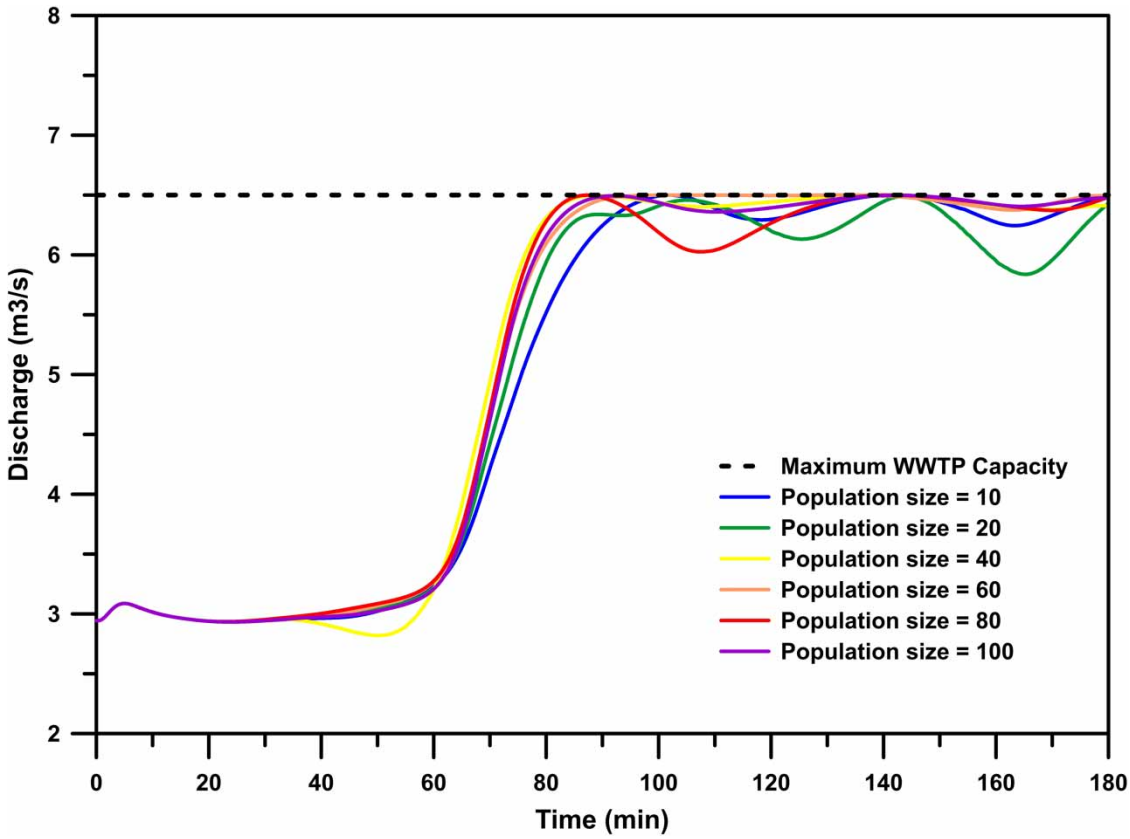

Figure 5 | Optimized flow for different population sizes.

computing performance decreases exponentially as a function of the number of threads employed in the simulation. Above 32 threads, the number of threads has no significant impact on the solution time. Moreover, for more proactivity, the computation time could be reduced further by parallelizing computation on several processors.

Figure 8 exhibits that the MPC developed as part of this work gives good results and enhances the efficiency of the sewer system of Casablanca, thereby allowing conveyance to the WWTP, in addition to strict wastewater, a volume of 146,830 m^3 of polluted rainwater without exceeding the maximum flow of the WWTP. The MPC managed the rainy event of 11 December 2017 by generating a schedule (Supplementary Material, Fig. S5) for controlling the gate valves at the interception structures. Furthermore, we can notice that a lack of a control strategy would cause disturbances and flooding at the lifting station at the entrance of the treatment plant, with a peak flow rate exceeding 8.5 m^3/s.

CONCLUSIONS

This paper presented a novel MPC based on neural networks for predicting flows and a GA for optimizing the operation of the sewer system of Casablanca. The MPC demonstrates high efficiency in reducing CSOs in the receiving environment by generating optimal temporally and spatially varied dynamic control strategies of the gate valves of the sewer system. This MPC could benefit municipalities around the world facing environmental issues and their consequences, such as CSOs and floods. As part of this work, we determined the best population size and the generation number that present a compromise between the algorithm performance in finding an optimal solution and the computation time. The parallelization of calculations allows the reduction of the computation time considerably and makes the MPC more proactive. However, since the MPC relies on weather forecasts, handling the uncertainty is required to successfully introduce the use of rainfall forecasts in operational management systems. Long-term verification analysis is needed to assess the quality of the forecasts for a particular sewer system. If this is satisfactory, a verification analysis is needed to test the decision rules and control strategies, given the forecasts, so that operators can see the effect of potential management strategies and avoid disasters.

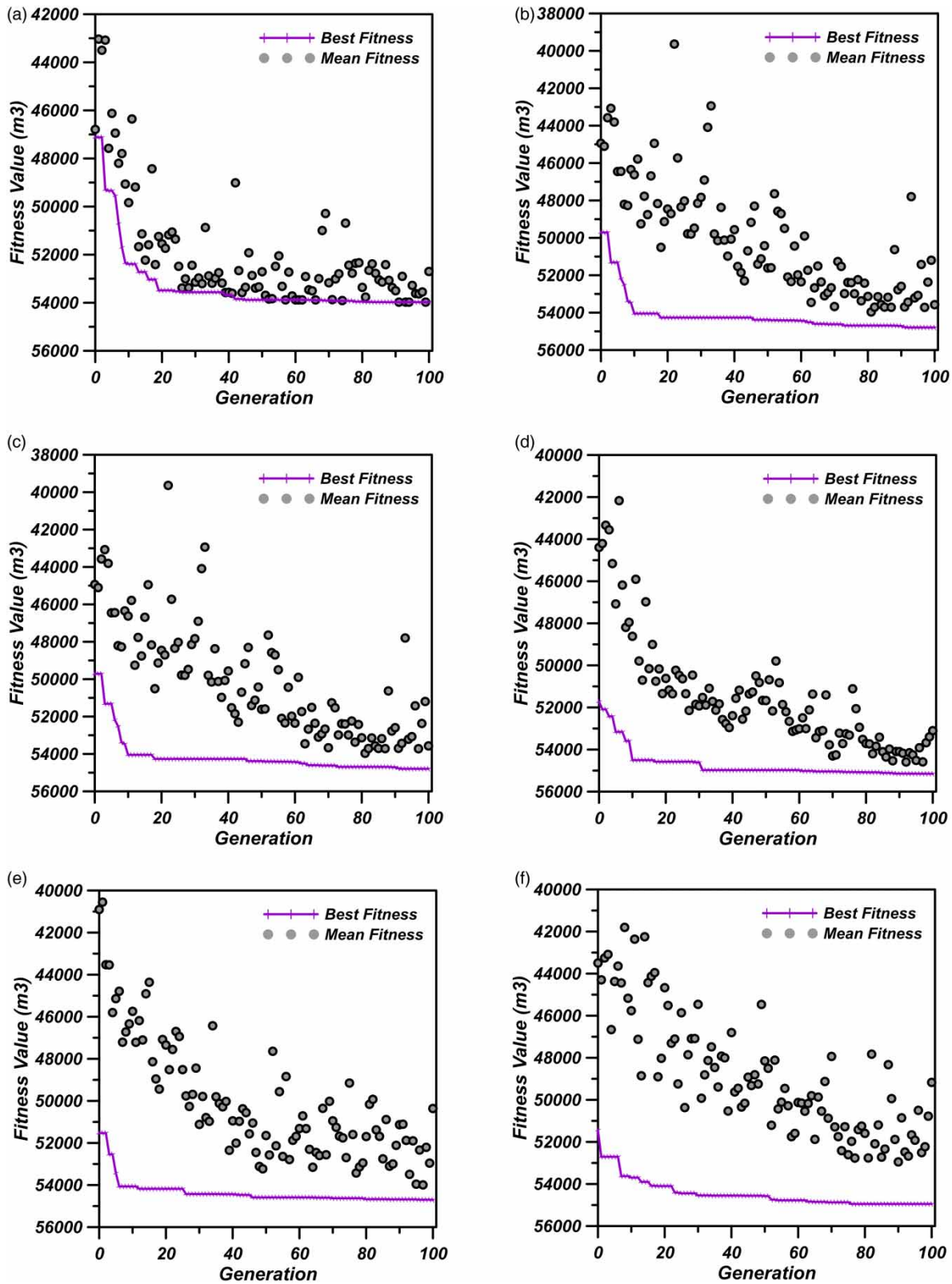

Figure 6 | Fitness with populations equal to (a) 10; (b) 20; (c) 40; (d) 60; (e) 80; and (f) 100.

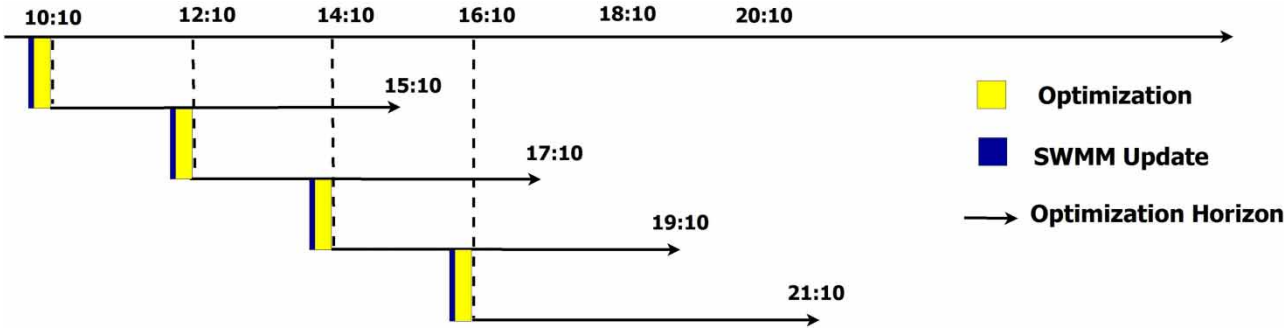

Figure 7 | Process of the MPC strategy.

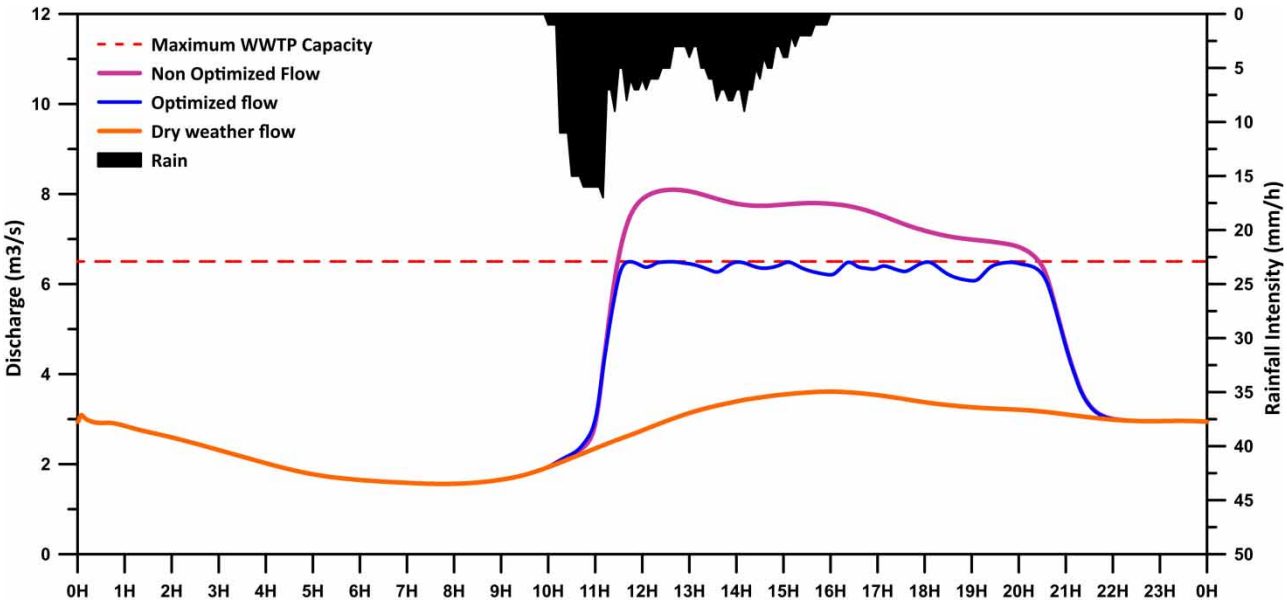

Figure 8 | Optimized flow for the rainfalls of 11 December 2017.

In the continuity of this work, a pollution measurement campaign will be conducted at the outlet of each watershed to determine the impact of CSOs on the natural environment and will be completed by two-dimensional hydraulic modeling of the dispersion of pollution into the sea. Thus, on the basis of these future results, the objective function will be adapted by weighting the volumes intercepted at the level of each branch according to the identified impact risk.

DATA AVAILABILITY STATEMENT

All relevant data are included in the paper or its Supplementary Information.

REFERENCES

Alliot, J. M. & Schiex, T. 1993 *Intelligence artificielle et informatique théorique*. Cepadues, Toulouse, France.

Alves, A., Sanchez, A., Vojinovic, Z., Seyoum, S., Babel, M. & Brdjanovic, D. 2016 Evolutionary and holistic assessment of Green-grey infrastructure for CSO reduction. *Water* **8** (9), 402.

Berenguer, M., Sempere-Torres, D. & Pegram, G. G. S. 2011 SBMcast – an ensemble nowcasting technique to assess the uncertainty in rainfall forecasts by Lagrangian extrapolation. *Journal of Hydrology* **404** (3–4), 226–240.

Bonamente, E., Termite, L. F., Garinei, A., Menculini, L., Marconi, M., Piccioni, E., Biondi, L. & Rossi, G. 2020 Run-time optimisation of sewer remote control systems using genetic algorithms and multi-criteria decision analysis: CSO and energy consumption reduction. *Civil Engineering and Environmental Systems* **37** (1–2), 62–79.

Bostan, M., Akhtari, A. A., Bonakdari, H. & Jalili, F. 2019 Optimal design for shock damper with genetic algorithm to control water hammer effects in complex water distribution systems. *Water Resources Management* **33** (5), 1665–1681.

Botturi, A., Ozbayram, E. G., Tondera, K., Gilbert, N. I., Rouault, P., Caradot, N., Gutierrez, O., Daneshgar, S., Frison, N., Akyol, Ç., Foglia, A., Eusebi, A. L. & Fatone, F. 2020 Combined sewer overflows: a critical review on best practice and innovative solutions to mitigate impacts on environment and human health. *Critical Reviews in Environmental Science and Technology* **51** (15), 1585–1618.

Bowler, N. E., Pierce, C. E. & Seed, A. W. 2006 STEPS: a probabilistic precipitation forecasting scheme which merges an extrapolation nowcast with downscaled NWP. *Quarterly Journal of the Royal Meteorological Society* **132** (620), 2127–2155.

Brokamp, C., Beck, A. F., Muglia, L. & Ryan, P. 2017 Combined sewer overflow events and childhood emergency department visits: a case-crossover study. *Science of the Total Environment* **607–608**, 1180–1187.

Chocat, B. 1997 *Encyclopédie de l'hydrologie urbaine et de l'assainissement*. Tec & doc-Lavoisier, Paris, pp. 529–543.

Darwin, C. 1859 In: *On the Origin of Species by Means of Natural Selection or the Preservation of Favoured Races in the Struggle for Life* (Murray, J., ed.). John Murray, London.

Davis, L. 1987 *Genetic Algorithms and Simulated Annealing*. Morgan Kaufmann Publishers, Pitman, London.

El Ghazouli, K., El Khattabi, J., Shahrour, I. & Soulhi, A. 2019 Comparison of M5 model tree and nonlinear autoregressive with exogenous inputs (NARX) neural network for urban stormwater discharge modelling. *MATEC Web of Conferences* **295**, 02002. https://doi.org/10.1051/matecconf/201929502002.

El Ghazouli, K., El Khattabi, J., Shahrour, I. & Soulhi, A. 2021 Wastewater flow forecasting model based on the nonlinear autoregressive with exogenous inputs (NARX) neural network. *H2Open Journal*. https://doi.org/10.2166/h2oj.2021.107.

Fogel, D. B., Bäck, T. & Michalewicz, Z. 2000 *Evolutionary Computation: Basic Algorithms and Operators*. Institute of Physics Publishing Bristol, PA.

Forrest, S. 1993 Genetic algorithms: principles of natural selection applied to computation. *Science* **261**, 872–878.

Garofalo, G., Giordano, A., Piro, P., Spezzano, G. & Vinci, A. 2017 A distributed real-time approach for mitigating CSO and flooding in urban drainage systems. *Journal of Network and Computer Applications* **78**, 30–42.

Goldberg, D. E. 1989 *Genetic Algorithms in Search, Optimization, and Machine Learning*. Addison-Wesley Publishing Company, Boston, Massachusetts, USA.

Hassan, W. H., Attea, Z. H. & Mohammed, S. S. 2020 Optimum layout design of sewer networks by hybrid genetic algorithm. *Journal of Applied Water Engineering and Research* **8** (2), 108–124.

Holland, J. H. 1962 Outline for a logical theory of adaptive systems. *Journal of the ACM* **9** (3), 297–314.

Jean, M. È., Duchesne, S., Pelletier, G. & Pleau, M. 2018 Selection of rainfall information as input data for the design of combined sewer overflow solutions. *Journal of Hydrology* **565**, 559–569.

Launay, M. A., Dittmer, U. & Steinmetz, H. 2016 Organic micropollutants discharged by combined sewer overflows – characterisation of pollutant sources and stormwater-related processes. *Water Research* **104**, 82–92.

Li, M., Zhang, J., Cheng, X. & Bao, Y. 2020 Application of the genetic algorithm. In: *Water Resource Management* (Atiquzzaman, M., Yen, N. & Xu, Z., eds). Springer Singapore, Big Data Analytics for Cyber-Physical System in Smart City, Singapore, pp. 1681–1686.

Lund, N. S. V., Borup, M., Madsen, H., Mark, O. & Mikkelsen, P. S. 2020 CSO reduction by integrated model predictive control of stormwater inflows: a simulated proof of concept using linear surrogate models. *Water Resources Research* **56** (8), 1–15.

McLellan, S. L., Hollis, E. J., Depas, M. M., Van Dyke, M., Harris, J. & Scopel, C. O. 2007 Distribution and fate of Escherichia coli in Lake Michigan following contamination with urban stormwater and combined sewer overflows. *Journal of Great Lakes Research* **33** (3), 566.

Montes, C., Berardi, L., Kapelan, Z. & Saldarriaga, J. 2020 Predicting bedload sediment transport of non-cohesive material in sewer pipes using evolutionary polynomial regression – multi-objective genetic algorithm strategy. *Urban Water Journal* **17** (2), 154–162.

Passerat, J., Ouattara, N. K., Mouchel, J. M., Rocher, V. & Servais, P. 2011 Impact of an intense combined sewer overflow event on the microbiological water quality of the Seine River. *Water Research* **45** (2), 893–903.

Phillips, P. J., Chalmers, A. T., Gray, J. L., Kolpin, D. W., Foreman, W. T. & Wall, G. R. 2012 Combined sewer overflows: an environmental source of hormones and wastewater micropollutants. *Environmental Science & Technology* **46** (10), 5336–5343.

Rathnayake, U. & Faisal Anwar, A. H. M. 2019 Dynamic control of urban sewer systems to reduce combined sewer overflows and their adverse impacts. *Journal of Hydrology* **579**, 124150.

Tayfur, G., Barbetta, S. & Moramarco, T. 2009 Genetic algorithm-based discharge estimation at sites receiving lateral inflows. *Journal of Hydrologic Engineering* **14** (5), 463–474.

Viviano, G., Valsecchi, S., Polesello, S., Capodaglio, A., Tartari, G. & Salerno, F. 2017 Combined use of caffeine and turbidity to evaluate the impact of CSOs on river water quality. *Water, Air, & Soil Pollution* **228** (9), 330.

Weyrauch, P., Matzinger, A., Pawlowsky-Reusing, E., Plume, S., von Seggern, D., Heinzmann, B., Schroeder, K. & Rouault, P. 2010 Contribution of combined sewer overflows to trace contaminant loads in urban streams. *Water Research* **44** (15), 4451–4462.

Yazdanfar, Z. & Sharma, A. 2015 Urban drainage system planning and design – challenges with climate change and urbanization: a review. *Water Science and Technology* **72** (2), 165–179.

Zhao, W., Beach, T. H. & Rezgui, Y. 2019 Automated model construction for combined sewer overflow prediction based on efficient LASSO algorithm. *IEEE Transactions on Systems, Man, and Cybernetics: Systems* **49** (6), 1254–1269.

First received 30 May 2021; accepted in revised form 15 November 2021. Available online 29 November 2021